Departamento de Química Orgánica.

Centro de Reconocimiento Molecular y Desarrollo Tecnológico.

Doctorado en Química

Functionalized gold nanoparticles for the detection of biologically active molecules

PhD Thesis

Submitted by:

Almudena Martí Morant

PhD supervisor:

Professor Margarita Parra Álvarez

Dr. Pablo Gaviña Costero

Valencia, November 2015

Margarita Parra Álvarez , PhD in Chemistry and Professor at the Universitat de València, and Pablo Gaviña Costero, PhD in Chemistry and Associate Professor at the Universitat de València

CERTIFY,

That the work **"Functionalized Gold nanoparticles for the detection of biologically active molecules"** has been developed by Almudena Marti Morant under their supervision in the Centro de Reconocimiento Molecular y Desarrollo Tecnólogico (IDM) of the Universitat de València, as a Thesis Project in order to obtain the degree of PhD in Chemistry at the Univeristat de València.

Valencia, November 2015

Margarita Parra Álvarez

Pablo Gaviña Costero

Dedicada a la meua familia pel seu suport al llarg d'aquest camí.

“En el fondo, los científicos somos gente con suerte: podemos jugar a lo que queramos durante toda la vida.”

(Lee Smolin)

“Nuestra recompensa se encuentra en el esfuerzo y no en el resultado. Un esfuerzo total es una victoria completa.”

(Mahatma Gandhi)

Arribats a aquest punt, cal pensar en el camí recorregut. Un camí que va començar quan vaig decidir fer el projecte final de carrera al grup de la professora Ana M. Costero. Eixe va ser el moment en el que vaig decidir que el món de la investigació també podria ser el meu. L'arribada a meta ha segut un camí llarg, el qual he sabut seguir.

És ben sabut que durant la Tesi augmentem el nostre bagatge al món de la investigació així com, el coneixement. I a banda, generem vincles amb tota la gent amb la que ens trobem i que t'ajuden dia a dia.

En primer lugar me gustaría dar las gracias a la Prof. Ana M. Costero, por haber contado conmigo y darme la oportunidad de desarrollar la tesis en su grupo de investigación así como,por ayudarme en todo momento, por estar siempre ahí y por intentar solucionar cualquier duda.

En segundo lugar me gustaría darles las gracias a mis directores de tesis Pablo y Marga. Gracias a los dos por guiarme y aconsejarme, porque los tres hemos aprendido muchas cosas sobre las nanopartículas de oro, y lo más importante por enseñarme a hacer investigación. Y como no, gracias a ti también Salvador por ayudarme en todo lo que podías y con algún que otro espectro de RMN.

Gràcies als meus companys del laboratori tant del 4.27 com del 4.34, des d'aquells que heu estat amb mi des del primer dia, com als que esteu amb mi des de fa poc. Gràcies a Raül, Úrsula, Kathe, per totes les rises que hem passat al 4.34 i peels bons moments, ja que fóreu els meus primers companys de laboratori. Gràcies també a Santi i Andrea del 4.27, per tot el que hem compartit. I com no a tots els que esteu ara ací amb mi, perquè feu que vindre al laboratori valga la pena, ens ho passem molt be i a banda som amics, Dani, Estefania i Carlos. Vull donar-vos les gràcies per estar sempre ahí i saber aconsellar-me. Com no també agrair a Alberto, Elena i Samuel per formar part d'aquest equip, al igual que als companys del laboratori 2.6 del politècnic

Aquesta tesi m'ha fet guanyar una cosa, molt important per a mi, que són els meus amics. O podem dir que ja som un petita família. Moltes gràcies a tots i cadascun de vosaltres, perquè ningú millor que vosaltres m'ha comprés degut a, que estem al mateix món.

És bonic mirar enrere i vore que em compartit molts *combois* i moltes coses junts. Gràcies Cristina G., Núria, Dani, Neus, Mar, Lluís, María R. I també a vosaltres Santi i Carles que encara que no sou químics heu donat el pego, jajaja. En especial vull agrair a Mar i Neus, la vostra paciència, així com per ser i demostrar-me que sou les meues incondicionals i per estimar-me tant.

Fora del laboratori també voldria agrair a les meus amics el seu suport i per estar ahí estos anys. A les meues incondicionals i companyes de camí, a Mª del Mar i a Paula, sé que sempre puc comptar amb vosaltres. I com no, a les meues germanes postisses, las germanes Escrivà. A tu Àngela i Andrea per ser com sou i recolzar-me d'una manera especial.

Finalment, m'agradaria fer una menció especial a aquells que sempre; haja passat el que haja passat; han estat preguntant-me com va la cosa, o mostrant interés, moltes vegades sense acabar d'entendre el que contava, sempre amb l'objectiu d'ajudar-me i comprendrem. Ells són; la meua família: a ma mare, perquè sóc tot el que m'has donat i ensenyat. Gràcies per l'esforç, per cuidar-me i ajudar-me a créixer en tots els aspectes de la vida. A la meua germana, gràcies perquè sempre estàs ahí i per ajudar-me en tot moment, i per ensenyar-me que quan una finestra es tanca, un porta més gran està esperant-me. A la meua *uelita*, gràcies pels teus savis consells. Enrique no em podia oblidar-me de tu, gràcies per ser tant crític i demostrar interés. Gràcies família per donar-me i mostrar-me que tot té solució, quan no veig més enllà dels meus ull.

Abstract

The present PhD thesis entitled “Functionalized Gold Nanoparticles for the detection of biologically active molecules” is based in the blending of Supramolecular Chemistry and Materials Science principles for the preparation of new functional gold nanoparticles and some fluorescein derivatives with the ability of detecting small molecules in liquid environments.

The first part of this thesis is focused on the design, synthesis, characterization and evaluation of suitable organic compounds anchored onto gold nanoparticles as a chromogenic sensor. Different sensors were obtained to detect nerve agent mimics, nitric oxide and dicarboxylates. The strategy is based on the aggregation of gold nanopartilcles, as a consequence of the aggregation provide a color change appreciable by naked eye and a change in the Plasmon band, with remarkable limits of detection.

The remaining part of this thesis are centered in the design, synthesis and evaluation of suitable fluorescein derivatives compounds as a fluorescence sensor for dicarboxylates ω-amino acids. These chemosensors were designed containing different binding sites in order to bind with a specific molecule. The fluorescein-probes allowed discrimination of amino acid with different chain length and distinguish different dicarboxylate.

Resumen

La presente tesis doctoral titulada “Nanopartículas de oro funcionalizadas para la detección de moléculas biológicamente activas” está centrada en la combinación de principios de la Química Surpamolecular y de la Ciencia de los Materiales para la preparación de nuevas nanopartículas funcionalizadas y de derivados de fluoresceina capaces de detectar pequeñas moléculas en disolución.

La primera parte de la tesis, se concentra en el diseño, síntesis, caracterización y evaluación de compuestos orgánicos que son anclados a nanopartículas de oro y utilizados como sensores cromogénicos. Se han obtenido distintos sensores para detectar simulantes de agentes de guerra, óxido nítrico y dicarboxilatos. La estrategia seguida se basa en que el analito provoque la agregación de las nanopartículas de oro, y como consecuencia un cambio en la banda de plasmón que da lugar al cambio de color correspondiente; con remarbles límites de detección.

El resto de la tesis se centra en el diseño, síntesis y evaluación de compuestos derivados de fluoresceína apropiados como sensores fluorogénicos de dicarboxilatos y de ω-amino ácidos. Estos quimiosensores fueron diseñados con diferentes centros reactivos con el fin de interaccionar con una molécula específica. Dichos sensores químicos permiten discriminar entre las diferentes longitudes de cadena de los aminos ácidos y la distinción entre los dicarboxilatos

Result of this thesis and other contributions have resulted in the following scientific publications:

- Ana M. Costero, Margarita Parra, S. Gil, Josep V Colomer, **Almudena Martí, "***Fluorescein-based thiourea derivatives as fluorogenic sensors for mono and dicarboxylates. "* Sensor Letters, **2010**, 8, 818-823.

- Estela Climent; **Almudena Martí**; Santiago Royo; Ramón Martínez-Máñez, M. Dolores Marcos; Félix Sancenón; Juan Soto; Ana M Costero; Salvador Gil; Margarita Parra. "*Chromogenic detection of nerve agent mimics by mass transport control to the surface of bi-functionalized* silica nanoparticles". *Angew. Chem. Int. Ed*., **2010**, 49, 5945 –5948.

- **Almudena Martí**; Ana Maria Costero; Pablo Gaviña; Salvador Gil; Margarita Parra; Mauro Brotons-Gisbert; Juan F. Sánchez-Royo. "*Functionalized gold nanoparticles as an approach to the direct colorimetric detection of DCNP nerve agent* simulant".*Eur. J. of Org. Chem.*, **2013**, 4770-4779.

- **Almudena Martí**; Ana M. Costero; Pablo Gaviña; Margarita Parra. "*Triarylcarbinol functionalized gold nanoparticles for the colorimetric detection of nerve agent simulants.",* Tet. Let., **2014**, 55, 3093-3096

- **Almudena Martí**; Ana M. Costero; Pablo Gaviña; Margarita Parra. "*Selective colorimetric NO (g) detection based on the use of modified gold nanoparticles using click chemistry." Chem. Commun*., **2015**, 51, 3077-3079.

- **Almudena Martí**, Ana M. Costero, Pablo Gaviña, Margarita Parra. "*A simple system for ω-amino acids discrimination based on a thiourea modified fluorescein*." Accepted *Eur. J. Org. Chem.* **DOI**: 10.1002/ejoc.201500991.

- **Almudena Martí**, Ana M. Costero, Pablo Gaviña, Margarita Parra, *"Selective recognition and sensing of succinate vs. other dicarboxylates by thiourea-functionalized gold nanoparticles". Chem. Eur. J., Submitted.*

A	Acceptor
Ac	Acetyl
AcoEt	Ethyl acetate
Ala	Alanine
Aunps	Gold nanoparticles
^{13}C-NMR	Carbon nuclear magnetic resonance
$CDCl_3$	Chloroform- *d*
CT	Charge transer
CTAB	Trimethylammonium bromide
CWA	Chemical warfare agent
Cys	Cysteine
D	Donor
d	doublet
δ	Chemhical shift
DCNP	Diethylcyanophosphonate
DCP	Diethylchlorophosphate
dd	Doublet of doubets
4,4'-DDD	1-chloro-4-[2,2-dichloro-1-(4-chlorophenyl)ethyl]benzene
4,4'-DDE	1,1-*bis*-(4-chlorophenyl)-2,2-dichloroethene
DCM	Dicloromethane
Dcet	Dichloroethane
DDC	Diciclohexylcarbodimide
DFP	Diisopropylfluorophosphate
DLS	Dynamiclight scattering
DMAP	Dimethylamino piridine
DMF	Dimethylformamide
DMSO	Dimethylsulfoxide
dt	Doublet of triplets
EDC	N-(3-Dimethylaminopropyl)-N'-ethylcarbodiimide
Et	Ethyl
Et_3N	Triethyl amine
Etoh	Ethanol
FRET	Fluorescence Resonance Energy Transfer
GABA	γ-aminobutiric acid
Gly	Glycine
GV	2-(dimethylamino)ethyl-N,N-dimethylphosphoramido fluorinate
H_2	Hydrogen
$HAuCl_4$	Hydrochloric acid
Hex	Hexane

Hz	Hertz
ICT	Internal charge transfer
J	J-coupling
LOD	Limit of detection
m	multiplet
Malathion	Diethyl 2-[(dimethoxyphosphorothioyl) sulfanyl]butanedionate
Me	Methyl
MeCN	Acetonitrile
MeOH	Methanol
min	minutes
mL	milliliters
µL	microliters
NaOH	Sodium hydroxide
NBS	N-Bromosuccinimide
n-BuLi	n-Buthylithiuml
NH_4OAc	Ammonium acetate
NMR	Nuclear magnetic resonance
NO	Nitric oxide
Pd/C	Palladium on carbon
PET	Photoinduced charge transfer
Ph	Phenyl
ppm	Parts per million
Pr	Propyl
q	quartet
R	Organic residue
RNS	Reactive nitrogen species
ROS	Reactive oxygen species
SAMs	Self-Assembled Monolayer Surfaces
SEM	Scanning Electron Microscopy
SERS	Surface Exchange Raman Spectroscopy
SQ	Squaridine dye
Sarin	(RS)-O-isopropyl methylphosphonofluoridate
Soman	O-pinacolyl methylphosphoramidocyanidate
t	triplet
Tabun	(RS)-ethyl-N,N-dimethylphosphoramidocyanidate
TBA	Tetrabutylammonium
TBAOH	Tetrabutylammonium hydroxide
TBS	Tert-butyldimethylsilyl
TEM	Transmission electron microscpy
TFA	Trifluoroacetic acic

THF	Tetrahydrofurane
UV	Ultraviolet
VG	Amiton, Tetram, O,O-diethyl S-2-(diethylamino)ethyl phosphorothionate
Vis	Visible
VX	O-ethyl S-[2-(diisopropylamino)ethyl]methylphosphono-thioate
λ	Wavelength
ε	Molar absoption coefficient

Table of contents

CHAPTER 1:
General Introduction

1.1. Supramolecular Chemistry

Chemistry is the science that studies the nature, structure, properties, and composition of matter. Chemistry also studies how matter undergoes changes during reactions and the energetic balance in these processes. The main basis of chemistry is the creation of molecular assemblies employing a controlled formation or breaking of covalent bonds. In the same context, supramolecular chemistry examines the weaker and reversible non covalent interactions between molecules. These forces include hydrogen bonding, metal coordination, hydrophobic forces, van der Waals forces, π-π interactions and electrostatic effects, [1] with the aim to easily generate unique nanostructured supermolecules that presented different properties (often better) than the sum of the properties of each individual component.[2]

J. M. Lehn, D. J. Cram and C. J. Pedersen are considered the founding fathers of Supramolecular Chemistry and the great importance of their job was universally recognized in 1987 when they received the Nobel Prize for their fundamental contributions to the development of this new area inside chemistry. According to Dr. Lehn, who introduced the term, a *supermolecule* is an organized complex entity that is created from the association of two or more chemical species held together by intermolecular forces, whereas the term *supramolecular chemistry* may be defined as "chemistry beyond the molecule", focusing on the organized entities of higher complexity that result from the association of two or more chemical species held together by intermolecular forces. [3]

The emergence of *supramolecular* chemistry has a deep effect on how efficiently chemists prepare structures of different sizes and shapes with dimension in the range of 1 to 100 nm. Molecules can be associated by their geometric or electronic affinity yielding supramolecular aggregates that presented new properties and characteristics that are very difficult to achieve by the isolated molecular entities. Due to this fact, incorporation of molecules onto materials offers new developments in the area of nanoscience and nanotechnology.

---

[1] Taylor & Francis Group, Encyclopedia of Supramolecular Chemistry, Vols. 1, 2 (Ed.: Atwood, J.L.; Steed, J.W.), LLC, New York, **2004**.

[2] K. Ariga, T. Kunitake, *Supramolecular Chemistry-Fundamentals and application*, Springer-Verlag Heidelberg.

[3] M. Lehn, Supramolecular Chemistry, Ed. VCH, 1995; J.-M. Lehn, Nobel lecture, **1987**.

1.2. Molecular Recognition and Sensing.

Molecular recognition is the basis of the supramolecular chemistry because the construction of any supramolecular aggregate involves selective molecular combination. In particular a molecular recognition event can take place only if a host molecule (or receptor) selectively interacts with a guest molecule (substrate) usually through non-covalent bonds.

In order to form a supermolecule, the receptor and guest must have mutual spatial and electronically complementary binding sites, or, in other words, they must follow the lock and key principle, (Figure 1) in which the guest has a geometric size or shape complementary to the receptor or host. This concept laid the basis for molecular recognition; i.e. the discrimination by a host between a number of different guests

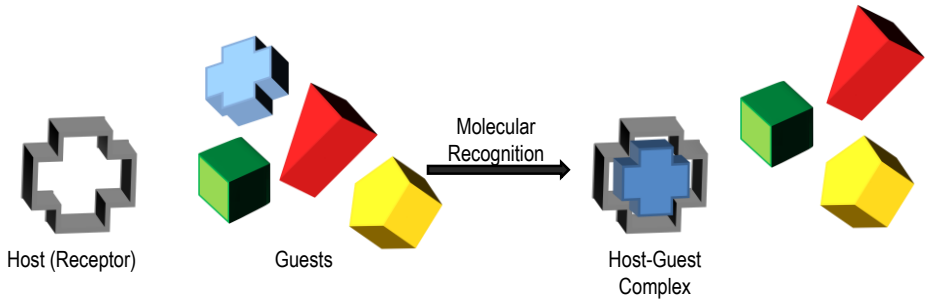

Figure 1. Scheme of a molecular recognition event by an specific host-guest interaction.

Bearing in mind this concept, in order to design a suitable receptor for a specific guest, some factors of the guest should be considered, as for example, the size, charge, geometry, hydrophilicity or lipophilicity or the possible formation of hydrogen bonds. On this basis, a myriad of receptors that mimic the behavior of biological systems have been described. These synthesized abiotic receptors are able to recognize cations, anions and neutral molecules.[4]

---

[4] a) M. D. Best, S. L. Tobey, E. V. Anslyn, *Coord. Chem. Rev*., **2003**, *240*, 3. b) J. M. Llinares, D. Powell, K. Bowman-James, *Coord. Chem. Rev*., **2003**, *240*, 57. c) K. A. Schug, W. Lindner, *Chem. Rev*., **2005**, *105*, 67. d) J. Yoon, S. K. Kim, N. J. Singh, K. S. Kim, *Chem. Soc. Rev*., **2006**, *35*, 355. e) P. Blondeau, M. Segura, R. Pérez-Fernández, J. de Mendoza, *Chem. Soc. Rev*., **2007**, *36*, 198. f) Z. Xu, S. K. Kim J. Yoon, *Chem. Soc. Rev*., **2010**, *39*, 1457. g) J. W. Steed, Chem. Soc. Rev., **2009**, 38, 506. h) V. Amendola, L. Fabbrizzi, Chem. Commun., **2009**, 513.

Molecular recognition chemistry is closely related with the concept of chemical sensing. A *chemosensor* is a molecule or supermolecule that recognizes and interacts with a specific analyte producing a detectable signal wich reveals the presence of the guest[5]. The signals most widely used to detect the presence of guest molecules are changes in color, fluorescence or modulations in the electrochemical properties of the host. In this sensing process, information at the molecular level, such as the presence or not of a certain guest in solution, is amplified to a macroscopic level; hence, molecular sensing opens the door to the determination (qualitative or quantitative) of certain guests.[6] In this sense, one interesting goal in the development of sensors deals with the synthesis of highly selective systems. Reversibility and fast response will be also appealing features for an applicable sensor to be taken into account in its design.

Thus, a chemical sensor must be featured by the presence of two fundamental subunits:

- ***Receptor unit*** that grants the specificity of the interaction with a particular analyte and allows the sensor to discriminate between a number of different substrates

- ***Signaling unit*** whose function is to transduce the recognition event into a measurable signal related to the concentration of the analyte.

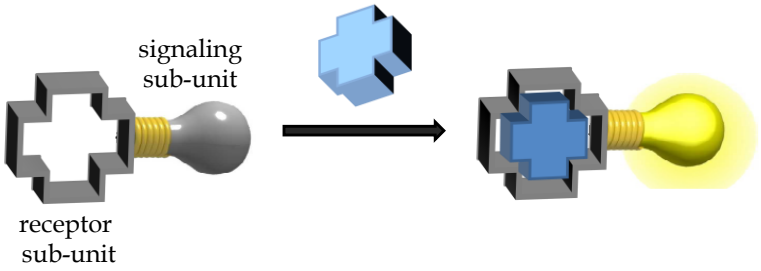

Figure 2: Schematic representation of the mechanism of a chemosensor**.**

Chromo-fluorogenic sensors offers significative advantages over other analytical detection methods such as: no need a sample pretreatment, non-

[5] W. C. Rogers, M. O. Wolf, Coord. *Chem. Rev*., **2002**, 233, 341.

[6]a) R. Martínez-Máñez, F.Sancenón, *Chem. Rev*., **2003**, 103, 4419. b) M.Moragues, R.Martínez-Mañez, F. Sancenón, *Chem. Soc. Rev*., **2011**, 40, 2593.

destructive detection method, uses of simple and extended instrumentation need of small amounts of samples and, in some cases, *in situ* detection and in real-time measurements. Colorimetric sensors induced noticeable color changes, observable with the naked eye, and can be used for rapid qualitative determinations. On the other hand, fluorogenic sensors have a high degree of sensitivity and specificity due to the possibility of specifying excitation and emission wavelengths, and normally allow achieving lower detection limits when compared with colorimetric techniques.

Practically, all the reported examples of chromo-fluorogenic chemosensors described in the literature are constructed by the application of one of the three main approaches described below (see also Figure 3):

- Binding site–signalling subunit approach: in the chemosensors constructed using this approach the "binding site" and the "signaling subunit" are linked through covalent bonds. The interaction of a target molecule with the binding site changes the electronic properties of the signaling subunit (a dye or a fluorophore) resulting in a sensing event via color or emission modulation.[7]

- The displacement approach: In this approach the binding site and the signaling subunit are not covalently bonded but forming a molecular ensemble. The sensing paradigm relies on a displacement reaction: the coordination of the target molecule with the binding site induces the release of the signalling subunit. An optical response is obtained because the color or emission of the signaling subunit in the sensing ensemble is different from those presented when it is free in solution.[8]

- The ''chemodosimeter'' approach: This approach takes advantage of target induced irreversible chemical reactions that generate fluorescence or color changes.[9]

---

[7] a) T. Gunnlaugsson, M. Glynn, G. M. Tocci, P. E. Kruger, F. M. Pfeffer, *Coord. Chem. Rev*., **2006**, 250, 3094. b) V. Amendola, D. Esteban-Gómez, L. Fabbrizzi, M. Lichelli, *Acc. Chem. Res*., **2006**, 39, 343. c) T. Gunnlaugsson, H. D. P. Ali, M. Glynn, P. E. Kruger, G. M. Hussey, F. M. Pfeffer, C. M. G. Dos Santos, J. Tierney, *J. Fluoresc*., **2005**, 15, 287.

[8] a) S.L. Wiskur, H.Ait-Haddou, J.J. Lavagne, E. V.Anslyn, *Acc, Chem. Res*., **2001**, 34, 963. b) B. T. Nguyen, E. V. Anslyn*, Coord. Chem. Rev*., **2006**, 250, 3118.

[9] Z. Yu, X.Chen, H.N. Kim, J. Yoon, *Chem. Soc. Rev*. **2010**, 39, 127-137.

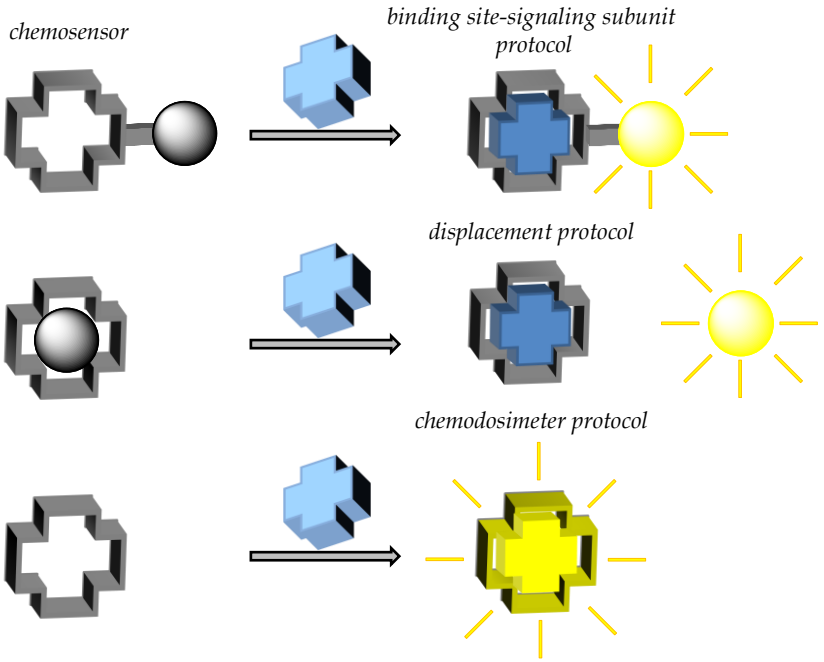

Figure 3: Schematic representation of the three three main approaches operation of a chemosensor.

Scientists working in the field of supramolecular chemistry are interested in the topology and arrangement of functional groups within molecules, always with the same aim: to improve the properties (such as selectivity) of these molecular devices.[10] For this aim, *translocation* (changes in the relative positions of molecules or ions in a controlled fashion) or *self-assembly processes* (where simple structural molecular units self-organize to yield supermolecules of nano or micrometric dimensions with new properties) have been used in the design of new chemosensors. In addition, these concepts and processes have been applied for designing hybrid organic-inorganic materials for their use in signalling applications. These hybrid organic-inorganic materials have been constructed by the anchoring of certain molecular receptors on the surface of selected 2D or 3D inorganic scaffoldings.

[10] P. D. Beer, P. A. Gale*, Angew. Chem. Int. Ed*., **2001**, 40, 486.

1.3 Organic-inorganic hybrid materials.

Within the area of receptor-guest interactions, the development of materials by assembling organic compounds (receptor) into nanoscopic inorganic materials (support) can lead to hybrid solids with considerably attractive properties different; (and often better); than those of isolated components.[11] The main advantages of anchoring receptors by covalent bonding on inorganic supports are the following:

- Molecular sensors can be organized into the inorganic surfaces in a monolayer (depending of the functionalization degree), improving the recognition process due to the restriction in movement on the solid.

- Modulation of the properties of the hybrid material by multifunctionalization in successive steps.

- Reusability of the system. If the host-guest interaction processes are reversible, the material could be reused several times, without losing its chemical recognition properties.

- Avoid leaching processes of the signaling units.

These heterogenous materials are usually easy to handle.[12] Furthermore, the possibility of controlling size, shape and surface area, can provide interesting changes on the physical and chemical properties of the inorganic surface, improving selectivity and sensitivity.[13]

---

[11] *The supramolecular chemistry of organic-inorganic hybrid materials*, Ed. K. Rurack, R. Martínez-Máñez, **2010**, Wiley.

[12] C. Sánchez, *J. Mater. Chem*., **2005**, 15, 3557.

[13] a) A. Verma, V. M. Rotello, *Chem. Commun*., **2005**, 3, 303. b) U. Drechsler, B. Erdogan, V. M. Rotello, Chem. Eur. J., 2004, 10, 5570. c) A. B. Descalzo, R. Martínez-Máñez, F. Sancenón, K. Hoffmann, K. Rurack, *Angew. Chem. Int. Ed*., **2006**, 45, 5924. d) F. Mancin, E. Rampazzo, P. Tecilla, U. Tonellato, Chem. Eur. J., 2006, 12, 1844. e) I. Willner, B. Basnar, B. Willner, *Adv. Funct. Mater*., **2007**, 17, 702.

1.4. Gold Nanoparticles in molecular sensing.

Detection of chemical and biological agents plays a fundamental role in biomedical, forensic and environmental science[14] as well as in anti-bioterrorism applications.[15] The development of highly sensitive, cost-effective; miniature sensors requires advanced technology coupled with fundamental knowledge in chemistry, biology, and material sciences.[16]

In general, chemical sensors feature two functional components: a ***recognition unit*** to provide selective/specific binding with the target analytes and a ***transducer component*** for signaling the binding event. An efficient sensor relies heavily on these two components for the recognition process in terms of response time, selectivity, and limits of detection (LOD).[17]

Designing sensors with higher efficacy depends on the development of novel materials to improve both the recognition and transduction processes. Nanomaterials feature unique physicochemical properties that can be of great utility in creating new recognition and transduction processes for chemical and biological sensors.

Gold nanoparticles (AuNPs) possess distinct physical and chemical attributes that make them excellent scaffolds for the fabrication of novel chemical and biological sensors[18] (Figure 4).

[14] a) Diamons, D. *Principles of Chemical and Biologial Sensors*; John Wiley & Sons, Inc.: New York, NY**, 1998**. b) Sadik, O. A.; Land, W.H.; Wang, J. *Electroanalysis* **2003**, 15, 1149. c) El-Sherif, M.; Bansal, L.; Yuan, J. M. *Sensors*, **2007**, 7, 3100. d) Sapsford, K.E.; Bradburne, C.; Detehanty, J.B.; Meditz,I. L. *Mater Today*, **2008**,11,38.

[15] a) Burnworth,M.; rowan, S. J.; Weder, C. *Chem Eur. J*, **2007,** 13, 7828. b) Paddle, B. M. *Biosens. Bioelectron*., **1996**, 11, 1079. c) Rusell, A. J.; Berberich, J. A.; Drevon, G. E.; Koepseñ, R.R. *Annu. Rev. Biomed. Eng.,* **200**3, 5, 1.

[16] a) De, M.; Ghosh, P. S.; Rotello, V. M. *Adv Mater* **2008**, 20, 4225. b) Anslyn, E. V.; Rotello, V. M *Curr. Opin. Chem. Biol*. **2010**, 14, 683.

[17] a) Anker, J. N.; Hall, W. P.; Lyandres, O.; Shah, N. C.; Zhao, J.; Van Duyne, R. P. *Nat. Mater*., **2008**, 7, 442 b) Shipway, A. N.; Katz, E.; Willner, I. *ChemPhysChem* **2000**, 1, 18

[18] a) Boisselier, E.; Astruc, D. *Chem. Soc. Rev*. **2009**, 38, 1759. b) Daniel, M. C.; Astruc, D. *Chem. Rev*. **2004**, 104, 293 c) Zhao, W.; Brook, M. A.; Li, Y. F. *ChemBioChem* **2008**, 9, 2363 d) Bunz, U. H. F.; Rotello, V. M., *Angew. Chem., Int. Ed*. **2010**, 49, 3268

- AuNPs can be synthesized in a straightforward manner and can be made highly stable

- They possess unique optoelectronic properties which can be easily tuned by varying their size, shape, and the chemical environment.

- They provide high surface/volume ratio with excellent biocompatibility using appropriates ligands.[19]

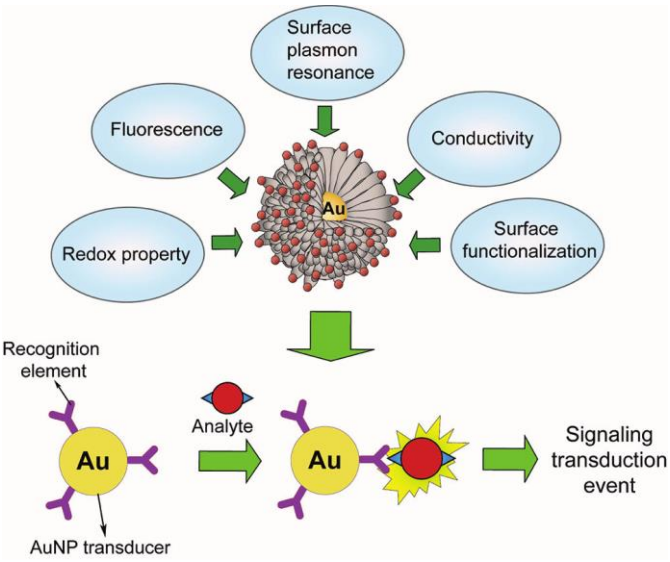

Figure 4: Physical properties of AuNPs and schematic illustration of a AuNP-based detection system

AuNPs offer a suitable platform for multifunctionalization with a wide range of organic ligands for the selective binding and detection of small molecules and biological targets.[20]

Each of these properties has allowed the development of novel sensing strategies with improved sensitivity, stability and selectivity.

---

[19] Daniel, M. C.; Astruc, D. *Chem. Rev.* **2004,** 104, 293

[20] a) Haick, H. *J. Phys. D: Appl. Phys* **2007**, 40, 7173. b) Zayats, M.; Baron, R.; Popov, I.; Willner, I. *Nano Lett***. 2005**, 5, 21. c) Radwan, S. H.; Azzazy, H. M. E. *Expert Rev. Mol. Diagn*. **2009**, 9, 511.

1.4.1 Synthesis of AuNPs and surface functionalization.

Numerous preparative methods for AuNPs synthesis have been reported, including both "top-down" (physical manipulation) and "bottom-up" (chemical transformation) approaches. During the last two decades, considerable effort has been developed to synthesis of AuNPs, focusing on control over the size, shape, solubility, stability, and functionality. It is worth noting that the term colloid and cluster are frequently used interchangeably; the former generally refers to particles having diameters more than 10 nm, while the latter commonly refers to smaller particles. The most extended methods to generate AuNPs are:

- ***Citrate –based preparation methods.***

The preparative synthesis of colloidal gold can be traced back to Michael Faraday's work in 1857, in which the gold hydrosols were prepared by reduction of an aqueous solution of chloroaurate with phosphorus dissolved in carbon disulfide.

Turkevich et al developed a synthetic method for creating AuNPs in 1951 by treating hydrogen tetrachloroaurate ($HAuCl_4$) with citric acid in boiling water, where the citrate acts as both reducing and stabilizing agent.[21] Frens further refined this method by changing the gold/citrate ratio to control the particle size.[22] This protocol has been widely employed to prepare dilute solutions of moderately stable spherical AuNPs with diameters from 10 to 20 nm, though larger AuNPs (e.g, 100 nm) can also be prepared. These citrate-stabilized AuNPs can undergo irreversible aggregation during functionalization processes with thiolated ligands. Several strategies have been developed to conquer this problem including the use of a surfactant, Tween 20, prior to the modification to prevent aggregation, or using thioactic acid as an intermediate via a two-step functionalization.[23]

[21] J. Turkevich, P. C. Stevenson and J. Hillier, *Discuss. Faraday Soc*., **1951**, 11, 55–75.
[22] G. Frens, *Nature: Phys. Sci*., **1973**, 241, 20–22.
[23] S. Y. Lin, Y. T. Tsai, C. C. Chen, C. M. Lin and C. H. Chen, *J. Phys.Chem. B*, **2004**, 108, 2134–2139.

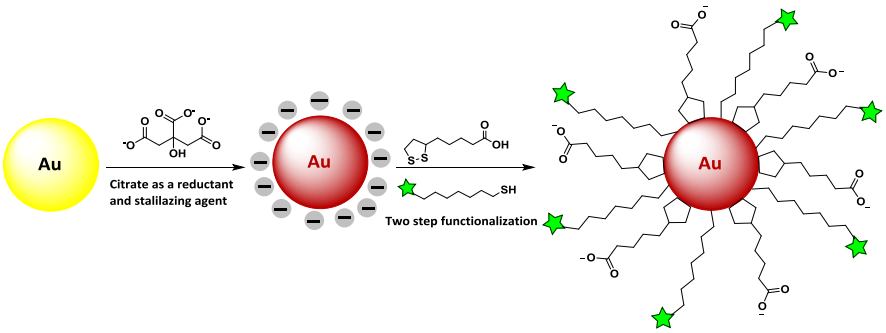

Figure 5: Representation of stabilizing synthesis of AuNPs by Turkevich method

❖ *The Brust-Schiffrin method for thiol –protected AuNPs.*

After Mulcaney's initial attempt of stabilizing AuNP with alkanethiols,[24] a significant breakthrough in the field of modified AuNP synthesis was achieved by Brust and Schiffrin in 1994. These authors reported a two-step synthetic strategy, using strong thiol-gold interactions to protect AuNPs with thiol ligands. In this method, $AuCl_4^-$ is transferred from an aqueous phase using to toluene using tetraoctylammonium bromide (TOAB) as a surfactant, and then reduced by sodium borohydride ($NaBH_4$) in the presence of dodecanethiol.[25] On addition of $NaBH_4$, a quick color change from orange to deep brown takes place in the organic phase. The AuNPs are generated in toluene with controlled diameters in the range of 1.5-5 nm. These thiol-protected AuNPs feature superior stability because of the strong thiol-gold interaction and they can be easily handled, characterized, and functionalized. The nanoparticles can be thoroughly dried and then re-dispersed in organic solvents without any aggregation or decomposition process observed.

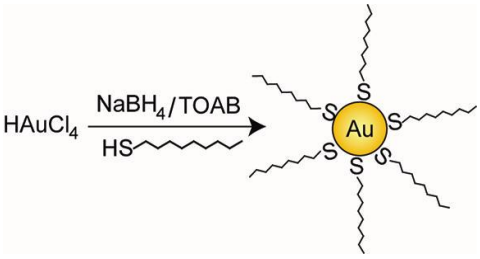

Figure 6: Representation of Brust-Schiffrin synthesis of AuNPs

---

[24] Giersig, M.; Mulvaney, P. *Langmuir* **1993**, 9, 3408.

[25] Brust, M.; Walker, M.; Bethell, D.; Schiffrin, D. J.; Whyman, R. J.*,Chem. Soc., Chem. Commun*. **1994**, 801

1.4.2 Properties of gold nanoparticles

Spherical AuNPs possess useful attributes such as size and shape related optoelectronic properties,[26] large surface volume/ratio, excellent biocompatibility; and low toxicity.[27] These properties make AuNPs an important tool in bionanotechnology (Table 1).

Table 1: Properties of AuNPs and their area of application.[28]

Properties	Application Data
Redox activity	Electronic devices and electrochemical sensing
Raman scattering (SERS)	
Surface plasmon resonance (SPR)	Colorimetric sensing and photothermal therapy
Fluorescence quenching	Sensor fabrication and material science

Among the most important optoelectronic properties of AuNPs includes surface plasmon resonance (SPR) absorption bands and their ability to quench fluorescence. Spherical AuNPs exhibit a range of colors (e.g., brown orange, red and purple) in aqueous solution as the core size increases from 1 to 100 nm, and generally show a size relative absorption peak from 500 to 550 nm.[29] This absorption band rises from the collective oscillation of the conduction electrons due to the resonant excitation by the incident photons (**Figure 7**) which is called "surface plasmon band".[30]

[26] a) T. K. Sau, A. L. Rogach, F. Jaeckel, T. A. Klar and J. Feldmann, *Adv. Mater*., **2011**, 22, 1805–1825; b) M. Hu, J. Chen, Z.-Y. Li, L. Au, G. V. Hartland, X. Li, M. Marquez and Y. Xia, *Chem. Soc.Rev.*, **2006**, 35, 1084-1094.

[27] a) N. Khlebtsov and L. Dykman, *Chem. Soc. Rev*., **2011**, 40, 1647– 1671; b) C. J. Murphy, A. M. Gole, J. W. Stone, P. N. Sisco, A. M. Alkilany, E. C. Goldsmith and S. C. Baxter, *Acc. Chem. Res.*, **2008**, 41, 1721–1730.

[28] Yi-C. Yeh, B. Creran and V. M. Rotello*Nanoscale*, **2012**, 4, 1871

[29] a) A. C. Templeton, W. P. Wuelfing and R. W. Murray, *Acc. Chem. Res*., **2000**, 33, 27–36; b) R. Hong, J. M. Fernandez, H. Nakade, R. R. Arvizo, T. Emrick and V. M. Rotello, *Chem. Commun*., **2006**, 2347–2349

[30] a) G. Mie, *Ann. Phys*., **1908**, 25, 377–445; b) A. C. Templeton, J. J. Pietron, R. W. Murray and P. Mulvaney*, J. Phys. Chem. B*, **2000**, 104, 564–570

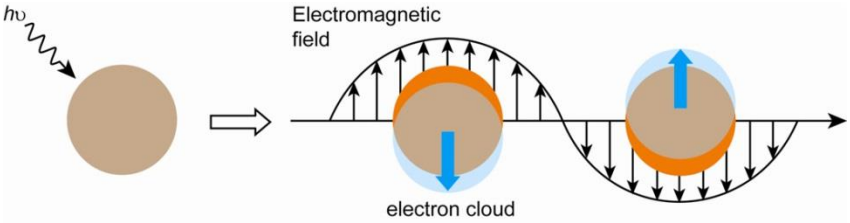

Figure 7: Schematic representation of the oscillation of conduction electrons across the nanoparticles in the electromagnetic field of the incident light.

This phenomenon is influenced not only by the size of the nanoparticles, but also by their shape, the solvent, the ligand on the surface, the core charge, temperature and even to the proximity of other nanoparticles.[31] The aggregation of nanoparticles results in significant red-shifting of the SPR frequency, broadening of surface plasmon band and changing the solution color from red to blue due to the interparticle plasmon coupling.[32] This phenomenon constitutes the cornerstone for their application in colorimetric sensing.

For the application of AuNPs in solution, it is not a trivial task to determine their concentrations.[33] The extinction coefficients of AuNPs with different sizes and capping ligands have also been measured experimentally.[34] A linear relationship is observed between logarithms of molar extinction coefficient (ε) and core diameter (*d*), essentially irrespective of the ligands and solvents:

$$\ln \varepsilon = k \cdot \ln d + c \qquad (\mathbf{1.1})$$

Where k =3.32 and c = 10.8 (λ = 506 nm). Therefore, the nanoparticles concentrations can be readily deduced from the Beer-Lambert Law once the nanoparticle size is known (from TEM). According to equation (1.1), it is estimated that AuNP of 20 nm diameter have a molar excitation coefficient of $1 \cdot 10^9$ M^{-1} cm^{-1}.

---

[31] a) F. Toderas, M. Baia, D. Maniu and S. Astilean, *J. Optoelectron. Adv. Mater*., **2008**, 10, 2282–2284; b) S. Srivastava, B. L. Frankamp and V. M. Rotello, *Chem. Mater*.**, 2005**, 17, 487–490; c) K. L. Kelly, E. Coronado, L. L. Zhao and G. C. Schatz, *J. Phys. Chem. B,* **2003**, 107, 668–677; (d) S. Link and M. A. El-Sayed, *Int. Rev. Phys.Chem*., **2000**, 19, 409–453

[32] K. H. Su, Q. H. Wei, X. Zhang, J. J. Mock, D. R. Smith and S. Schultz, *Nano Lett*., **2003**, 3, 1087–1090.

[33] Link, S.; Wang, Z. L.; El-Sayed, M. A., *J. Phys. Chem. B* **1999**, 103, 3529.

[34] Liu, X.; Atwater, M.; Wang, J.; Huo, Q., *Colloid Surf. B: Biointerfaces* **2007**, 58, 3-7.

This value is at least three orders higher than that of common organic dyes (10^4-10^6 M^{-1} cm^{-1}), indicating that AuNPs may serve as excellent light collectors.[35]

1.4.3 Colorimetric sensing

The aggregation of AuNPs of appropriate size (d > 3.5 nm) induces interparticle surface plasmon coupling, resulting in a visible color change from red to blue at nanomolar concentrations.[36] The color change during AuNP aggregation (or redispersation of an aggregate) provides a practical platform for absorption-based colorimetric sensing of any target analyte that directly triggers the AuNPs aggregation or redispersion.[37] Some examples of the use of functionalized AuNPs as sensor through an aggregation-disaggregation process are described below:

- ***Alkali and Alkaline Earth Metal Ions.***

AuNPs-based colorimetric sensing for metal ions generally requires the incorporation of chelating agents onto the nanoparticles surface. The presence of analyte ion induces the nanoparticle aggregation by forming multidentate interparticle complexes. For instance, AuNPs carrying 15-crow-5 moieties have been fabricated for the colorimetric detection of potassium ions (K^+). This sensor system showed micromolar recognition and colorimetric response toward K^+ even in the presence of physiologically important cations, such as Li^+, Cs^+, NH_4^+, Mg^{2+}, Ca^{2+} and excess Na^+.[38]

[35] a) Kamat, P. V.; Barazzouk, S.; Hotchandani, S. *Angew. Chem., Int.Ed*. **2002**, 41, 2764. b) Thomas, K. G.; Kamat, P. V. *Acc. Chem. Res*. **2003**, 36, 888.

[36] Srivastava, S.; Frankamp, B. L.; Rotello, V. M., *Chem. Mater*, **2005**, 17, 487.

[37] a) Rosi, N. L.; Mirkin, C. A. *Chem. Rev*. **2005**, 105, 1547; b) Jiang, Y.; Zhao, H.; Lin, Y. Q.; Zhu, N. N.; Ma, Y. R.; Mao, L. Q. *Angew. Chem., Int. Ed*. **2010**, 49, 4800

[38] Lin, S. Y.; Liu, S. W.; Lin, C. M.; Chen, C. H. *Anal. Chem*., **2002**, 74, 330.

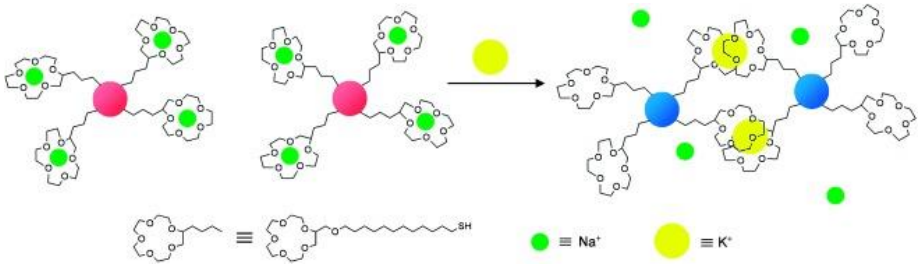

Figure 8: Schematic depiction of red to blue color colorimetric sensing of metal ions using AuNPs functionalized with chelating ligands.

- ***Detection of anions.***

Fast and sensitive detection of CN^- is important for environmental monitoring and the evaluation of food safety. Han et al. reported a colorimetric detection for cyanide anions in aqueous solution employing adenosine triphosphate-stabilized AuNPs and a Cu^{2+}-phenantroline complex as the receptor unit.[39] In their sensing ensemble, exposure CN^- to Cu^{2+}-phenantroline complex induced a decomplexation process to generate free phenantroline, wich subsequently caused the ATP-stabilized AuNPs to aggregate resulting in color change. This system detected concentrations of 10^{-5} M CN^- in neutral aqueous solution

Figure 9: Schematic representation of colorimetric sensing of cyanide anion in aqueous solution employing triphosphate stabilized AuNPs.

[39] Kim, M. H.; Kim, S.; Jang, H. H.; Yi, S.; Seo, S. H.; Han, M. S.*Tetrahedron Lett*. **2010**, 51, 4712.

- ***Detection of small molecules.***

2,4,6-Trinitrotoluene (TNT) is a leading example of a nitroaromatic explosive with significant detrimental effects on the environment and human health. Cysteamine was used both as the primary amine and as the stabilizer for AuNPs to facilitate the donor-acceptor interaction between TNT and cysteamine leading to aggregation, and a change in the color of the suspension to violet bue.[40]

The clear change in the color of the suspension could be used for the direct colorimetric visualization of TNT. As such a color change can be readily seen by the naked eye, the method demonstrated herein is relatively simple and does not requires the use of expensive instrumentation.

This simple assay for the direct colorimetric visualization of TNT by inducing aggregation, changed the color from red to blue. The limit of detection was found to be in the concentration range from $5 \cdot 10^{-9}$ M to $5 \cdot 10^{-13}$ M

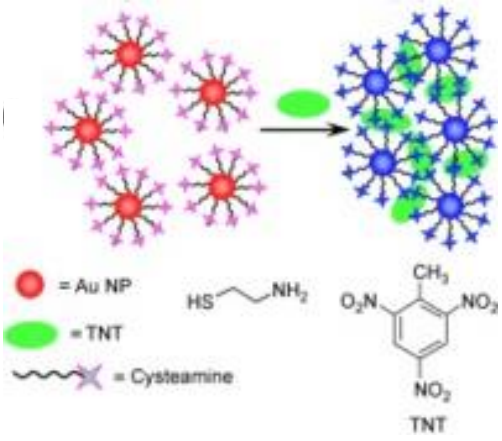

Figure 10: Assay for direct colorimetric visualization of TNT based on the D-A interaction between TNT and cysteamine at the AuNP solution interface.

[40] Jiang, Y.; Zhao, H.; Zhu, N. N.; Lin, Y. Q.; Yu, P.; Mao, L. Q. *Angew. Chem., Int. Ed*. **2008**, 47, 8601-8603.

CHAPTER 2:
Detection of Nerve Agents

2.1 Introduction

Nerve Agents

In the modern era, chemicals warfare agents have been divided into five categories: nerve agents, vesicants, choking agents, blood agents, and incapacitants.[41,42] The development of chemical-warfare agents during the Second World War led to the so-called "nerve agents", which are fast-acting poisons that attack the nervous system. Among chemical-warfare agents, nerve agents are extremely dangerous and their high toxicity and ease of production underscore the need to detect these lethal chemicals via quick and reliable procedures.

Nerve agents are capable of interfering with the action of the nervous system. Their primary mode of action is the inhibition of acetylcholinesterase, resulting in acetylcholine accumulation in the synaptic junctions that hinders muscles from relaxing.[43]

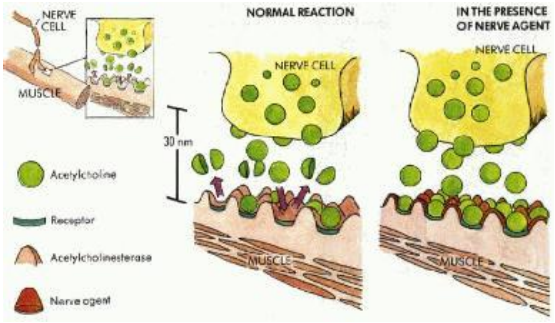

Figure 1: The effect of the nerve agents is to inhibit the hydrolysis of acetylcholine resulting in a buildup of acetylcholine in the synaptic cleft.

Nerve agents have been studied extensively due to their rapid and severe effects on human and animal health systems.[44]. Intoxication with nerve agents may

[41] O. A. Sadik , W. H. Land , J. Wang , *Electroanalysis*, **2003** , 15 , 1149

[42] a) W. S. Augerson , Chemical and Biological Warfare Agents , A Review of the Scientifi Literature as it Pertains to Gulf War Illnesses , Vol. 5 , RAND , Santa Monica, CA **2000** ; b) D. R. Walt , D. R. Franz , *Anal. Chem*, **2000**, 72, 738A.

[43] S. M. Somani, Chemical Warefare Agents, Academic Press, San Diego**, 1992**.

[44] a) A. Silver , *The Biology of Cholinesterases* , Elsevier , New York **1974** ,p 449 ; b) Goodman and Gilman's *The Pharmacological Basis of Therapeutics*, 10th ed. (Eds: J. G. Hardman , L. E. Limbird , A. Goodman Gilman), McGraw–Hill , New York **2001**

occur by inhalation, contact with skin, or through the intake of contaminated foods or liquids. After intoxication, nerve agents irreversibly bind to a free serine residue of acetylcholinesterase to inhibit its enzymatic function.[45]

Chemically, nerve agents are highly toxic phosphoric acid ester, which are structurally related to the larger family of organophosphate compounds. There are two main classes of nerve agents: the G series and the V series.

The G-series have a fluoride (F^-) or cyanide (CN^-) as a leaving group and the V-series have a thiolate as a leaving group. The nerve gas mimics diethylcyanophosphonate (DCNP), diethylchlorophosphate (DCP) and diisopropylfluorophosphate (DFP) are normally used in laboratory detection studies as they are compounds that show the same reactivity as the real nerve agent, but lack their severe toxicity.

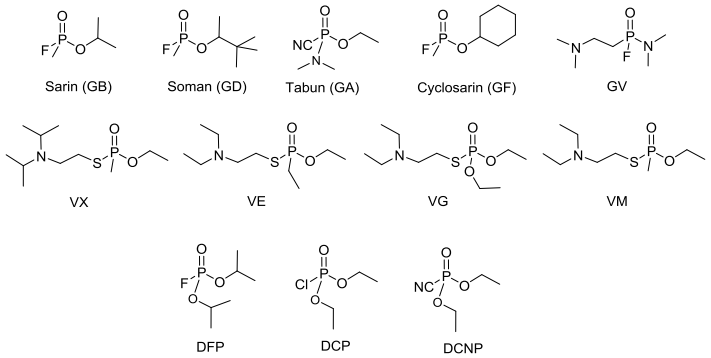

Figure 2: Principal nerve agent and nerve agent simulants.

The covalent binding of acetylcholinesterase to the nerve agents is carried through an S_N2 reaction: a hydroxyl group (-OH) of a serine residue of acetylcholinesterase attacks the electrophilic phosphorous atom of the nerve agent to displace F^- or CN^- (depending on the nerve agent used) as a leaving group.

[45] M. B. Colovic, D. Z. Krstic, T. D. Lazarevic-Pasti, A. M. Bondzic and V. M. Vasic., *Curr Neuropharmacol*., **2013**, 11, 315-335.

The electrophilic character of the phosphorous atom determines the stability of the agent since highly reactive nerve agents can be less persistent. The resulting product of hydrolysis is a non-toxic phosphoric acid derivative.

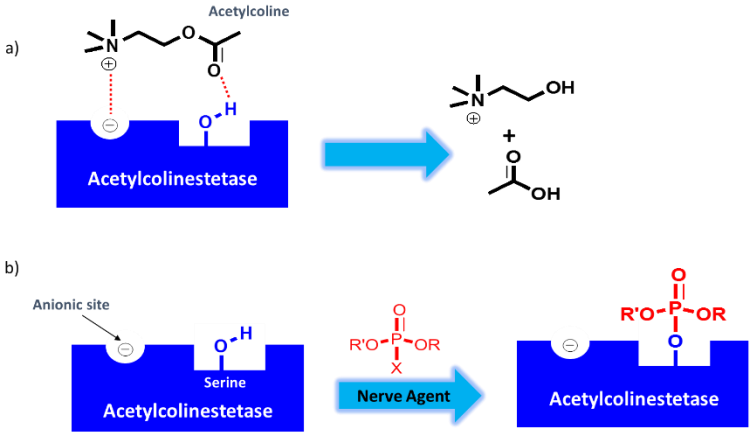

Figure 3: Acetylcholinesterase representation: a) enzymatic reaction with acetylcholine and b) inhibition mechanism mediated by nerve agents.

An intense research effort has been directed to develop sensitive and selective systems for detection of these compounds. Current methods for nerve-agents monitoring are mainly based on the use of biosensors,[46] ion-mobility spectroscopy (IMS), electrochemistry,[47] microcantilevers,[48] photonic crystals,[49] and optical-fiber arrays.[50] As an alternative to these instrumental methods, the

[46] a) M. T. McBride, S. Gammon, M. Pitesky, T. W. O'Brien, T. Smith, J. Aldrich, R. G. Langlois, B. Colston, K. S. Venkateswaran, *Anal. Chem*., **2003**, 75, 1924; b) A. J. Russell, J. A. Berberich, G. F. Drevon, R. R. Koepsel, *Annu. Rev. Biomed. Eng*., **2003**, 5, 1. c) H. Wang, J. Wang, D. Choi, Z. Tang, H. Wu, Y. Lin, *Biosens. Bioelectron*. **2009**,24, 2377

[47] a) M. A. K. Khan, Y. T. Long, G. Schatte, H. B. Kraatz, *Anal. Chem*., **2007**, 79, 2877; b) O. V. Shulga, C. Palmer, *Anal. Bioanal. Chem*., **2006**, 385, 1116; c) J. C. Chen, J. L. Shih, C. H. Liu, M. Y. Kuo, J. M. Zen, *Anal. Chem*., **2006**, 78, 3752; d) G. Liu, Y. Lin, *Anal. Chem*., **2006**, 78, 835.

[48] a) G. Zuo, X. Li, P. Li, T. Yang, Y. Wang, Z. Chen, S. Feng, *Anal. Chim. Acta* **2006**, 580, 123; b) C. Karnati, H. Du, H. F. Ji, X. Xu, Y. Lvov, A. Mulchandani, P. Mulchandani, W. Chen, *Biosens. Bioelectron*., **2007**, 22, 2636; c) Q. Zhao, Q. Zhu, W. Y. Shih, W. H. Shih, *Sens. Actuators B,* **2006**, 117, 74.

[49] a) W. He, Z. Liu, X. Du, Y. Jiang, D. Xiao, *Talanta*, **2008**, 76, 698; b) J. P. Walker, K. W. Kimble, S. A. Asher, *Anal. Bioanal. Chem*., **2007**, 389, 2115; c) J. P. Walker, S. A. Asher, *Anal. Chem*., **2005**, 77, 1596.

[50] M. J. Aernecke, D. R. Walt, *Sens. Actuators B*, **2009**, 142, 464.

development of easy-to-use fluorogenic and chromogenic reagents has been gaining interest in recent years.[51] For instance, systems involving PET-based fluorescent probes,[52] assays using oximate-containing derivates[53] molecular imprinting polymers,[54] nanoparticles,[55] carbon nanotubes,[56] porous silicon,[57] or displacement-like procedures[58] have been recently reported. Most of these detection methods rely on changes in fluorescence properties, whereas few examples are related to color modulations.

For example, J. Xie and coworkers[59] reported, a simple colorimetric assay for the effective detection of organophosphorous (OP) nerve agents (GB, GD and VX) and highly toxic OP pesticide paraoxon with ultra-high sensitivity. In this method, stable lipoic acid (LA) capped gold nanoparticles (AuNPs) show an aggregation-induced change in the color (see chapter 1), from red to blue, in the presence of thiocholine (TCh), which is generated in situ by the enzymatic hydrolysis of acetylthiocholine (ATCh) by acethylcholinesterase (AChE). If there are OPs in the solution, the production of TCh is suppressed, and the AuNPs remain

---

[51] a) M. Burnworth, S. J. Rowan, C. Weder, *Chem. Eur. J*., **2007**, 13, 7828; b) S. W. Thomas III, G. D. Joly, T. M. Swager, *Chem. Rev.*, **2007**, 107, 1339; c) S. Royo, R. Martínez-Mañéz, F. Sancenón, A. M. Costero, M. Parra, S. Gil, *Chem. Commun*., **2007**, 4839; d) B. C. Giordano, G. E. Collins, Curr. *Org. Chem*., **2007**, 11, 255; e) G. J. Mohr, *Anal. Bioanal. Chem*. **2006**, 386, 1201;

[52] a) A. M. Costero, S. Gil, M. Parra, P. M .E. Mancini, R. Martínez-Máñez, F. Sancenon, S. Royo, *Chem. Commun*., **2008**, 6002. b) T.J. Dale and J. Rebek, *J. Am. Chem. Soc.*, **2006**, 128, 4500-4501.

[53] a) K. J. Wallace, J. Morey, V. M. Lynch and E. V. Anslyn, *New J. Chem*., **2005**, 29, 1469; b) K. J. Wallace, R. I. Fagbemi, F. J. Folmer-Andersen, J. Morey, V. M. Lynch and E. V. Anslyn, *Chem. Commun*., **2006**, 3886., c)F. Terrier, P. Rodríguez-Dafonte, E. Le Guével and G. Moutiers, *Org. Biomol. Chem*., **2006**, 4, 4352; H. S. Hewage, K. J. Wallace and E. V. Anslyn, *Chem. Commun*., **2007**,3909.

[54] a) A. L. Jenkins and S. Y. Bae, *Anal. Chim. Acta*, **2005**, 542, 32; b) G. E. Southard, K. A. Van Houten, E. W. Ott, Jr and G. M. Murray, *Anal. Chim. Acta*, **2007**, 581, 202; c) R. Shunmugam and G. N. Tew, *Chem.–Eur. J*., **2008**, 14, 5409

[55] a) V. Pavlov, Y. Xiao and I. Willner, *Nano Lett*., **2005**, 5, 649; b) L. Wang, K. D. Cole, A. K. Gaigalas and Y.-Z. Zhang, *Bioconjugate Chem*., **2005**, 16, 194.

[56] C. Y. Lee, R. Sharma, A. D. Radadia, R. I. Masel and M. S. Strano, *Angew. Chem. Int. Ed.*, **2008**, 47, 5018–5021

[57] a) S. Jang, Y. Koh, J. Kim, J. Park, C. Park, S. J. Kim, S. Cho, Y. C. Ko and H. Sohn, *Mater. Lett.*, **2008**, 62, 552–555. b) S. Jang, Y. Koh, J. Kim, K. Jung and H. Sohn, J. *Korean Phys. Soc*., **2009**, 55, 294–298

[58] D. Knapton, M. Burnworth, S. J. Rowan and C. Weder, *Angew. Chem., Int. Ed*., **2006**, 45, 5825.

[59] J. Sun , L. Guo , Y. Bao , J. Xie, *Biosensors and Bioelectronics*, **2011**, 28, 152-157.

well-dispersed and thus red colored. The basis of this signaling system is shown in Figure 4.

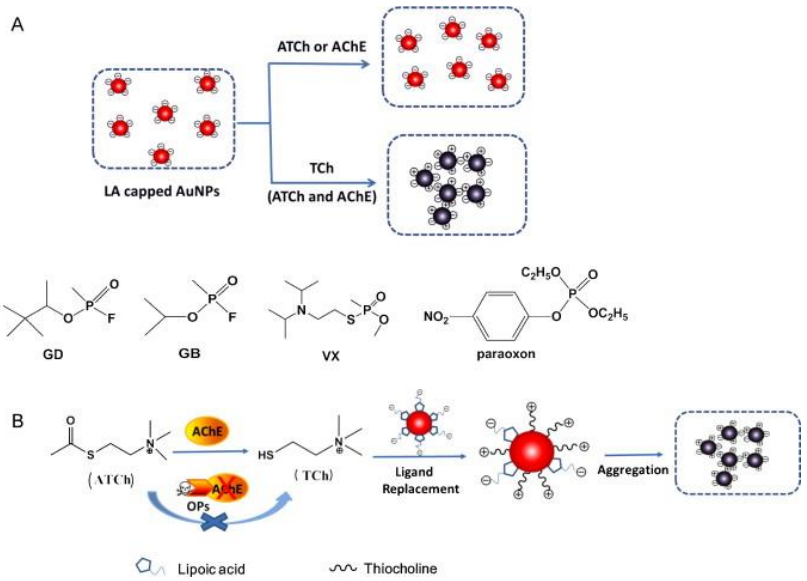

Figure 4: A) Thiocholine-induced aggregation of the LA capped AuNPs and chemical structures of investigated OPs, in which two are G-type (Sarin (GB) and Soman (GD)), one are V-type (VX), and one is a pesticide (paraoxon). B) Illustration of signaling strategy for OPs based on the AuNPs probe.

2.2. Strategies previously developed by Costeros´s group for the chromogenic detection of nerve agents.

In the last few years, our group has designed, and evaluated several chemodosimeters for the detection of nerve agents of the G series. Different transducing units were explored, including azopyridine derivates[60] and triarylcarbinols.[61]

2.2.1. Azo dyes derivatives

Studies have been published that indicate that aromatic amines such as pyridine can react with phosphates and phosphonates, containing a good leaving group such as nerve agents [62]

Our group reported a simple system that is able to colorimetrically respond to the presence of nerve-agent mimics, and in addition, capable of discriminating DCNP from other nerve agent mimics. [63] Chemosensor **I** is a push-pull azo dye containing a *N,N*-dimethylaniline donor group and a pyridine acceptor moiety electronically connected through an azo bridge.

The sensing strategy was based on the phosphorylation of the nitrogen of the pyridine unit to produce a change in the spectroscopic properties of the azo dye. If the piridine group was phosphorylated, this reaction would increase the electron-acceptor properties of the pyridine unit and grow the push-pull character of the chromophore producing a bathochromic shift of the absorption band,

---

[60] a) S. Royo, A. M. Costero,] M. Parra, S. Gil,R. Martnez-Mañez, and F. Sancenón., *Chem. Eur. J*., **2011**, 17, 6931–6934; b) H. J. Kim, J. H. Lee, H. Lee, J. H. Lee, J. H. Lee, J. H. Jung and J. S. Kim; *Adv. Funct. Mater*., **2011**, 4035-4040.

[61] (a) Gotor, R.; Royo, S.; Costero, A. M.; Parra, M.; Gil, S.; Martínez-Máñez, R.; Sancenón, F. *Tetrahedron*, **2012**, 68, 8612–8616; (b) Royo, S.; Gotor, R.; Costero, A. M.; Parra, M.; Gil, S.; Martínez-Máñez, R.; Sancenón, F. *New J. Chem*., **2012**, 38, 1485–1489; (c) Costero, A. M.; Parra, M.; Gil, S.; Gotor, R.; Martínez-Máñez, R.; Sancenón, F.; Royo, S. *Eur. J. Org. Chem*., **2012**, 4937–4946.

[62] (a) A. D. Guha, H. W. Lee, I. Lee, *J. Org. Chem*., **2000**, 65, 12; (b) N. Bourne, A. Williams, *J. Am. Chem. Soc*., **1984**, 106, 7591; (c) S. E. Pipko, L. V. Bezgubenko, A. D. Sinitsa, E. B. Rusanov, E. G. Kapustin, M. I. Povolotskii, V. V. Shadchak, *Heteroat. Chem*., **2008**, 19, 171. (d) Guha, A. K.; Lee, H. W.; Lee, I. *J. Chem. Soc., Perkin Trans. 2*, **1999**, 765.

[63] S. Royo, A. M. Costero,] M. Parra, S. Gil,R. Martnez-Mañez, and F. Sancenón., *Chem. Eur. J*., **2011**, 17, 6931–6934

whereas if the phosphorylation reaction takes place in the nitrogen of the aniline, the donor properties of the aniline decrease and an hypsochromic shift in the maximum absorption peak of the chromophore would be observed. This latter reaction was only observed in the presence of DCNP due to the release of CN^-.

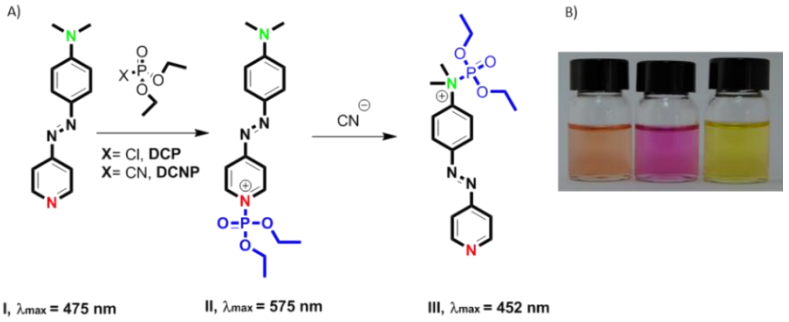

Figure 5: A) Phosphorilation reaction of chemosensor **I** with nerve agent mimics. λmax values observed in acetonitrile/water (25:75 v/v. pH 5.6). B) The colour change observed of chemosensor **I** (orange), in presence of DCP (pink) and DCNP (yellow).

The reactivity and signaling properties of 2-(2-(dimethylamino) phenyl) ethanol derivatives (**IV**) were also evaluated in nerve agent detection (see Figure 6). [64] This moiety contains a nucleophile, the hydroxyl group, which is known to undergo acylation reactions with phosphonate substrates to form intermediate **V** that suffers a rapid intramolecular N-alkylation to yield **VI**, a quaternary ammonium salt.[65] In order to design colorimetric probes the dimethylaminophenyl donor group was coupled with an acceptor moiety (A) to build up a push pull dye. The detection strategy is depicted in Figure 6. The conversion of the tertiary amine **IV** into the quaternary ammonium salt **VI** upon reaction with organophosphorus (OP) substrates dramatically changes the electronic donor properties of the nitrogen atom thus resulting in a decrease of the push–pull character of the dye and in a colour modulation.

[64] **a)** A**.** M. Costero, S**.** Gil, M**.** Parra, P**.** M. E. Mancini, R**.** Martínez-Máñez, F**.** Sancenón and S**.** Royo**,** *Chem. Commun*., **2008**, 6002-6004**.** b) A. M. Costero, ,S. Gil, R. Gotor, P**.** M. E. Mancini, R**.** Martínez-Máñez, F**.** Sancenón and S**.** Royo**, *Chem. Asian J.*,** 2010**, 5, 1573-1585.**

[65] T. J. Dale and J. Rebek, Jr, *J. Am. Chem. Soc*., 2006, 128, 4500.

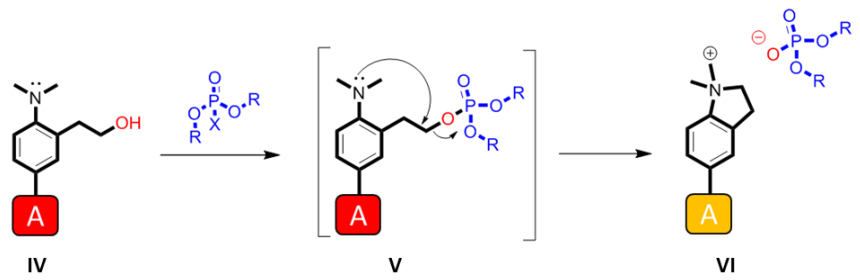

Figure 6: Colorimetric detection paradigm using 2-(2-(dimethylaminophenyl)ethanol containing puch-pull dyes.

2.2.2. Triaryl carbinol derivatives.

Another approximation for the chromogenic detection of nerve agents, developed by Costero's group, is based on the use of triaryl carbinols.[66] Triaryl carbinols can be converted into strongly colored triaryl carbonium dyes, by protonation or acylation of the hydroxyl group followed by an E1 process. The sensing protocol is shown is Figure 7. The hydroxyl group present in the carbinols (**VII**) is able to experiment phosphorylation reactions with the nerve agent mimics to form the intermediates **VIII**, which easily undergoes an elimination reaction giving rise to the corresponding carbocation (**IX**). Transformation of **VII** into **IX** is concomitant with formation of a highly delocalized system that is responsible for a significant color modulation.[67]

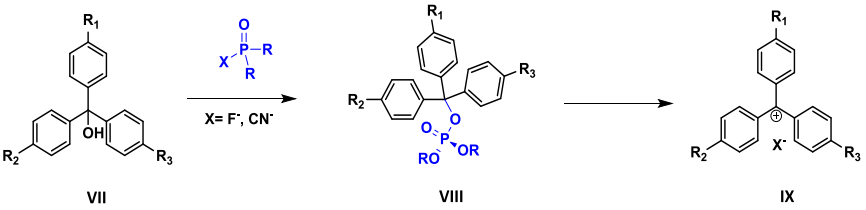

Figure 7: Mechanism of the chromogenic response of carbinols in the presence of warfare agent simulants.

---

[66] R. Gotor, A. M. Costero, S. Gil, M. Parra, R. Martínez-Máñez and F. Sancenón, *Chem Eur J*, 2011, 17, 11994.

[67] S. Royo, R. Gotor, A. M. Costero, M. Parra, S. Gil, R. Martínez-Máñez and F. Sancenón, *New J. Chem*., **2012**, 36, 1485-1489

2.3. Objectives

The main goal of this chapter is the design, synthesis and evaluation of new chemodosimetes for the colorimetric detection of nerve agent mimics, based on the use of gold nanoparticles as a traducer unit, and azopiridine, 2-(2-dimethylaminophenyl)ethanol and triaryl carbinol as receptor units.

In particular our aim were:

- ·To explore the capabilities of various derivatives bearing the previously cited moieties, (azopyridine, 2-(2-dimethylaminophenyl)ethanol, and triaryl carbinol), as reacting units towards nerve agents.

- To attach this compounds onto the surface of gold nanoparticles as a thioctic acid derivatives.

- To evaluate the response of these functionalized gold nanoparticles in solution in front of the nerve agent mimics DCP, DCNP and DFP.

2.4. Functionalized Gold Nanoparticles as an approach to the Direct Colorimetric Detection of DCNP Nerve Agent Simulant.

Functionalized Gold Nanoparticles as an approach to the Direct Colorimetric Detection of DCNP Nerve Agent Simulant

Almudena Martí,[a,b] Ana M. Costero,[a,b] Pablo Gaviña,*[a,b] Salvador Gil,[a,b] Margarita Parra,*[a,b] Mauro Brotons-Gisbert,[c] and Juan Francisco Sánchez-Royo[c]

[a] Centro de Reconocimiento Molecular y Desarrollo Tecnológico (IDM), Unidad Mixta Universidad de Valencia-Universidad Politécnica de Valencia, Valencia, Spain Fax: +34-963543151 E-mail: pablo.gavina@uv.es margarita.parra@uv.es Homepage: http://www.uv.es/idm

[b] Departamento de Química Orgánica, Universidad de Valencia, c/ Dr. Moliner 50, 46100 Burjassot, Valencia, Spain Homepage: http://www.uv.es

[c] Instituto de Ciencia de los Materiales, Universidad de Valencia, c/ Dr. Moliner 50, 46100 Burjassot, Valencia, Spain Homepage: http://www.uv.es

Received: 6th March 2013
Published online: 17th June 2013

Eur. J. Org. Chem., **2013**, 4770–4779.

Introduction

The use of chemical warfare (CW) agents in terrorist attacks has proven the need for the development of reliable and accurate methods for detecting these lethal compounds.[1] Among CW weapons, nerve agents are especially dangerous and the United Nations classifies them as weapons of mass destruction. Nerve agents are capable of interfering with the action of the nervous system. Their primary mode of action is the inhibition of acetylcholinesterase, resulting in an accumulation of acetylcholine in the synaptic junctions, which hinders the relaxing of muscles.[2]

Analytical methods based on enzymatic assays and physical measurements have generally been used to detect these agents.[3] However, these protocols usually have limitations, such as low selectivity, poor portability and a certain level of complexity. In recent years several chromo- and fluorogenic sensors and probes for nerve agents have been described.[4] Colorimetric detection is particularly appealing because it uses low-cost, widely available instruments and allows assays to be detected by the naked eye. Our research group has developed a new family of reagents for the chromogenic detection of the nerve agent simulants DFP, DCP and DCNP (Figure 1) based on the use of 2-[2-(dimethylamino)phenyl]ethanol reactive groups that are part of the conjugated π system of donor–acceptor dyes.[5] The nucleophilic hydroxy group of this moiety is easily phosphorylated by nerve agent simulants to give the intermediate **II** (Scheme 1, a), which undergoes rapid intramolecular *N*-alkylation to afford the quaternary ammonium salt **III**. The change in the electronic distribution promoted by these processes allows the colorimetric detection of DCP, DFP and DCNP, whereas the reagents remain silent in the presence of other organophosphorus derivatives. On the other hand, the nucleophilic reactivity of the pyridine moiety of a push–pull azo dye towards nerve gases has allowed us to develop off–on colorimetric sensors (Scheme 1, b).[6]

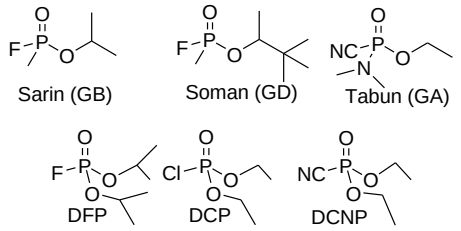

Figure 1. Chemical structures of different organophosphorus nerve reagents and their simulants.

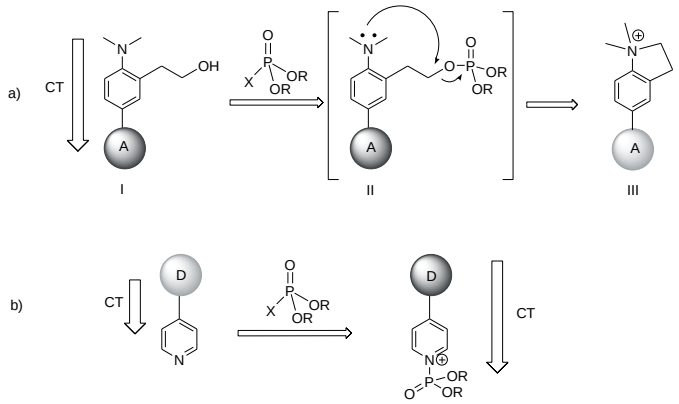

Scheme 1. Colorimetric sensing paradigm developed by our group

In both cases, the reaction between the probe and the simulant generates a positive charge on the molecule. Based on this fact, we focused on the study of the behavior of gold nanoparticles (AuNPs) functionalized with this type of moiety towards nerve agents. The functionalization of AuNPs has attracted research interest, especially in receptor-based sensor applications.[7] Gold nanoparticles have unique optoelectronic properties that can easily be tuned by changing their size, shape or chemical environment.[7–9] Colorimetric assays based on gold nanoparticles have recently become useful for many types of analytes without the need for advanced instrumentation because the molecular recognition events can be transformed into color changes.[10] The selective and sensitive strategy for sensing is based on the color change that arises from the interparticle plasmon coupling that occurs during aggregation of AuNPs or the dispersion of AuNP aggregates. The red color of dispersed nanoparticles turns to dark blue upon aggregation, and this color change can be observed by the naked eye even at low concentrations.[11] Thus, the generation of positive charges on the surfaces of dispersed functionalized anionic AuNPs as a result of their reaction with nerve agents will induce their aggregation with the concomitant color change.

Recently, the detection of highly toxic organophosphate pesticides by using thioctic acid capped AuNPs as colorimetric probes in an indirect strategy with very low detection limits has been described.[7c,12,13] In that research sensors were developed for the detection of thiocholine obtained by catalytic hydrolysis of acetylthiocholine by acetylcholinesterase. The ligand-exchange reaction between cationic thiocholine and the negatively charged thioctic carboxylate induces the aggregation of Au nanoparticles. The irreversible inhibition of acetylcholinesterase by the organophosphorus pesticides prevents aggregation and the red color of the Au nanoparticles remains.

Following a completely different approach, we report herein the results obtained in the direct detection of DCNP (as simulant of tabun) by using thioctic acid capped AuNPs functionalized with pyridines or 2-[2-(dimethylamino)phenyl]ethanol derivatives.

Results and Discussion

The sensing paradigm of the detection process, which is presented in Scheme 2, involves the generation of positive charges on the surfaces of the gold nanoparticles through the reactions of the terminal nucleophilic ligands with molecules of the nerve agent simulant. These positive charges partially neutralize the original negative charges of the nanoparticles, inducing their aggregation and thus a change in their surface plasmon resonance absorption and consequently a change in their color.

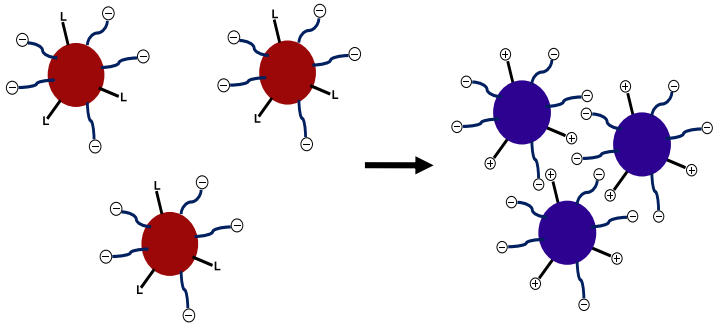

Scheme 2. Paradigm of the sensing mechanism. Reaction of the terminal ligands with the simulant produces positive charges that can compensate the negative charges of the AuNPs and induce aggregation processes.

Synthesis of the Ligands

AuNPs have affinity for both reduced (thiols) and oxidized (disulfide) sulfur groups through Au–S bonds, and thus both groups can be used as anchors for the functionalization of nanoparticles. The different ligands used in this study are presented in Figure 2.

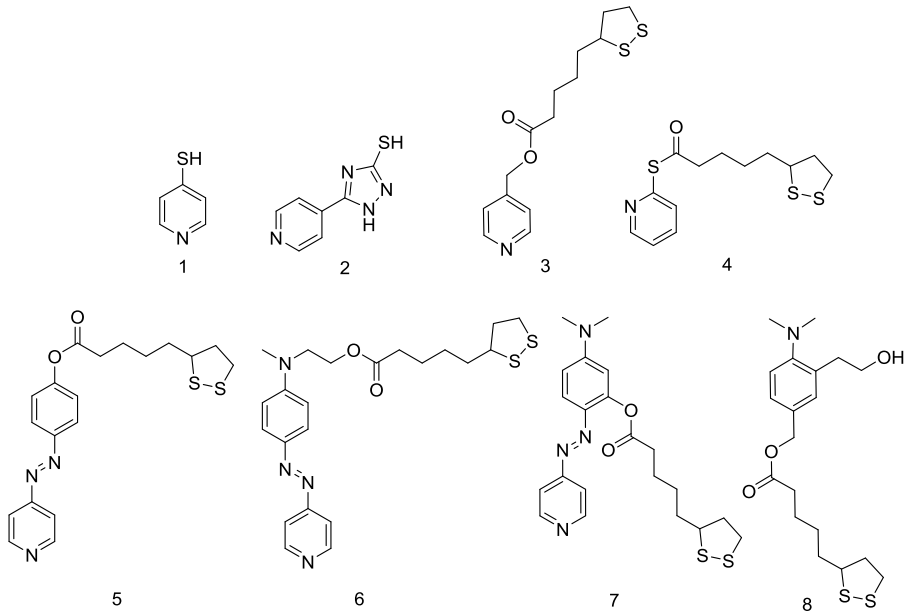

Figure 2. Ligands 1–8 synthesized for the functionalization of AuNPs.

Ligands **1** and **2** are commercially available, whereas **3** and **4** were obtained by the esterification of the corresponding alcohol or disulfide derivatives with thioctic acid (TA) under Steghich[14] or Mitsunobu[15] conditions. Ligands **5–7** were synthesized by an azo-coupling reaction between pyridine-4-diazonium (obtained from 4-aminopyridine by diazotization) and phenol, *N*-phenyl-*N*-methyl-2-aminoethanol or 3-(dimethylamino)phenol, respectively, followed by esterification with TA. Ligand **8** required a seven-step synthesis and is depicted in Scheme 3. Thus, 2-(2-nitrophenyl)ethanol (**9**) was reduced in the presence of formaldehyde to the corresponding dimethylamino derivative **10**. This amino compound was transformed into the 4-bromo derivative **11** by reaction with *N*-bromosuccinimide (NBS). Protection of the hydroxy group as a silyl ether yielded **12**, which was lithiated with BuLi and then transformed into the formyl derivative **13** by reaction with DMF. Compound **13** was subsequently reduced to the corresponding benzylic alcohol **14**. After esterification with thioctic acid and deprotection of the silyl-protected hydroxy moiety with *tert*-butylammonium fluoride (TBAF), ligand **8** was obtained in a 20 % overall yield. The chemical structures and purity of ligands **1–8** were confirmed by spectroscopic techniques

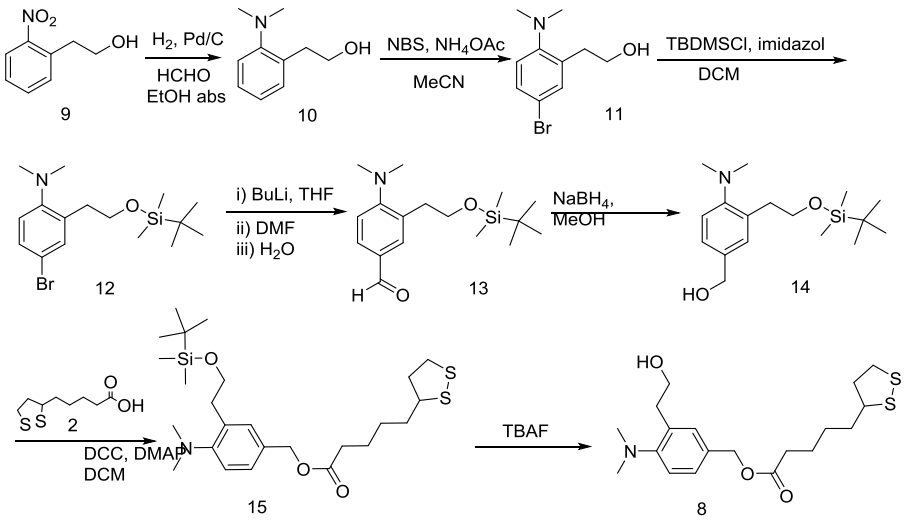

Scheme 3. Synthesis of ligand **8.**

Synthesis of the Functionalized Gold Nanoparticles

AuNPs can be synthesized by different procedures, [16-18] the size, stability and optical properties of the resulting nanoparticles being strongly dependent upon the method used. The functionalized gold nanoparticles AuNP**1**-AuNP**8** were synthesized by a two-step procedure. First, citrate-stabilized nanoparticles were prepared by reducing tetrachloroauric acid with trisodium citrate in boiling water.[8,19] In this step we found that both the relative concentration of the reagents and thorough cleaning of the glassware with aqua regia were crucial to avoid either nucleation during the synthesis or aggregation of the gold colloid solutions. Monodisperse citrate-stabilized nanoparticles were thus obtained with an average size of 13 nm, as determined by TEM. The surface plasmon peak appears at 526 nm, in perfect agreement with the experimental data for particle sizes smaller than 25 nm.[8] The molar extinction coefficient was estimated to be $\varepsilon = 2.47 \times 10^8\ M^{-1}\ cm^{-1}$ (obtained from the plot of ε vs. nanoparticle size reported by Huo and co-workers [20]). The initial concentration of the citrate-capped AuNPs was calculated from the Beer–Lambert law to be 5.3×10^{-9} M.

In the second step, in a ligand-exchange reaction, the citrate was displaced from the surface of the nanoparticles by a mixture of thioctic acid and the different ligands **1**–**8**. In each case it was necessary to optimize the ligand/TA molar ratio (from 1:1 to 1:4) to improve the stabilization of the nanoparticles as well as the response with respect to the analyte.

As an alternative, a three-step protocol was tested for the functionalization of AuNPs in which the citrate was first displaced by TA and the resulting TA-capped AuNPs were stirred in the presence of ligands for a second ligand-exchange reaction. However, the degree of functionalization was much lower by this method, as evidenced by a weaker response towards the war agent simulant.

In this study, the nanoparticles were centrifuged and redissolved in a buffered aqueous solution (MOPS) at pH 7. In this medium, no obvious change neither in color nor in the characteristic peak at 526 nm was observed.

The resulting functionalized gold nanoparticles were characterized by UV/Vis and zeta-potential measurements, and the results are summarized in Table 1. In some cases the AuNPs were also characterized by TEM or XPS.

Table 1. Characterization of the gold nanoparticles.[a]

AuNP	Optimized TA:L molar ratio	SPR peak λ_{max} [nm]	c [M]	ζ-potencial [mV] [b]
AuNP**2**	1:1	526	$1.29 \cdot 10^{-8}$ M	-32.5
AuNP**3**	1.2:1	526	$9.47 \cdot 10^{-8}$ M	-35.6
AuNP**4**	1.2:1	526	$9.47 \cdot 10^{-8}$ M	
AuNP**5**	1.2:1	524	$1.18 \cdot 10^{-8}$ M	-37.3
AuNP**6**	1.2:1	520	$5.79 \cdot 10^{-9}$ M	-35.9
AuNP**7**	4:1	525	$8.32 \cdot 10^{-9}$ M	-36.2
AuNP**8**	1.5:1	524	$1.13 \cdot 10^{-8}$ M	-24.0 [c]

[a] Dispersed in buffered aqueous solution (MOPS, pH 7). [b] ZP= -37.5mV for TA-capped AuNPs. [c] Suspended in deionized water.

AuNP1 experienced aggregation during the functionalization reaction and this prevented its use in the detection studies. The other gold nanoparticles remained stable in cold, buffered aqueous solution for at least a month, which is in agreement with their high zeta-potential values in this medium.

Figure 3 (a) shows the Au 4f core level spectra measured by XPS for the samples AuNP**2**, AuNP**5** and AuNP**7** as well as for TA- and citrate-capped AuNPs. The presence of Au was detected in all of them, although the Au 4f doublets measured in the functionalized samples tend to shift to higher binding energies with respect to the unfunctionalized sample. This fact can be attributed to charge

transfer effects between the Au nanoparticles and the incorporated ligands, indicating that Au tends to donate electrons.

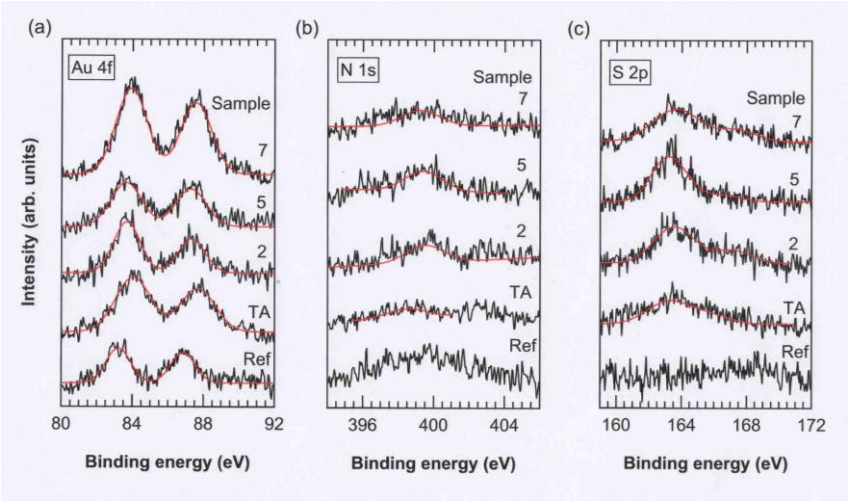

Figure 3. XPS spectra for Au, N and S atoms in AuNP2, AuNP5, AuNP7, TA-capped and citrate-capped (reference) AuNPs.

Figure 3 (b,c) show the N 1s and S 2p core level spectra measured by XPS, respectively. In most of the samples a weak but distinguishable feature attributable to a signal of the N 1s core level can be observed at binding energies of around 400 eV, but is not detectable in the TA-functionalized AuNP nor in the reference sample. In the binding energy region corresponding to the S 2p core level, a clear structure emerges between 160 and 172 eV in the functionalized samples. In these samples, the S 2p spectra appear to be dominated by photoelectrons with binding energies of around 162–163 eV, which can be attributed to sulfur atoms bound and unbound to the gold surface, accompanied by a weaker structure appearing at around 168 eV attributable to oxidized S atoms.

Sensing Studies

To verify the reactivity of the pyridine ligands with the DCNP simulant, a preliminary study was conducted with free ligands **5**–**7** in acetonitrile (the lack of absorption of ligands **1**–**4** in the UV/Vis region precluded their study).

The UV/Vis spectra of ligands **5** and **6** in acetonitrile (5×10^{-5}M) show a band centred at 316 and 431 nm (log ε = 4.36 and 4.31 M^{-1} cm^{-1}), respectively. The addition of 30 equiv. of DCNP to each ligand induced in both cases a bathochromic

shift to give a new band centred at 340 and 532 nm, respectively, corresponding to the phosphorylation of the pyridine moiety, which enhances the intramolecular charge-transfer process in the dyes. The UV spectrum of ligand **7** in acetonitrile (5×10^{-5} M) shows a band centred at 454 nm (log ε = 4.15 $M^{-1}\,cm^{-1}$). In this case, addition of 30 equiv. of DCNP induced the appearance of two broad absorption bands, which, upon deconvolution, split into four well-defined bands at 394, 431, 507 and 537 nm (see Figure 4). Based on previous studies, [6] these bands were assigned to ligand **7** protonated at the dimethylamino group (band centred at 431 nm, confirmed by the addition of 30 equiv. of HCl to a sample of ligand **7** in acetonitrile) and ligand **7** phosphorylated in three different places. The band centred at 537 nm, which corresponds to the phosphorylation of the pyridine moiety, increases the pull–push character of the chromophore, which accounts for the bathochromic shift similar to ligand **6**. The bands at 394 and 507 nm can be assigned to the phosphorylation of the dimethylamino and azo groups of the ligand. The phosphorylation of the aniline moiety was expected to induce a decrease in the charge-transfer character of dye **7**, as we previously observed for a similar system.[6]

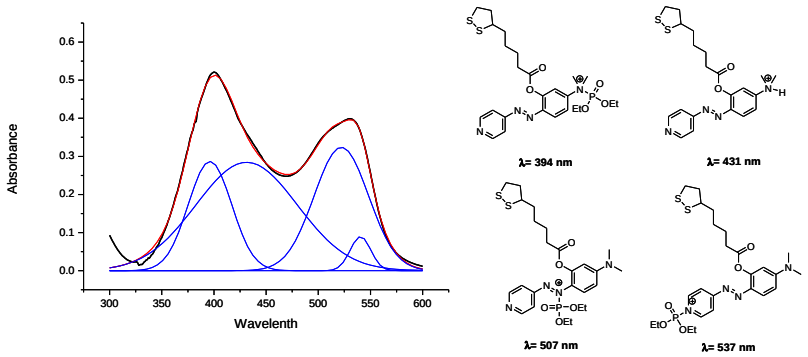

Figure 4. UV/Vis spectrum of ligand 7 (5 × 10–5 m in acetonitrile) on addition of 30 equiv. of DCNP. Deconvolution of the two bands and assigned products.

On the basis of these results we expected that the phosphorylation of the pyridine moiety in nanoparticles AuNP**2**–AuNP**7** or the formation of an ammonium salt in AuNP**8** promoted by the presence of DCNP would change the overall electrostatic charge on the surfaces of the nanoparticles, triggering an aggregation process coupled with a bathochromic shift of the SPR absorption band and a change in the color of the solution.

In fact, when DCNP (5×10^{-2} M, in acetonitrile) was added to a suspension of the prepared AuNP**2**–AuNP**8** in aqueous MOPS solutions, a color change from red wine to purple blue was readily observed by the naked eye. This change is indicative of the aggregation of AuNPs. The sensing experiments were carried out in buffered solutions to prevent any acidic system slowing or even interfering in the sensing process. DFP and DCP could not be studied because they were hydrolysed in this medium.

The ability of these functionalized AuNPs to act as probes for DCNP detection was studied by UV/Vis spectroscopy. The UV/Vis spectra are consistent with the observed color changes. Thus, the intensity of the surface plasmon peak of the monodispersed AuNPs at 526 nm (A_{526}) decreased and a new peak at around 660 nm (A_{660}) appeared as clusters of AuNP formed. Figure 5 shows the results of UV/Vis titration studies performed with AuNP**3** and AuNP**6**, as representative examples, in the presence of increasing amounts of DCNP. Such changes in the spectra, concomitant with the change in color of the solution, can be well explained by the DCNP-induced aggregation of the nanoparticles through charge neutralization at the surface. The aggregation of the AuNPs was further confirmed by TEM analysis (see Figure 6 for AuNP**3**).

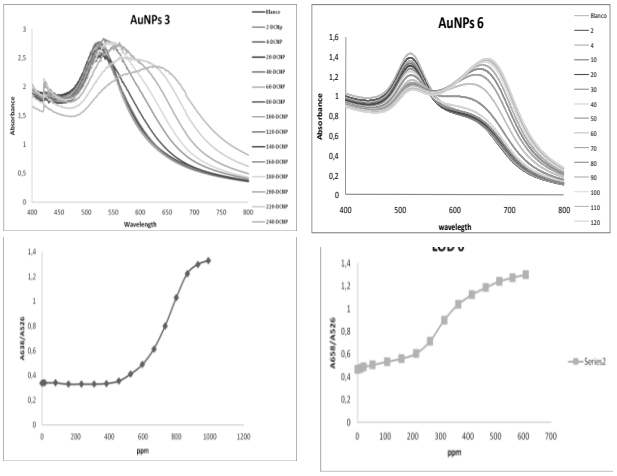

Figure 5. UV/Vis spectra of AuNP3 (top left) and AuNP6 (top right) on addition of increasing amounts of DCNP (5×10^{-2} M in acetonitrile) expressed in ppm (mg/L). Plots of A_{660}/A_{526} vs. DCNP concentration for AuNP3 (bottom left) and AuNP6 (bottom right).

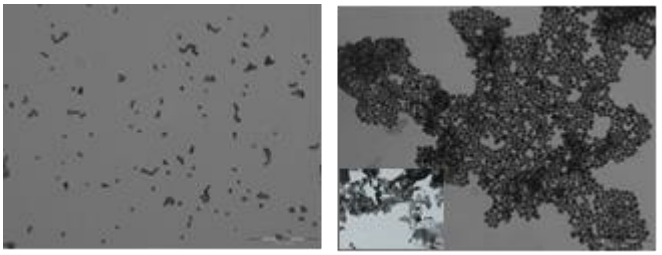

Figure 6. TEM images of a stabilized AuNP**3** dispersion (left) and its aggregates (right) upon addition of excess DCNP at a resolution of 200 nm (inset: the same aggregates at a resolution of 1000 nm).

The variation in A_{670}/A_{526} versus DCNP concentration for AuNP**3** and AuNP**6** is also presented in Figure 5. A very significant increase in theA_{660}/A_{526} ratio was observed as the concentration of DCNP was increased, above 600 ppm for AuNP**3** and above 200 ppm for AuNP**6**, which reflects the greater nucleophilic character of ligand **6**. The visual limits of detection (visual LODs, defined as the minimum concentration of simulant necessary for an observable colour change) and calculated LODs (from the changes in UV/Vis spectra, see the Supporting Information) observed for DCNP are presented in Table 2.

Table 2. Visual and calculated LODs of DCNP with AuNP1–AuNP8.

	AuNP**2**	AuNP**3**	AuNP**4**	AuNP**5**	AuNP**6**	AuNP**7**	AuNP**8**
Visual LOD [ppm]	456	597	1151	310	158	796	106
Calcd. LOD [ppm]	229	470	>1100	340	76	750	81

As expected, AuNP**4** and AuNP**7** showed modest results, probably due to strong steric hindance of the aliphatic ester chain near the pyridine nucleophile, which prevents access of the organophosphate agent to the nitrogen centre. The greater nucleophilic character of the azo-substituted pyridines in ligands **5** and **6** in comparison with ligand **3** would explain the higher LOD observed for the latter.

The best results were obtained with the gold nanoparticles functionalized with azo dye **6** (AuNP**6**) and the dimethylaminophenylethanol ligand **8** (AuNP**8**; Figure 7), which can detect 76 and 81 ppm of DCNP, respectively, thus improving

the limit previously obtained by us in solution by a similar approach (see Scheme 1, b).[6]

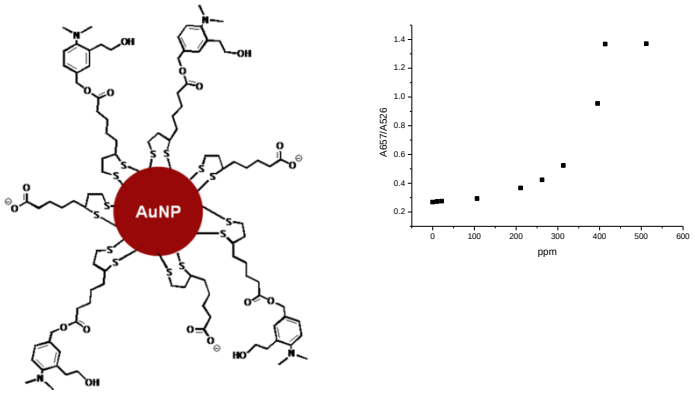

Figure 7. Representation of a AuNP functionalized with ligand **8** (top). Plot ofA_{660}/A_{526} vs. DCNP concentration (left)

Conclusions

Functionalized AuNPs have proven to be an interesting alternative for the direct colorimetric detection of nerve agents in buffered aqueous media provided suitable ligands are anchored to the surfaces of the AuNPs. We have achieved detection limits of 76 and 81 ppm (mg/L) for ligands **6** and **8** and found that both steric and electronic effects are crucial for obtaining good results.

Experimental Section

General Procedures: All reagents were commercially available and used without purification. Silica gel 60 F_{254} (Merck) plates were used for TLC. Milli-Q ultrapure water was used for the synthesis of the AuNPs and in the sensing experiments. ^{1}H and ^{13}C NMR spectra were recorded with a Bruker 300 MHz spectrometer. Chemical shifts are reported in ppm with tetramethylsilane as an internal standard. High-resolution mass spectra were recorded in the positive ion mode with a VG-AutoSpec mass spectrometer. UV/Vis absorption spectra were recorded in a 1 cm pathlength quartz cuvette with a Shimadzu UV-2101PC spectrophotometer. All measurements were carried out at 293 K (thermostatted). Zeta potentials were measured with a Malvern Zetasizer ZS three times in 10–25 cycles. X-ray photoelectron spectroscopy (XPS) was employed to verify the success of the molecular modification of the AuNP surfaces. The spectra were recorded with an Escalab 210 spectrometer from Thermo VG Scientific. The base pressure in

the analysis chamber was 1.0×10^{-10} mbar. Photoelectrons were extracted by using the Mg-K_α excitation line ($h\nu$ = 1253.6 eV). The binding energy of the spectra refers to the Fermi level. The electronic images were obtained with a JEOL-1010 transmission electron microscope operating at 100 kV.

Ligands 1 and 2 were commercially available and were used as received.

Synthesis of Ligand 3: Dicyclohexylcarbodiimide (DCC; 5.19 g, 25.2 mmol) was added portionwise to a cold solution of pyridine-4-methanol (2.72 g, 13.2 mmol) in dichloromethane (DCM; 20 mL). Then thioctic acid (2.72 g, 13.2 mmol) and 4-(dimethylamino)pyridine (DMAP; catalytic amounts) in DCM (20 mL) were added and the mixture was stirred for 72 h at room temperature. Then aq. NH_4Cl was added and the resulting precipitate was removed and the remaining solution was extracted with DCM (3 × 10 mL). The combined organic layers were washed with water and then dried with $MgSO_4$. The solvent was evaporated and the crude product was purified by column chromatography (silica gel, DCM/AcOEt, 1:1) to yield the corresponding ester **3** (2.04 g, 52 %) as a yellow oil.^{1}H NMR (300 MHz, CD_3OD): δ = 8.52 (dd, J= 4.5, 1.7 Hz, 2 H), 7.45–7.38 (m, 2 H), 5.19 (s, 2 H) 3.56 (ddd, J= 12.2, 8.6, 6.3 Hz, 1 H), 3.22–3.03 (m, 2 H), 2.51–2.38 (m, 3 H), 1.94–1.80 (m, 1 H), 1.76–1.59 (m, 4 H), 1.55–1.41 (m,2 H) ppm. ^{13}C NMR (75 MHz, CD_3OD): δ = 175.0, 150.7, 124.0, 65.5, 58.0, 41.7, 39.8, 36.1, 35.1, 30.2, 26.2 ppm. HRMS: calcd. for $C_{14}H_{19}NO_2S_2$ $[M]^+$ 297.0857; found 297.0832.

Synthesis of Ligand 4: Thioctic acid (2.00 g, 9.69 mmol), Ph_3P (3.05 g, 11.6 mmol) and 2,2'-dipyridyl disulfide (2.56 g, 11.6 mmol) were dissolved in THF (30 mL). The solution was stirred at room temperature for 24 h under argon and then concentrated in vacuo to give the crude product. Purification by column chromatography (hexane/EtOAc, 2:1) afforded 2.26 g (78 %) of ligand **4**[21] as a yellow oil.^{1}H NMR (400 MHz, $CDCl_3$): δ = 8.58 (ddd ,J = 4.8, 2.0, 0.8 Hz, 1 H), 7.59 (d, J = 7.6 Hz, 1 H), 7.71 (dt, J = 8.0, 2.0 Hz, 1 H), 7.26 (ddd, J = 7.6, 5.2, 1.2 Hz, 1 H), 3.53 (q, J = 6.4 Hz, 1 H), 3.17–3.04 (m, 2 H), 2.69 (t, J = 7.4 Hz, 2 H), 2.42 (sext, J = 6.8 Hz, 1 H), 1.87 (sext, J = 6.8 Hz, 1 H), 1.77–1.63 (m, 4 H), 1.43–1.53 (m, 2 H) ppm. ^{13}C NMR (75 MHz, $CDCl_3$): δ = 196.0, 151.2, 150.1, 137.2, 130.1, 123.5, 56.1, 43.8, 40.1, 38.4, 34.5, 28.4, 25.0 ppm.

Synthesis of Ligand 5: Phenol (5.0 g, 53 mmol) and sodium nitrite (4.0 g, 58 mmol) in aqueous NaOH (10 % w/w, 20 mL) was added dropwise to a solution of 4-aminopyridine (6.0 g, 64 mmol) in 7.3 M HCl (45 mL) at 0 °C. The pH of the mixed solution was adjusted to pH 6–7 by the addition of a 10 % aqueous solution of NaOH. The resulting mixture was stirred at 0 °C for 2 h. After neutralization of the solution with sodium hydrogen carbonate, an orange precipitate was obtained. Purification by crystallization with methanol and DCM afforded 4-(4-

hydroxyphenylazo)pyridine [22](4.6 g, 44 %) as an orange solid. ^{1}H NMR (300 MHz, $CDCl_3$): δ = 10.57 (s, 1 H), 8.77 (d, *J* = 6.0 Hz, 2 H), 7.90–7.85 (m, 2 H), 7.68 (dd, *J* = 4.5, 1.6 Hz, 2 H), 7.02–6.94 (m, 2 H) ppm.

DCC (0.988 g, 4.79 mmol) was added portionwise to a cold solution of 4-(4-hydroxyphenylazo)pyridine (0.454 g, 2.28 mmol) in DCM (20 mL),. Then a cold solution of thioctic acid (0.518 g, 2.51 mmol) and a catalytic amount of DMAP in DCM (20 mL) was added and the mixture was stirred for 72 h at room temperature. After this time, a saturated aqueous solution of ammonium chloride was added and the resulting precipitate was removed. The mixture was extracted with DCM (3 × 10 mL). The combined organic layers were washed with water, dried with $MgSO_4$, evaporated and further purified by column chromatography (DCM/AcOEt, 1:1) to yield the corresponding ester 5 (0, 353 g, 40 %) as an orange solid. ^{1}H NMR (300 MHz, CD_3OD): δ = 8.77 (d, *J* = 6.4 Hz, 2 H), 8.06 (d, *J* = 9.1 Hz, 2 H), 7.84 (d, *J* = 6.4 Hz, 2 H), 7.36 (d, *J* = 9.1 Hz, 2 H), 3.68–3.54 (m, 1 H), 3.22–3.06 (m, 2 H), 2.67 (t, *J* = 7.3 Hz, 2 H), 2.57–2.43 (m, 1 H), 1.95–1.86 (m, 1 H), 1.84–1.69 (m, 4 H), 1.65–1.55 (m, 2 H) ppm. ^{13}C NMR (75 MHz, CD_3OD): δ = 172.37, 153.42, 144.38, 134.38, 134, 06, 129.61, 127.14, 123.05, 121.49, 56.81, 40.23, 38.56, 34.66, 33.57, 28.01, 24.64 ppm. HRMS: calcd. for $C_{19}H_{22}N_3O_2S_2$ $[MH]^+$ 388.1153; found 388.1157.

Synthesis of Ligand 6: 4-aminopyridine (0.367 g, 4 mmol) was dissolved in a mixture of concentrated phosphoric acid (25 mL) and concentrated nitric acid (12 mL). This solution was slowly added to a solution containing sodium nitrite (0.334 mg, 4.8 mmol) and water (8 mL) at –5 °C. The generated diazonium salt was immediately added to a solution containing 2-[methyl(phenyl)amino]ethanol (0.609 mg, 4.03 mmol) and 30 % phosphoric acid (20 mL). The reaction mixture was allowed to react for 30 min at –5 °C and then for 60 min at room temperature. The final dark-red crude was neutralized with a saturated sodium carbonate solution and the organic product extracted with DCM. The organic layer was dried with $MgSO_4$, filtered and the solvent eliminated in a rotary evaporator. 4-Azidopyridine (0.234 g, 0.53 mmol, 45 %) was isolated as a dark-red solid by column chromatography using AcOET/hexane (1:1) as eluent. ^{1}H NMR (300 MHz, $CDCl_3$): δ = 8.71 (dd, *J* = 4.6, 1.6 Hz, 2 H), 7.90 (d, *J* = 9.3 Hz, 2 H), 7.63 (dd, *J* = 4.6, 1.6 Hz, 2 H), 6.82 (d, *J* = 9.3 Hz, 2 H), 3.89 (m, 2 H), 3.66 (t, 2 H), 3.16 (s, 3 H) ppm. ^{13}C NMR (75 MHz, $CDCl_3$): δ = 149.72, 159.68, 148.34, 130.95, 120.83, 113.14, 11.52, 63.92, 58.47, 41.04 ppm. HRMS: calcd. for $C_{14}H_{16}N_4O$ $[M]^+$ 256.303; found 256.286.

DCC (1.04 mmol) was added portionwise to a cold solution of (*E*)-2-{methyl[4-(pyridin-4-yldiazenyl)phenyl]amino}ethanol (0.87 mmol) in DCM (25 mL). Then a cold solution of thioctic acid (1.04 mmol) and DMAP (catalytic amount) in DCM (25 mL) was added and the mixture was stirred for 48 h at room temperature. After this time a saturated solution of ammonium chloride was added

and the precipitated removed. The mixture was extracted with DCM (3 × 10 mL) and the combined organic layers were washed with water, dried with $MgSO_4$, evaporated and further purified by column chromatography (DCM/ethyl acetate, 1:1) to yield the corresponding ester 6 (0.243 g, 45 %) as a dark-orange solid. ^{1}H NMR (300 MHz, MeOD): δ = 8.70 (d, J = 6.2 Hz, 2 H), 7.96–7.85 (m, 2 H), 7.72–7.64 (m, 2 H), 6.84–6.73 (m, 2 H), 4.31 (t, J = 5.8 Hz, 2 H), 3.73 (t, J = 5.8 Hz, 2 H), 3.56–3.42 (m, 1 H), 3.14–3.09 (m, 2 H), 3.14–3.09 (s, 3 H), 2.48–2.33 (m, 1 H), 2.24 (t, J = 7.3 Hz, 2 H), 1.92–1.76 (m, 1 H), 1.69–1.51 (m, 4 H), 1.47–1.32 (m, 2 H) ppm. ^{13}C NMR (75 MHz, $CDCl_3$): δ = 173.70, 158.93, 150.09, 126.74, 116.82, 112.04, 60.81, 56.70, 51.22, 40.62, 39.29, 38.87, 34.95, 29.97, 24.88 ppm. ^{13}C NMR (75 MHz, $CDCl_3$): δ = 173.7, 159.2, 153.0, 144.4, 126.8, 116.9, 112.0, 61.6, 56.7, 51.2, 40.6, 38.9, 35.0, 34.3, 29.1, 24.9 ppm. HRMS: calcd. for $C_{22}H_{28}N_4O_2S_2$ $[M]^+$ 444.165; found 444.169.

Synthesis of Ligand 7: 4-Aminopyridine (0.121 g, 1.29 mmol) was dissolved in water (10 mL). Then concentrated sulfuric acid (0.5 mL, 9.2 mmol) was added and the reaction mixture was heated to give a solution. The reaction mixture was cooled to 0 °C and then a solution of $NaNO_2$ (0.089 g, 1.29 mmol) in water (5 mL) was added dropwise. Then a solution of (dimethylamino)phenol (0.206 g, 1.5 mmol) was added dropwise during 30 min. The resulting orange solution was stirred for 30 min at 0 °C and then for 30 min at room temperature. Then the reaction mixture was neutralized with an aqueous saturated solution of potassium acetate (30 mL). The precipitate was purified by column chromatography (hexane/ethyl acetate, 9:1) to yield (*E*)-5-(dimethylamino)-2-(pyridin-4-yldiazenyl)phenol (0.122 g, 39 %) as a brown solid. ^{1}H NMR (300 MHz, $CDCl_3$): δ = 15.62 (s, OH), 8.59 (s, 1 H), 7.45 (d, J = 6.1 Hz, 2 H), 7.32 (d, J = 9.3 Hz, 1 H), 6.52 (dd, J = 9.2, 2.6 Hz, 1 H), 5.91 (d, J = 2.6 Hz, 1 H), 5.30 (s, 1 H), 3.17 (s, 6 H) ppm. ^{13}C NMR (75 MHz, $CDCl_3$): δ = 159.72, 158.91, 151.87, 148.37, 131.14, 114.01, 104.12, 99.18, 96.25, 41.29 ppm. HRMS: calcd. for $C_{13}H_{14}N_4O$ $[M]^+$ 242.1168; found 242.1194.

DCC (1.392 mmol) was added portionwise to a cold solution of (*E*)-5-(dimethylamino)-2-(pyridin-4-yldiazenyl)phenol (0.87 mmol) in DCM (25 mL). Then a cold solution of thioctic acid (1.04 mmol) and DMAP (catalytic amount) in DCM (25 mL) was added and the mixture was stirred for 48 h at room temperature. After this time, a saturated solution of ammonium chloride was added and the precipitate removed. The mixture was extracted with DCM (3 × 10 mL) and the combined organic layers were washed with water, dried with $MgSO_4$, evaporated and further purified by column chromatography (DCM/ethyl acetate, 1:1) to yield the corresponding ester 7 (0.150 g, 40 %) as an orange solid. ^{1}H NMR (300 MHz, $CDCl_3$): δ = 8.64 (dd, J = 4.6, 1.6 Hz, 1 H), 7.79 (d, J = 9.3 Hz, 1 H), 7.49 (dd, J = 4.6, 1.6 Hz, 2 H), 6.54 (dd, J = 9.3, 2.8 Hz, 1 H), 6.36 (d, J = 2.7 Hz, 1 H), 3.50 (dq, J = 13.2, 6.6 Hz, 1 H), 3.07 (s, 2 H), 3.08–3.04 (m, 3 H), 2.62 (t, J = 7.4 Hz, 1 H), 2.40 (dq, J = 6.6, 5.5 Hz, 1 H), 2.30 (t, J = 7.3 Hz, 2 H), 1.93–1.78 (m, 3 H) ppm. ^{13}C NMR (75 MHz,

$CDCl_3$): δ = 172.4, 159.7, 151.7, 148.2, 142.0, 130.1, 113.0, 108.3, 104.7, 96.4, 56.4, 41.2, 40.3, 38.7, 34.6, 33.5, 28.1, 24.6 ppm. HRMS: calcd. for $C_{21}H_{26}N_4O_2S_2$ $[M]^+$ 430.150; found 430.146.

Synthesis of Ligand 8: 2-(2-Nitrophenyl)ethanol (2.3 g, 19.67 mmol), formaldehyde (4.83 mL, 32.3 mmol, 36 %) and Pd/C (480 mg, 10 %) were dissolved in absolute ethanol (200 mL) and placed under H_2 until uptake of hydrogen had ceased. After filtration through Celite, the solvent was evaporated and the product was purified by extraction with ethyl acetate and washed with water. The organic layer was washed with brine and dried with $MgSO_4$ to give 2-(dimethylaminophenyl)ethanol (10; 3.22 g, 95 %) as a yellow oil. ^{1}H NMR (300 MHz, $CDCl_3$): δ = 7.19–6.95 (m, 4 H), 3.76 (t, J = 5.9 Hz, 2 H), 2.91 (t, J = 5.7 Hz, 2 H), 2.62 (s, 6 H) ppm. ^{13}C NMR (75 MHz, $CDCl_3$): δ = 152.6, 136.5, 131.5, 128.0, 125.4, 120.4, 64.7, 45.4, 36.5 ppm.

NBS (0.187 g, 1.05 mmol) was added to a mixture of 2-(dimethylaminophenyl)ethanol (10; 0.165 g, 1 mmol) and NH_4OAc (10 mol-%) in MeCN (5 mL) and the mixture was stirred at room temperature. After completion of the reaction as indicated by TLC, the mixture was concentrated in vacuo and extracted with EtOAc/H_2O (1:1, 3 × 5 mL). The organic portion was separated from the extract, dried and concentrated. The residue was subjected to column chromatography (silica gel, hexane/EtOAc, 10:1) to obtain pure 2-(5-bromo-2-dimethylaminophenyl)ethanol (11) as a brown oil. (0.237, 97 %). ^{1}H NMR (300 MHz, $CDCl_3$): δ = 7.23 (dt, J = 8.4, 2.4 Hz, 2 H), 6.95 (t, J = 7.1 Hz, 2 H), 4.86 (s, 1 H), 3.73 (t, J = 6.2 Hz, 2 H), 2.92–2.8 (m, 2 H), 2.57 (s, 6 H) ppm. ^{13}C NMR (75 MHz, $CDCl_3$): δ = 151.8, 138.9, 134.2, 130.9, 122.3, 118.2, 64.5, 45.4, 36.2 ppm.

2-(5-Bromo-2-dimethylaminophenyl)ethanol (11; 1.75 g, 7.14 mmol) and imidazole (1.46 g, 21.44 mmol) was dissolved in anhydrous DCM (5 mL). *tert*-Butyldimethylsilyl chloride (1.19 g, 7.86 mmol) was added and the reaction mixture was stirred at room temperature until the complete disappearance of the starting material (by TLC). The solvent was evaporated and the residue dissolved in ethyl acetate (20 mL) and washed with concentrated aqueous $NaHCO_3$ (2 × 10 mL). The organic layer was dried with $MgSO_4$ and the solvents evaporated. The product was purified by column chromatography (DCM/MeOH, 95:5) to give 4-bromo-2-{2-[(*tert*-butyldimethylsilyl)oxy]ethyl}-*N*,*N*-dimethylaniline (12; 0.2106 g, 83 %) as a pale-yellow oil. ^{1}H NMR (300 MHz, $CDCl_3$): δ = 7.37–7.18 (m, 2 H), 6.94 (d, J = 8.5 Hz, 1 H), 3.81 (t, J = 7.25 Hz, 2 H), 2.87 (t, J = 7.0 Hz, 2 H), 2.62 (s, 6 H), 0.86 (s, 9 H), 0.00 (s, 6 H) ppm. ^{13}C NMR (75 MHz, $CDCl_3$): δ = 152, 137.03 133.18, 131.2, 121.82, 118.1, 63.82, 45.60, 34.64, 26.33, 18.74, –5.01 ppm. HRMS: calcd. for $C_{16}H_{28}BrNOSi$ $[M]^+$ 357.1124; found 357.1192.

A solution of bromide **12** (1.49 g, 4.15 mmol) dissolved in THF (30 mL) was cooled to –78 °C under Ar. *n*-Butyllithium (6.5 mL, 5 mmol) was added dropwise

with stirring and then warmed to 0 °C and kept at this temperature for an additional 1 h. Again the solution was cooled to –78 °C and dry dimethylformamide (0.96 mL, 12.48 mmol) was added. The reaction was stirred at room temperature for 2 h and water (15 mL) was added. The solvents were removed in vacuo and the residue redissolved in DCM. The organic extract was dried with anhydrous $MgSO_4$and filtered. 3-{2-[(*tert*-Butyldimethylsilyl)oxy]ethyl}-4-dimethylaminobenzaldehyde (13) was obtained after silica gel column chromatography (ethyl acetate/hexane, 1:5) in 98 % yield (1.26 g). ^{1}H NMR (300 MHz, $CDCl_3$): δ = 9.83 (s, 1 H), 7.76 (d, J = 2.1 Hz, 1 H), 7.68 (dd, J = 8.3 and 2.1 Hz, 1 H), 7.07 (d, J = 8.3 Hz, 1 H), 3.86 (t, J = 7.0 Hz, 2 H), 2.93 (t, J = 7.0 Hz, 2 H), 2.78 (s, 6 H), 0.84 (s, 9 H), –0.02 (s, 6 H) ppm. ^{13}C NMR (75 MHz, $CDCl_3$): δ = 191.8, 159.2, 133.2, 132.8, 130.9, 129.7, 118.9, 67.9, 63.5, 50.3, 45.8, 44.7, 35.2, 31.4, 26.4, 26.3, 18.7, –5.0 ppm. HRMS: calcd. for $C_{17}H_{29}NO_2Si$ $[M]^+$ 307.1968; found 307.2036.

$NaBH_4$ (0.034 g, 9.0 mmol) was added to a solution of 13 (0.461 g, 15 mmol) in MeOH (30 mL), and the mixture was heated at 60 °C for 2.5 h. After addition of water (20 mL) at 0 °C, work-up was performed with ethyl acetate and water, and the combined organic layers were washed with brine and dried with $MgSO_4$. After filtration followed by evaporation, the residue was subjected to column chromatography through silica gel (ethyl acetate/hexane, 3:7) to afford pure 3-{2-[(*tert*-butyldimethylsilyl)oxy]ethyl}-4-[(dimethylamino)phenyl]methanol (14; 0.424 g, 91 %) as a pale-yellow solid. ^{1}H NMR (300 MHz, $CDCl_3$): δ = 7.23–7.13 (m, 2 H), 7.13–7.05 (m, 1 H), 4.59 (s, 2 H), 3.82 (t, J = 7.3 Hz, 2 H), 2.92 (t, J = 7.3 Hz, 2 H), 2.64 (s, 6 H), 1.61 (s, 2 H), 1.35–1.28 (m, 1 H), 0.87 (s, 9 H), 0.01 (s, 6 H) ppm. ^{13}C NMR (75 MHz, $CDCl_3$): δ = 153.3, 136.1, 134.7, 130.1, 126.3, 120.3, 65.7, 64.3, 45.7, 35.1, 26.4, 18.8 ppm. HRMS: calcd. for $C_{19}H_{29}NO_2Si$ $[M]^+$ 309.5190; found 309.1402.

DCC (0.480 g, 2.32 mmol) was added portionwise to a cold of solution of **14** (0.343 g, 1.1 mmol) in DCM (25 mL). Then a solution of thioctic acid (251 mg, 1.65 mmol) and 4-(dimethylamino)pyridine (catalytic amount) in DCM (25 mL) was added and the mixture was stirred for 24 h at room temperature. Then brine was added and the mixture was extracted with diethyl ether (3× 5 mL). The combined organic layers were washed with water, dried with $MgSO_4$, evaporated and further purified by column chromatography (dichloromethane/ethyl acetate, 1:1) to yield **15** (0.243 g, 44 %) as a yellow oil. ^{1}H NMR (300 MHz, $CDCl_3$): δ = 7.16 (dd, J = 10.2, 5.0 Hz, 2 H), 7.05 (dd, J = 8.0, 4.4 Hz, 1 H), 5.01 (s, 2 H), 3.81 (t, J = 7.1, 3.5 Hz, 2 H), 3.53 (dt, J = 13.0, 6.5 Hz, 1 H), 3.20–3.03 (m, 2 H), 2.90 (t, J = 7.3, 3.9 Hz, 2 H), 2.65 (s, 5 H), 2.48–2.38 (m, 1 H), 2.33 (t, J = 19.7, 7.0 Hz, 1 H), (dt, J = 19.7, 7.0 Hz, 1 H), 1.71–1.61 (m, 4 H), 1.46 (dt, J = 15.6, 6.8 Hz, 2 H), 0.87 (s, 9 H), 0.00 (s, 6 H) ppm. ^{13}C NMR (75 MHz, $CDCl_3$): δ = 173.8, 153.9, 134.6, 131.4, 130.9, 127.6, 120.1, 66.6, 64.2, 56.7, 45.6, 40.6, 38.9, 35.1, 35.0, 34.5, 29.1, 26.4, 25.1, 18.8, –4.94 ppm. HRMS: calcd. for $C_{25}H_{43}NO_3S_2Si$ $[M]^+$ 497.893; found 497.8244.

TBAF·$3H_2O$ (0.73 mL, 0.7 mmol) was added to a solution of **15** (0.243 mg, 0.5 mmol) in THF (4 mL) and the mixture was stirred at room temperature for 2 h. The reaction mixture was then diluted with water (10 mL) and the aqueous phase extracted with diethyl ether (5 × 5 mL). The combined organic layers were dried with $MgSO_4$, filtered and the solvent was removed in vacuo. The crude product was purified by column chromatography (hexane/ethyl acetate, 1:1) to furnish the ligand 4-(dimethylamino)-3-(2-hydroxyethyl)benzyl 5-(1,2-dithiolan-3-yl)pentanoate (8; 0.064 g, 35 %) as a colourless liquid. ^{1}H NMR (300 MHz, $CDCl_3$): δ = 7.18 (dd, J = 10.2, 5.0 Hz, 2 H), 7.05 (dd, J = 8.0, 4.4 Hz, 1 H), 5.01 (s, 2 H), 3.84 (t, J = 7.1, 3.5 Hz, 2 H), 3.53 (dt, J = 13.0, 6.5 Hz, 1 H), 3.20–3.03 (m, 2 H), 2.99 (t, J = 7.3, 3.9 Hz, 2 H), 2.65 (s, 5 H), 2.48–2.38 (m, 1 H), 2.33 (t, J = 19.7, 7.0 Hz, 1 H), (dt, J = 19.7, 7.0 Hz, 1 H), 1.71–1.61 (m, 4 H), 1.46 (dt, J = 15.6, 6.8 Hz, 2 H) ppm.^{13}C NMR (75 MHz, $CDCl_3$): δ = 173.7, 152.7, 136.8, 132.9, 131.7, 128.1, 120.6, 66.2, 64.7, 56.7, 45.4, 40.6, 38.9, 36.6, 35.0, 34.4, 29.1, 25.1 ppm. HRMS: calcd. for $C_{19}H_{29}NO_3S_2$ $[M]^+$ 383.5683; found 383.1694.

Preparation of the Functionalized AuNPs: All glassware was thoroughly cleaned with freshly prepared aqua regia (HCl/HNO_3, 3:1), rinsed thoroughly with deionized water and dried in air. AuNPs with a diameter of around 13 nm were synthesized as reported previously.[16] Briefly, an aqueous 38.8 mM trisodium citrate solution (10 mL) was added to a boiling solution of 1 mM $HAuCl_4$ (100 mL) and the resulting solution boiled for 30 min until a red solution was obtained. This solution was cooled to room temperature and then stored in a refrigerator at 4 °C for use. The AuNPs were modified by ligand-exchange reaction at room temperature as follows: A 0.01 M aqueous NaOH solution (20 µL) was added to the as-prepared citrate-capped AuNPs (10 mL). Then TA (200 µL, 10^{-3} M in ethanol) and the appropriate amount of ligand **2–8** (10^{-3}M in ethanol) were added simultaneously and the solution was stirred overnight. To purify the AuNPs, the mixture was centrifuged for 20 min at 14000 rpm and the supernatants were decanted. Then the resulting AuNPs were resuspended in MOPS buffer solution (0.1 M at pH 7). The size and shape of the modified AuNPs were characterized by TEM. The UV/Vis spectra absorbance spectra of the modified AuNPs were recorded.

The limits of detection (LODs) were determined as described in the Supporting Information

Supporting Information (see footnote on the first page of this article): Copies of the ^{1}H NMR and ^{13}C NMR spectra (Figures S1 to S11), UV/Vis spectra ligands **5–7** (Figure S12), UV/Vis spectra and A_{660}/A_{526} vs. DCNP concentration plots for AuNP2-AuNP8 and method of determination of LODs.

Acknowledgments

The authors thank to Spanish Government (grant numbers MAT2009-14564-C04-03 and MAT2012-38429-C04-02) and the Generalitat Valenciana (Project PROMETEO/2009/095) for support. A. M. is grateful to the Spanish Government for a fellowship. SCSIE (Universidad de Valencia) is gratefully acknowledged for all the equipment employed.

References

[1] A) H. H. Hill Jr.; S. J. Martin Pure Appl. Chem. 2002, 74, 2285-2291; B) M. Wheelis Pure Appl. Chem. 2002, 74, 2247-2251.

[2] S. M. Somani Chemical Warfare Agents, Academic Press, San Diego, 1992.

[3] A) J. J. Gooding Anal. Chim. Acta 2006, 559, 137-151; B) L. M. Eubanks; T. J. Dickerson; K. D. Janda Chem. Soc. Rev. 2007, 36, 458-470.

[4] S. Royo; R. Martinez-Mañez; F. Sancenón; A. M. Costero; M. Parra; S. Gil Chem. Commun. 2007, 4839-4847.

[5] A. M. Costero; M. Parra; S. Gil; R. Gotor; P. M. E. Mancini; R. Martinez-Mañez; F. Sancenón; R. Royo Chem. Asian J. 2010, 5, 1573-1585.

[6] S. Royo; A. M. Costero; M. Parra; S. Gil; R. Martinez-Mañez; F. Sancenón Chem. Eur. J. 2011, 17, 6931-6934.

[7] A) R. Elghanian; J. J. Storhoff; R. C. Mucic; R. L. Letsinger; C. A. Mirkin Science 1997, 227, 1078-1081; B) L. M. Wang; X. F. Liu; X. F. Hu; S. P. Song; C. H. Fan Chem. Commun. 2006, 3780-3782; C) D. B. Liu; W. S. Qu; W. W. Chen; W. Zhong; Z. Wang; X. X. Jiang Anal. Chem. 2010, 82, 9606-9610; D) K. Saha, S. S. Agasti, C. Kim, X. Li, V. M. Rotello, Chem. Rev. 2012, 112, 2739-2779; E) V. K. K. Upadhyayula Anal. Chim. Acta 2013, 715, 1-18.

[8] W. Haiss; N. T. K. Thanh; J. Aveyard; D. G. Fernig Anal. Chem. 2007, 79, 4215-4221.

[9] B. Kong; A. Zhu; Y. Luo; Y. Tian; Y. Yu; G. Shi Angew. Chem. Int. Ed. 2011, 50, 1837-1840.

[10] D. Liu; Z. Wang; X. Jiang Nanoscale 2011, 3, 1421-1433.

[11] A) K. M. Mayer; J. H. Hafner Chem. Rev. 2011, 111, 3828-3857; B) E. E. Bedford; J. Spadovecchia; C. M. Pradier; F. X. Gu Macromol Biosci. 2012, 12, 724-739.

[12] J. Sun; L. Guo; Y. Bao; J. Xie Biosensors and Bioelectronics 2011, 28, 152-157.

[13] H. Li; J. Guo; H. Ping; L. Liu; M. Zhang; F. Guan; C. Sun; Q. Zhang Talanta 2011, 87, 93-99.

[14] K. Bondyopadhyay; S. G. Lin; H. Lin; L. Echegoyen Chem. Eur. J. 2000, 6, 4385-4392.

[15] M. Kadalbajoo; J. Park; A. Opdahl; H. Suda; C. A. Kitchens; J. C. Garnó; J. D. Batteas; M. J. Tarlov; P. Deshong Lagmuir 2007, 23, 700-707.

[16] P- Zhao; N. Li; D. Astruc Coor. Chem. Rev. 2013, 257, 638-665.

[17] N. R. Jana; L. Gearheart; C. J. Murphy Lagmuir 2001, 17, 6782-6786.

[18] A) K. C. GRABAR; R. G. FREEMAN; M. B. HOMMER; M. J. NATAN ANAL. CHEM. 1995, 67, 735-743; B) K. R. BROW; A. P. FOX; M. J. NATAN J. AM. CHEM. SOC. 1996, 118, 1154-1157.

[19] S.-Y. LIN; Y.-T. TSAI; C.-C. CHEN; C.-M- LIN; C.-H. CHEN J. PHYS. CHEM. B 2004, 108, 2134-2139.

[20] X. LIU; M. ATWATER; J. WANG; Q. HUO COLLOIDS AND SURFACES B: BIOINTERFACES 2007, 58, 3-7.

[21] M. KADALBAJOO; J. PARK; A. OPDAHL; H. SUDA; C. A. KITCHENS; J. C. GARNO; J. D. BATTEAS; M. J. TARLOV; P. DESHONG LAGMUIR 2007, 23, 700-707.

[22] L. CUI, Y. ZHAO., CHEM. MATER., 2004, 16, 2076-2082

Supplementary Material

Functionalized Gold Nanoparticles as an approach to the Direct Colorimetric Detection of DCNP Nerve Agent Simulant

Almudena Martí,[a,b] Ana M. Costero,[a,b] Pablo Gaviña,*[a,b] Salvador Gil,[a,b] Margarita Parra,*[a,b] Mauro Brotons-Gisbert,[c] and Juan Francisco Sánchez-Royo[c]

[a] Centro de Reconocimiento Molecular y Desarrollo Tecnológico (IDM), Unidad Mixta Universidad de Valencia-Universidad Politécnica de Valencia, Valencia, Spain Fax: +34-963543151 E-mail: pablo.gavina@uv.es margarita.parra@uv.es Homepage: http://idm.webs.upv.es

[b] Departamento de Química Orgánica, Universidad de Valencia, c/ Dr. Moliner 50, 46100 Burjassot, Valencia, Spain Homepage: http://www.uv.es

[c] Instituto de Ciencia de los Materiales, Universidad de Valencia, c/ Dr. Moliner 50, 46100 Burjassot, Valencia, Spain Homepage: http://www.uv.es

Figure S1. ^{1}H NMR and ^{13}C NMR spectrum of ligand **3** in CD_3OD at 300 and 75 MHz

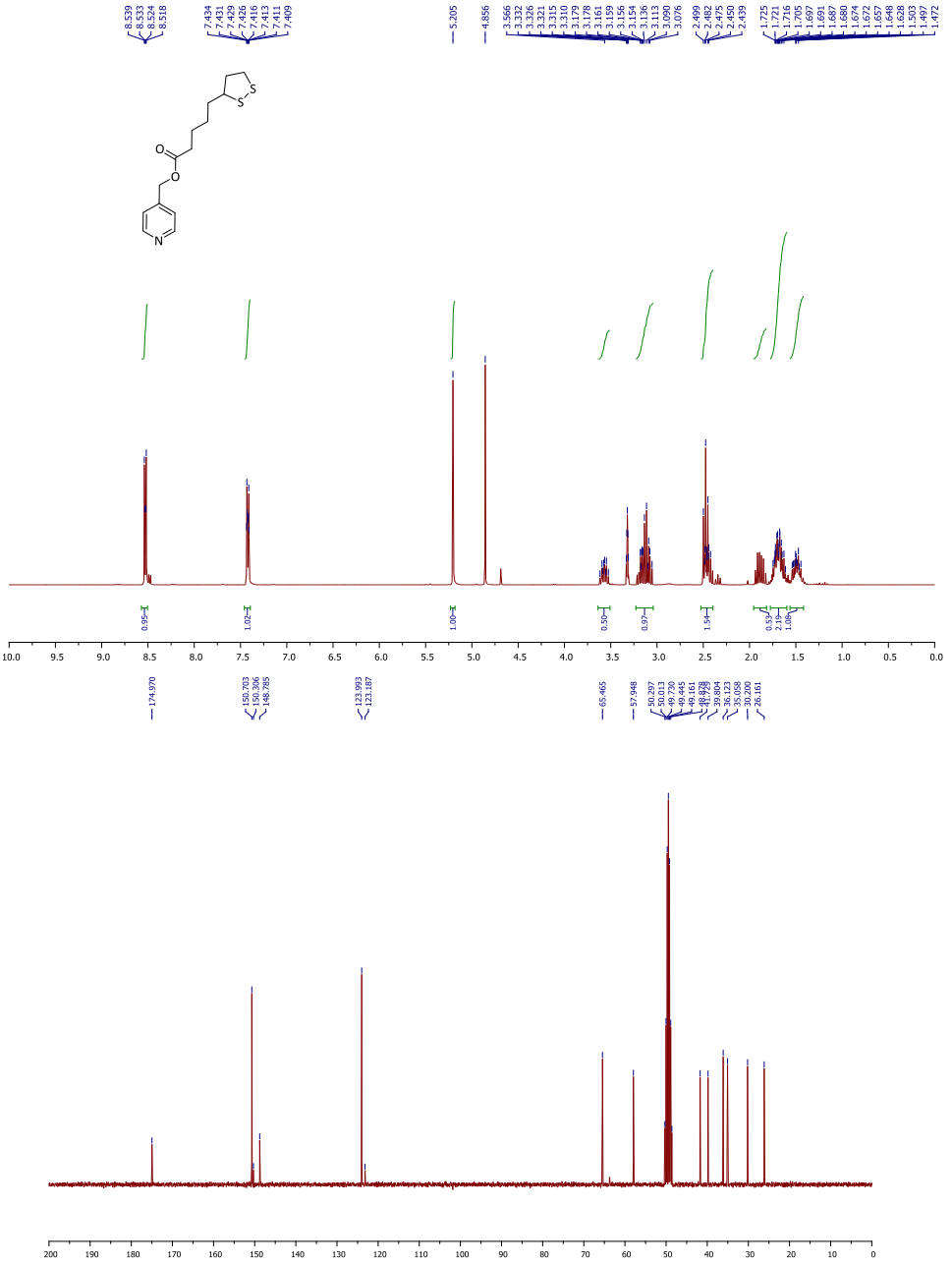

Figure S2. ^{1}H NMR and ^{13}C NMR spectrum of ligand **5** in CD_3OD at 300 and 75 MHz

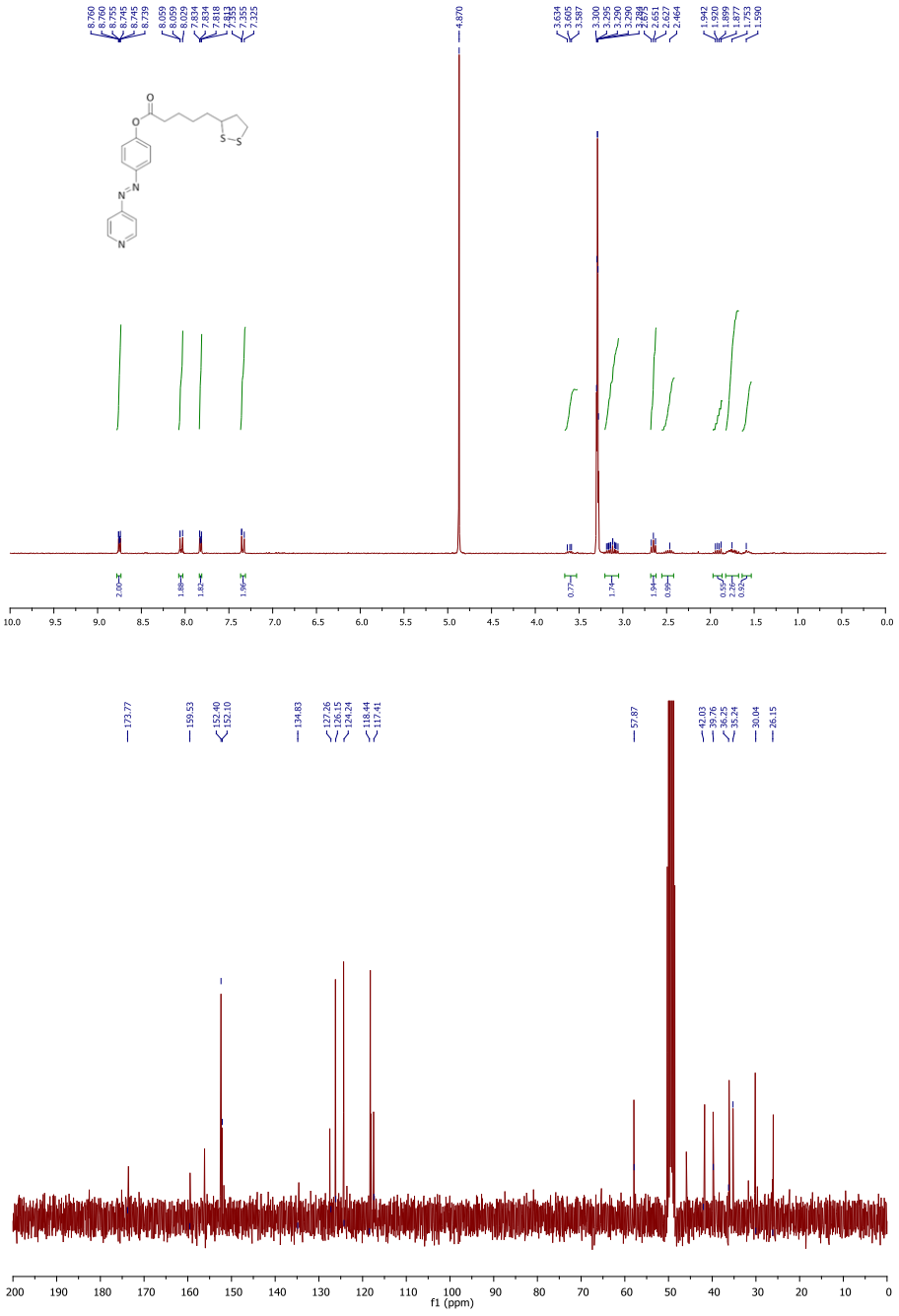

Figure S3. ^{1}H NMR and ^{13}C NMR spectrum of ligand **6** in CD_3OD at 300 and 75 MHz

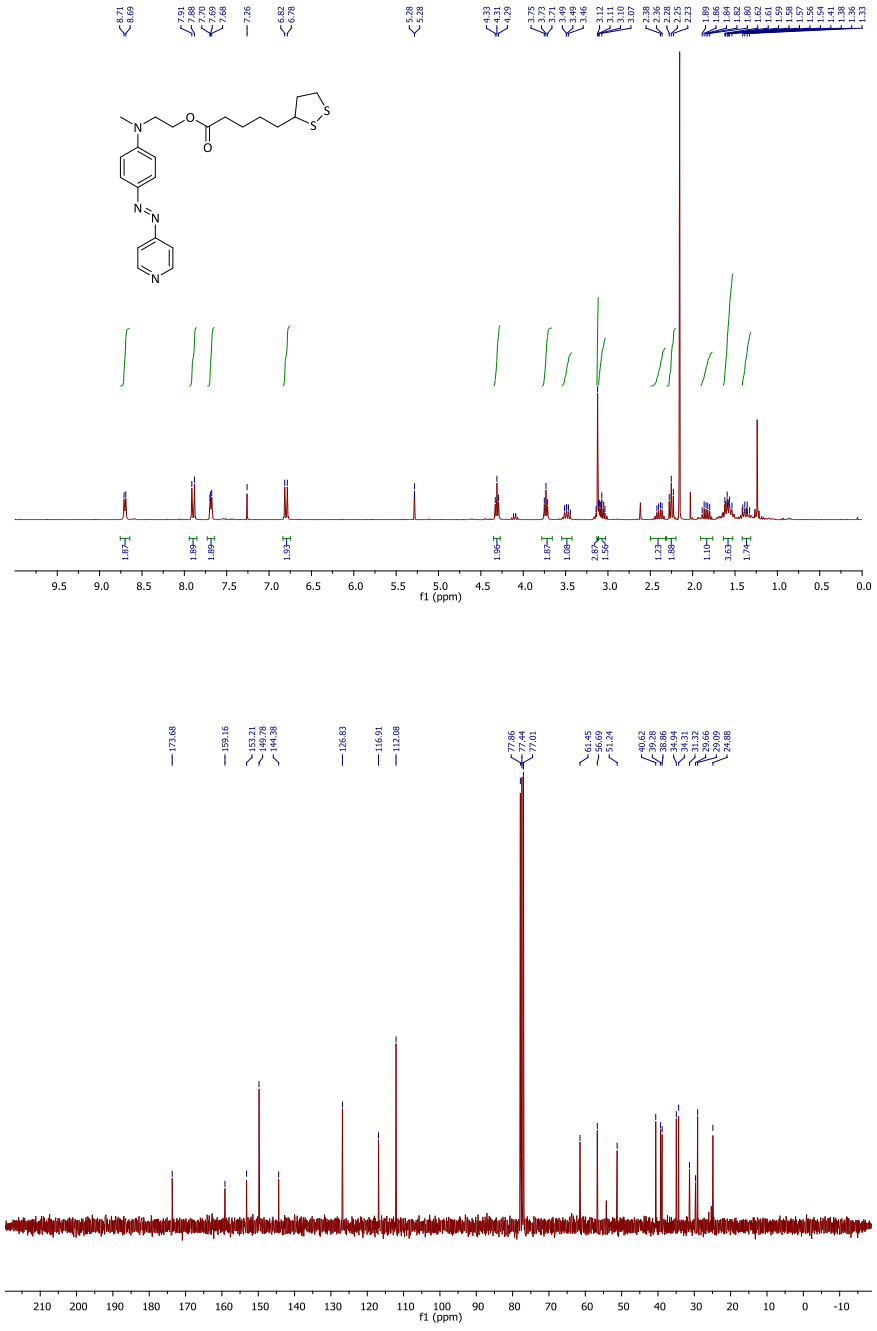

Figure S4. ^{1}H NMR and ^{13}C NMR spectrum of ligand **7** and precursor in $CDCl_3$ at 300 and 75 MHz

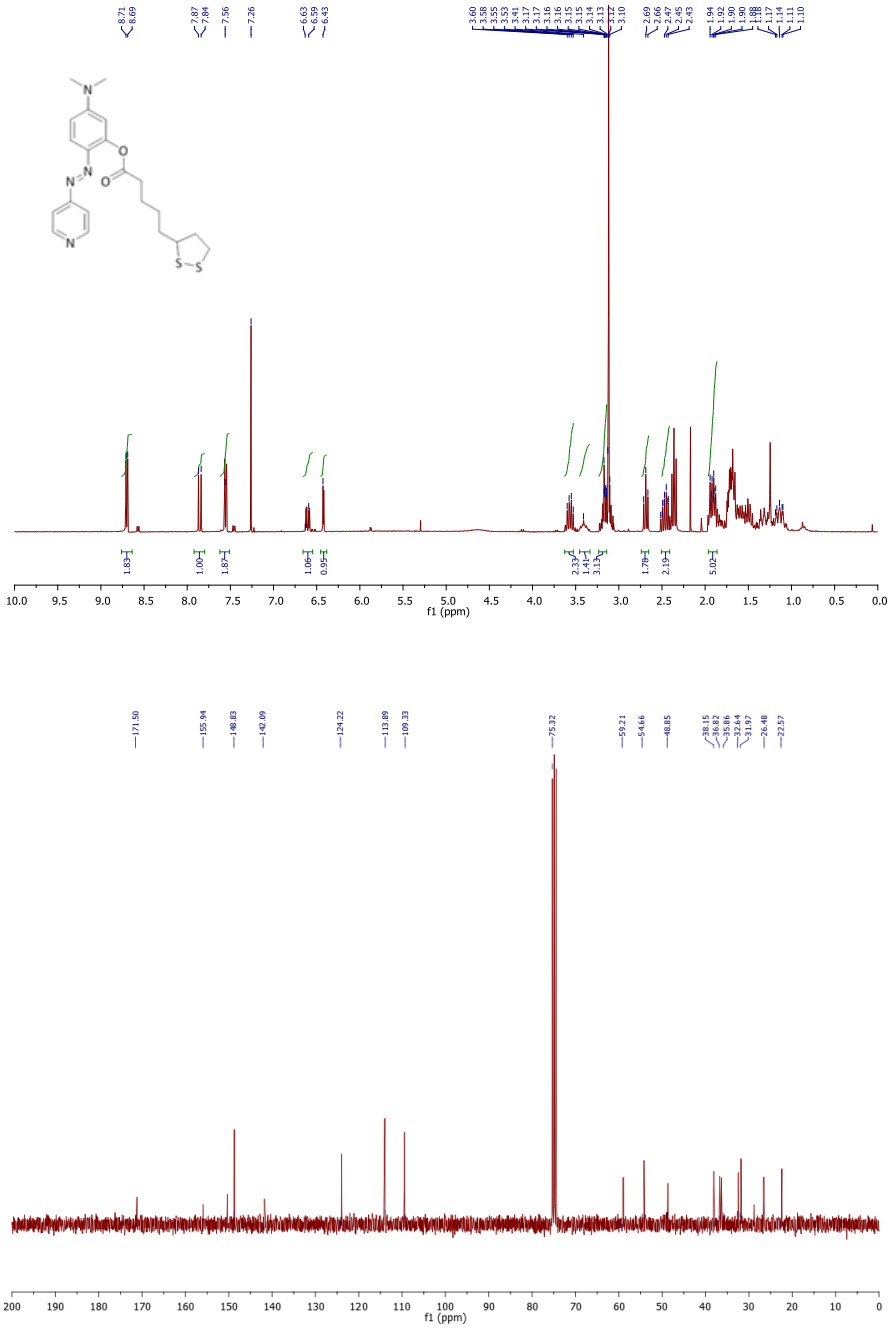

Figure S5. ^{1}H NMR and ^{13}C NMR spectrum of compound **10** in $CDCCl_3$ at 300 and 75 MHz

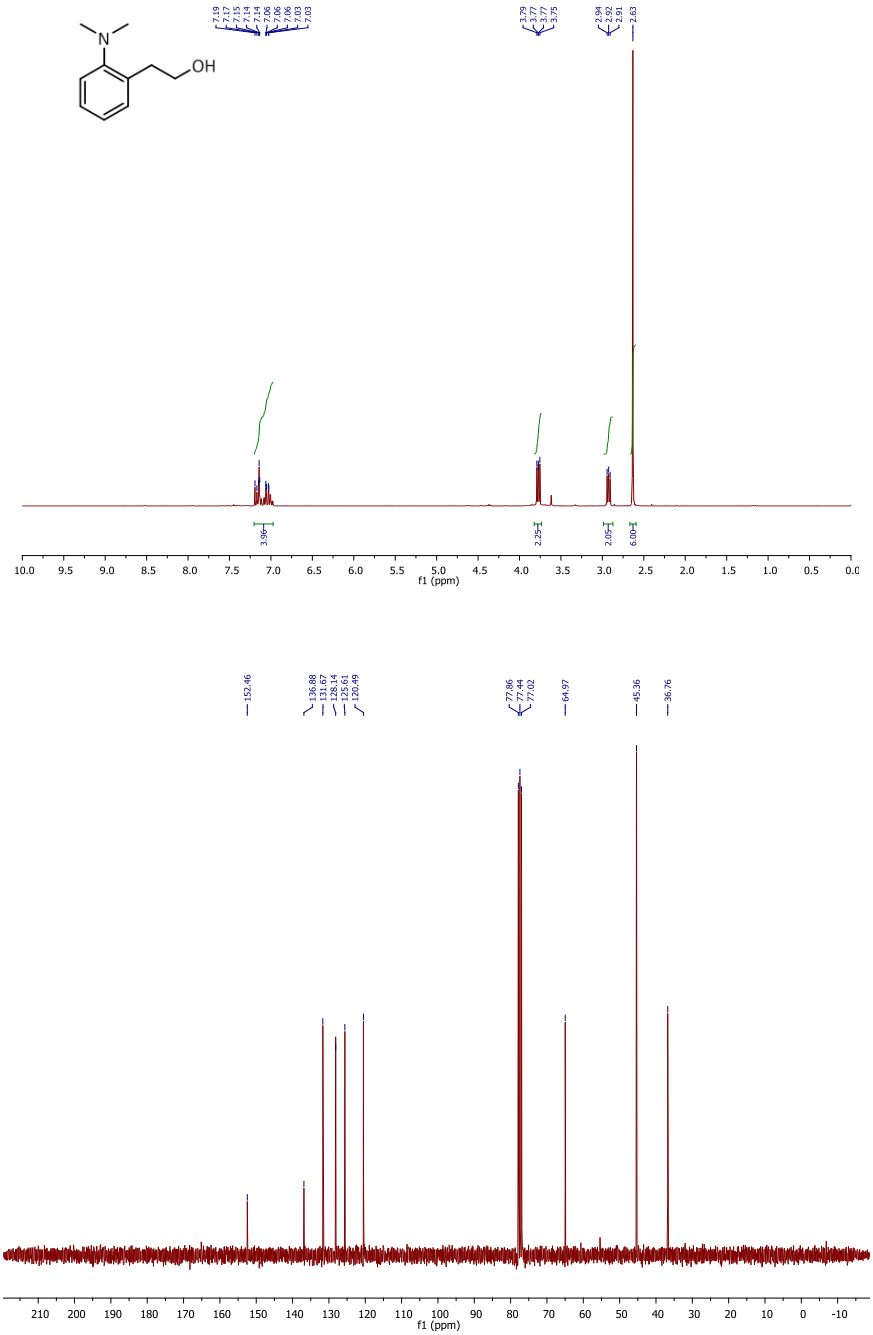

Figure S6. ^{1}H NMR and ^{13}C NMR spectrum of compound **11** in $CDCCl_3$ at 300 and 75 MHz

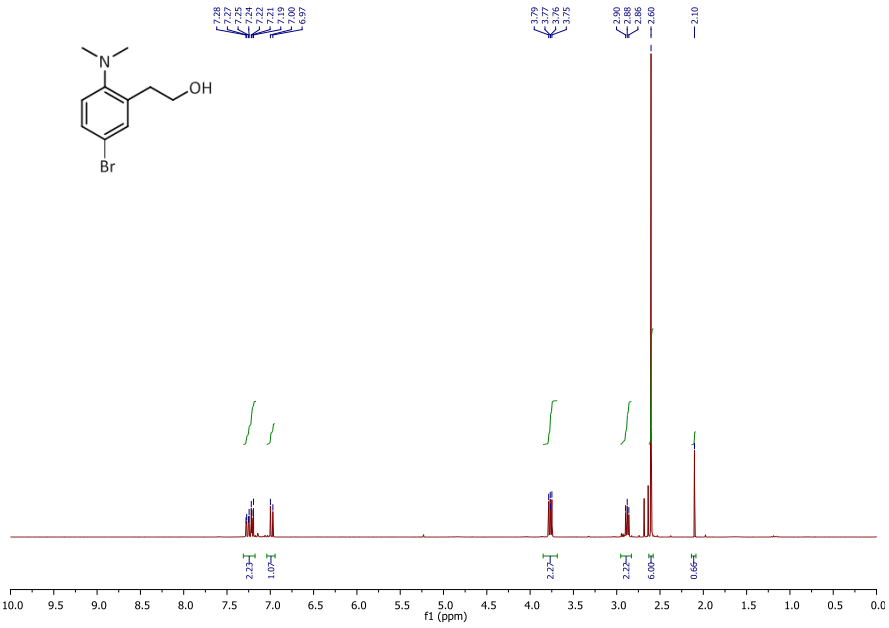

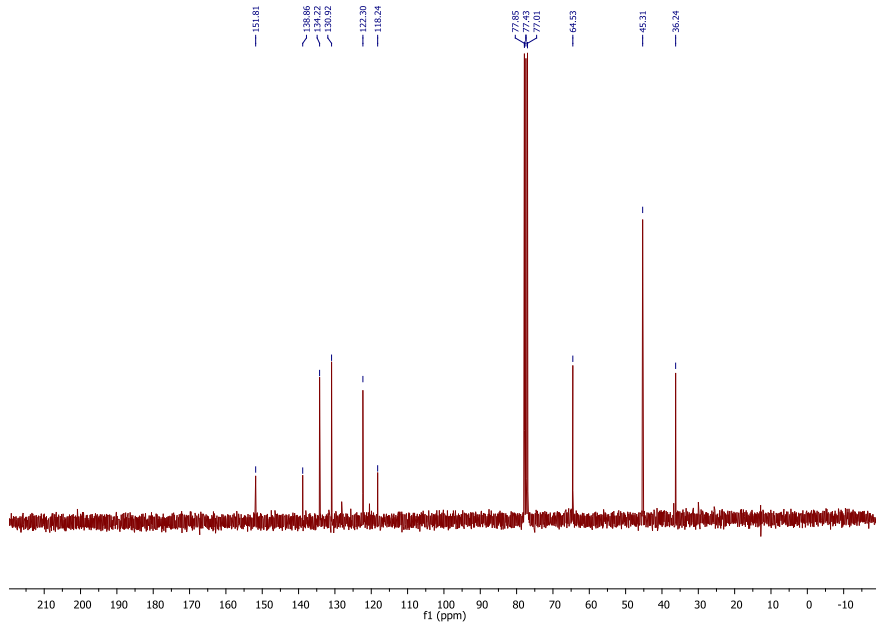

Figure S7. ^{1}H NMR and ^{13}C NMR spectrum of compound **12** in $CDCCl_3$ at 300 and 75 MHz

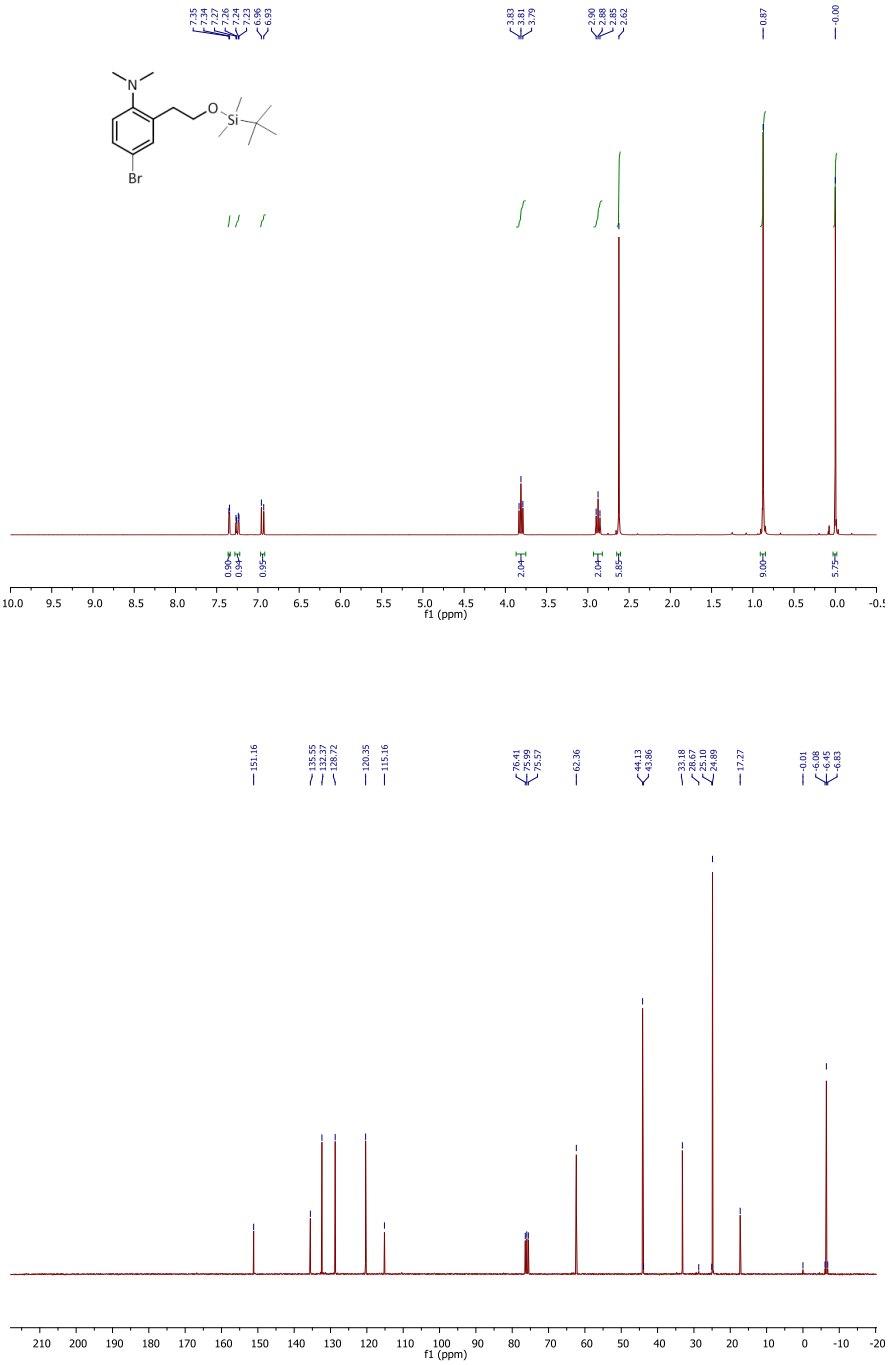

Figure S8. ^{1}H NMR and ^{13}C NMR spectrum of compound **13** in $CDCCl_3$ at 300 and 75 MHz

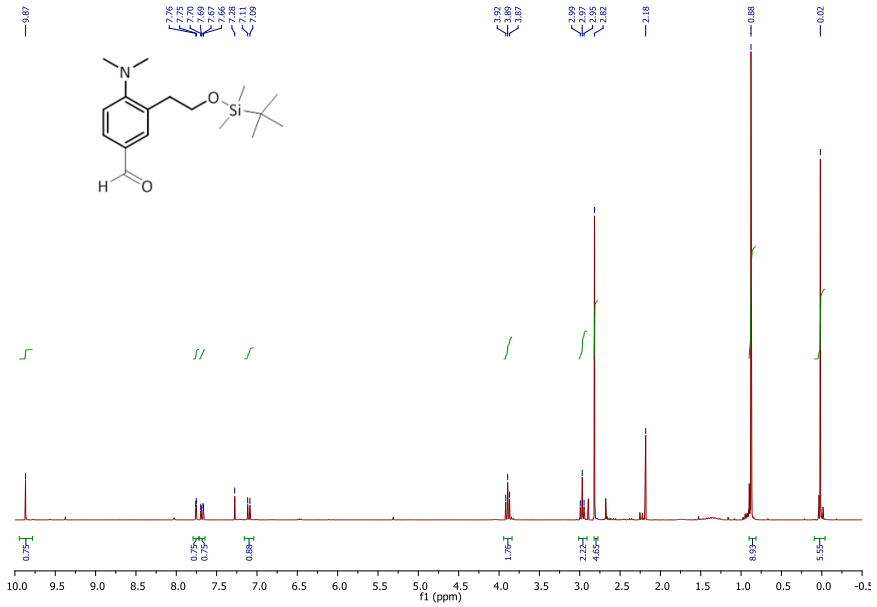

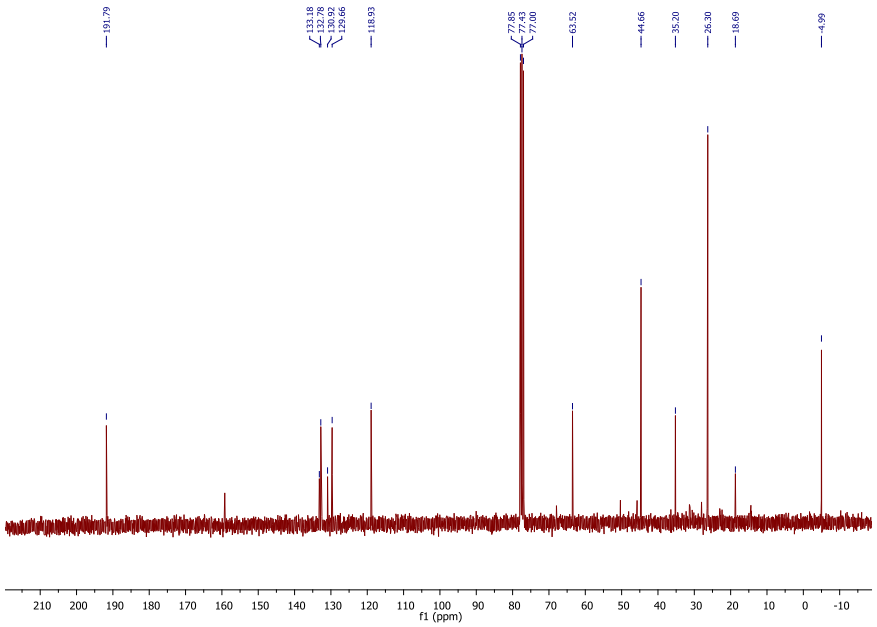

Figure S9. ^{1}H NMR and ^{13}C NMR spectrum of compound **14** in $CDCCl_3$ at 300 and 75 MHz

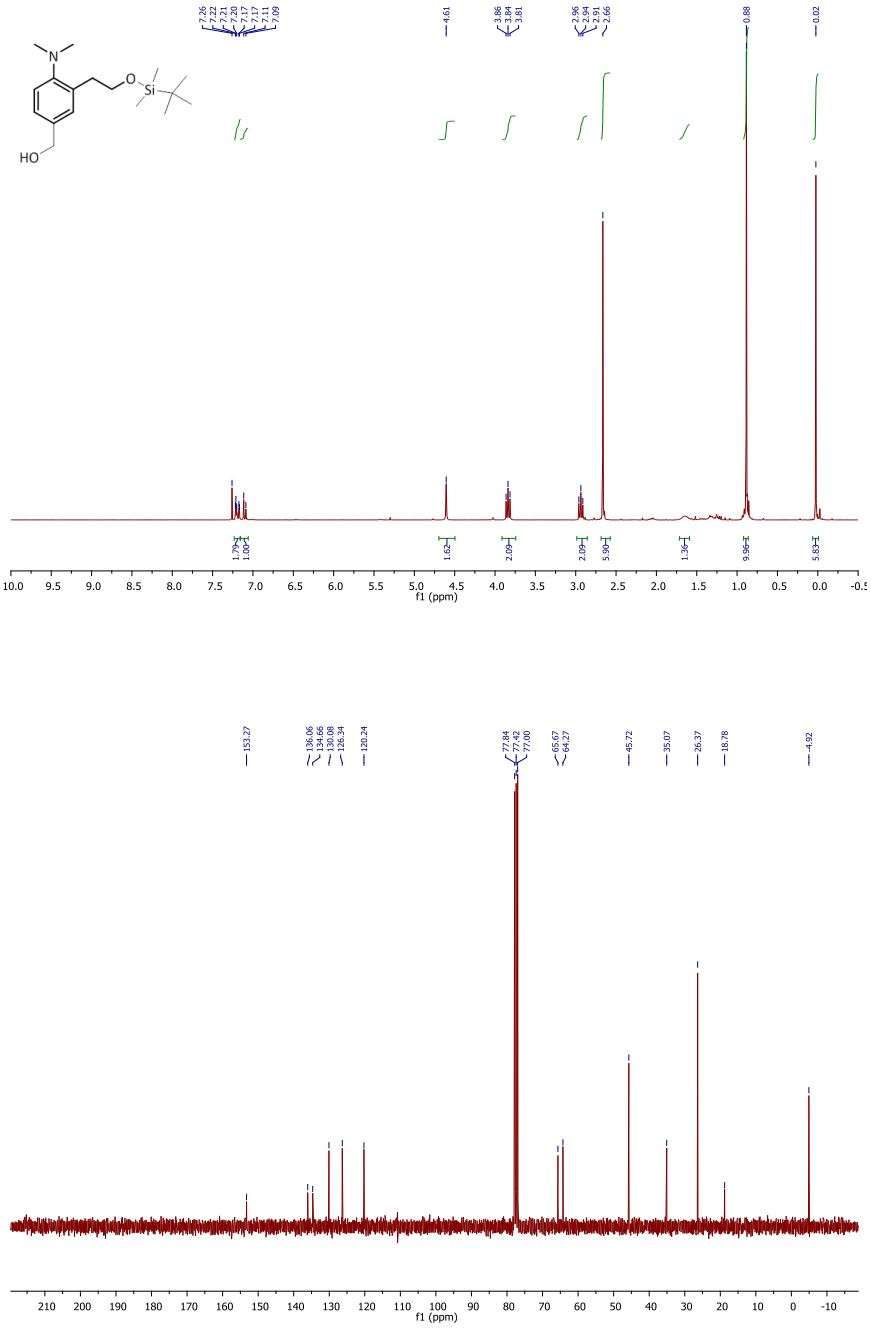

Figure S10. ^{1}H NMR and ^{13}C NMR spectrum of compound **15** in $CDCCl_3$ at 300 and 75 MHz

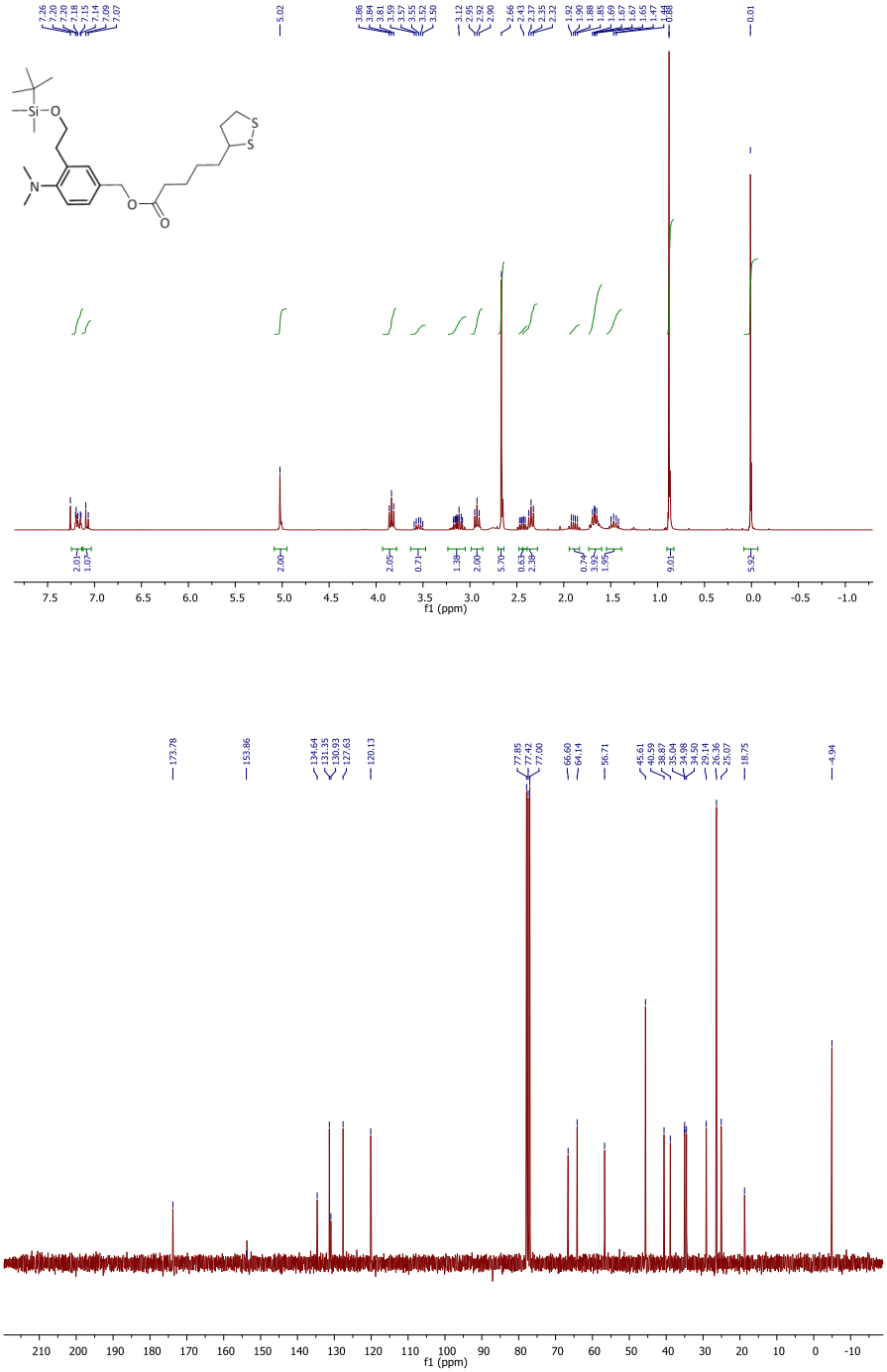

Figure S11. ^{1}H NMR and ^{13}C NMR spectrum of ligand **8** in CD_3OD at 300 and 75 MHz

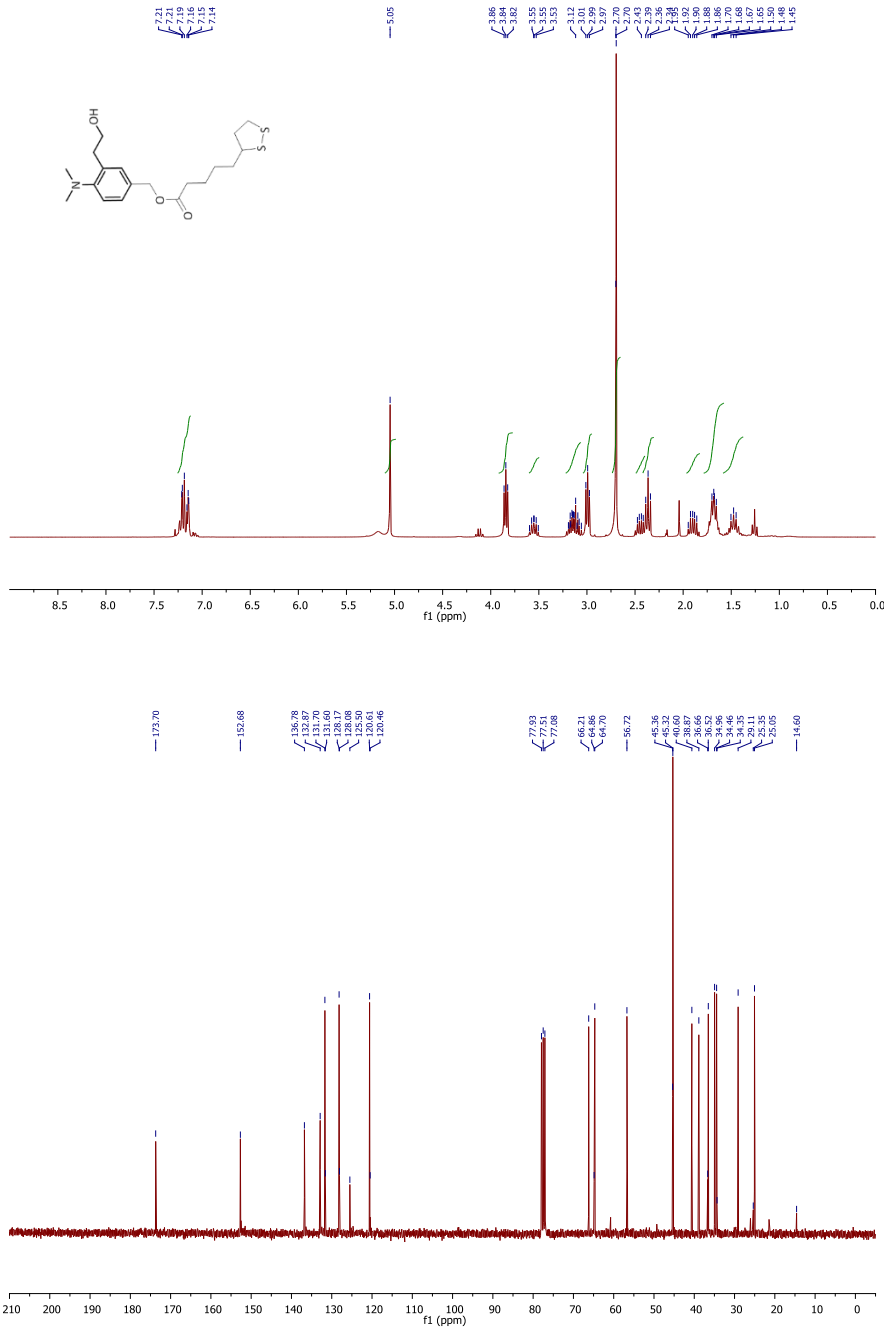

Figure S12. UV-vis spectra free ligands in CH_3CN solution.

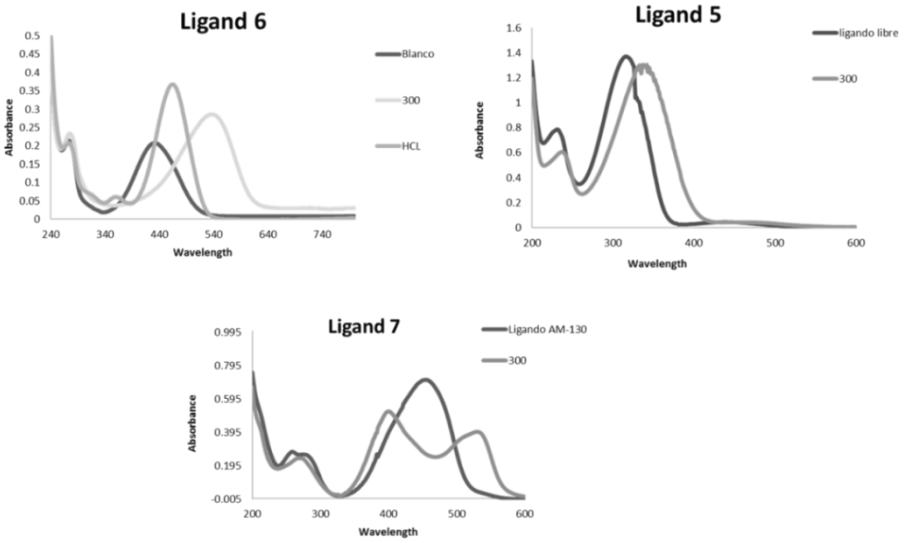

Figure S13. UV-vis spectra and A_{660}/A_{526} plots for AuNP

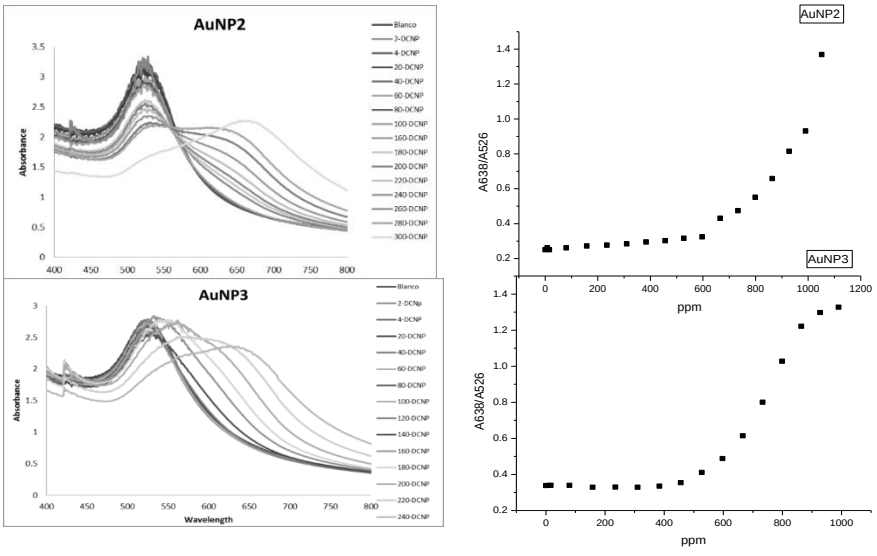

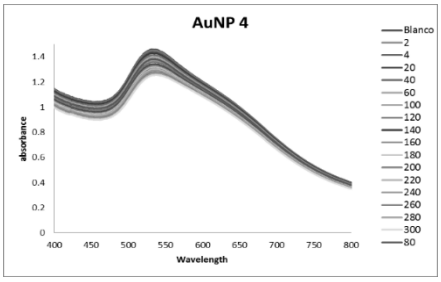
AuNP 4
absorbance
Wavelength
Blanco
2
4
20
40
60
100
120
140
160
180
200
220
240
260
280
300
80

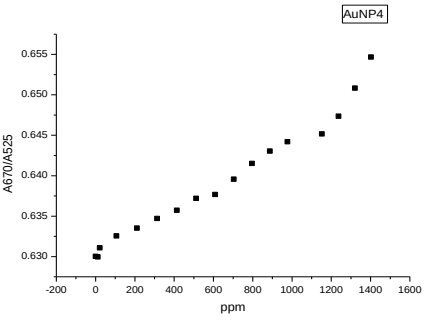
AuNP4
A670/A525
ppm

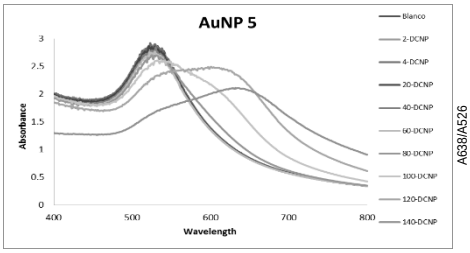
AuNP 5
Absorbance
Wavelength
Blanco
2-DCNP
4-DCNP
20-DCNP
40-DCNP
60-DCNP
80-DCNP
100-DCNP
120-DCNP
140-DCNP

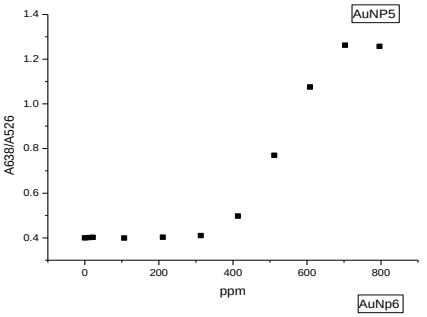
AuNP5
A638/A526
ppm

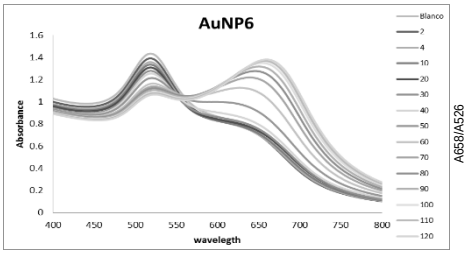
AuNP6
Absorbance
wavelegth
Blanco
2
4
10
20
30
40
50
60
70
80
90
100
110
120

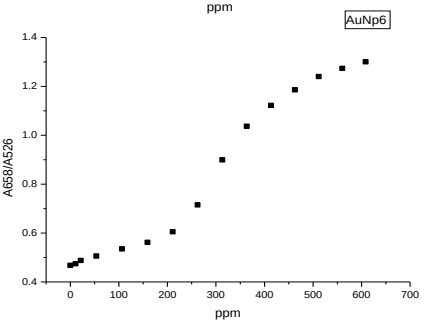
AuNp6
A658/A526
ppm

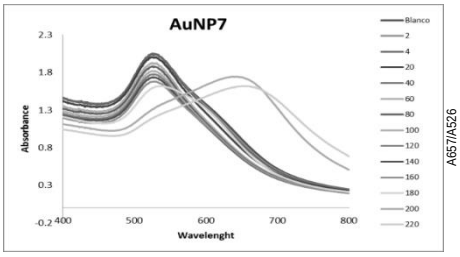
AuNP7
Absorbance
Wavelenght
Blanco
2
4
20
40
60
80
100
120
140
160
180
200
220

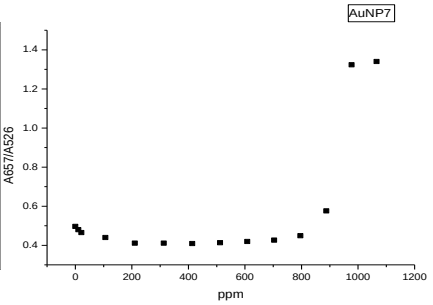
AuNP7
A657/A526
ppm

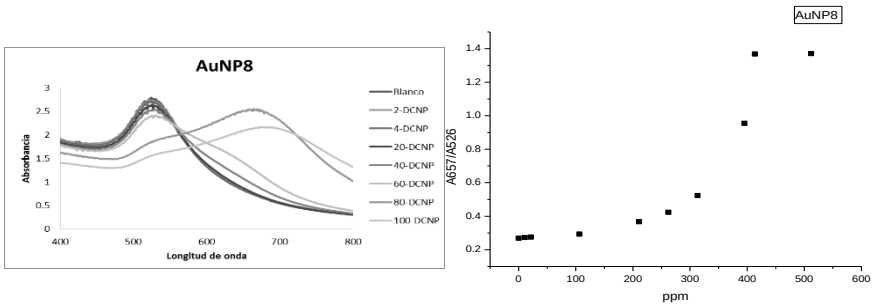

Determination of the Limits of Detection (LODs)

The limits of detection (LODs) were calculated from the plots of the ratio of the intensity of the absorbance at ca. 660 nm and ca. 526 (A_{660}/A_{526}) versus DCNP concentration expressed in ppm (mg/L). We arbitrarily define the LOD as the DCNP concentration at which a 10 % increase in the absorbance intensity ratio (A_{660}/A_{526}), can be measured.[1]

The A_{660}/A_{526} value of the blank solution (y_b), the LOD and the standard deviations were obtained from the slope of the calibration curves in the linear range.

As an example, the calculation of the LOD for **AuNP6** is described.

y_b= 0.470
$y_b + 0.1\ y_b = 0.517$
x = LOD = 76 ppm.

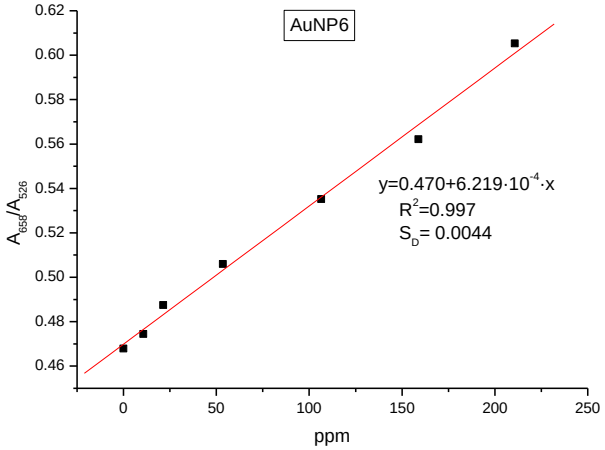

Table S1: Calculated LODs for AuNPs

	NPs2	**NPs3**	**NPs4**	**NPs5**	**NPs6**	**NPs7**	**NPs8**
y_b	0.251	0.335	0.631	0.399	0.470	0.406	0.270
LOD (ppm)	229	470	2400	340	76	750	81
S_D	0.0022	0.0087	$6.4 \cdot 10^{-4}$	0.069	0.0044	0.0062	0.0022

Figure S15. $A_{640}/A_{524} - (A_{640}/A_{524})_0$ changes of **AuNP5** in front of different interference agents and DCNP at analyte concentrations of 2.4 mM in buffered aqueous solution

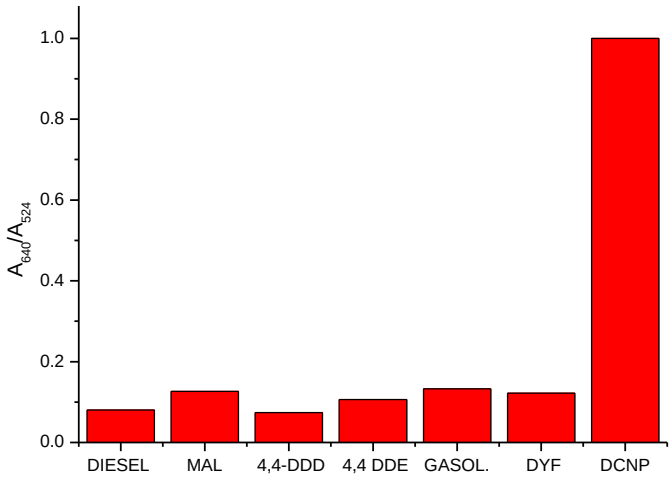

References

[1] B. Liu, H. Wang, T. Wang, Y. Bao, F. Du, J. Tian, Q. Li, R. Bai, *Chem. Commun.* **2012**, *48*, 2867-2869.

2.5. Triarylcarbinol functionalized gold nanoparticles for the colorimetric detection of nerve agent simulants

Triarylcarbinol functionalized gold nanoparticles for the colorimetric detection of nerve agent simulants.

Almudena Martí, Ana M. Costero, Pablo Gaviña*, Margarita Parra.

Centro Mixto de Reconocimiento Molecular y Desarrollo Tecnológico (IDM), Universidad de Valencia-Universidad Politécnica de Valencia, Dr. Moliner, 50, 46100 Burjassot,
Valencia, Spain

Revised: 27 March 2014.
Available online: 5 April 2014.

Tetrahedron Letters, **2014**, 55, 3093–3096.

The detection of chemical warfare (CW) through a simple colorimetric method is an area of increasing interest. Among CW, nerve agents have received a lot of interest in the last few years since they are especially dangerous species and poisoning may occur through inhalation or consumption of contaminated liquids or foods.[1] Chemically, nerve agents are highly toxic phosphonic acid esters, structurally related to the larger family of organophosphorus compounds. The extreme toxicity of these compounds is due to their ability to bind primarily and rapidly to acetylcholinesterase in the neuromuscular junction of the central nervous system.[2]

Detection protocols for nerve agents are mainly based on enzymatic assays and physical measurements.[3] However, these protocols usually have limitations such as a certain level of complexity, high cost, and low portability. In the last years, the detection systems based on fluorogenic and chromogenic sensors have gained interest to overcome many of the previous limitations.[4] Colorimetric detection is particularly appealing because it uses low-cost, widely available instruments and the presence of the analyte can be detected by the naked eye.

Functionalized gold nanoparticles (AuNPs) have recently attracted interest in sensor applications.[5] The sensing strategy is based on the color change that arises from the interparticle Plasmon coupling that occurs during the aggregation of AuNPs or the dispersion of AuNPs aggregates. The red color of dispersed nanoparticles turns to dark blue upon aggregation and the color change can be observed by the naked eye even at low concentrations.[6]

Our research group has recently reported a new approach for the direct colorimetric detection of the nerve agent simulant DCNP (Fig. 1) using thioctic acid capped AuNPs functionalized with pyridine ligands. Upon reaction with DCNP, positive charges are generated on the surface of the dispersed anionic nanoparticles triggering their aggregation with the resulting change in the color of the solution.[7]

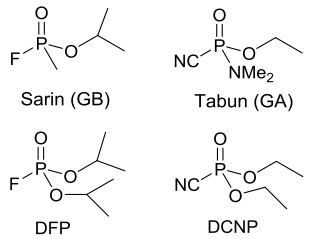

Figure 1. Chemical structures of nerve agents and the simulants used in this study.

On the other hand we have recently developed a new family of reagents for the chromogenic detection of nerve agent simulants DCNP and DFP based on the use of triarylcarbinols. Triarylcarbinols can be converted into their

corresponding carbocations in the presence of nerve agent simulants resulting in strong color changes (Fig. 2, bottom).[8]

Herein, we want to extend these studies toward the direct colorimetric detection of DCNP and DFP simulants using thioctic acid capped AuNPs functionalized with a triarylcarbinol derivative. Thus, the reaction of the anionic AuNPs with the nerve agent simulants should generate positive charges on the surface of the nanoparticles inducing their aggregation (Fig. 2, top). This should produce a change in the surface Plasmon resonance absorption of the AuNPs and consequently a change in their color. It is noteworthy that despite the growing interest in the use of functionalized AuNPs as sensors, only few articles have been published on the detection of organophosphorus compounds, always via an indirect process.[9] Therefore we believe that this is a field that requires deeper study.

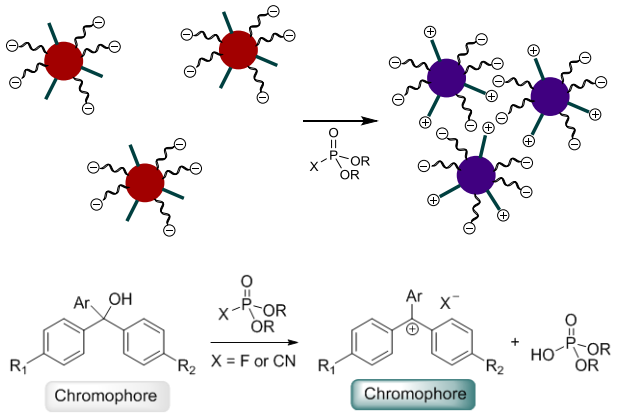

Figure 2. Paradigm of the sensing mechanism using functionalized anionic AuNPs: reaction of the terminal ligands with the simulant produces positive charges which can compensate the negative charges of the nanoparticles inducing their aggregation (top). Colorimetric sensing using triarylcarbinols: The hydroxyl group undergoes phosphorylation, followed by elimination to generate the corresponding colored carbocation (bottom).

Triarylcarbinol **1** (Scheme 1) was synthesized from 2-(4 bromophenoxy)ethanol, 4-(dimethylamino)benzophenone, and BuLi in THF. The carbinol was obtained in a 50% yield after column chromatography. In order to attach the triarylcarbinol to the surface of the AuNPs, taking advantage of the strong affinity of gold for disulfide groups, the less hindered primary alcohol was esterified with thioctic acid in the presence of DCC and DMAP[10] to yield ligand **L**. The chemical structure and purity of **L** were confirmed by spectroscopic techniques

(see SI). The absence of absorption bands in the visible region of the UV–vis spectrum is noteworthy, indicating the absence of carbocation from dehydration reactions.

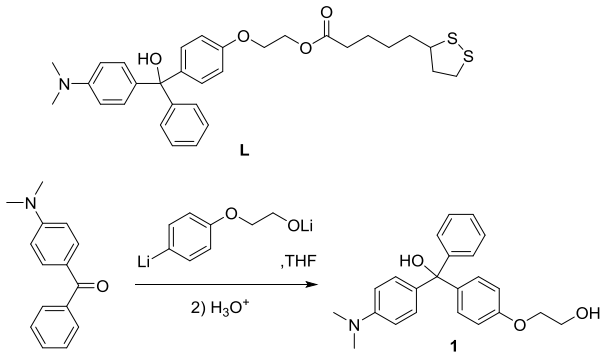

Scheme 1. Ligand L to be attached to the AuNPsans synthesis of triarylcarbinol **1.**

The corresponding triaryl carbonium ion, which was generated by the addition of concd HCl to DMF or acetonitrile solutions of the ligand, showed a broad UV–vis absorption band centered at 520 nm (5× 10^{-5} M in DMF).

The functionalized gold nanoparticles were synthesized by a two-step procedure. First citrate-stabilized nanoparticles were prepared by reducing tetrachloroauric acid with trisodium citrate in boiling water.[11] Monodisperse citrate-stabilized nanoparticles were obtained with an average size of 13 nm, as determined by TEM, and with a Z-potential value of -72.6 mV. The surface plasmon peak appeared at 526 nm. The initial concentration of the citrate capped AuNPs was calculated to be 3.4 × 10^{-9} M according to the Lambert–Beer's Law from an estimated molar extinction coefficient of ε = 2.47 × 10^{8} $M^{-}1$ $cm^{-}1$ (obtained from the plot of e vs nanoparticle size previously reported).[7] In a second step, in a ligand-exchange reaction the citrate was replaced from the surface of the nanoparticles by a mixture of thioctic acid and ligand L, in an optimized ratio of 1:2. The pH of the aqueous solution was previously adjusted to 9.0 by addition of NaOH. The functionalized AuNPs (**NP1**) were then centrifuged and re-dissolved in DMF. These nanoparticles were neither stable in water nor in aqueous buffer solutions probably due to a slow dehydration of the carbinols leading to aggregation processes. This item was confirmed by studying the behavior of the free ligand **L** in buffer aqueous solution by UV–vis spectroscopy. The appearance of a new band at 510 nm corresponding to the triaryl carbonium ion could be observed within minutes.

DMF solutions of the triarylcarbinol functionalized AuNPs (**NP1**) exhibited the characteristic surface plasmon resonance (SPR) band at 526 nm in the UV–vis spectrum. As expected, the presence of DCNP or DFP promoted a decrease in the intensity of this peak and the appearance of a new peak at around 640 nm indicating the formation of AuNP clusters. These results are consistent with the phosphorylation of the tertiary alcohol followed by an elimination reaction to generate the corresponding carbocation as shown in Figure 2.

Figure 3 shows the results of UV–vis titration studies performed with DMF solutions of our material in the presence of increasingamounts of DCNP and DFP. These changes in the spectra are concomitant with a change in the color of the solution from red to dark blue.

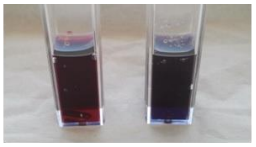

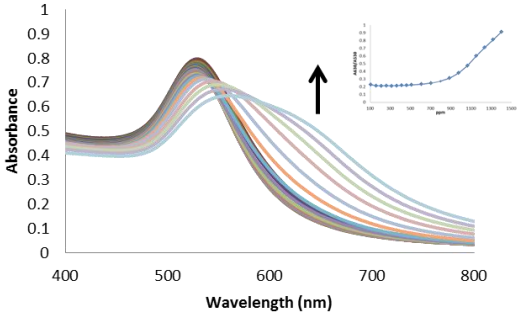

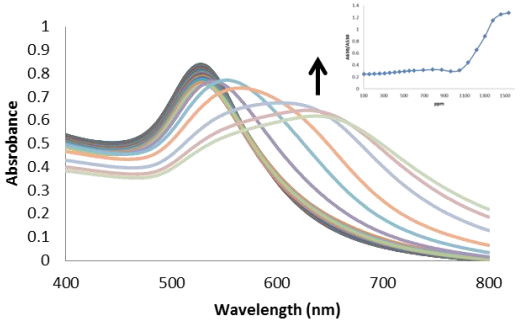

Figure 3. Color change observed on the solution of NP1 in DMF upon addition of the simulants (top). UV-vis spectra of the triarylcarbinol functionalized AuNPs on addition of increasing amounts of DCNP (middle) and DFP (bottom) expressed in ppm (mg/L). Insets: Plots A640/A526 vs. DCNP and DFP concentration respectively.

The variation of the ratio of the absorbance intensities of **NP1** at 640 nm and 526 (A_{640}/A_{526}) versus DCNP or DFP concentration is also presented (insets of Fig. 3). A very significant increase in the A_{640}/A_{526} ratio was observed as the concentration of stimulant was increased. The limits of detection (LODs) expressed in ppm (v/v) obtained from these plots were 560 for DCNP and 465 for DFP. To achieve a better understanding of the reaction, kinetic studies on the reactivity of the nanoparticles **NP1** in the presence of DFP were carried out in DMF solutions by using an excess of the simulant. The changes in the absorbance intensity of the aggregation band (A_{640}) in the UV–vis spectra versus the reaction time are shown in Figure 4. As expected, an increase in the absorbance with time is observed until a plateau is reached at about 9 min of reaction.

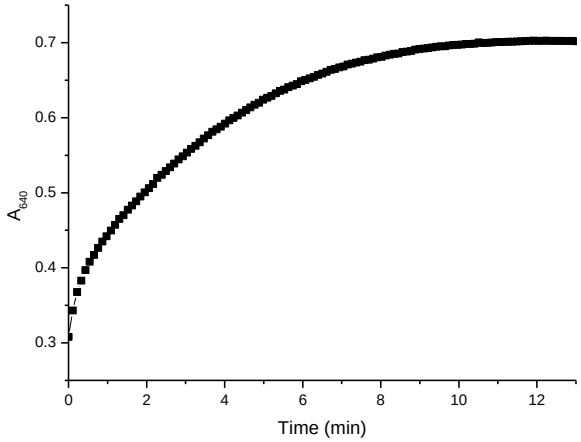

Figure 4. Changes in the aggregation absorbance band (A_{640}) vs. reaction time for NP1 in DMF upon addition of excess of DFP (8 mM).

It is well known that cyanide anions are capable of dissolving metals such as Au and Ag in the presence of oxygen upon the formation of soluble metal-cyanide complexes.[12] In order to evaluate if the cyanide which is released upon the reaction of our material with DCNP has influence in the obtained results, we studied the behavior of DMF solutions of NP1 in the presence of an excess of KCN.

TEM studies proved that there had been a gradual dissolution of the gold nanoparticles due to the etching by cyanide, reaching an average size of ca. 4–6 nm, which was not observed for solutions of **NP1** exposed to DCNP (Fig. 5). Additionally, the UV–vis spectra in DMF showed a slight bathochromic displacement of the Plasmon band to 540 nm which can be attributed to the corresponding change in

the nanoparticle size. These results confirm that the behavior of **NP1** in the presence of DCNP or excess cyanide is clearly different.

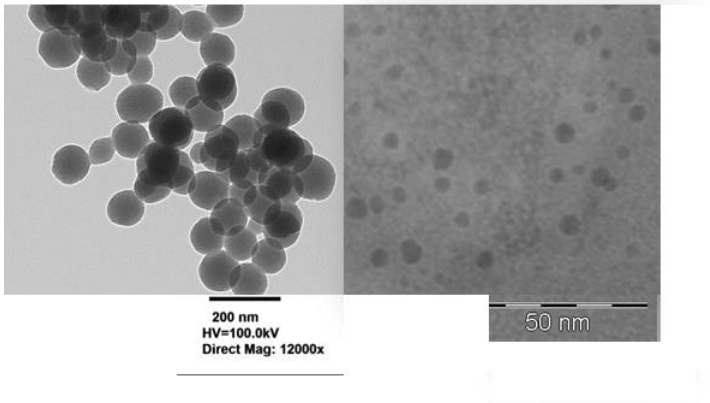

Figure 5. TEM images of NP1 upon addition of excess DCNP (left) and upon addition of excess KCN (right) at a resolution of 200 nm.

In order to demonstrate the selectivity of the system, studies were undertaken which confirmed that **NP1** only showed modest responses (or no response at all) in its UV–vis spectra with some of the interference agents that may be present in a military or civilian settings such as some pesticides (malathion, dyfonate, 4,4'-DDD, 4,4'-DDE), gasoline, and diesel fuel at concentrations of 2.4 mM in DMF solution (see Fig. S4). No changes in the color of the solutions could be observed with any of these interferents, the gold nanoparticles remaining stable as a red monodispersion.

In summary, we have synthesized triarylcarbinol functionalized gold nanoparticles **NP1** for the colorimetric detection of DCNP and DFP nerve agent simulants. The detection process is based on the compensation of charges at the surface of the nanoparticles, which triggers their aggregation resulting in a bathochromic shift in the Plasmon resonance band.

Acknowledgments

We thank the Spanish Government and the European FEDER funds (project MAT2012-38429-C04-02) for support. A.M. is grateful to the Spanish Government for a fellowship. SCSIE (Universidad de Valencia) is also gratefully acknowledged for all the equipment employed.

Supplementary data

Supplementary data (General synthetic procedures. Synthesis and spectroscopic data of compounds 1 and L. Copies of 1H and 13C NMR and HRMS spectra. Interference studies.) Associated with this article can be found, in the online version, at http://dx.doi.org/10.1016/j.tetlet.2014.03.139.

References and notes

1. (a) Kim, H. J.; Lee, J. H.; Lee, H.; Lee, J. H.; Lee, J. H.; Jung, J. H.; Kim, J. S. *Adv. Funct. Mater*., **2011**, 21, 4035–4040; (b) Hill, K. H., Jr.; Martin, S. J. Pure Appl. Chem. 2002, 74, 2285–2291.

2. Somani, S. M. *Chemical Warfare Agents*; Academic Press: San Diego, **1992.**

3. Sun, Y.; Ong, K. Y. *Detection Technologies for Chemical Warfare Agents and Toxic Vapors*; CRC Press: Boca Ratón (Florida), **2005**.

4. (a) Kim, K.; Tray, O. G.; Atwood, S. A.; Churchill, A. G., *Chem. Rev*. **2011**, 111, 5345–5403; (b) Royo, S.; Martínez-Máñez, R.; Sancenón, F.; Costero, A. M.; Parra, M.; Gil, S., *Chem. Commun*., **2007**, 4839–4847.

5. (a) Chen, Y.-C.; Lee, I.-L.; Sung, Y.-M.; Wo, S.-P., *Sens. Actuators, B*, **2013**, 188, 354–359; (b) Li, H.; Yong, Y.-W., *Chin. Chem. Lett*., **2013**, 24, 545–552; (c) Knighton, R. C.; Sambrook, M. R.; Vincent, J. C.; Smith, S. A.; Serpell, C. J.; Cookson, J.; Vickers, M. S.; Beer, P. D. *Chem. Commun*. **2013**, 2293–2295; (d) Kumar, V.; Anslyn, E. V. *J. Am. Chem. Soc*. **2013**, 135, 6338–6344; (e) Wang, A.-J.; Guo, H.; Zhang, M.; Zhou, D.-L.; Wang, R.-Z.; Feng, J.-J. *Microchim. Acta* **2013**, 180, 1051–1057.

6. (a) Rastegarzadeh, S.; Rezaei, Z. B. *Environ. Monit. Assess*. **2013**, 185, 9037–9042; (b) Mayer, K. M.; Hafner, J. M. *Chem. Rev*. **2011**, 111, 3828–3857.

7. Martí, A.; Costero, A. M.; Gaviña, P.; Gil, S.; Parra, M.; Brotons-Gisbert, M.; Sánchez-Royo, J. F. *Eur. J. Org. Chem*. **2013**, 4770–4779.

8. (a) Gotor, R.; Royo, S.; Costero, A. M.; Parra, M.; Gil, S.; Martínez-Máñez, R.; Sancenón, F. *Tetrahedron* **2012**, 68, 8612–8616; (b) Royo, S.; Gotor, R.; Costero, A. M.; Parra, M.; Gil, S.; Martínez-Máñez, R.; Sancenón, F. *New J. Chem*. **2012**, 38, 1485–1489; (c) Costero, A. M.; Parra, M.; Gil, S.; Gotor, R.; Martínez-Máñez R.; Sancenón, F.; Royo, S. *Eur. J. Org. Chem*. **2012**, 4937–4946.

9. (a) Wei, M.; Zeng, G.; Lu, Q. *Microchim. Acta* **2013**. http://dx.doi.org/10.1007/s00604-013-1078-4; (b) Liu, B.; Qu, W. S.; Chen, W. W.; Zhong, W.; Wang, Z.; Jiang, X. X. *Anal. Chem*. **2010**, 82, 9606–9610; (c) Sun, J.; Guo, L.; Bao, Y.; Xie, J. *Biosens. Bioelectron*. **2011**, 28, 152–157; (d) Li, H.; Guo, J.; Ping, H.; Liu, L.; Zhang, M.; Guen, F.; Sun, C.; Zhang, Q. *Talanta* **2011**, 87, 93–99.

10. Yin, J.; Wu, T.; Song, J.; Zhang, Q.; Liu, S.; Xu, R.; Duan, H. Chem. Mater. 2011, 23, 4756–4764.

11. (a) Haiss, W.; Thanh, N. T. K.; Aveyard, J.; Fernig, D. G. *Anal. Chem*. **2007**, 79, 4215–4221; (b) Kong, B.; Zhu, A.; Luo, Y.; Tian, Y.; Yu, Y.; Shi, G. *Angew. Chem*., *Int. Ed*. **2011**, 50, 1837–1840.

12. (a) Kim, M. H.; Kim, S.; Jang, H. H.; Yi, S.; Seo, S. H.; Han, M. S. Tetrahedron Lett. 2010, 51, 4712–4716; (b) Shang, L.; Jin, L.; Dong, S. Chem. Commun. 2009, 3077–3079; (c) Liu, X.; Basu, A. Langmuir 2008, 24, 11169–11174.

Supplementary Material

Triarylcarbinol functionalized gold nanoparticles for the colorimetric detection of nerve agent simulants

Almudena Martí, Ana M. Costero, Pablo Gaviña* and Margarita Parra

Centro Mixto de Reconocimiento Molecular y Desarrollo Tecnológico (IDM), Universidad de Valencia-Universidad Politécnica de Valencia, Dr. Moliner, 50, 46100 Burjassot, Valencia, Spain

General procedures:

All reagents were commercially available, and were used without purification. Silica gel 60 F_{254} (Merck) plates were used for TLC. Milli-Q ultrapure water was used for the synthesis of AuNPs. ^{1}H-NMR spectra were recorded on a Bruker 300 MHz spectrometer. Chemical shifts are reported in ppm units with tetramethylsilane as an internal standard. UV-vis absorption spectra were recorded using a 1 cm path length quartz cuvette on a Shimadzu UV-2101PC spectrophotometer. All measurements were carried out at 293 K (thermostated). Z-potential values were measured in a Malvern Zetasizer ZS, for 3 times in 10-25 cycles. The electronic images were made on a JEOL-1010 transmission electron microscope operating at 100 KV. High resolution mass spectrum was recorded in the positive ion mode on an AB Sciex Triple TOF 5600 mass spectrometer.

Syntheses

2-(4-((4-(dimethylamino)phenyl)(hydroxy)(phenyl)methyl)phenoxy)ethan-1-ol (1)

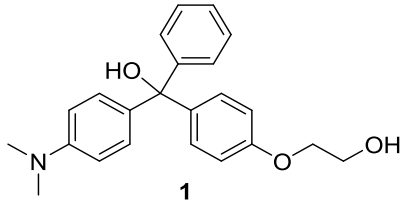

1

2-(4-bromophenoxy)ethanol (217 mg, 1 mmol) was dissolved in 20 mL of anhydrous THF under Ar atmosphere. The solution was cooled to -70 ^{o}C. n-Butyllithium (2,2 mmol of 2.88 M solution in hexane) was added dropwise via a syringe under continuous stirring. The mixture was left at -70 ^{o}C for 30 min. After this time 4-(dimethylamino)benzophenone (227 mg, 0.7 mmol) was added as a solid under stirring, and the mixture was allowed to warm to room temperature and left for 2 h. Saturated aqueous solution of $NaHCO_3$ (50 mL) was added to quench the reaction, and ethyl acetate (50 mL) was used to extract the crude product. The organic phase was washed with 50 mL of brine and dried over anhydrous $MgSO_4$. The insoluble solids were removed by filtration, and ethyl acetate was concentrated using a rotary evaporator. The crude product was further purified by silica gel column chromatography using hexane/ethyl acetate (3:7, v/v) as eluent. After removing all the solvents, carbinol **1**, was isolated as a pale green solid (196 mg, 50% yield).

^{1}H NMR (300 MHz, $CDCl_3$) δ 7.30-7.22 (m, 5H), 7.18 (d, *J*= 9.0 Hz, 2H), 7.07 (d, *J* = 9.0 Hz, 2H), 6.80 (d, *J* = 9.0 Hz, 2H), 6.65 (d, *J* = 9.0 Hz, 2H), 4.04-3.99 (m, 2H), 3.92-3.87 (m, 2H), 3.20 (br. s, 1H), 2.92 (s, 6H).

^{13}C NMR (75.5 MHz, $CDCl_3$): δ 157.6, 149.7, 147.7, 140.4, 135.3, 129.4, 128.9, 127.9, 127.0, 113.8, 111.9, 81.6, 69.3, 61.6 and 40.6.

Ligand L

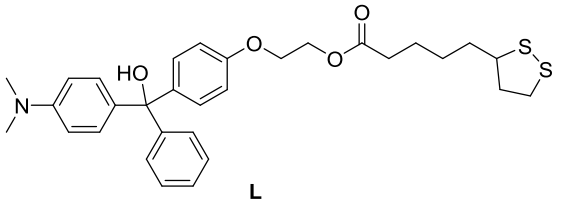

L

A 100 mL round-bottom flask was charged with lipoic acid (31 mg, 0.15 mmol), DCC (31 mg, 0.15 mmol), and anhydrous CH_2Cl_2 (20 mL). The reaction mixture was cooled to 0°C in an ice-water bath, and a solution of **1** (48 mg, 0.13 mmol), DMAP (cat. amount), and anhydrous CH_2Cl_2 (20 mL) was added dropwise over a period of 1 h under magnetic stirring. After the addition was completed, the reaction mixture was stirred at 0°C for 1 h and then allowed to warm to room temperature overnight. After removing the insoluble salts by filtration, the filtrate was concentrated and further purified by silica gel column chromatography using hexane/ethyl acetate (1:6, v/v) as an eluent. After removing all the solvents, the product **L** was obtained as a pink solid (23 mg, 32% yield).

^{1}H NMR (300 MHz, $CDCl_3$) δ 7.29–7.19 (m, 5H), 7.18 (d, *J*= 9.0 Hz, 2H), 7.05 (d, *J* = 9.0 Hz, 2H), 6.81 (d, *J* = 9.0 Hz, 2H), 6.63 (d, *J* = 9.0 Hz, 2H), 4.42-4.37 (m, 2H), 4.16-4.11 (m, 2H), 3.58–3.45 (m, 1H), 3.16-3.03 (m, 2H), 2.92 (s, 6H), 2.46-2.32 (m, 3H), 1.90 – 1.40 (m, 7H).

^{13}C NMR (75.5 MHz, $CDCl_3$): δ 173.5, 157.5, 149.7, 147.7, 140.5, 135.2, 129.3, 128.9, 127.9, 127.0, 113.9, 111.8, 81.6, 66.1, 62.9, 56.4, 40.6, 40.3, 38.6, 34.7, 34.1, 32.9, 28.8.

HRMS (ESI): *m/z* calcd. for $C_{31}H_{38}NO_4S_2$ $[M+H]^+$ 552.224; found 552.225.

Preparation of the functionalized gold nanoparticles NP1

All glassware was thoroughly cleaned with freshly prepared aqua regia (HCl: HNO_3, 3:1), rinsed thoroughly with deionized water and dried in air. AuNPs with a diameter of 13 nm ca. were synthesized as reported previously.[S1] Briefly, 10 mL of aqueous 38.8 mM trisodium citrate solution was added into 100 mL of 1 mM $HAuCl_4$ boiling solution and the resulting solution was kept continuously boiling for 30 min until a red solution was obtained. The solution was cooled to room temperature and was then stored in a refrigerator at 4°C for use. Modification of Au-NPs through the ligand-exchange reaction was performed at room temperature as follows: 20 µl of 0.01 M aqueous NaOH were added to 10 mL of the as-prepared citrate capped AuNPs. Then, 200 µl of TA (10^{-3} M in ethanol) and 400 µl of ligand **L** (10^{-3} M in DMF) were added simultaneously and the solution was stirred overnight. To purify the AuNPs, the mixture were centrifuged for 20 min at 14000 rpm and supernatants were decanted; then the resulting AuNPs were resuspended in DMF.

Figure S1. 1H NMR and 13C NMR spectra of compound 1 in CDCl3.

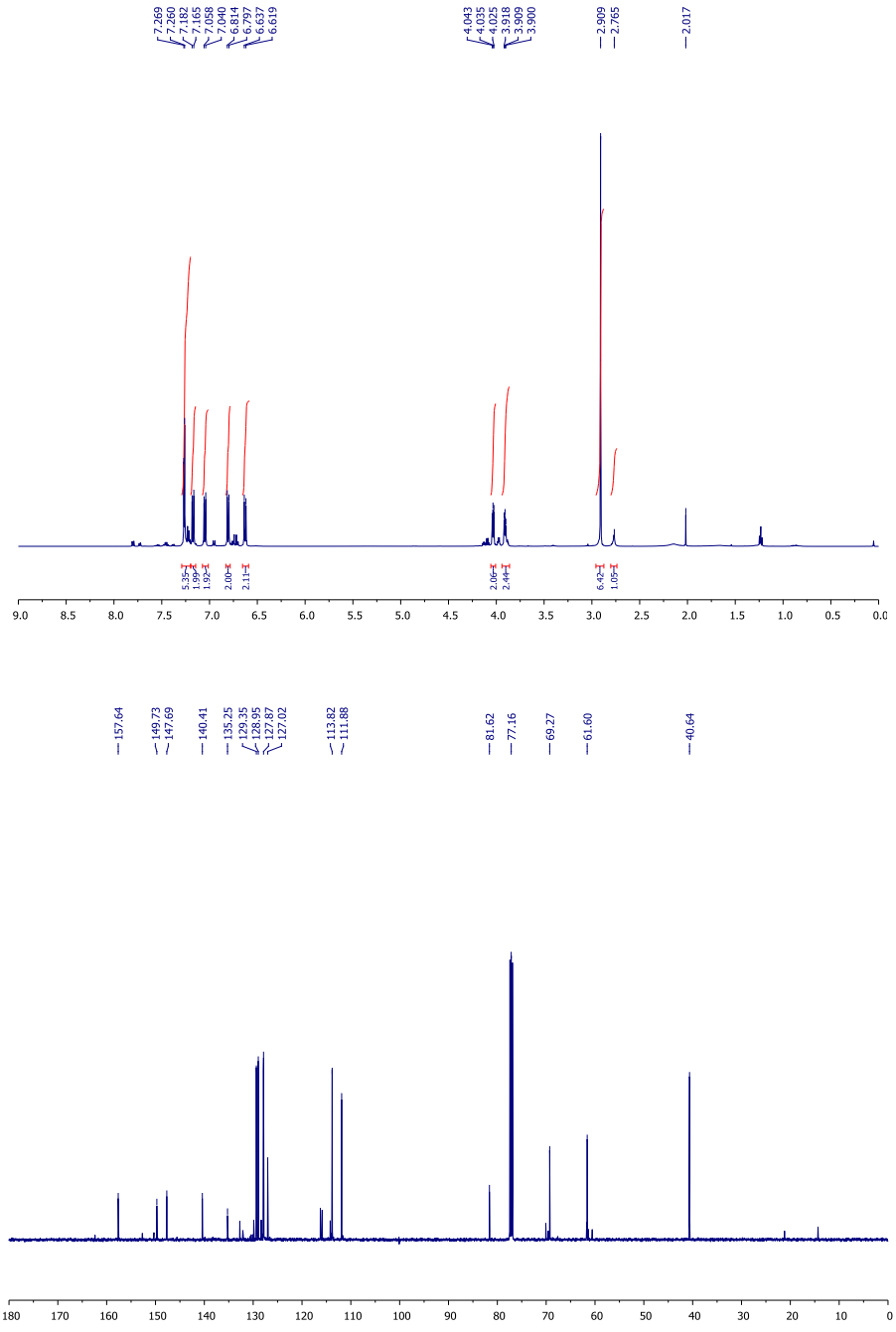

Figure S2. ^{1}H NMR and ^{13}C NMR spectra of ligand **L** in $CDCl_3$

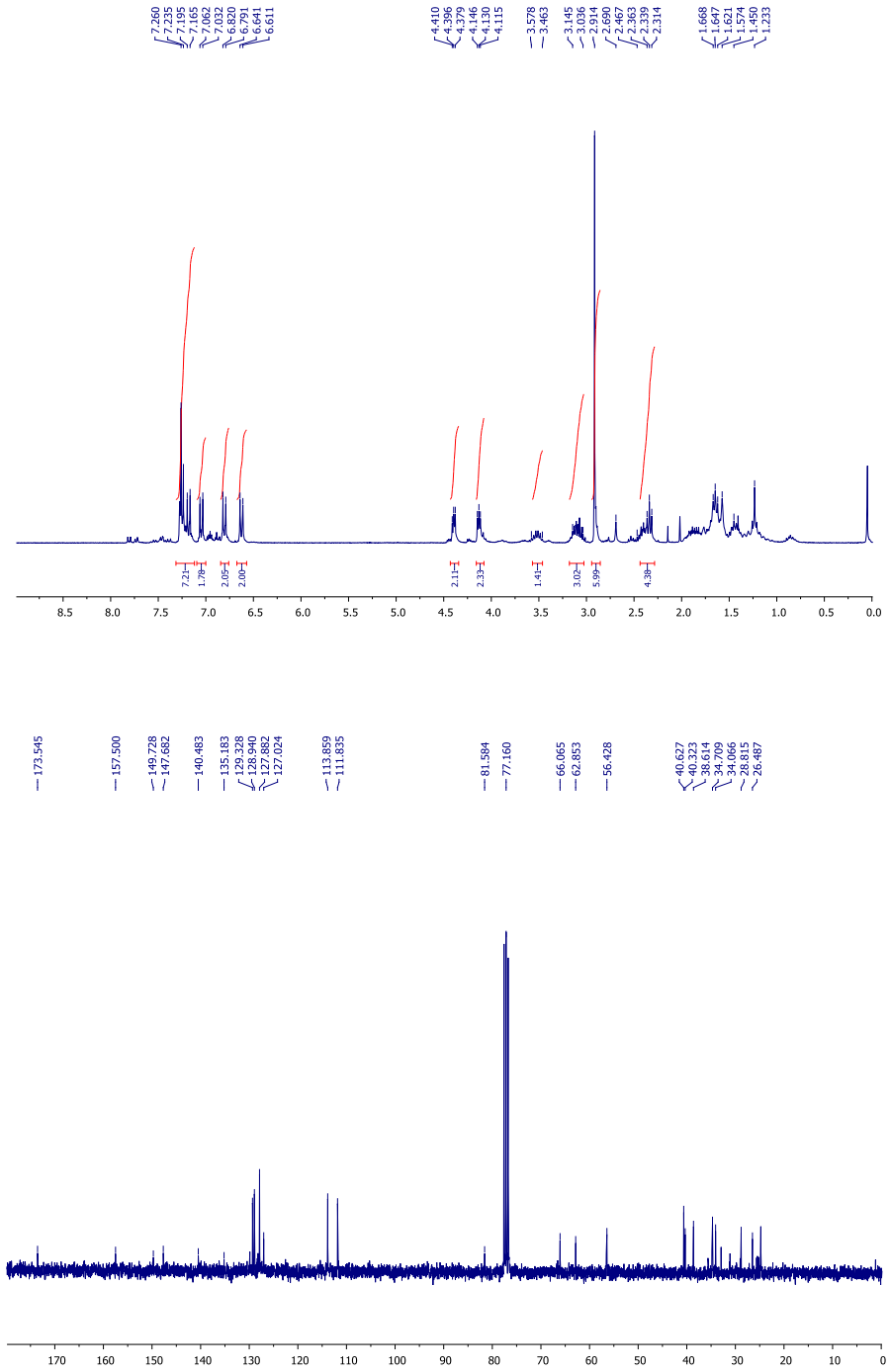

Figure S3. HRMS (ESI) of Ligand **L**

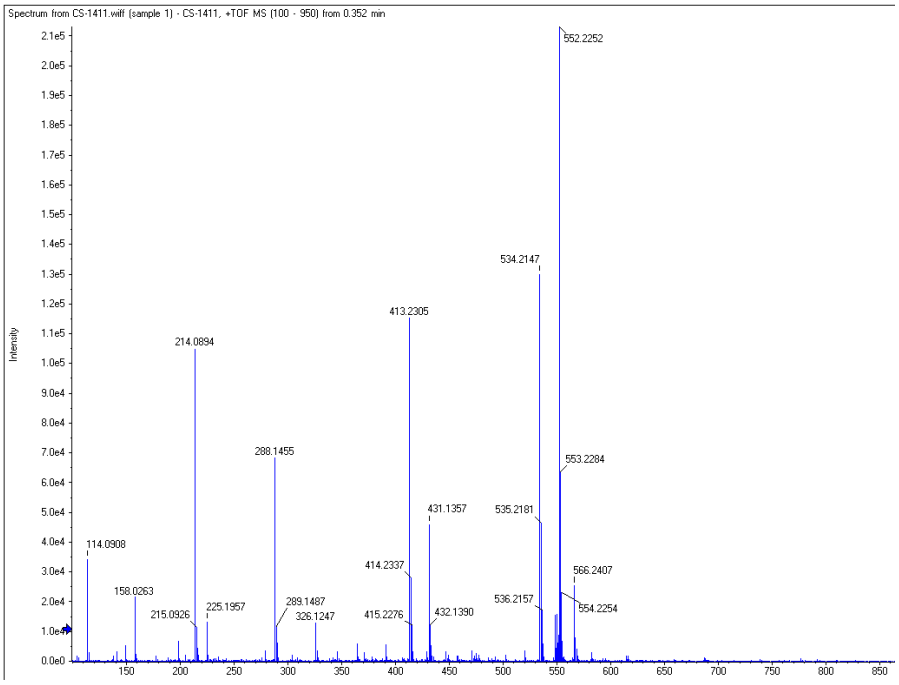

Figure S4. $A_{640}/A_{526} - (A_{640}/A_{526})_0$ changes of **NP1** in front of different interference agents and DCNP at analyte concentrations of 2.4 mM in DMF solution.

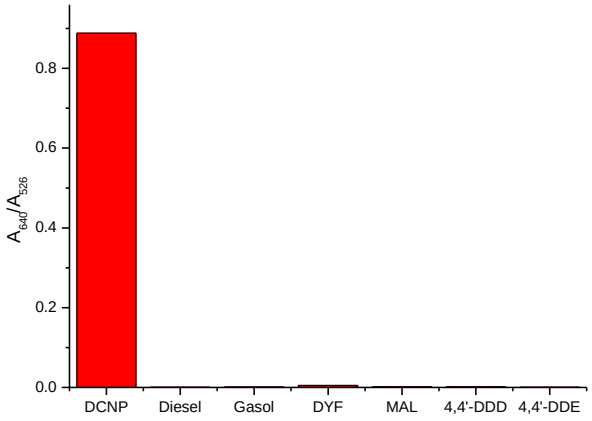

References

[S1] Kong, B.; Zhu, A.; Luo, Y.; Tian, Y.; Yu, Y.; Shi, G. *Angew. Chem. Int. Ed.* **2011**, *50*, 1837-1840.

CHAPTER 3:
Detection of Nitric Oxide

3.1. Chemical properties of NO relevant to Biology

Nitric oxide (NO) is a small uncharged gaseous free radical containing one unpaired electron. NO exist in space as an interstellar molecule and it has been detected in the atmosphere of Venus and Mars. On earth, NO has been recognized as an atmospheric pollutant and a potential health hazard.[68]

On the ither hand, in 1987 NO was reported to be the long-sought endothelium-derived relaxing factors (EDRF) known to regulate blood vessel relaxation in the cardiovascular system. This finding initiated tremendous research efforts to understand how NO functions in the organism. Consequent discoveries of its involvement in a range of processes such as signal transduction in the brain and inmate defense against and parasitic infections in the immune system led the magazine *Science* to designate NO as Molecule of the Year in 1992. In 1998, the discovery of NO as a signaling molecule in cardiovascular system was honored by the Nobel Prize in Physiology or Medicine awarded to Fuchgott, Ignarro and Murad. With this increasing attention given to NO studies, new measurement techniques have contributed to our understanding of this enigmatic molecule.

A growing body of evidence demonstrates that the role that NO plays in diverse systems is concentration dependent, and thus it is not surprising that defective NO production has been implicated in a range of disorders. For example, underproduction of NO is related to hypertension, impotence, arteriosclerosis, and susceptibility to infection. Diseases due to excessive NO production include immune-type diabetes, neurotoxicity associated with aneurysm, stroke and reperfusion injury, inflammatory bowel disease, rheumatoid arthritis, cancer, septic shock, multiple sclerosis, and transplant rejection.[69]

Unquestionably, reliable measurement of both NO production and its levels is important. Detection and quantification of NO in biological systems present significant analytical challenges for several reasons with the low concentration of NO produced *in vivo* being a major concern. NO is endogenously generated by NO synthase (NOS), of which there are three isoforms. In general, *nNOS* and *eNOS* release NO in the nanomolar range, whereas *iNOS* can release NO in the micromolar range for extended periods of time. NO can also be scavenged by reactions with electron-rich biomolecules such as hemoglobin and interaction with the d-orbitals of transition metal (particularly iron), or by oxidation with endogenous reactive oxygen species to form nitrite and nitrate in the cells. As a result, the average lifetime of NO is in the range of milliseconds to seconds.

---

[68] T. Nagano, *Chem. Rev*., **2002**, 102, 2135-1269.
[69] X. Ye, S. S. Rubakhin, and V. Sweedler, *Analyst*, **2008**, 133, 423-433.

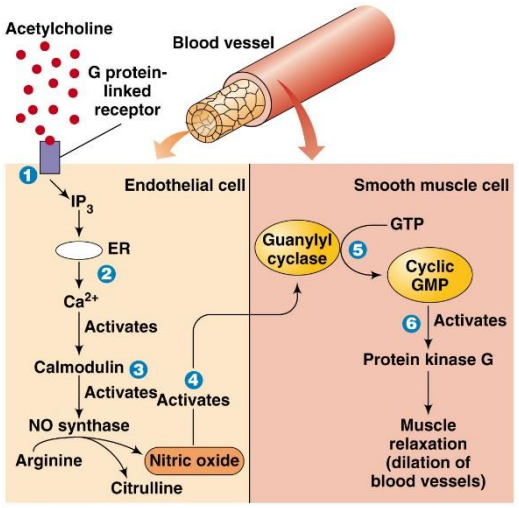

Figure 1: Nitric oxide couples G protein-linked receptor stimulation in endothelial cells to relaxation of smooth muscle cells in blood vessels. NO synthase converts arginine to citrulline and NO.

3.2. Environmental effects.

Air pollution constitutes on of the major problems in urban areas where many sources of air born pollutant are concentrated. The main source of air pollution are the combustion processes of fossil fuels used in power plants, vehicles and other incineration process. Key combustion–generated air contaminants are sulfur oxides (principally SO_2), particulate matter carbon monoxide, unburned hydrocarbons and nitrogen oxides (NO_x), which are mixtures of NO and NO_2. In the atmosphere, the ratio NO/NO_2 is determined by the intensity of sunshine (wich converts NO_2 to NO) and the concentration of ozone (which reacts with NO to again from NO_2). NO_x emission contributes too many environmental problems like acid rain, photochemical smog, greenhouse effect, etc. NO_x and many volatile organic compounds (VOC) are considered ground-level ozone precursors. Furthermore, the mixture of NO_x and VOC in the atmosphere exposed to sunlight can result in the formation of photochemical smog, whereas NO_2 together with sulfur dioxide SO_2 are the major contributors to acid rain. Acid rain is likely to generate further environmental effects like deforestation and soil and water acidification. It also

causes material losses, e.g. destruction of buildings and monuments, and crop damage.[70,71]

Restrictions regarding NO_x emission, which are being imposed by the Gothenburg and Kyoto Protocols. Interest in NO_x emission has been steadily increasing since 1952, when the role of nitrogen oxides in the formation of photochemical smog was formulated.[72]

Regardless of being the major component of NO_x, nitric oxide is much less toxic than nitric dioxide. It causes eye and throat irritation. As most radicals, NO is unstable and reacts readily with oxygen to form NO_2 which even at low doses can be a source of acute lung injury with pneumonitis and fulminant pulmonary edema.

3.3. Chemosensors and chemodosimeters for NO (g).

A number of strategies for NO detection, such as those based on chemiluminescence,[73] colorimetry,[74] electron paramagnetic resonance[75] and electrochemistry[76] have been reported.[77]

3.3.1 Fluorescence sensors

The reaction between *ortho*-diaminophenyl and NO is the most well know and widely used modulating mechanism in the design of fluorogenic NO probes. Aromatic vicinal diamines can efficiently quench the emission of a fluorophore subunit through a photoinduced electron transfer (PET) mechanism. The reaction of an aromatic vicinal diamine with NO in the presence of oxygen leads to the

[70] K. Skalska, J. S. Miller, S. Ledakowicz, *Sci. Total Environ*., **2010**, 408, 3976-3989.
[71] Brüggemann TC, Keil FJ., *J Phys Chem C*., **2008**;112:17378–17387.
[72] a) Anon, *Air Pollut Consult*, **1995**, 13–16.; b) Devahasdin S, Fan Ch, Li K, Chen DH., *J. Photochem. Photobiol. A*, **2003**, 156, 161– 170.
[73] J. F. Brien, B. E. McLaughlin, K. Nakatsu and G. S. Marks, *Methods Enzymol*., **1996**,268, 83
[74] F. Brown, N. J. Finnerty, F. B. Bolger, J. Millar and J. P. Lowry, *Anal. Bioanal. Chem*., **1982**, 126, 131**.**
[75] a) H. Kosaka, M. Watanabe, H. Yoshihara, N. Harada and T. Shiga, *Biochem. Biophys. Res. Commun.*, **1992**, 184, 1119. b) Y. Katayama, N. Soh and M. Maeda, *Chem.PhysChem*., **2001**, 2, 655
[76] a) T. Malinski and Z. Taha, *Nature*, **1992**, 358, 676. b) F. Bedioui and N. Villeneuve, *Electroanalysis*, **2003**, 15, 5.
[77] a) M. D. Pluth, M. R. Chan, L. E. McQuade and S. J. Lippard, *Inorg. Chem*., **2011**, 50, 9385. b) S. Ma, D.-C. Fang, B. Ning, M. Li, L. He and B. Gong, *Chem. Commun*., **2014**, 50, 6475-6478

formation of triazole that blocks the non-radiative PET relaxation pathway and restores fluorescence emission of the fluorophore.[78] For example, Nagano reported the synthesis of probe **DAF** (see Figure 2), a diaminofluorescein derivative in which the two vicinal amine groups react with NO in the presence of O_2, forming a highly fluorescent triazole product.

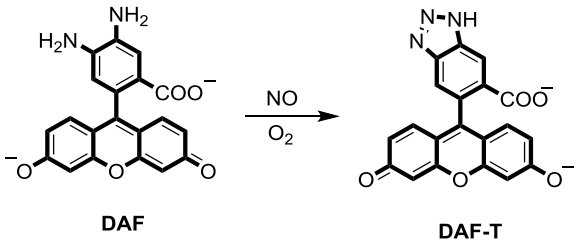

Figure 2: Reaction of NO with DAF-2 to form DAF-2 triazole (DAF- T).

A series of fluorescence-based NO indicators combine transition metal complexes with coordinated fluorophores. The fluorescence of the complexes is significantly quenched compared to that of the free ligands and is restored in presence of NO. This NO-induced fluorescence enhancement of probe is based on a NO-induced demetallation of the complex.

For example, the copper fluorescein complex (CuFL) developed by Lippard[79] (see Figure 3) exhibits NO-triggered fluorescence enhancement. NO reduces the Cu (II) of CuFL to Cu (I), forming NO^+. NO^+ nitrosates the ligand and releases Cu (I), which immediately turns on the fluorescence.

[78] a) H. Kojima, N. Nakatsubo, K. Kikuchi, S. Kawahara, Y. Kirino, H. Nagoshi, Y. Hirata and T. Nagano, *Anal. Chem*., **1998**, 70, 2446. b) H. Kojima, M. Hirotani, N. Nakatsubo, K. Kikuchi, Y. Urano, T. Higuchi, Y. Hirata and T. Nagano, *Anal. Chem*., **2001**, 73, 1967.

[79] a) Z. J. Tonezetich, L. E. Mc. Quade, S. L. Lippard, *Inorg. Chem*., **2010**, 49, 6338-6348. b) M. H. Lim, S. J. Lippard, *Acc. Chem. Res*., **2007**, 40, 41-51.

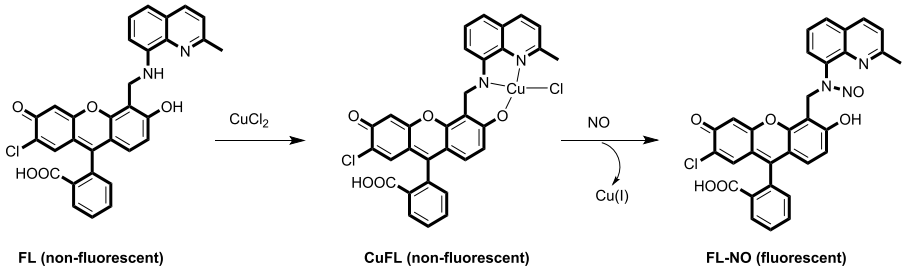

Figure 3: Nitric oxide sensor with copper developed for S. J. Lippard and coworkers.

3.4. Functionalized gold nanoparticles for detection of Cu (II)

Gold nanoparticles (AuNPs) based methods for visual or colorimetric sensing,[80] are interest because of the intense red colour arising from surface plasmon absorption. In the literature there are some references based on a colorimetric method for the detection of copper ions using the "click"[81] reaction. Furthermore v the "click" reaction can tolerate a wide range of solvents, temperatures and pH values.[82]

Appropriate functionalization of AuNPs with alkyne and/ or azide terminated groups is therefore required. This principle has been demonstrated by Zhou and coworkers.[83] By using alkyne and azide tagged AuNPs in the presence of sodium ascorbate, the authors reported the analytes-triggered AuNPs aggregation was accompanied by a colour change and thus gave direct indication of the copper (II) content in the analyte. A detection limit for Cu (II) of 50 μM was reported, where other metal ions were found not to interfere with the colorimetric assay.

[80] Z.-q. Tan, J.-f. Liu, R. Liu, Y.-g. Yin and G.-b. Jiang, *Chem. Commun*., **2009**, 7030.
[81] H. C. Kolb, M. G. Finn and K. B. Sharpless, *Angew. Chem., Int. Ed*., **2001**, 40, 2004
[82] M. Meldal and C. W. Tornoe, *Chem. Rev*., **2008**, 108, 2952.
[83] Y. Zhou, S. Wang, K. Zhang and X. Jiang, *Angew. Chem. Int. Ed*., **2008**, 47, 7454-7456

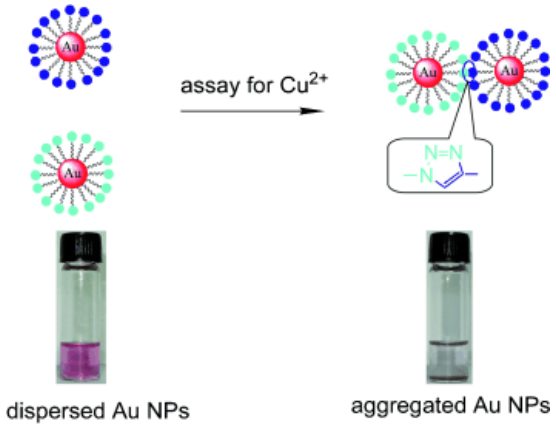

Figure 5: In the presence of Cu (II) with sodium ascorbate as a reductant, gold nanoparticles that have azide- and alkyne-terminated groups undergo aggregation as the result of Cu (I)-catalyzed click chemistry.

A simplified colorimetric method for the detection of copper (II) by using azide-tagged AuNPs was also reported by Xu *et al*.[84] Azide functionalized AuNPs undergo a "click" reaction with a dialkynyl cross-linker, 1, 4-diethynylbenzene (DEB), in the presence of Cu^{2+} and sodium ascorbate to form the triazole-linked aggregates. The lowest concentration at which there was a distinct colour change detectable by eye was 1.8 µM of Cu(II).

-

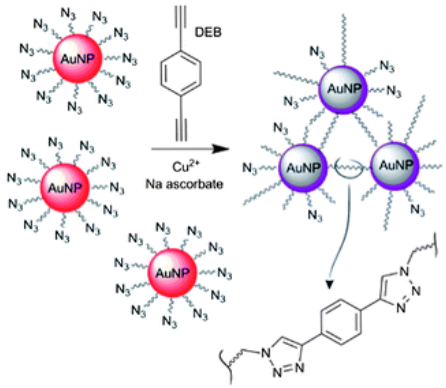

Figure 6: Schematic depiction of the copper trigged aggregation of AuNPs for Cu (II) detection developed by J. Justin Gooding and coworkers.

[84] C. Hua, W. H. Zhang, S. R. M. De Almeida, S. Ciampi, D. Gloria, G. Liu, J. B. Harper and J. J. Gooding; *Analyst*, **2012**, 137, 82

3.5. Objectives.

Based on the fact that (i) the copper-catalized azyde alkyne cycloaddition ("click" reaction) needs Cu (I) to proceed, (ii) NO (g) reduce Cu(II) to Cu(I) and (iii) gold nanoparticles undergo color changes (from red to blue) upon aggregation, in this chapter we aim to develop a new sensor containing gold nanoparticles functionalized with alkyne and azide terminated ligands to detect NO(g).

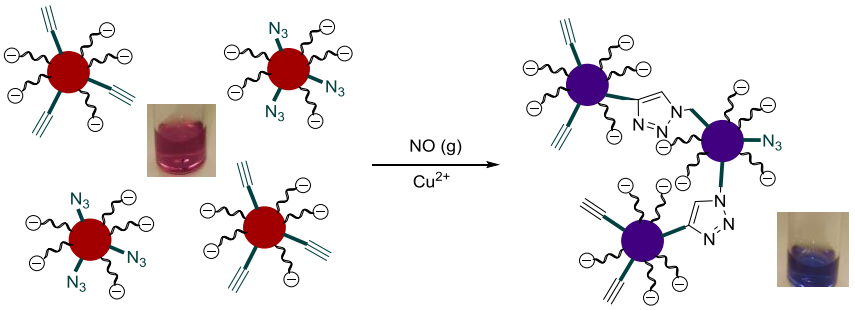

Figure 7: A new colorimetric probe for detection of NO (g) based on the use of functionalized gold nanoparticles is described. The sensing protocol is based on a click reaction catalized by Cu(I) which is generated in situ from the reduction of Cu(II) by NO(g).

3.6. Selective colorimetric NO (g) detection with modified gold nanoparticles using click chemistry

Selective colorimetric NO (g) detection with modified gold nanoparticles using click chemistry.

Almudena Martí, Ana M. Costero,* Pablo Gaviña,* and Margarita Parra

Centro de Reconocimiento Molecular y Desarrollo Tecnológico (IDM), Unidad Mixta Universidad de Valencia-Universidad Politécnica de Valencia, Dr. Moliner, 50, 46100 Burjassot, Valencia, Spain. Email: ana.costero@uv.es, pablo.gavina@uv.es

Received: 19 December 2014.
Available: 15 January 2015.

Chem. Commun., **2015**, 51, 3077-3079.

Nitric oxide (NO) is a gaseous free-radical species which exists in the atmosphere. NO is produced from the reaction of N_2 and O_2 during high-temperature combustion processes from car engines, power plants or industrial processes and naturally by lightning during a thunderstorm. NO is one of the components of the air pollutants known as nitrogen oxides (NOx), which are responsible for the acid rain and the smog pollution. High NOx levels in the atmosphere can cause serious diseases such as carcinogenesis and asthma.[1] NO is also a ubiquitous bioactive signaling molecule. Biological NO is generated in the oxidation of L-arginine to L-citrulline catalyzed by nitric oxide synthases and participates in the regulation of a variety of physiological and pathological processes, such as in the control of vascular smooth muscle relaxation and vasodilation, platelet adhesion, regulation of the immune response and as neurotransmitter in the brain.[2]

Several analytical methods for NO detection have been developed such as electrophoresis, electron paramagnetic resonance (EPR) or GC-mass spectroscopies, chemiluminescence or electrochemical methods.[1,3] In comparison to these protocols, colorimetric and/or fluorescence-based techniques present a large number of advantages such as simple detection in situ or at site without any sample pre-treatment or use of low-cost, widely available equipment. Colorimetric detection is particularly appealing because it allows assays to be followed by the naked eye. However, whereas a large number of fluorescent probes for NO detection have been described,[4] studies on colorimetric detection of this gas are scarce.

In the last few years, functionalized gold nanoparticles (AuNPs) have attracted enormous interest in colorimetric sensing due to their unique optoelectronic properties.[5] The detection strategy is based on the color change that arises from the interparticle plasmon coupling during analyte-induced aggregation or dispersion of AuNPs. The red color of dispersed nanoparticles turns into dark blue upon aggregation, and this color change can be observed by the naked eye even at nanomolar concentrations.[6] Recently, the copper(I)-catalyzed azide-alkyne cycloaddition (the archetypal “click” reaction), between alkyne- and azide-tagged AuNPs has been used in the design of colorimetric methods for the detection of Cu(II) ions in water.[7] The detection method is based on the in situ reduction of Cu(II) to Cu(I) in the presence of sodium ascorbate as the reductant. The Cu (I) catalyst promotes the “click” reactions on the surface of the AuNPs leading to interparticle-crosslinking aggregation.[8]

On the other hand it is well established that the copper centre in Cu(II) complexes undergo reduction to Cu(I) in the presence of NO,[9] and several Cu(II) complexes have been reported as colorimetric and/or fluorescent probes for nitric

oxide detection.[10] Combining these two facts, herein we report a colorimetric method for the detection of NO (g) based on the aggregation-induced color change of a mixture of azide- and alkyne-functionalized AuNPs and Cu(II).

The paradigm of the detection system is depicted in Scheme 1. The initial aqueous solution containing a mixture of azide- and terminal-alkyne functionalized AuNPs remains dispersed in the presence of Cu(II), with its characteristic red-wine color. However upon reduction of Cu(II) to Cu (I) by NO, the click reaction between azide and alkyne-terminated nanoparticles takes place leading to interparticle-crosslinking aggregation and subsequent change in the plasmon absorption band and in the color of the solution.

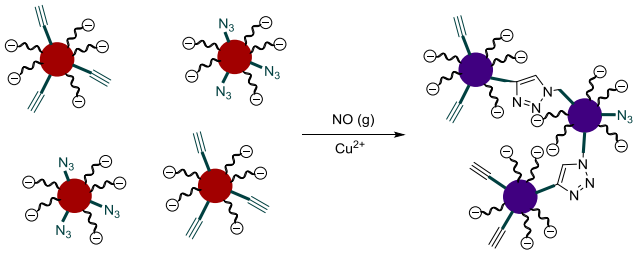

Scheme 1. Paradigm of the sensing mechanism: reaction of alkyne-AuNPs with azide-AuNPs by a Cu (I) catalyzed "click" reaction results in aggregation processes. The Cu(I) catalyst is generated in situ by the reduction of Cu(II) in the presence of NO (g).

The synthesis of both, azide- and alkyne-terminated lipoic acid derivatives **1** and **2**, used for the functionalization of the surface of the AuNPs, is depicted in Scheme 2.

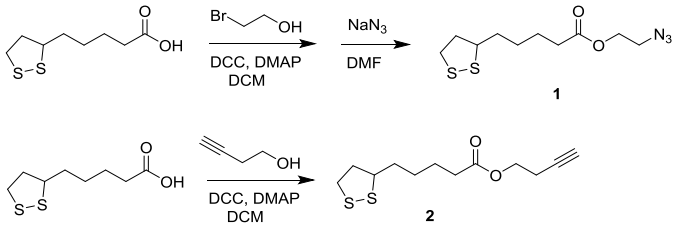

Scheme 2. Synthesis of lipoic acid derivatives 1 and 2.

Compound **1** was obtained by the Steglich esterification of lipoic acid with 2-bromoethanol, followed by reaction with sodium azide in 62% overall yield. Alkyne-terminated lipoic acid derivative **2** was obtained in 65% yield from the

esterification of lipoic acid with 3-butyn-1-ol. The chemical structure and purity of compounds 1 and 2 were confirmed by spectroscopic techniques (see ESI).

Azide- and terminal alkyne-functionalized gold nanoparticles (AuNP1 and AuNP2 respectively) were synthesized by a two-step procedure. First, citrate-stabilized AuNPs were prepared by reducing tetrachloroauric acid with trisodium citrate in boiling water.[11] Then, by ligand-exchange reactions, citrate was displaced from the surface of the nanoparticles by a mixture of lipoic acid (LA) and compounds **1** or **2** in an optimized 1:2 (LA/ligand) molar ratio. The functionalized nanoparticles were purified by repeated centrifugation and redispersion in water.

The resulting functionalized gold nanoparticles were characterized by UV-vis, transmission electron microscopy (TEM) and dynamic light scattering (DLS). Monodisperse stabilized AuNPs were obtained with an average size of 13 (AuNP1) and 13.5 nm (AuNP2), as determined by TEM. Both AuNPs displayed a surface plasmon absorption peak at 525 nm, in perfect agreement with the experimental data for particle sizes smaller than 25 nm.[11] The initial concentration of the AuNPs was calculated to be 5.3 10^{-9} M by UV-vis spectroscopy, from an estimated molar extinction coefficient of $\varepsilon = 2.5 \cdot 10^{8}$ M^{-1} cm^{-1}.[12] The red wine aqueous dispersions of AuNP1 and AuNP2 remained stable in the fridge for more than 2 months, with no observable changes in their characteristic plasmon absorption band.

In order to verify the reaction of AuNP1 with AuNP2 under click conditions, a preliminary study was conducted with aqueous solutions containing equimolecular mixtures of both AuNPs ($4 \cdot 10^{-10}$ M), copper (II) acetate (40 μM) and different amounts of sodium ascorbate as the reducing agent. The click reaction of the nanoparticles was monitored by UV-vis spectroscopy. In the absence of ascorbate, stable red-wine dispersions of the nanoparticles in water were obtained, exhibiting the characteristic plasmon absorption band at 525 nm. Upon addition of increasing amounts of sodium ascorbate (from 4 μM to 400 μM), and after an induction period of 5 min, the color of the solution gradually changed to dark blue, as was clearly appreciable by the naked-eye. The UV-vis spectra (see Fig. S4, ESI) were consistent with the observed color changes. Thus, the intensity of the surface plasmon peak at 525 nm (A_{525}) corresponding to the monodispersed AuNPs gradually decreased and a new peak at ca. 627 nm (A_{627}) characteristic of aggregated AuNPs appeared. The ascorbate-induced aggregation of the AuNPs was further confirmed by TEM analysis (see Fig. S5, ESI).

When the previous aqueous mixture of both AuNPs and Cu(II) was exposed to a N_2 atmosphere containing low concentrations of NO (g) as the reductant, no change in the color of the solution was appreciated by the eye. Only when excess of NO was bubbled into the solution for 20 min, the color turned into blue, accompanied by the gradual appearance of a precipitate as a result of the

aggregation process. However, when instead of water, a mixture of water/methanol (1:7, v/v) was used as a solvent a clear change in the color of the solution was observed after 5 min of exposure of the nanoparticles to low concentrations of NO (g) without any bubbling.[13]

To evaluate the minimum concentration of NO (g) detectable by our system, titration experiments were carried out by exposing a water-MeOH solution (1:7, v/v) containing a mixture of **AuNP1** and **AuNP2** ($3.3 \cdot 10^{-10}$ M) and Cu(AcO)2 (30 μM) to a N2 atmosphere containing increasing amounts of gaseous NO for 5 min, and then allowing the solution to stand in the air for other 5 min. The experiments were followed by UV-vis spectroscopy (see Figure 1).

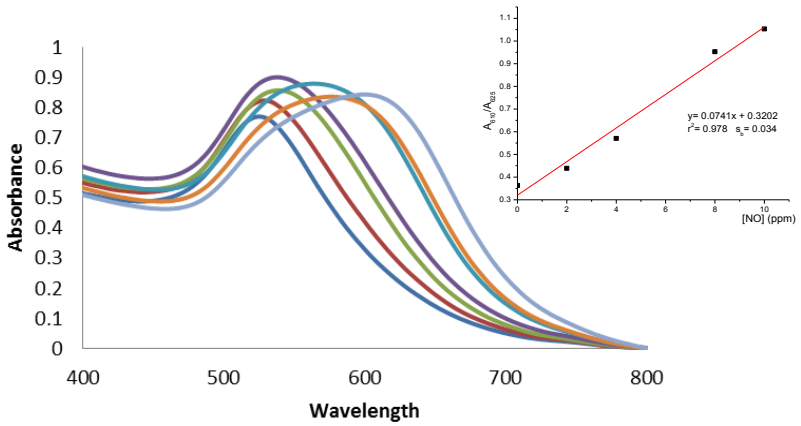

Figure 1. Left: UV-vis spectra of titration of a mixture of AuNP1, AuNP2 and Cu(AcO)2 in MeOH:H2O (7:1), upon exposition to increasing amounts of NO (g). Inset: Plot of A610/A525 vs NO concentration (in ppm).

The observed red shift from 525 to 610 nm in the surface plasmon band was indicative of the aggregation of the gold nanoparticles. The gradual change in the color of the solution from red to blue could be detectable by the naked eye for concentrations as low as 4 ppm of NO (g) (see Fig. 2). The interparticle-crosslinking aggregation was also confirmed by TEM studies at different NO concentrations (see Fig. S7, ESI)

A detection limit of 1.4 ppm (v/v) for NO (g) was obtained from the plot of the ratio of the absorbance intensities at 525 and 610 nm (A610/A525) versus NO concentration (Fig. 1, right).

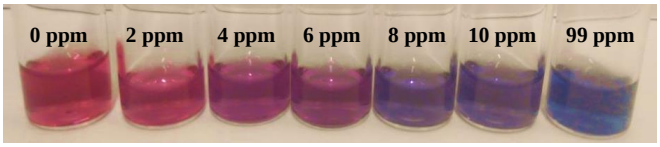

Figure 2: Photograph of solutions of AuNP1, AuNP2 and Cu (II) in MeOH:H2O (7:1) after exposure to a nitrogen atmosphere containing increasing amounts of NO (g)

Finally, to demonstrate the selectivity of the system, several possible interferents (SO_2 (g), CO_2 (g), CO (g) and NO_2 (g), 50 ppm each) were tested by UV-vis spectroscopy following the same protocol. As can be observed in the UV-vis spectra (Fig. 3) only a modest response was observed in the presence of excess of NO2. Furthermore, when all the gases and NO were exposed to the AuNPs dispersion, the change in color (Fig. 3, bottom and Fig. S8, ESI) and the red shift of the SPR absorption band clearly showed that this detection system is highly selective towards NO (g) with no appreciable interference from other common atmospheric gases

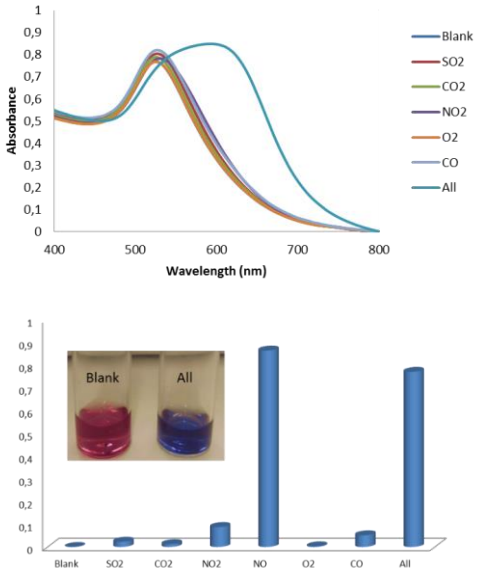

Figure 3. Up: UV-vis spectra of a mixture of AuNP1, AuNP2 and Cu(II) in the presence of various interferents (50 ppm, v/v); Botton: Representation of A_{610}/A_{525} for the interferents and photograph of color change.

In summary, azide- and terminal alkyne-functionalized AuNPs in the presence of Cu (II) have demonstrated to be an interesting alternative for the direct colorimetric detection of NO (g) in aqueous media. The detection process is based on the aggregation of the AuNPs through a Cu(I) catalyzed click reaction promoted by the in situ reduction of Cu(II) by NO (g). With this method detection, limits of 1.4 ppm (mL/m^3) have been achieved. This methodology can to find uses in many scenarios where sensors for NO (g) are required. Furthermore, the biocompatibility of the AuNPs allows the possibility of extending their applications for NO detection in bioassays.

We acknowledge the Spanish Government (MAT2009-14564-C04-03 and MAT2012-38429-C04-02) for financial support. A. M. is grateful to the Spanish Government for a fellowship. SCSIE (Universidad de Valencia) is gratefully acknowledged for all the equipment employed.

Notes and References

Electronic Supplementary Information (ESI) available: Materials and synthetic procedures ^{1}H- and ^{13}C-NMR spectra, procedures for the titration and interference studies, calculation of the detection limit, supplemental spectra. See DOI: 10.1039/c000000x/

1. T. Nagano, *Luminescence* 1999, **14**, 283-290.

2. L. J. Ignarro, Nitric Oxide: Biology and Pathobiology, Academic Press, San Diego, 2010.

3. S. Ma, D.-C. Fang, B. Ning, M. Li, L. He and B. Gong, *Chem. Commun*., 2014, **50**, 6475-6478 and references therein.

4. (a) H. Kojima, N. Nakatsubo, K. Kikuchi, S. Kawahara, Y. Kirino, H. Nagoshi, Y. Hirata and T. Nagano, *Anal. Chem*., 1998, **70**, 2446-2453; (b) X. Chem, X. Tian, I. Shin and J. Yoon, *Chem. Soc. Rev*. 2011, **40**, 4783-4804; (c) A. Beltrán, M. I. Burguete, D. R. Abánades, D. Pérez-Sala, S. V. Luis and F. Galindo, *Chem. Commun*., 2014, **50**, 3579-3581; (d) X. Lv, Y. Wang, S. Zhang, Y. Liu, J. Zhang and W. Guo, *Chem. Commun*., 2014, **50**, 7499-7502.

5. (a) K. Saha, S. S. Agasti, C. Kim, X. Li and V. M. Rotello, *Chem. Rev*., 2012, **112**, 2739-2779; (b) K. M. Mayer and J. H. Hafner, *Chem. Rev*., 2011, **111**, 3828-3857.

6. A. Marti, A. M. Costero, P. Gaviña, S. Gil, M. Parra, M. Brotons-Gisbert and J. F. Sánchez-Royo, *Eur. J. Org., Chem*., 2013, 4770-4779.

7. (a) Y. Zhou, S. Wang, K. Zhang and X. Jiang, *Angew. Chem. Int. Ed*., 2008, **47**, 7454-7456; (b) C. Hua, W. H. Zhang, S. R. M. De Almeida, S. Ciampi, D. Gloria, G. Liu, J. B. Harper and J. J. Gooding, *Analyst*, 2012, **137**, 82-86.

8. Y. Zhang, B. Li and C. Xu, *Analyst*, 2010, **135**, 1579-1584.

9. (a) D. Tran and P. C. Ford, *Inorg. Chem*., 1996, **35**, 2411-2412; (b) K. Tsuge, F. DeRosa, M. D. Lim and P. C. Ford, *J. Am. Chem. Soc*., 2004, **126**, 6564-6565.

10. (a) M. H. Lim and S. J. Lippard *J. Am. Chem. Soc*, 2005, **127**, 12170-12171; (b) U.-P. Apfel, D. Buccella, J. J. Wilson and S. J. Lippard, *Inorg. Chem*., 2013, **52**, 3285-3294.

11. (a) W. Haiss, N. T. K. Thanh, J. Aveyard and D. G. Fernig, *Anal. Chem*., 2007, **79**, 4215-4221; (b) S.-Y. Lin, Y.-T. Tsai, C.-C. Chen, C.-M. Lin and C.-H. Chen, *J. Phys. Chem. B*, 2004, **108**, 2134-2139.

12. X. Liu, M. Atwater, J.Wang and Q. Huo, C*olloids and Surfaces B: Biointerfaces*, 2007, **58**, 3-7.

13. It has been recently reported that the presence of aliphatic alcohols seems to accelerate the reduction of Cu (II) to Cu(I) in azide-alkyne cycloadditions. See W. S. Brotherton, H. A. Michaels, J. T. Simmons, R. J. Clark, N. S. Dalal and L. Zhu, *Org. Lett*., 2009, **11**, 4954-4957.

Supplementary Information

Selective colorimetric NO (g) detection with modified gold nanoparticles using click chemistry

Almudena Martí, Ana M. Costero*, Pablo Gaviña*, Margarita Parra

Centro Mixto de Reconocimiento Molecular y Desarrollo Tecnológico (IDM), Universidad de Valencia – Universidad Politécnica de Valencia, Dr. Moliner, 50 46100 Burjassot (Valencia), Spain

E-mail: ana.costero@uv.es and pablo.gavina@uv.es

General procedures:

All reagents were commercially available, and were used without purification. Silica gel 60 F254 (Merck) plates were used for TLC. Milli-Q ultrapure water was used for the synthesis of AuNPs and the sensing experiments. NO (g), NO_2 (g) and CO (g) were obtained from commercially available gas cylinders. SO_2 (g) and CO_2 (g) were generated in situ following standard protocols. ^{1}H-NMR and ^{13}C-NMR spectra were recorded on a Bruker 300 MHz spectrometer. Chemical shifts are reported in ppm with tetramethylsilane as an internal standard. High resolution mass spectra were recorded in the positive ion mode on a VG-AutoSpec mass spectrometer. UV-vis absorption spectra were recorded using a 1 cm path length quartz cuvette on a Shimadzu UV-2101PC spectrophotometer. All measurements were carried out at 293 K (thermostated). Z-potential values were measured in a Malvern Zetasizer ZS, for 3 times in 10-25 cycles. The TEM electronic images were made on a JEOL-1010 transmision electron microscope operating at 100 KV.

Synthesis of 2-azidoethyl 5-(1,2-dithiolan-3-yl)pentanoate (1)

A 100 mL round-bottom flask was charged with (±)-α-lipoic acid (1.5 g, 7.27 mmol), DCC (1.5 g, 7.27 mmol), and anhydrous CH_2Cl_2 (20 mL). The reaction mixture was cooled to 0°C in an ice-water bath and a solution of 2-bromoethanol (0.5 mL, 6.9 mmol) and a catalytic amount of DMAP in anhydrous CH_2Cl_2 (20 mL) was added dropwise over a period of 1 h under magnetic stirring. After the addition was completed, the reaction mixture was stirred at 0°C for 2 h and then allowed to warm to room temperature for 24 h. After removing the insoluble salts by filtration, the filtrate was concentrated and further purified by silica gel column chromatography using hexane/ethyl acetate (4:6, v/v) as eluent. 2-Bromoethyl 5-(1,2-dithiolan-3-yl)pentanoate was obtained as a yellow oil (1.36 g, 60% yield).

^{1}H NMR (300 MHz, $CDCl_3$): δ= 4.39 (t, *J*= 6.2 Hz, 2H), 3.60-3.50 (m, 1H), 3.51 (t, *J*= 6.2 Hz, 2H), 3.25-3.10 (m, 2H), 2.52-2.42 (m, 1H), 2.37 (t, *J*= 7.3 Hz, 2H), 1.96-1.86 (m, 1H), 1.75-1.63 (m, 4H), 1.55-1.45 (m, 2H).

^{13}C NMR (75 MHz, $CDCl_3$) δ= 173.1, 63.8, 56.5, 40.4, 38.6, 34.7, 34.0, 29.0, 28.9, 24.8.

HRMS (ESI): *m/z* calcd. for $C_{10}H_{18}BrO_2S_2$ ($[M+H]^+$), 314.993 (100%) and 312.993 (93%); found 314.990 and 312.992.

2-Bromoethyl 5-(1,2-dithiolan-3-yl)pentanoate (2.0 g, 6.4 mmol) and sodium azide (1.25 g, 19.2 mmol) were dissolved in DMF (10 mL) and stirred at 60 ^{o}C for 48 h. The reaction mixture was diluted with dichloromethane, washed with water and $NaHCO_3$ (aq), dried over anhydrous $MgSO_4$ and concentrated to obtain 2-azidoethyl 5-(1,2-dithiolan-3-yl)pentanoate (**1**) as a light yellow liquid (1.38 g, 78%).

^{1}H NMR (300 MHz, $CDCl_3$) δ (ppm)= 4.25 (t, *J*= 5.1 Hz, 2H), 3.57 (qt, J = 6.6 Hz, 1H), 3.48 (t, J = 5.1 Hz, 2H), 3.25–3.07 (m, 2H), 2.54–2.42 (m, 1H), 2.38 (t, *J*= 7.4 Hz, 2H), 1.97–1.85 (m, 1H), 1.75–1.63 (m, 4H), 1.54–1.44 (m, 2H).

^{13}C NMR (75 MHz, $CDCl_3$) δ (ppm)= 173.2, 63.0, 56.4, 49.9, 40.4, 38.6, 34.7, 34.0, 28.8, 24.7.

HRMS (ESI): *m/z* calcd. for $C_{10}H_{18}N_3O_2S_2$ ($[M+H]^+$): 276.084; found 276.082.

Synthesis of but-3-yn-1-yl 5-(1,2-dithiolan-3-yl)pentanoate (2)

A 100 mL round-bottom flask was charged with lipoic acid (1.5 g, 7.27 mmol), DCC (1.5 g, 7.27 mmol), and anhydrous CH_2Cl_2 (20 mL). The reaction mixture was cooled to 0^{o}C and a solution of 3-butyn-1-ol (0.53 mL, 6.9 mmol) and DMAP (cat. amount) in anhydrous CH_2Cl_2 (20 mL) was added dropwise over a period of 1 h under magnetic stirring. After the addition was completed, the reaction mixture was stirred at 0 ^{o}C for 2 h and then allowed to warm to room temperature for 24 h. After removing the insoluble salts by filtration, the filtrate was concentrated and the residue was purified by silica gel column chromatography using hexane/ethyl acetate (4:6, v/v) as eluent. Compound **2** was obtained as yellow oil (1.02 g, 45% yield).

^{1}H NMR (300 MHz, $CDCl_3$): δ (ppm)= 4.18 (t, *J*= 6.7 Hz, 2H), 3. 56 (qt, *J*= 6.6 Hz, 1H), 3.22–3.07 (m, 2H), 2.53–2.41 (m, 3H), 2.35 (t, *J*= 7.4 Hz, 2H), 2.00 (t, *J*= 2.5 Hz, 1H), 1.96–1.85 (m, 1H), 1.76–1.59 (m, 4H), 1.53–1.43 (m, 2H).

^{13}C NMR (75 MHz, $CDCl_3$) δ (ppm)= 173.3, 80.2, 70.0, 62.1, 56.5, 40.4, 38.6, 34.7, 34.1, 28.9, 24.8, 19.2.

HRMS (ESI): *m/z* calcd. for $C_{12}H_{19}O_2S_2$ ($[M+H]^+$), 259.0826; found, 259.0810

Preparation of the functionalized AuNPs.

All glassware was thoroughly cleaned with freshly prepared aqua regia (HCl: HNO_3, 3:1), rinsed thoroughly with deionized water and dried in air. AuNPs with a diameter of ca. 13 nm were synthesized as reported previously.[1] Briefly, 10 mL of aqueous 38.8 mM trisodium citrate solution was added to an aqueous boiling solution of $HAuCl_4$ (100 mL, 1 mM) and the resulting solution was kept continuously boiling for 30 min until a red solution was obtained. The solution was cooled to room temperature and was then stored in a refrigerator at 4°C for use. Modification of AuNPs through the ligand-exchange reaction was performed at room temperature as follows: 20 µl of 0.01 M NaOH aqueous were added to the 10 mL of the as-prepared citrate capped AuNPs. Then, 200 µl of LA ($1 \cdot 10^{-3}$ M in methanol) and the corresponding amount of compounds **1** or **2** (10^{-3} M in methanol) were added simultaneously and the solution was stirred overnight. To purify the AuNPs, the mixture were centrifuged for 20 min at 14000 rpm and supernatants were decanted; then the resulting AuNPs were resuspended in water. The whole process was repeated twice. The AuNPs were characterized by UV-vis spectroscopy, TEM and zeta-potential measurements.

Zeta-potential values (mV) for the AuNPs suspended in deionized water: **AuNP1**, -45.4; **AuNP2**, -38.9.

Ascorbic acid and NO titration studies

The ascorbic acid titration studies were carried out as follows: The initial aqueous mixture (750 µL) containing **AuNP1** and **AuNP2** ($4 \cdot 10^{-10}$ M) and $Cu(OAc)_2$ (40 µM) was prepared by adding 10 µL of $Cu(OAc)_2$ (3 mM) to a solution containing equimolecular amounts of **AuNP1** and **AuNP2** in deionized water. The UV-vis spectrum was registered. Then increasing amounts of sodium ascorbate (3mM in water, 1 µL aliquots) were added, and the UV-spectra were recorded. The total sodium ascorbate concentration during the titration varied from 3 µM to 36 µM.

The NO titration studies were carried out as follows: A mixture of 750 µL of **AuNP1** ($5.3 \cdot 10^{-9}$ M in water) and 750 µL of **AuNP2** ($5.3 \cdot 10^{-9}$ M in water) at pH 7.8 was diluted to 12 mL with methanol (final AuNPs concentration of $3.3 \cdot 10^{-10}$ M). 1mL of the previously prepared water/methanol solution was placed in a vial and 10 µL of aqueous $Cu(OAc)_2$ (3 mM) were added. The vial was introduced inside a 250 mL round bottom flask filled with a N_2 atmosphere containing NO (g) (2 ppm) for 5 min.

Then the vial was taken out of the flask and let stand in the air for 5 more minutes and the UV-vis spectrum was immediately registered (from 400 to 800 nm with a scan rate of 0.125 nm/seg). The same procedure was repeated with different NO concentrations.

Calculation of LOD

The limit of detection for NO (g) was obtained from the plot of the ratio of the absorbance intensities at 525 and 610 nm (A_{610}/A_{525}) versus NO concentration (in ppm). LOD was calculated by using the equation (1), where K=3; S_b is the standard deviation of the blank and m is the slope of the calibration curve.

$$\mathrm{LOD} = \mathrm{K} \cdot \frac{S_b}{m} \quad (1)$$

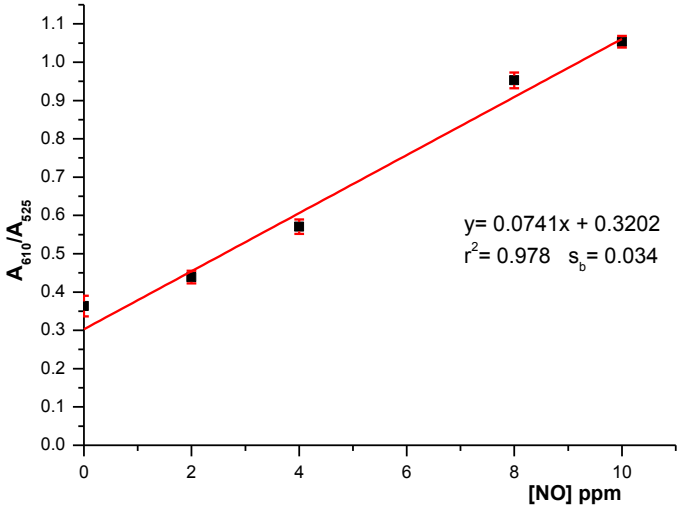

Interference Studies

The same experimental procedure previously described for NO detection was followed for the interference studies. In this case 1 mL H_2O/MeOH solutions (1:7 v/v) containing the AuNPs and Cu(II) were exposed for 5 min to a nitrogen atmosphere containing 50 ppm of the different interferents. The solutions were allowed to stand for 5 min in the air and the corresponding UV-vis spectra were recorded. Finally the solution of the AuNPs and Cu(II) was exposed a nitrogen atmosphere containing 50 ppm of the interferents and 50 ppm of NO, in the same conditions than above, and the UV-vis spectra was registered. In the absence of NO, no color changes were observed and the UV-vis spectra were almost identical to that of the original NPs. However in the presence of the interferents plus NO a clear change in the color of the solution was observed (Figure S7) with the corresponding red shift in the UV-spectrum indicative of the aggregation process.

NO, NO_2 and CO where obtained from commercially available gas cylinders. SO_2 (g) was generated from a mixture of granulated copper and 96 % H_2SO_4; CO_2 (g) was generated from a mixture sodium carbonate and concentrated hydrochloric acid.

Figure S1. ^{1}H NMR and ^{13}C NMR spectra of 2-bromoethyl 5-(1,2-dithiolan-3-yl)pentanoate in $CDCl_3$ at 300 and 75 MHz

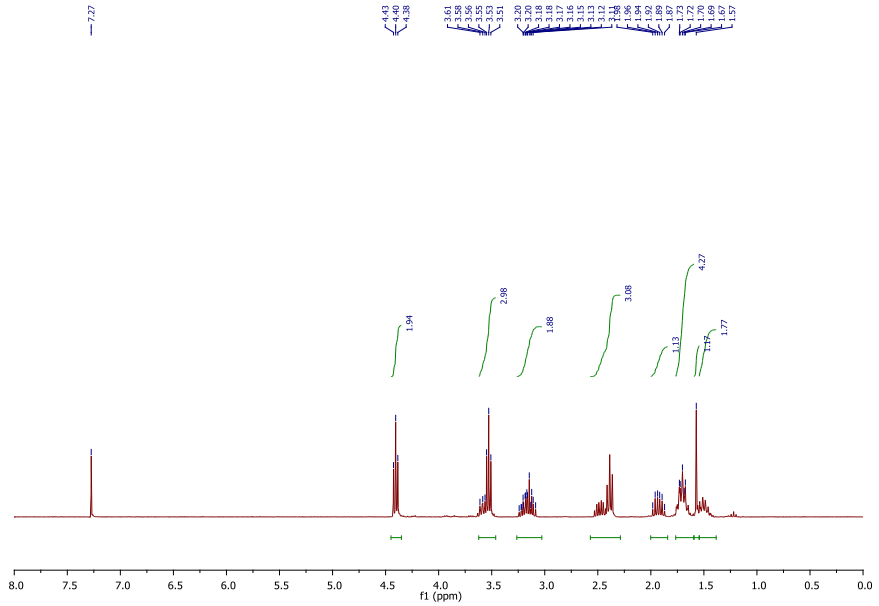

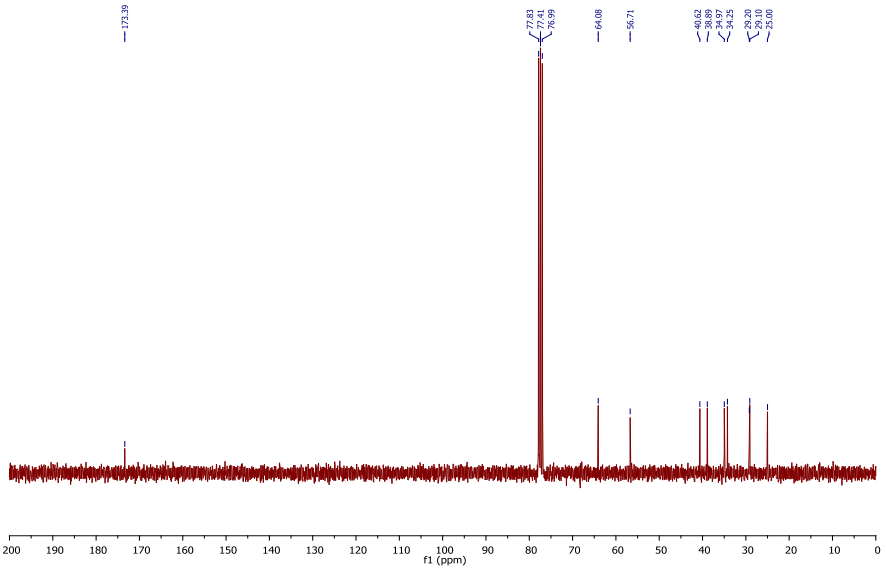

Figure S2. ^{1}H NMR and ^{13}C NMR spectra of azide derivative **1** in $CDCl_3$ at 300 and 75 MHz

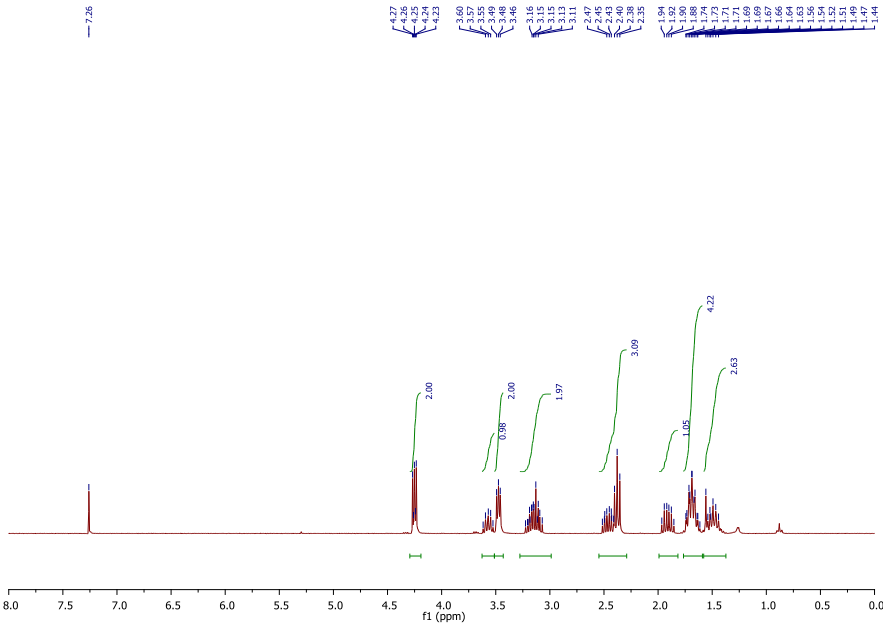

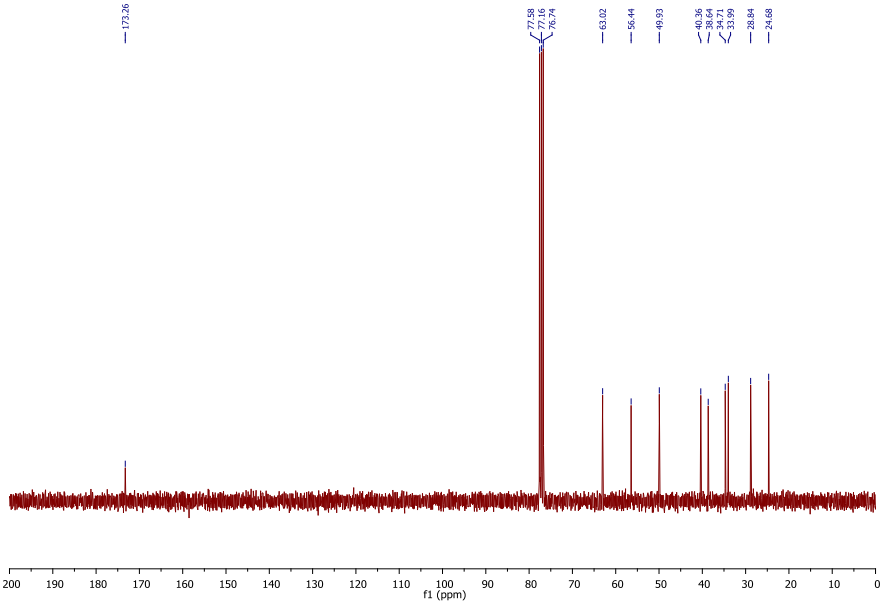

Figure S3. ^{1}H NMR and ^{13}C NMR spectra of compound **2** in $CDCl_3$ at 300 and 75 MHz.

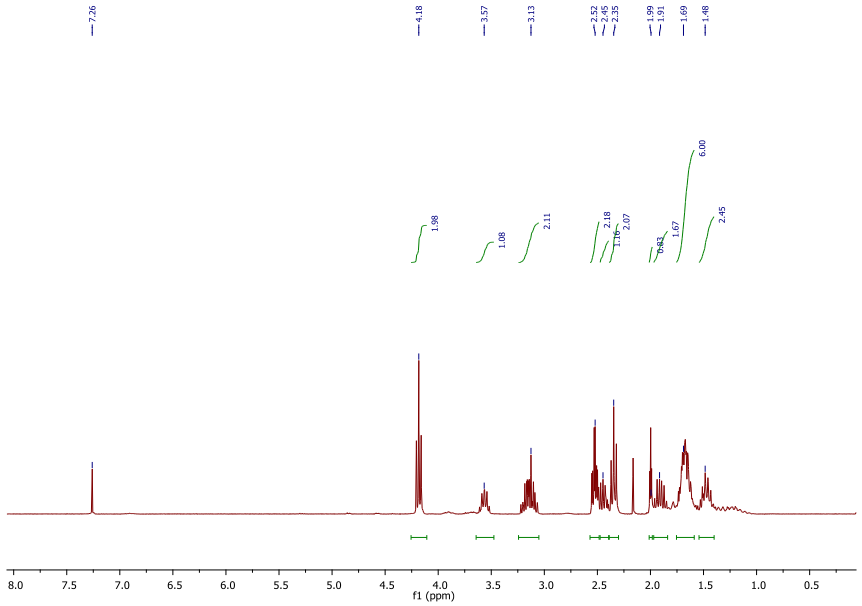

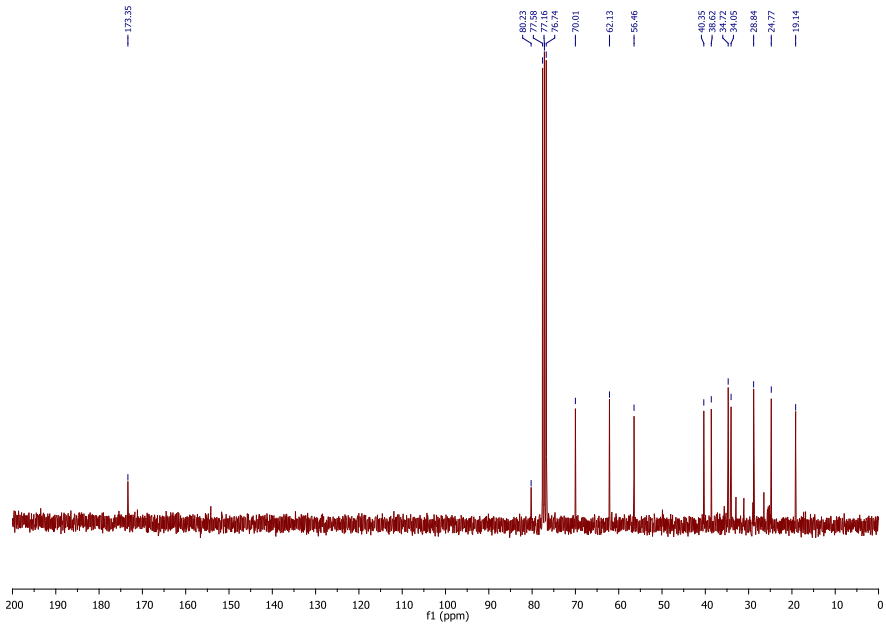

Figure S4. UV-vis spectra of the titration of a mixture of **AuNP1**, **AuNP2** and $Cu(OAc)_2$ ($4 \cdot 10^{-5}$ M) in water upon addition of increasing amounts of sodium ascorbate ($4 \cdot 10^{-6}$M to $4 \cdot 10^{-4}$ M).

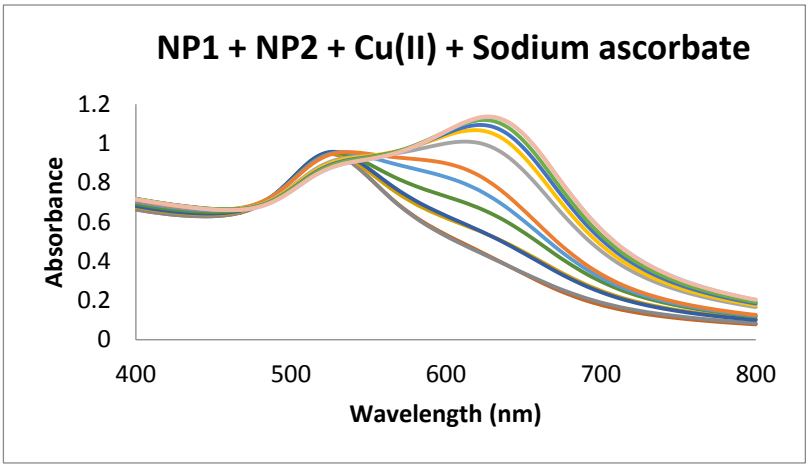

Figure S5. TEM images of an equimolecular mixture of **AuNP1** and **AuNP2** (left); and aggregated AuNPs upon addition of excess of sodium ascorbate in presence of copper acetate, at 200 nm resolution.

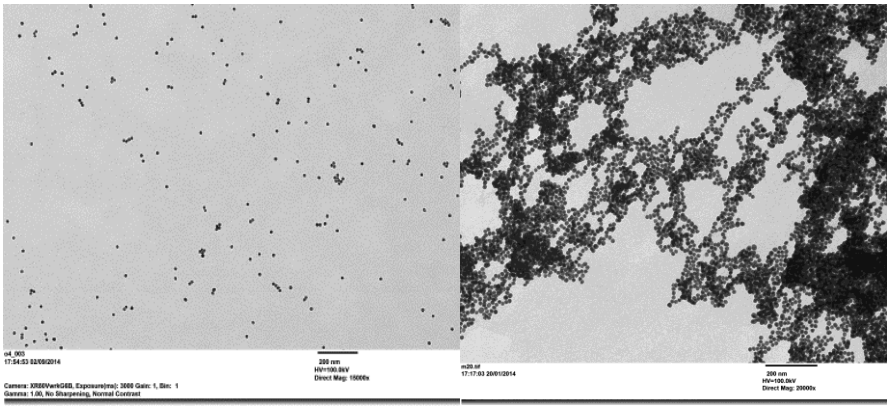

Figure S6 Up: UV-vis spectra of titration of a mixture of **AuNP1**, **AuNP2** and Cu(AcO)2 in MeOH:H2O (7:1), upon exposition to increasing amounts of NO (g). Bottom: Plot of A610/A525 vs NO concentration (in ppm).

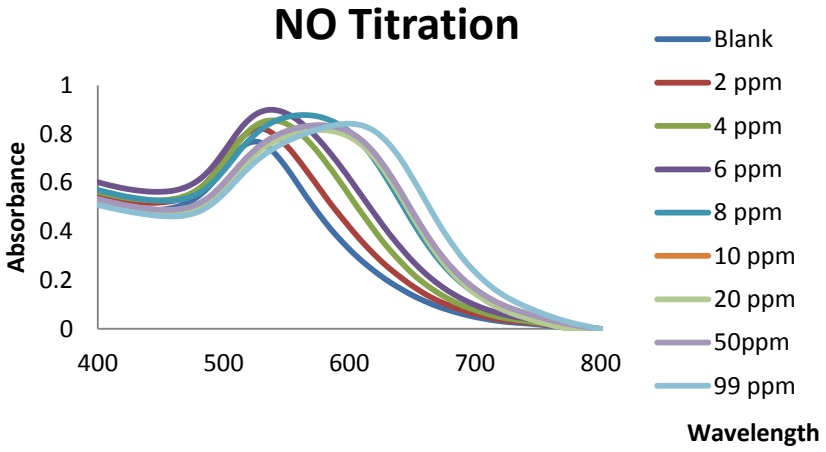

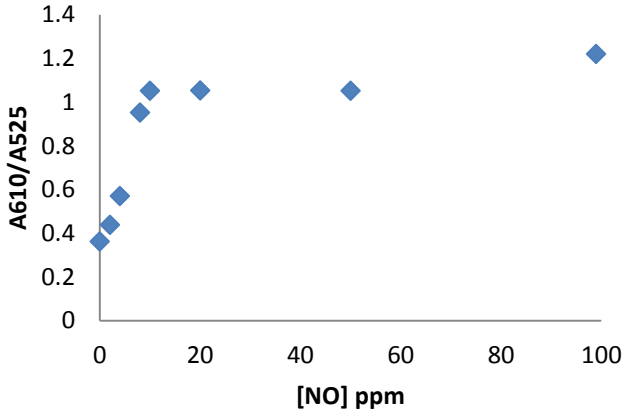

Figure S7. TEM images of an equimolecular mixture of **AuNP1**, **AuNP2** and Cu(II), in the absence (up left), and in the presence of 6 ppm of NO (g) (up right) and 99 ppm of NO (g) (bottom).

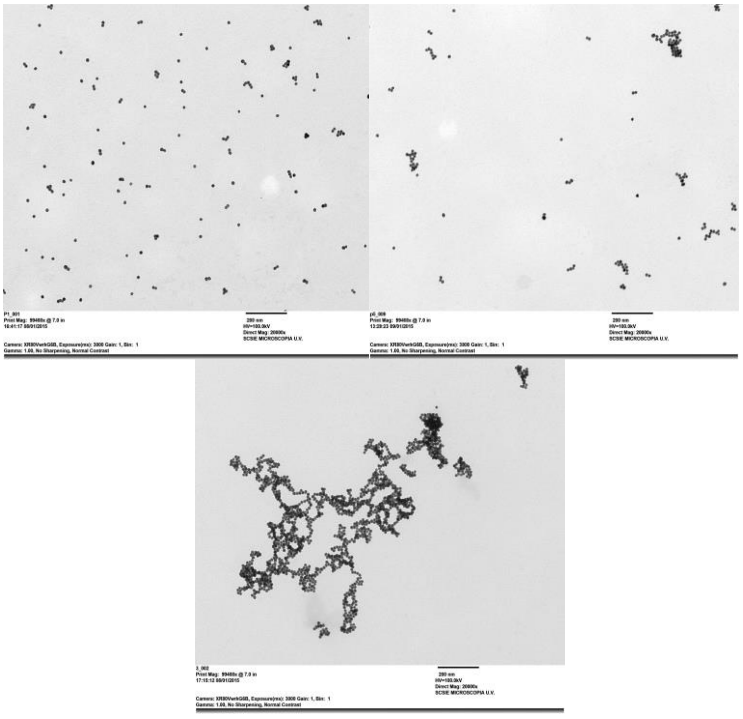

Figure S8. Photograph of solutions of **AuNP1**, **AuNP2** and Cu(II) in MeOH:H2O (7:1) after exposure to the different interferents (SO_2, CO_2, CO and NO_2, 50 ppm each) (left); photograph of the blank solution and the same solution after exposure to a mixture of SO_2, NO_2, CO_2 and NO (right)

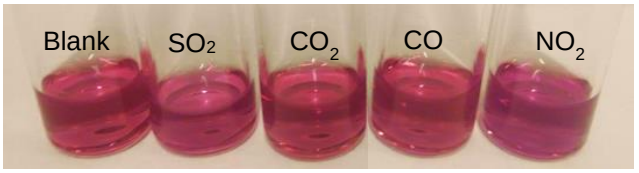

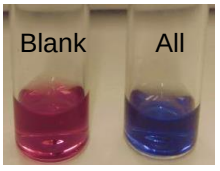

References

[1] A. Martí, A. M. Costero, P. Gaviña, S. Gil, M. Parra, M. Brotons-Gisbert, J. F. Sánchez-Royo, *Eur. J. Org. Chem.* **2013**, 4770-4779.

CHAPTER 4:
Detection of dicarboxylates.

4.1. Introduction

Dicarboxylic species including both dicarboxylate anions and dicarboxylic acids are ubiquitous in living systems. Their participation in cellular metabolism (malonate, succinate, fumarate, malate, aspartate, glutarate, citrate. . .) controls the activity of many enzymatic receptors and several biosynthetic processes.[85] That is why their abnormal regulation is related to several pathologies and physiological disorders.

Moreover, poly-carboxylic species such as tartrate, glutamate, adipate or citrate are important in alimentary industry as food additives. Dicarboxylic acids and dicarboxylates are also common chemicals in the pharmaceutical and cosmetics industries. Besides, aromatic carboxylates are widely used in the industry of plastics.[86] And many raw materials in the industry of inks and paints are also related to dicarboxylic acids.[87]

All these roles exemplify the relevance of dicarboxylic species as analytical targets to be detected and quantified.

Among the different approaches applied to the detection of dicarboxylate anions and dicarboxylic acids, the design of synthetic receptors which can produce an easily readable analytical response represents an area of intense research activity. Systems which offer a colorimetric, fluorescent or electrochemical signaling have enabled the development of fast and easy analytical protocols. The polytopic nature of dicarboxylic species requires special attention in the design of receptors which should include a manifold of interacting sites. Another important aspect, to be considered in the recognition of dicarboxylate anions and dicarboxylic acids, is the effect of pH and water solubility, due to the requirement of having to perform certain studies under physiological conditions.[88]

---

[85] a) J.G. Zeikus, M.K. Jain, P. Elankovan, *Appl. Microbiol. Biotechnol*., **1999**, 51, 545–552. b) D.L. Nelson, A.L. Lehninger, M.M. Cox, Lehninger, *Principles of Biochemistry*, W.H. Freeman, New York, **2008**.

[86] a) T.A.M. Msagati, *Food acids and acidity regulators, in: Chemistry of Food Additives and Preservatives*, Blackwell Publishing Ltd., **2012**, pp. 125–130. b) B. Ward Jr., C. Force, A. Bills, F. Woodward, *J. Am. Oil Chem. Soc*., **1975**, 52, 219–224. c) G. Wypych, *Handbook of Plasticizers*, second ed., ChemTech Publishing, **2012**.

[87] R.J. Fitzmaurice, G.M. Kyne, D. Douheret, J.D. Kilburn, *J. Chem. Soc., PerkinTrans*. 1, **2002**, 841–864.

[88] D. Curiel, M. Más-Montoya, G. Sánchez, *Coord. Chem. Rev*., **2015**, 284, 19-66.

All these challenging conditions have attracted the interest of many research groups and have rendered a wide structural variety of synthetic receptors which have exploited the use of different intermolecular interactions to tackle dicarboxylic recognition. These synthetic receptors can be divided into two mains groups: neutral molecules and charged species. In the first group we can find H-bond donors such as ureas, thioureas, amides or pyrroles.[89] In the second group we can find molecules bearing positively charged groups such as an ammonium, guanidinium, imidazole or pyridinium salts. In this thesis we focused in the use of thiourea receptors as a neutral H-bond donors for dicarboxylate recognition.[90]

4.2. Urea and thiourea-based receptors.

The use of urea and thiourea functional groups as receptors represents a widespread synthetic approach in carboxylate anion recognition. The good orientation of two hydrogen bond donor groups (NH) becomes especially useful for the association with Y-shaped carboxylate anions due to an optimum geometrical correspondence. It is common to resort to thiourea derivatives due to the higher acidity of their protons, when compared to those of urea groups, and to the less hydrogen bond acceptor characteristics of the sulphur atom.

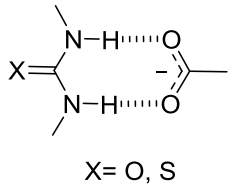

Scheme 1: Hydrogen bonding interaction between urea or thiourea and carboxylate anion**.**

The binding site defined by bis-thiourea **1** has been used for the complexation many aliphatic (oxalate, malonate, succinate and glutarate) and aromatic dicarboxylates (phthalate, isophthalate and terephthalate) in CH_3CN.

[89] S. A. Kadam, K. Martin, K. Haav, L. Toom, C. Mayeux, A. Pung, P. A. Gale,. J. R. Hiscock, S. J. Brooks, I. L. Kirby, N. Busschaert and I. *Leito, Chem. Eur. J*. **2015**, 21, 5145 – 5160

[90] T. Gunnlaugsson, A. P. Davis, J. E. O'Briena and .M.Glynn, *Org. Biomol. Chem*., **2005**,3, 48-56

[91]Chirality was introduced into the structure of the receptor **1** with the aim of comparing the complexation of the two enantiomers of chiral dicarboxylic aminoacids (*D*- and *L*-glutamate and *D* - and *L* –aspartate). However, due to the flexibility of the side branches only a subtle enantioselectivity was detected. The incorporation of the anthracene unit enabled the monitoring of the binding event by emission spectroscopy.

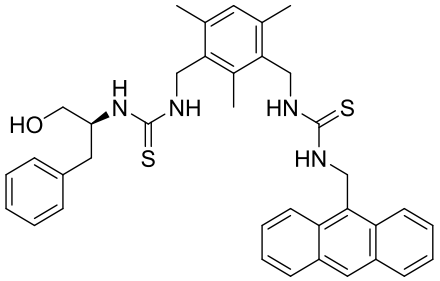

1

Figure 1: Sensor described for Chan and coworkers.

The discrimination between isomeric dicarboxylates was also described by Costero *et al*. who synthesized chiral bisthioureas derived from trans-transoid-trans-1,2,4,5-tetrasubstitutes cyclohexanes.[92] Compound **2** led to the formation of 1:1 complexes with the maleate anion in DMSO solution. Two-dimensional NMR experiments demonstrated that a conformational change in the cyclohexane ring, which adopted a boat or twisted boat arrangement, happened upon maleate complexation. This conformation released steric hindrance around the ethoxycarbonyl substituents and brought the naphthalene units in close proximity enabling the detection of an excimer band in the fluorescence spectrum. Conversely, the trans configuration of the fumarate anion did not induce any conformational change after binding and only a minor emission quenching could be detected, which was ascribed to the formation of a 2:1 (host:guest) complex.

[91] X.B. Zhou, Y.W. Yip, W.H. Chan, A.W.M. Lee, *Beilstein J. Org. Chem*., **2011**, 7, 75-81.
[92] A.M. Costero, M. Colera, P. Gaviña, S. Gil, *Chem. Commun*., **2006**, 7, 761–763.

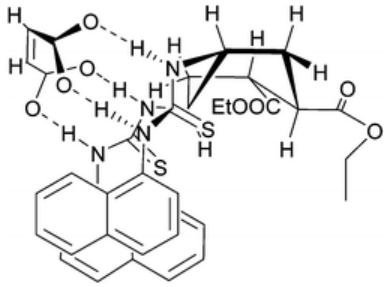

Figure 2: Structural proposal for the complex formed between ligand 2 and TMA maleate.

Hosts with multiple hydrogen bonding functional groups promote the synergistic binding of dicarboxylate anions. Ghosh *et al*. reported the fluorescent triphenylamine-based receptor **3** containing a combined amide–urea binding site, which responded to the presence of linear aliphatic dicarboxylates (malonate, succinate, glutarate, adipate, pimelate and suberate). [93] In the case of malonate, an excess of this dianion originated a drastic colour change from yellow to red. The origin of this colour change was ascribed to an intramolecular charge transfer between the amide–urea binding site and the p-nitrophenyl moiety, which was enhanced by the deprotonation of the urea function.

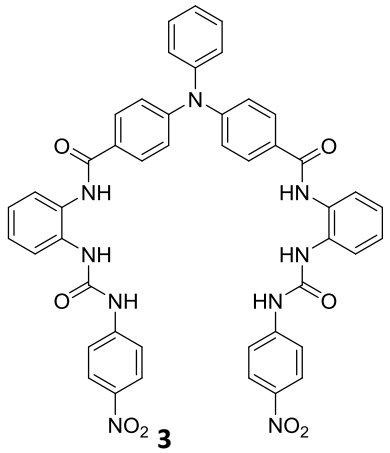

3

Figura 3: Triphenylamine-based receptor for the selective recognition of dicarboxylates.

[93] K. Ghosh, I. Saha, G. Masanta, E.B. Wang, C.A. Parish, *Tetrahedron Lett*, **2010**, 51, 343–347.

4.3. Hybrid Materials.

The attachment of a synthetic receptor to a surface is a very elegant way to increase both selectivity and sensitivity of a particular sensory system. There are several options to accomplish the anchoring of molecules as well as a wide range of substrates. Perhaps the most common methodology consists in the linkage of thiols, sulfides or disulfides onto the surface of gold substrates. Likewise, the employment of silanes over SiO_2 surfaces is also important due to the compatibility of such systems with spectrophotometric techniques which cannot be used with gold substrates.

4.3.1. Gold Nanoparticles

Isothiouronium decorated gold nanoparticles **4** have been used for the selective colorimetric sensing of malonate.[94] This dianion induced a significant colour change, from red to bluish-violet, in a nanoparticle suspension in 10% H_2O/MeOH. The response was due to an aggregation process induced by the presence of the dicarboxylate which acted as a linker between nanoparticles, as demonstrated by field emission scanning electron microscopy. Although other anions also caused small changes on the surface plasmon band, the mentioned colour change was exclusive of malonate anion.

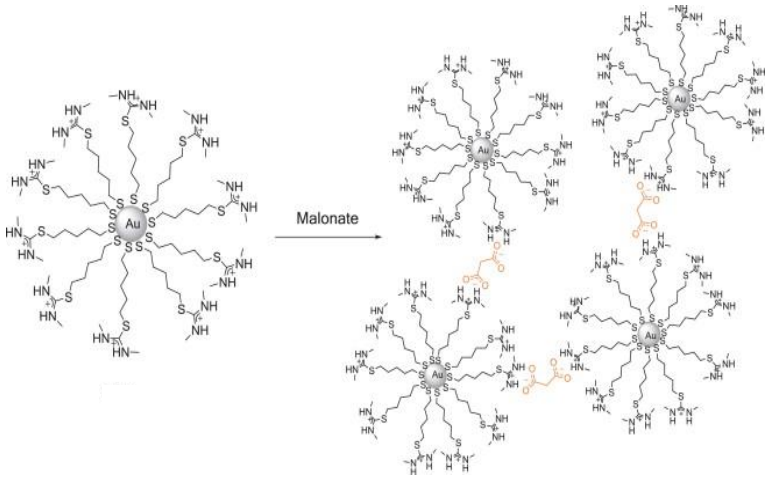

Figure 4: Isothiouronium-modified gold nanoparticles showed a selective sensor material for malonate.

[94] Y. Kubo, S. Uchida, Y. Kemmochib, T. Okubo, *Tetrahedron Lett*., **2005**, 46, 4369–4372.

Ahn and collaborators have reported the preparation of gold nanoparticles functionalized with o-(carboxamido)trifluoroacetophenone. A colour change from red to purple, resulting from the broadening of the plasmon band, could be observed in aqueous solution upon titration with certain dicarboxylate anions. Interestingly, only rigid dianions with both carboxylate groups pointing in opposite directions (fumarate and terephthalate) could promote the aggregation of nanoparticles which caused the colour change.[95]

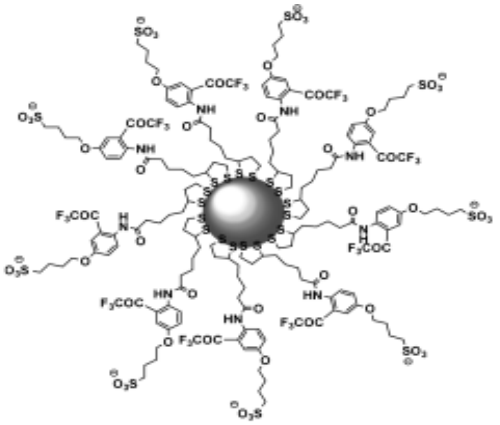

Figure 5: Functionalized gold nanoparticles able to discriminates fumarate from its cis-isomer maleate, and benzene-1,4-dicarboxylate from its isomeric benzene-1,2-and benzene-1,3-dicarboxylates.

Gold nanoparticles with bis-thiourea arms, (Figure 6), have been tested as anion receptors.[96] The presence of dicarboxylates provoked an enhancement of the surface plasmon absorption band as a result of intra-particle 1:1 complexes being formed in DMSO. A good response was achieved for a number of aliphatic dicarboxylates (malonate, succinate, glutarate, adipate, pimelate and sebacate). Conversely, no alteration of the spectrum was detected with monocarboxylates, halides and phosphates. Interestingly, control experiments carried out with monothiourea receptors did not show any evidence of binding, which reinforces the intra-particle nature of the interactions on the functionalized nanoparticles.

[95] A. Chatterjee, D.J. Oh, K.M. Kim, K.-S. Youk, K.H. Ahn, *Chem. Asian J.*, **2008**, 3, 1962–1967.
[96] Y. Liu, Y. Liu, Z. Liang, X. Li, S. Liu, J. Yu, *Chin. J. Chem. Phys*., **2011**, 29, 531–538.

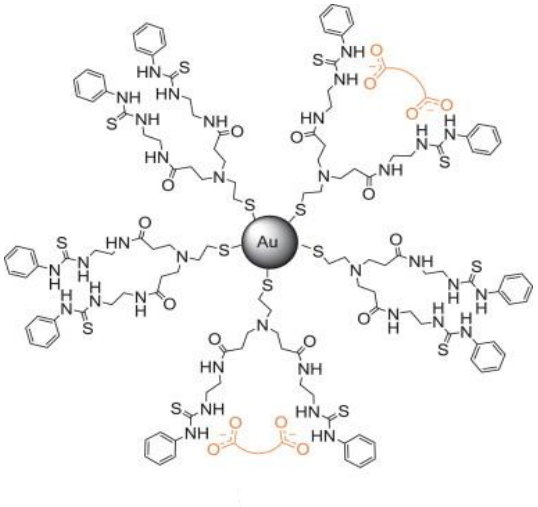

Figure 6: Selective chemosensor for malonate.

Finally, Lu and co-workers designed a novel sensory system using a fluorescein-doped silica nanoparticle functionalized with an [Eu(EDTA)(H_2O)$_3$] complex.[97] By exposure of the nanoparticles to solutions of calcium dipicolinate, a fluorescence enhancement was observed as a consequence of the displacement of coordinated water molecules by the dicarboxylate. The detection limit obtained for this sensor was 0.2 nM and no interference induced by other aromatic carboxylic acids such as phthalic, isophthalic and benzoic acid was detected.

[97] K. Ai, B. Zhang, L. Lu, *Angew. Chem. Int. Ed*., **2009**, 48, 304–308.

4.4. Objectives

The objective of this chapter is the design, synthesis and evaluation of optical sensors and probes for mono- and dicarboxylates, based on the use of thiourea moieties as a receptor units.

In the first part, we will discuss the use of a fluorescein derivative as signaling unit in the design of a fluorogenic sensor for mono and dicarboxylates. In the second part, thiourea-based receptors will be attached onto the surface of gold nanoparticles for the colorimetric sensing of dicarboxylates through analyte-induced aggregation.

4.5. Fluorescein-based thiourea derivatives as fluorogenic sensors for mono and dicarboxylates

Fluorescein-based thiourea derivatives as fluorogenic sensors for mono and dicarboxylates

Ana M. Costero, Margarita Parra, Salvador Gil, Josep Vicent Colomer, Almudena Martí.

Centro mixto de Reconocimiento Molecular y Desarrollo Tecnológico (IDM), Universidad Politécnica de Valencia–Universidad de Valencia, Valencia, Spain. Departamento de Química Orgánica, Facultad de Químicas, Universidad de Valencia, Doctor Moliner 50, 46100 Burjassot, Valencia, Spain.

Received: 31 March 2010

Accepted: 26 May 2010.

Sensor Lett., **2010**, 8, 818-823.

1. Introduction

Fluorescent sensors for ions and neutral species have demonstrated their potential in different fields such as biological probes,[1-3] environmental sensors,[4-5] nerve gas sensors,[6-8] etc. Fluorescein is one of the most commonly used fluorophores due to its high molar absorptivity, large fluorescence quantum yield and high photostability. In addition, the fluoresceine unit absorbs and emits light in the visible region. Among the different commercially available fluorescein derivatives, fluorescein isothiocyanate has proved very useful because it is able to react with amino groups to give thiourea derivatives. Even though this probe has been mainly used in biological studies, some applications in anion sensing have been recently reported.[9-11] The photophysical properties of fluorescein strongly depend on pH and, for this reason, anion recognition experiments must be carefully designed to distinguish real complexation processes from mere acid-base reactions. On the other hand, thiourea moiety has proved to be an appropriate binding site for anion and, more specifically, for carboxylate recognition.[12-13] This functional group is able to form strong hydrogen bonds with carboxylate to give rise to clear modifications in the sensor photophysical properties. However, some particular characteristics of the thiourea group should be considered in order to understand its complexing and sensing properties: (1) the role that positional isomers play in the complexation proccess14-16 and (2) the tendency of ligands to aggregate in solution.[17-19]

Our research group has been interested in preparing fluorescent thiourea-based sensors for the selective sensing of carboxylates and dicarboxylates. In this sense, specific interest has been paid to diastereoisomers discrimatation (maleate vs. fumarate).[20-21] The previously prepared ligands contained naphtalene groups as fluorescent motifs. As these groups are moderately fluorescent, we decided to susbtitute naphthyl groups for the most fluorescent fluorescein system to increase the sensititivity in the process. Thus, we herein report the preparation of three new ligands (see Chart 1) and their use in sensing different anions.

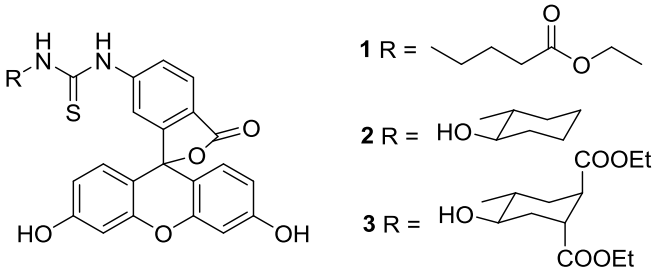

Chart 1: Structure of the prepared sensors

2. Experimental Methods

2.1 General procedures and materials.

All the other reagents were commercially available and were used without purification. THF was distilled from Na/benzophenone under Ar prior to use. Silica gel 60 F254 (Merck) plates were used for TLC. ^{1}H and ^{13}C NMR spectra were recorded with the deuterated solvent as the lock and the residual solvent as the internal reference. High-resolution mass spectra (FAB) were recorded in the positive ion mode on a VG-AutoSpec. UV-vis spectra were recorded using a 1 cm path length quartz cuvette. All the measurements were carried out at 293 K. Fluorescence spectra were carried out in a Varian Cary Eclipse Fluorimeter. TMA salts were obtained from the corresponding acid and TMA hydroxide.

2.2 Synthesis of ligand 1.

Fluoresceinisothiocyanate (0.300 g, 0.77 mmol) was added drop-wise into a solution of ethyl 5-aminopentanoate hydrochloride (0.117 g, 0.7 mmol) and triethylamine (0.070 g, 0.7 mmol) in THF (30 mL) at 70ºC. The resulting mixture was refluxed for 16 h under an Ar atmosphere. Then the mixture was allowed to cool to room temperature and was poured over hexane (25 mL), yielding 1 as an orange precipitate (91% yield).

^{1}H NMR (400 MHz, DMSO-d6): δ = 1.19 (t, J = 7.1Hz, 3H, CH3); 1.84 (quint, J = 7.1Hz, 2H, CH2); 2.38 (t, J = 7.1Hz, 2H, CH2CO); 3.52 (broad s, 2H, CH2N); 4.07 (q, J = 7.1Hz, 2H, CH2O-); 6.5-6.6 (m, 4H, CHAr); 6.68 (d, J = 2.1Hz, 2H, -OCCHAr); 7.17 (d, J = 8.2Hz, 1H, CHAr); 7.76 (broad d, J = 8.2Hz, 1H, NCCHAr); 8.25 (broad s, 2H, OH+NCCHAr); 10.1 (broad s, 2H, 2HN).

^{13}C NMR (100 MHz, DMSO-d6): δ = 14.6 (CH3), 24.4 (CH2), 31.5 (CH2), 44.0 (CH2), 60.3 (CH2O), 81.5 (C-OCO), 102.7 (CAr), 110.2 (CHAr), 113.1 (CHAr), 116.5 (CHAr), 124.0 (CHAr), 129 (CHAr), 129.4 (CHAr), 141.5 (CAr), 147.5 (NCAr), 152.4 (OCAr), 159.9 (HOCAr), 169.0 (COO), 173.0 (COOEt), 180.5 (CS).

MS: m/z (%) = 520 [M+1, 100%]; 390 [C21H12NO5S +, 21%].

HRMS: m/z [M+1] + calcd for C27H25N2O7S: 521.1382; found: 521.1398.

2.3 Synthesis of ligand 2.

Fluoresceinisothiocyanate (0.778 g, 2.0 mmol) was added drop-wise into a solution of trans-2-aminecyclohexanol (0.30 g, 2.0 mmol) and triethylamine (0.37 g, 3.7 mmol) in THF (40 mL) at 70ºC. The resulting solution was refluxed for 24 h. Then the mixture was allowed to cool to room temperature and was poured over hexane (25 mL), yielding 2 as a yellow precipitate (40% yield);

^{1}H NMR (300 MHz, DMSO-d6): δ = 1.18 – 1.24 (m, 3H); 1.59-1.67 (m, 3H); 1.8 – 1.9 (m, 2H); 3.42 (m, 1H); 3.99 (m, 1H); 4.7 (broad s, 1H); 6.5-6.6 (m, 4H); 6.73 (d, J = 2 Hz, 2H); 7.14 (d, J = 8.2, 1H); 7.79 (dd, J1 = 8.2, J2 = 1.5, 1H); 8.3 (broad s, 1H); 8.44 (d, J = 1.5, 1H); 10.4 (broad s, 1H).

^{13}C NMR (100 MHz, DMSO-d6): δ = 23.2 (CH2), 24.2 (CH2), 25.6 (CH2), 34.3 (CH2), 59.0 (CHN), 70.4 (CHO), 102.7 (CHAr), 110.3 (CAr), 113.3 (CHAr), 115.9 (CHAr), 124.2 (CHAr), 124.7 (CAr), 126.9 (CAr), 129.2 (CHAr), 129.4 (CHAr), 142.3 (CAr), 147.0 (NCAr), 152.4 (OCAr), 160.1 (HOCAr), 169.1 (COO), 180.4 (CS).

3. Results and Discussion

The synthesis of ligands **1** and **2** was easily carried out from commercial fluoresceinisothiocyanate and the corresponding amine under standard conditions. Compound **3** was prepared from racemic trans-transoid-trans- 4,5-bis(ethoxycarbonyl)-2-aminociclohexanol[20-21] and fluoresceinisothiocyanate. Ligands were spectroscopically identified. Before starting the sensing studies, different properties of the free ligands (such as positional isomers in solution and aggregation) were considered. In addition, the influence of pH was also explored. Thus, NMR experiments carried out with ligand **1** in DMSO demonstrate that the fluorescein moiety was present in its spirolactone form in this solvent, which was determined by the signal at 81.5 ppm in the 13C NMR spectrum corresponding to the spirolactone carbon.[22] In addition, the thiourea group of the molecule in solution was mainly present in its Z,Z conformation (clear ROE signals were observed between H_6 and H_7 (Chart 2)). In addition, ROESY experiments clearly show ROE between H_4 and H_{13}. This finding supports the idea that some kind of aggregation was present in the concentrated solutions. Chart 2 shows a model of a possible dimer following the well-known aggregation of thioureas.[17-19,23]

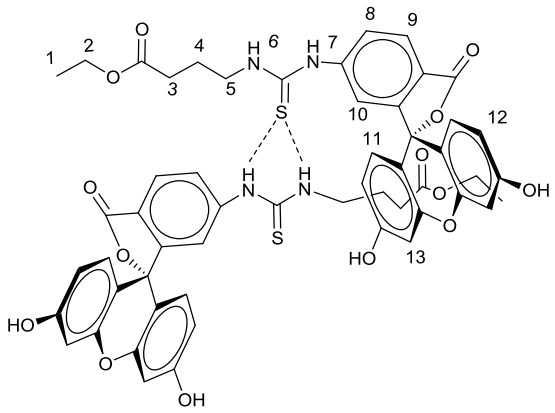

Chart 2: Model for the possible dimer of ligand 1.

Finally, the addition of 1 equiv of TMAOH to the DMSO solution of compound 1 induced strong modifications in the system as all the starting ligands were converted into different species. One of these species was monoanion **4** and the second was a by-product whose spectrospic data are compatible with compound **5** (Chart 3).

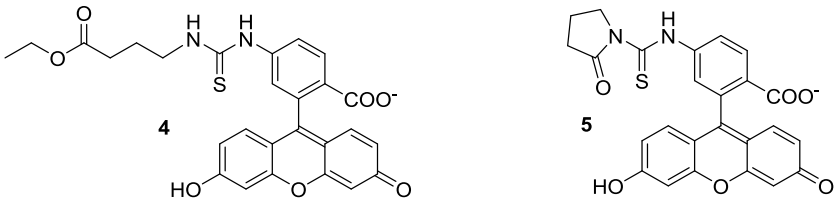

Chart 3: products obtained after treatment of ligand 1 with TMAOH.

Compounds **2** and **3** also show deprotonation when TMAOH was added, but no by-products were detected. The absorption spectra of compounds **1**-**3** can be accounted for by the superposition of the corresponding chromophors: fluorescein moiety (λmax= 520, 490 and 330 nm) and thiourea group (λmax= 258 nm). Compounds **1** and **3** also show a band at λmax= 275 nm, corresponding to the ester group (see Figure 1 (a) for compound **1**).[24] The absorption bands of compounds **1**-**3** in 10^{-5} M solutions in DMSO are summarized in Table 1. These values demonstrate that the three compounds have similar characteristics.

Table 1: Absorption bands of ligands **1-4** (10^{-5} M in DMSO).

Ligand	λ (nm) (ε M^{-1} cm^{-1})						
1	260	280	330		450	490	520
	(33100)	(30640)	(2670)		(260)	(610)	(1210)
2	260		340	420	450	482	522
	(36570)		(8320)	(5650)	(6870)	(7970)	(13550)
3	260	272	300	420	450	482	521
	(22880)	(4730)	(9710)	(3390)	(4600)	(6540)	(16550)

The fluorescence spectrum of ligand **1** (10-5 M in DMSO) exhibits the typical fluorescein dianion spectrum (λem = 540 nm) at both λexc = 490 nm (the usual excitation wavelength) and λexc = 330 nm. However in this latter case, a more complex emission pattern ((λem = 540, 465 and 415 nm) was observed (Figure 1 (b)). It has been established by ^{13}C NMR experiments in DMSO that the fluorescein moiety was present in the spirolactone form. Therefore, the protolytic equilibrium to generate the anionic systems must take place in the excited state.[25] On the other hand, different excitation spectra were obtained at 415, 465, and 540 nm, indicating that three species were present under these conditions.

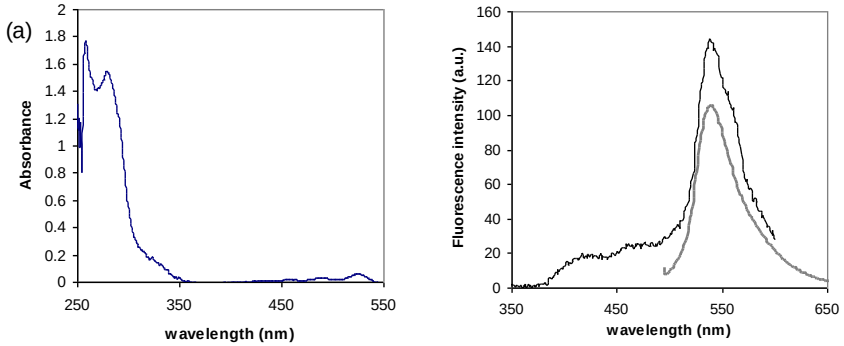

Figure 1. (a) UV spectrum of ligand 1 (b) emission spectrum of ligand 1 (λexc= 330 nm (blak) and 490 nm (grey)) in both cases the sample was 10^{-5} M in DMSO.

The influence of the concentration on the photophysical properties of ligands 1-3 was studied by both UV and fluorescence spectroscopy. Figure 2 shows the UV spectra of ligand **2** at different concentrations (10^{-4}, 10^{-5} and 10^{-6} M in

DMSO). As can be seen, the spectra present clear differences, of which the most important is the lack of absorption around 520 nm in the more concentrated solution. These results are consistent with a monomer-dimer equilibria of the ligand, as the NMR experiments suggest. Furthermore from the normalized UV spectra, an isosbestic point is observed at λ = 489 nm (see supplementary material) for ligand **2** and a monomer-dimer equilibrium constant (log K= 6) can be stimated. Close values have been obtained for ligands **1** and **3**.[26]

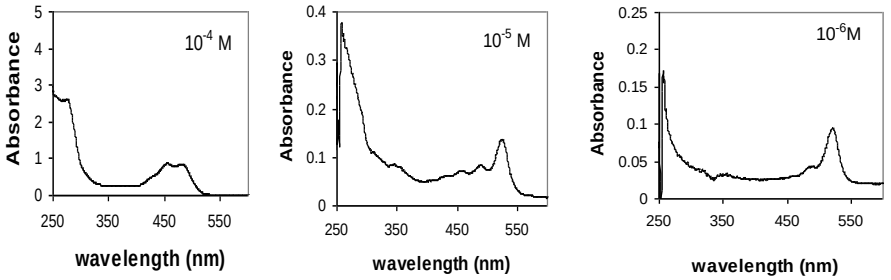

Figure 2. UV spectra of ligand 2 at different concentrations (10-4, 10-5 and 10-6 M in DMSO)

The emission spectra reveal that two emission bands (λ= 415 and 540 nm) appear when λexc= 330 nm. Nonetheless, the band at 415 nm was the main one in the most concentrated solutions (10^{-4} M and 10^{-5} M), whereas the main emission band appeared at 540 nm in the most diluted solution (10^{-6} M) (Figure 3). The band at 415 nm had a higher intensity in the spectrum of the 10^{-5} M solution than in the 10^{-4} M solution one owing to the different absorptions of both solutions at 330 nm.

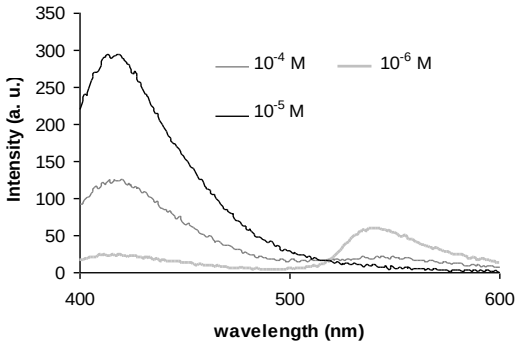

Figure 3. Emission spectra of ligand 2 at different concentration (in DMSO, (exc= 330 nm, slit=5).

The influence of concentration on the photophysical properties of ligands 1 and 3 was similar to that previously indicated for ligand **2**.

In order to know the influence of pH on the fluorescent properties of these compounds, experiments in buffered solutions (HEPES 10-**2** M, DMSO/water 2/1) were carried out. The influence of these conditions on the photophysical properties of the compounds was minimum (see Supplementary Information).

3.1 Complexation experiments.

Interactions of the ligands with anions were first studied in DMSO solutions with mono- and dicarboxylates, all of them as their tetramethyl amonium (TMA) salts. Under these conditions, two different processes must be considered: (a) acid-base reactions and (b) complexation with the thiourea groups. Figure 4 shows the fluorescent behavior of compound **2** upon the addition of increasing amounts of TMA acetate.

These results clearly support the notion that a first acid-base process generates the corresponding anion (emission band at 535 nm); this process finalizes when 1 equiv of anion has been added, and then it is followed by a real complexation process (Scheme 1) that is characterized by a quenching of the fluorescence. In addition a blue shift of the band to 525 nm was observed (Figure 4).

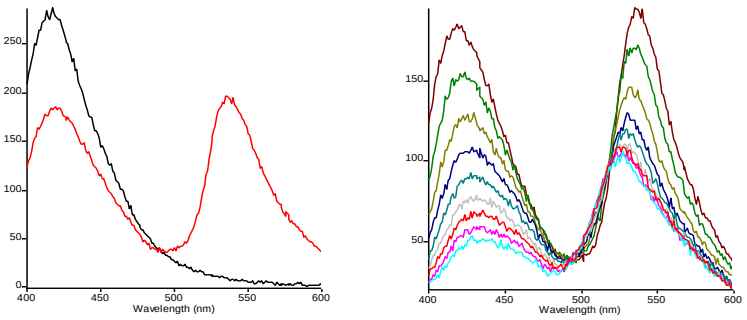

Figure 4. Fluorescence spectra of ligand 2 10^{-5} M in DMSO (λexc = 330 nm). (left) (a) free ligand, (b) free ligand after the addition of 1 equiv of TMA acetate. (right) free ligand after addition of TMA acetate from 1 equiv to 5 equiv.

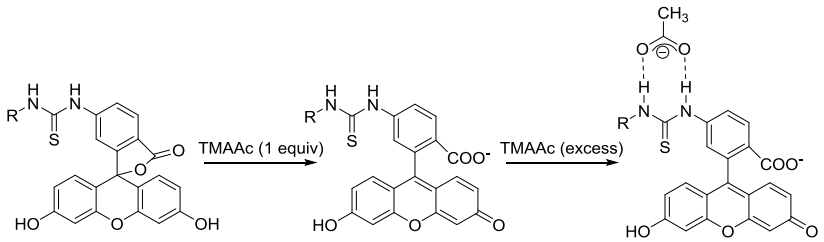

Scheme 1. Proposed steps in titration experiments with TMAAc.

As expected, the acid-base mechanism in buffered solutions (HEPES 10^{-2} M, DMSO:water (3:1)) was inhibited and only complexation took place. Under such conditions, the log β and the stoichiometry of the complexes for ligand **1-3** and TMA acetate were calculated by performing UV-titration experiments and by fitting all the spectrophotometric curves with the SPECFIT program.27 (see Table 2)

Table 2. Complexation constant and stoichiometry of complexes formed between ligands 1-3 and TMA acetate (10-5M, HEPES 10-2 M in DMSO:water (3:1)).

Ligand	Stoichiometry	log β
1	1:1	4.2 ± 0.1
2	1:1	5.9 ± 0.3
3	1.1	4.3 ± 0.2

Similar behavior was observed with malonate, succinate, maleate, fumarate and phthalate (all of them as their TMA salts). Thus, until the addition of 1 equiv, an increment of the emission at 535 nm, stronger than that with TMA acetate, was observed. In the presence of larger amounts of anion, a gradual quenching of fluorescence was induced, even though no modification in wavelength was observed in these cases. When buffered solutions were used, only the quenching of fluorescence was observed in accordance with the behavior previously observed with acetate (for example, see Figure 5 for ligand **1**).

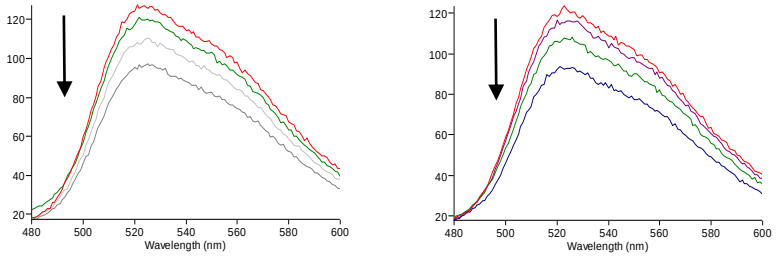

Figure 5. Fluorescent spectra of ligand 1 in the presence of increasing amounts of (left) TBA fumarate and (right) TBA maleate (10-5M, HEPES 10-2 M in DMSO:water (3:1), exc = 330 nm).

More interesting results were observed when excitation was carried out at 280 nm. Under these conditions, ligand **1** was able to discriminate maleate among all the studied anions. Thus, whereas fumarate, phthalate, succinate and malonate gave rise to slight changes in fluorescence intensity, maleate enhanced the fluorescence emission by 80% (Figure 6). A similar behavior was observed with ligands **2** and **3**, although the effect was slighter

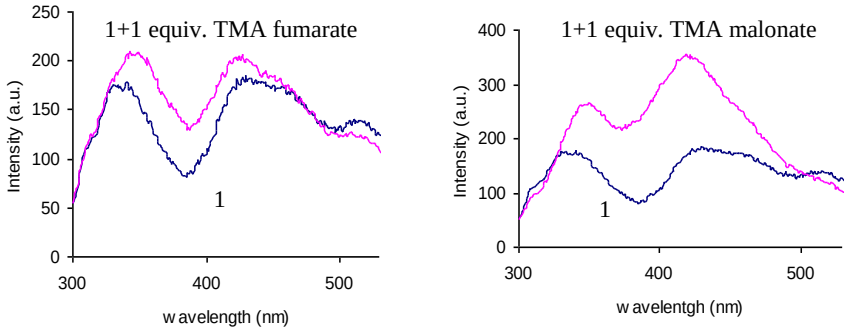

Figure 6. Fluorescent spectra of ligand **1** with (left) without and with 1 equiv. of TBA fumarate and (right) without and with 1 equiv. of TBA maleate (10-5M, HEPES 10-2 M in DMSO:water (3:1), λexc = 280 nm).

The different behavior observed between maleate and fumarate cannot be explained upon the basis of their cis or trans geometry because phthalate with a similar spatial disposition to that of maleate did not present any increase in fluorescence (see Supplementary Material) under similar conditions. Thus, the

different behavior observed with the studied dicarboxylates could relate to the different salts that these ligands can form depending on different factors.[28]

4. Conclusions

The three new synthesized ligands show photophysical properties that are strongly dependent on pH because of the presence of flourescein moiety. In addition, concentration is also a very important issue due to the aggregation tendency shown by the thiourea groups. The complexation experiments in DMSO demonstrate that two proccesses should be considered: deprotonation of fluorescein moiety and a real complexation by the thiourea group. Finally, ligand 1 is able to distinguish between maleate and fumarate when excitation is carried out at 280 nm. The special behavior shown by maleate could relate to the different aggregation species formed in the salt synthesis process.

Acknowledgments: This research has been financed by the Spanish DGCYT (CTQ2006-15456-C04-02 and MAT2009-14564-C04-02) and by the Regional Valencian Government (Generalitat Valenciana) (Acciones Complementarias ACOMP07/080). SCSIE (University of Valencia) is gratefully acknowledged for all the equipment employed.

References and Notes

1. M. Goncalves, T. Sameiro, Chem. Rev. 109, 190 (2009).

2. O. Minet, J. Beuthan, V. Mildaziene, R. Baniene, Rev. Fluor. 1, 195 (2004).

3. M.K. Johansson, R. M. Cook, Chem.–Eur. J. 9, 3466 (2003).

4. T. Matsuya, N. Hoshino, T. Okuyama, Current Analytical Chemistry 2(4), 397 (2006).

5. P. Scully, R. Chandy, R. Edwards, D. Merchant, R. Morgan, Environ. Sci. Res. 56, 175 (2001)

6. S. Royo, R. Martínez-Máñez, F. Sancenón, A. M. Costero, M. Parra, S. Gil, Chem. Commun. 4839 (2007)

7. B. C. Giordano, G. E.Collins, Curr. Org. Chem. 11, 255 (2007).

8. M. Burnworth, S. J. Rowan, C. Werder, Chem.–Eur. J. 13, 7828 (2007).

9. X-F. Yang, L. Wang, H. Xu, M. Zhao, Anal. Chim. Acta 631, 91 (2009).

10. J-S. Wu, Kim, H. J. Lee, J. H. Yoon, J. H. Lee, J. S. Kim, Tetrahedron Lett. 48, 3159 (2007).

11.. X. Zhang, Y. Shiraishi, T. Hirai, Tetrahedron Lett. 48, 8803 (2007).

12.. C. Caltagirone, P. A. Gale, Chem. Soc. Rev. 38, 520 (2009).

13.. Z.-h. Lin, L.-x. Xie, Y.-g. Zhao, C.-y. Duan, J.-p. Qu, Org. Biomol. Chem. 5, 3535 (2007).

14.. K. Rang, J. Sandström, C. Svensson, Can. J. Chem. 76, 811 (1998).

15.. D. A. Jose, D. K. Kumar, P. Kar, S. Verma, A. Ghosh, B. Ganguly, H. N. Ghosh, A. Das, Tetrahedron 63, 12007 (2007).

16.. F. Sansone, E. Chierici, A. Casnati, R. Ungaro, Org. Biomol. Chem. 1, 1802 (2003).

17.. A. M. Costero, P. Gaviña, G. M. Rodríguez-Muñiz, S. Gil, Tetrahedron 63, 7899 (2007).

18.. K.-J. Kim, J.-M. Lee, S.-K. Ryu, Sep. Technol. 6, 211 (1996).

19.. A. Mosunov, J. J. Dannenberg, J. Phys. Chem. B 104, 806 (2000).

20.. A. M. Costero, M. Colera, P. Gaviña, S. Gil, M. Kubinyi, K. Pál, M. Kállay, Tetrahedron 64, 3217 (2008).

21.. A. M. Costero, M. Colera, P. Gaviña, S. Gil, Chem. Commun., 761 (2006).

22.. H. N. Kim, M. H. Lee, H. J. Kim, J. S. Kim, Chem Soc Rev. 37, 1465 (2008).

23. R. Custelcean, Chem Commun., 295 (2008)

24. M. Nickoleit, A. Uhl, J. Bendig, Laser Chem. 17, 161 (1977)

25. R. Sjöback, J. Nygren, M. Kubista, Spectrochim. Acta, Part A 51, L7 (1995).

26. C. Lee, Y. W. Sung, J. W. Park, J. Phys. Chem. B 103, 893 (1999).

27. SPECFIT/32 Global Analysis System v. 3.0, Spectrum Associates (Marlborough, MA, USA). www.bio-logic.info/rapid-kinetics/specfit.html.

28. J. E. Barry, M. Finkelstein, S. D. Ross, J. Org. Chem. 47, 64 (1982).

4.6. Selective recognition and sensing of succinate vs. other dicarboxylates by thiourea-functionalized gold nanoparticles

Selective recognition and sensing of succinate *vs.* other aliphatic dicarboxylates by thiourea-functionalized gold nanoparticles

Almudena Martí, Ana M. Costero*, Pablo Gaviña*, Margarita Parra

Centro Mixto de Reconocimiento Molecular y Desarrollo Tecnológico. Facultad de Química. Universidad de Valencia. Dr. Moliner, 50, 46100 Burjassot, Valencia, Spain

Chem. Eur. J., Submitted

Abstract: Gold nanoparticles functionalized with thiourea moieties have been used as selective colorimetric sensors for the naked-eye detection of succinate *versus* other aliphatic dicarboxylates, all of them as their TBA salts. The detection process is based on the interparticle aggregation triggered by coordination of the end-carboxylates to the thiourea moieties of two different nanoparticles. This nanoparticle aggregation results in a batochromic shift of the plasmon resonance band and a visual color change from red to blue..

INTRODUCTION

Anions are involved in a large number of chemical, biological, environmental and industrial processes; for this reason, the establishment of new methods for the detection of these species is an area of great interest.[1] Particularly important are dicarboxylates since some of them have critical roles in the most important metabolic cycles of living organisms.[2] Specifically, succinate is an inhibitor of mitochondrial lipid peroxidation, preventing or delaying most of the damage caused by the peroxidation on different mitochondrial structures and functions. Moreover, selective ischaemic accumulation of succinate is responsible for ischaemia-reperfusion injury, which occurs when the blood supply to an organ is disrupted and then restored[3] However, although a large number of systems for the molecular recognition or sensing of dicarboxylates have been reported in the last years,[4] few examples of the selective recognition [5] or sensing of succinate versus other linear aliphatic dicarboxylates are known [6]

On the other hand, functionalized gold nanoparticles (GNPs) have recently attracted interest in colorimetric sensing applications.[7] The sensing strategy is based on the color change that arises from the interparticle Plasmon coupling that occurs during the aggregation of GNPs or the dispersion of GNPs aggregates. The red color of dispersed nanoparticles turns to dark blue upon aggregation and the color change can be observed by the naked eye even at low concentrations. This fundamental optical property of GNPs has been successfully used for the development of sensors for biological macromolecules as well as small organic molecules and metal cations.[8] However there are less references reporting the use of functionalized gold nanoparticles for the detection of small anions. In these examples ureas, thioureas, amides or isothiouronium-modified surfaces were synthesized as receptors for anion recognition. [9]

To the best of our knowledge, only two authors have studied the sensing ability of functionalized gold nanoparticles in front of dicarboxylate anions. Liu, Yu and col. synthesized GNPs functionalized with bis-thiourea arms that showed higher selectivity for dicarboxylate anions (and particularly for malonate) than for

simple monoanions. The sensing mechanism is based on conformational changes on the surface of the nanoparticles, due to an intraparticle complexation, which lead to slight changes in the surface plasmon band of the nanoparticles.[10] On the other hand, Ahn and col. developed GNPs functionalized with *o*-(carboxamido)trifluoroacetophenone derivatives as sensing systems to distinguish geometrical isomers of dicarboxylates (fumarate *versus* maleate).[11] The change of colour was induced by the analyte-triggered aggregation of the nanoparticles.

We describe herein the synthesis of new thiourea functionalized gold nanoparticles as well as their evaluation as colorimetric sensors for aliphatic dicarboxylates. The sensing mechanism, depicted in Figure 1, is based on the coordination of the terminal carboxylates to the thiourea moieties of two different GNPs, leading to interparticle-crosslinking aggregation. This reaction was expected to produce a change in the surface plasmon resonance absorption of the GNPs and consequently a change in their colour, from red to blue (figure 1).

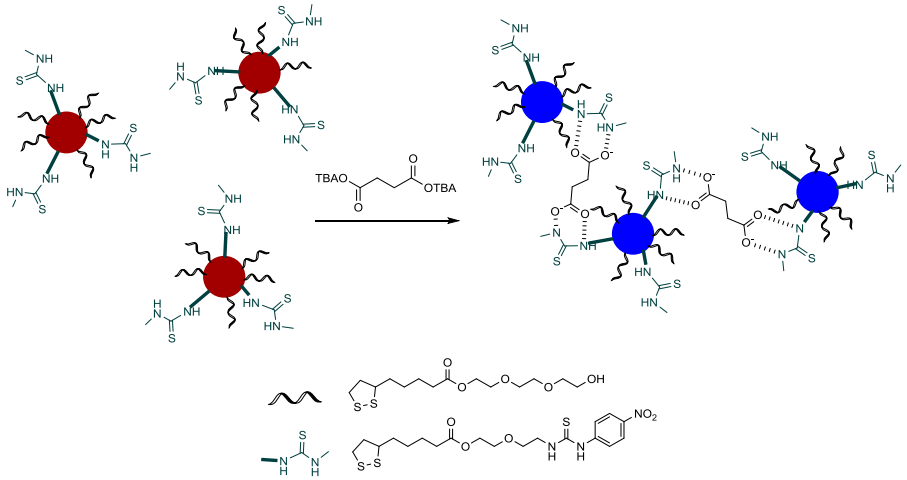

Figure 1: Paradigm of the sensing mechanism using functionalized gold nanoparticles: complexation of dicarboxylates with the thiourea group of two nanoparticles induces aggregation and consequently colour change.

RESULTS AND DISCUSSION

p-Nitrophenyl thiourea derivative 1 was synthesized from 4-nitrophenyl isothiocyanate and 2-(2-aminoethoxy)ethanol. In order to attach the thiourea moiety to the surface of the GNPs, and provide the strong affinity of gold for disulfide groups, the alcohol was esterified with thioctic acid in the presence of EDC and DMAP to yield ligand **L1** (51 % yield overall). In the same conditions triethylene

glycol was esterified with thioctic acid to obtain **L2** with 40 % yield (Scheme 1). This chain was used to stabilize the system as it is described that oligo(ethylene glycol) moieties prevented the nanoparticles aggregation process in nonionic gold surfaces. [12] The chemical structure and purity of the prepared ligands were confirmed by spectroscopic techniques (see SI).

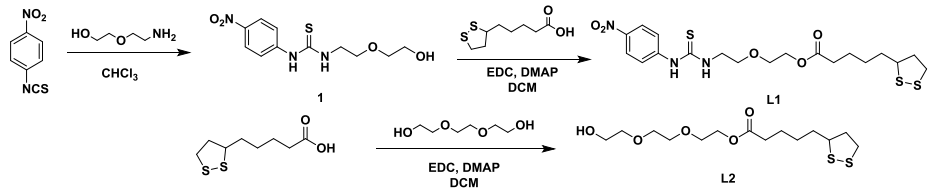

Scheme 1: Synthesis of ligands L1 and L2.

Thiourea-functionalized gold nanoparticles GNP1 were synthetized by a two-step procedure. First, citrate-stabilized nanoparticles was prepared by reducing tetrachloroauric acid with trisodium citrate in boiling water.[13, 14] Then, in a ligand-exchange reaction the citrate was displaced from the surface of the nanoparticles by a mixture of ligands L1 and L2, in a 1:5 (L1 : L2) optimized ratio. The functionalized GNPs were centrifuged and re-dissolved in water, giving rise to a stable aqueous suspension of GNP1. The obtained functionalized-GNPs showed an average size of 13 nm as determined by TEM. Water solutions of GNP1 exhibited the characteristic surface plasmon resonance band at 530 nm in the UV-vis spectra.

Our first studies were focused on the evaluation of the behaviour of water solutions of GNP1 in the presence of various linear aliphatic dicarboxylates with increasing chain lengths: oxalate (**C2**), malonate (**C3**), succinate (**C4**), glutarate (**C5**), adipate (**C6**), pimelate (**C7**), suberate (**C8**), azeleate (**C9**) sebacate (**C10**) and dodecanodiolate (**C12**). In addition, two unsaturated aliphatic dicarboxilates: fumarate (**t-C4**) and maleate (**c-C4**), were chosen to study the influence of the geometry of the double bond, and an aromatic dicarboxylate, 2,6-napthalenedicarboxylate (**NDC**) to evaluate the influence of the rigidity of the system. Finally, acetate was also studied as a model of monocarboxylates. Acetate and all the dicarboxylates were used as their tetrabutylammonium(TBA) salts.

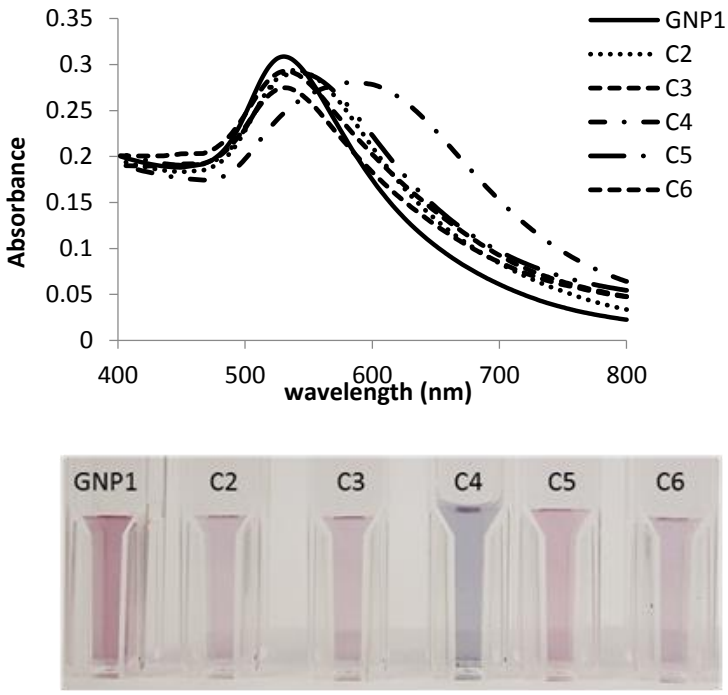

Figure 2: (top) UV-vis spectra of a water solution of GNP1 ($4 \cdot 10^{-10}$ M) free and after addition of an excess of oxalate (C2), malonate (C3), succinate (C4) , glutarate (C5) , and adipate (C6)as their TBA salts (50µL of a 1mM water solution, corresponding to a final concentration of 4.76×10^{-5}M); (bottom) Colors of the resulting solutions of GNP1 after the addition of excess of dicarboxylates C2–C6.

Figure 2 shows the UV-spectra of a solution of **GNP1** in water ($4 \cdot 10^{-10}$ M) before and after addition of an excess of TBA salts of oxalate (**C2**), malonate (**C3**), succinate (**C4**) and glutarate (**C5**) (50µL of a 1mM solution in water) (for aliphatic dicarboxylates **C6–C12** see Supporting Information). Surprisingly, only with succinate, a color change of the GNPs solution from red to blue, clearly visible by the naked eye, was observed (Figure 2, bottom). The colour change corresponds to the appearance of a new surface plasmon resonance band at λ= 615 nm (aggregated GNPs). For the rest of the linear aliphatic dicarboxylates only small bathochromic shifts in SPR

band of the dispersed **GNP1** were observed for some of them, whereas almost no change was observed in the presence of acetate.

The aggregation of **GNP1** in the presence of excess of succinate was further confirmed by TEM studies (Figure 5).

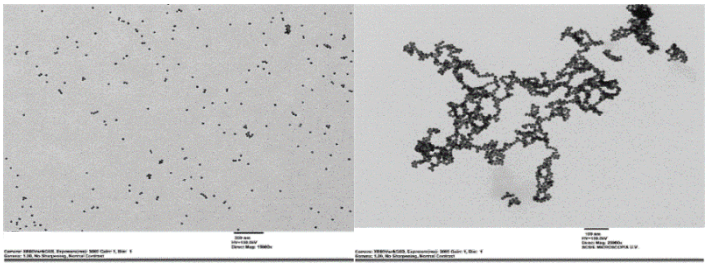

Figure 5: TEM images of stabilized GNP1 dispersions (left) and their aggregates upon addition of excess of succinate (right).

In the case of unsaturated dicarboxylates, only a small difference was observed between maleate (*c*-**C4**) and fumarate (*t*-**C4**) (see Figure 3). Thus, in the case of **c-C4** a small bathochromic shift of the main absorption band was observed whereas a broadening of the right part UV-vis spectra of **GNP1** towards higher wavelenghts was observed for **t-C4**. Finally no changes were observed in the presence of the aromatic 2,6-naphthalenedicarboxylate.

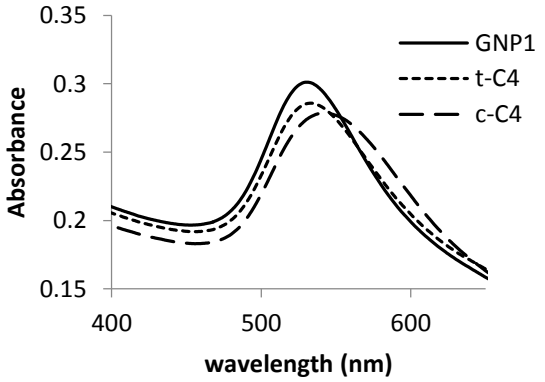

Figure 3. UV-spectra of a solution of GNP1 ($6 \cdot 10^{-11}$ M) free and after addition of an excess of fumarate and maleate as TBA salts, (100µL of a solution 1mM in water, corresponding to a concentration of 9.09×10^{-5}M).

The selective response observed for succinate *vs* the other aliphatic dicarboxylates allows to use this system for the selective colorimetric detection of this anion in aqueous solutions. With this goal titration studies were performed with **GNP1** and TBA succinate in water. The absortion band at 530 nm (A_{530}) corresponding to red dispersed **GNP1** gradually suffers a batochromic displacement to 615 nm (A_{615}), resulting in a purple colour of the solution which can be observed by the naked eye (Figure 4).

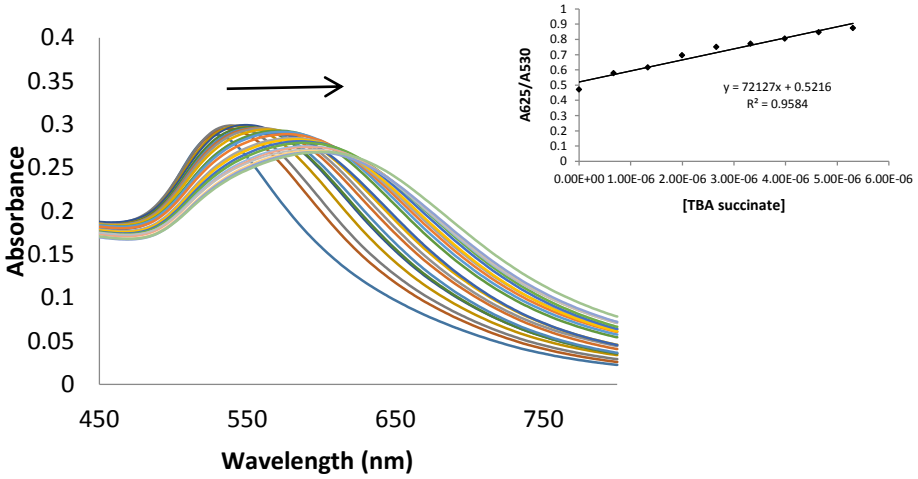

Figure 4: UV-vis spectra of GNP1 ($1.37 \cdot 10^{-9}$ M) upon addition of increasing amounts (2 µl) of succinate (1x 10^{-3} M in water). (Inset). Plots A_{615}/A_{530} *versus* TBA succinate concentration obtained with GNP1.

The linearity of detection was kept until $6x10^{-6}$M. The visual limit of detection (visual LOD, defined as the minimum concentration of dicarboxylate necessary for an observable color change) was 5 µM. When the LOD was calculated from the changes in UV-vis spectra (see S.I.), the value was 0.5 µM.

Figure 6 shows a plot of A615/A630 vs dicarboxylate concentration to compare the behaviour of succinate with that of shorter or longer aliphatic dicarboxylates (**C2** to **C6**). For succinate, a linear response was observed until approximately $1x10^{-5}$M of dicarboxylate, reaching a plateau around $3x10^{-5}$M. In the case of C5 a linear but much less pronounce response was observed between 10^{-6} to 10^{-5} M of dicarboxylate and almost no response was observed for the rest of dicarboxylates.

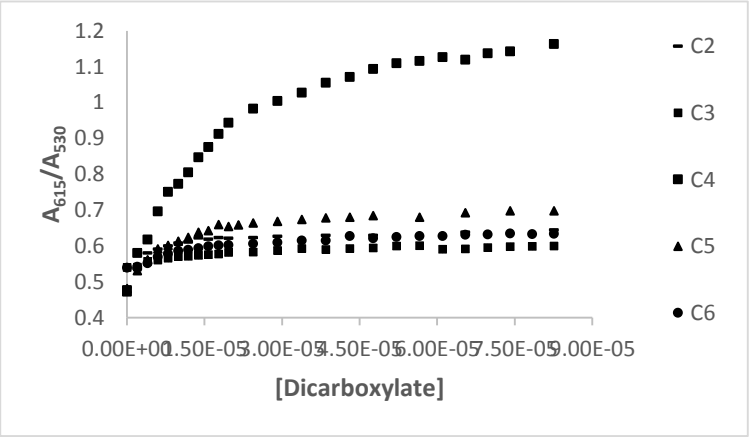

Figure 6: Comparative titrations: Plots A_{615}/A_{530} *versus* dicarboxylate concentration obtained with GNP1s for TBA oxalate (C2), malonate (C3), succinate (C4), glutarate (C5) and adipate (C6) (for the other anions see supporting information)

As it has been previously described [11] for other functionalized GNPs, there is a competition between inter- and intra-particle binding processes in the complexation of dicarboxylates, being critical both the geometry and the flexibility of the analytes, and the geometry and particular arrangement of the binding groups on the surface of the nanoparticles. In our case, succinate seems to be the only dicarboxylate able to cause an effective inter-particle cross linking aggregation with **GNP1**, giving place to the clusters formation. Very likely, the small bathochromic shifts of the SPR band of dispersed GNPs observed for the other dicarboxylates is related to intra-particle binding events (figure 6).

The observed selectivity could be related to the distance between the nanoparticles after complexation. It has been established that the red shift takes places when the interparticle distances in the aggregates decrease to less than the average particle radius [15] and this situation can be achieved with succinate and in less extension with maleate whereas the longer dicarboxylates do not give rise to this situation. Oxalate present and odd behavior that can be related to the lower complexation constants usually showed by this carboxylate when it is complexed with ligands functionalized with thioureas.

In summary, we have synthesized thiourea functionalized gold nanoparticles (**GNP1**) for the selective colorimetric detection of TBA succinate *versus* others dicarboxylates. The detection process is based on the interparticle

cross linking aggregation triggered by coordination of the carboxylate group with the thiourea moieties of two different GNPs. This aggregation results in a batochromic shift in the SPR band and a color change of the solution, from red to blue which is easily observable by the eye.

ACKNOWLEDGMENTS

We thank the Spanish Government, European FEDER funds (MAT2009-14564-C04) and Generalitat Valenciana (PROMETEOII/2014/047) for support. A. M. is grateful to the Spanish Government for a fellowship. SCSIE (Universidad de Valencia) is gratefully acknowledged for all the equipment employed.

REFERENCES

1.- (a) L. Fabbrizzi; A. Poggi *Chem. Soc. Rev*. **2013**, *42*, 1681-1699; (b) R. Custelcean *Topics in Curr. Chem*. **2012**, *322*, 193-216; (c) V. Amendola; L. Fabbrizzi; L. Mosca *Chem. Soc. Rev*. **2010**, *39*, 3889-3915.

2.- A. Lehninger, D, Nelson y M. Cox. "Principios de bioquímica". Ed. Omega, Spain, 2000, pp. 515-517.

3.- E. T. Chouchani, V. R. Pell, E. Gaude, D. Aksentijević, S. Y. Sundier, E. L. Robb, A. Logan, S. M. Nadtochiy, E. N. J. Ord, A. C. Smith, F. Eyassu, R. Shirley, C.-H. Hu, A. J. Dare, A. M. James, S. Rogatti, R. C. Hartley, S. Eaton, A. S. H. Costa, P. S. Brookes, S. M. Davidson, M. R. Duchen, K. Saeb-Parsy, M. J. Shattock, A. J. Robinson, L. M. Work, C. Frezza, T. Krieg , M. P. Murphy *Nature* **2014**, *515*, 431-435.

4.- (a) C. Curiel; M. Mas.Montoya; G. Sanchez *Coordination Chem. Rev*. **2015**, *284*, 19-66; (b) A. M. Costero; M. Parra; S. Gil; M. R. Andreu "Springer Series on Chemical Sensors and Biosensors" **2013**, *12*, 1-32.

5.- (a) M. Bonizzoni, A. Moletti, D. Pasini, A. Taglietti *New J. Chem*. **2007**, *31*, 352-356; (b) I. V. Korendovych, M. Cho, O. V. Makhlynets, P. L. Butler, R. J. Staples, E. V. Rybak-Akimova *J. Org. Chem.* **2008**, *73*, 4771-4782.

6.- A. M. Costero, M. Colera, Pablo Gaviña, Salvador Gil, Úrsula Llaosa *Tetrahedron*, **2008**, *64*, 7252-7257

7.- (a) Chen, Y.-C.; Lee, I.-L.; Sung, Y.-M.; Wo, S.-P. *Sensor Actuat. B-Chem*. **2013**, *188*, 354-359; (b) Knighton, R. C.; Sambrook, M. R.; Vincent, J. C.; Smith, S. A.; Serpell, C. J.; Cookson, J.; Vickers, M. S.; Beer, P. D. *Chem. Commun.* **2013**, *49*, 2293-2295; (c) Kumar, V.; Anslyn, E. V. *J. Am. Chem. Soc.* **2013**, *135*, 6338-6344; (d) Wang, A.-J.; Guo, H.; Zhang, M.; Zhou, D.-L.; Wang, R.-Z.; Feng, J.-J. *Microchim. Acta* **2013**, *180*, 1051-1057; (e) A. Martí, A. M. Costero; P. Gaviña; M. Parra *Tetrahedron Lett*. **2014**, *55*, 3093-3096; (f) C. Wang; C. Yu *Rev Anal Chem* **2013**, *32*, 1–14.

8.- (a) K. Saha, S. S. Agasti, C. Kim, X. Li, V. M. Rotello Chem. Rev. 2012, 112, 2739-2779; (b) A. Martí, A. M. Costero; P. Gaviña; M. Parra *Chem. Commun*. **2015**, *51*, 3077-3079.

9.- (a) S. Watanabe; M. Sonobe; M. Arai; Y. Tazume; T. Matsuo; T. Nakamura; K. Yoshida *Chem. Commun*. **2002**, 2886-2867; (b) Y. Kubo; S. Uchida; Y. Kemmochi; T. Okubo *Tetrahedron Lett.* **2005**, *46*, 4369-4372; (c) S. Kado; A. Furui; Y. Akiyama; Y. Nakahara; K. Kimura *Anal. Sci*. **2009**, *25*, 261-265; (d) K. Tomita; T. Ishioka; A. Harata *Anal. Sci.* **2012**, *28*, 1139-1144.

10.- Y. Liu; Y. Liu; Z. Liang; X. Li; S. Liu; J. Yu *Chin. J. Chem*. **2011**, *29*, 531-538.

11.- (a) K.-S. Youk; K. M. Kim; A. Chatterjee; K. H. Ahn *Tetrahedron Lett*. **2008**, *49*, 3652-3655; (b) A. Chatterjee; D. J. Oh; K. M. Kim; K.-S. Youk; K. H. Ahn *Chem. Asian J.* **2008**, *3*, 1962-1967.

12.- M. Kadalbajoo; J. Park; A. Opdahl; H. Suda; C. A. Kitchens; J. C. Garno; J. D. Batteas; M. J. Tarlov¡; P. DeShong *Langmuir* **2007**, *23*, 700-707.

13.- S.-Y. Lin; Y.-T. Tsai; C.-C. Chen; C.-M. Lin; C.-h. Chen *J. Phys. Chem. B* **2004**, *108*, 2134-2139.

14.- W. Haiss; N. T. K. Thanh; J. Aveyard; D. G. Fernig; *Anal. Chem*. **2007**, *79*, 4215-4221.

15.- A. A. Lazarides; G. C. Schatz*, J. Chem*. *Phys.* **2000**, *112*, 2987-2993.

Supplementary Information

Selective recognition and sensing of succinate *vs.* other aliphatic dicarboxylates by thiourea-functionalized gold nanoparticles

Almudena Martí, Ana M. Costero, Pablo Gaviña*, Margarita Parra

Centro Mixto de Reconocimiento Molecular y Desarrollo Tecnológico (IDM), Universidad de Valencia – Universidad Politécnica de Valencia, Dr. Moliner, 50 46100 Burjassot (Valencia), Spain

E-mail: pablo.gavina@uv.es

General procedures:

All reagents were commercially available, and were used without purification. Silica gel 60 F254 (Merck) plates were used for TLC. Milli-Q ultrapure water was used for the synthesis of AuNPs and the sensing experiments. ^{1}H-NMR and ^{13}C-NMR spectra were recorded on a Bruker 300 MHz spectrometer. Chemical shifts are reported in ppm with tetramethylsilane as an internal standard. High resolution mass spectra were recorded in the positive ion mode on a VG-AutoSpec mass spectrometer. UV-vis absorption spectra were recorded using a 1 cm path length quartz cuvette on a Shimadzu UV-2101PC spectrophotometer. All measurements were carried out at 293 K (thermostated). The TEM electronic images were made on a JEOL-1010 transmision electron microscope operating at 100 KV.

Synthesis of L1

A solution of 4-Nitrophenyl isothiocyanate (3.42 g, 19 mmol) in dry toluene (5 mL) was added to a solution of 2-(2-aminoethoxy)ethanol (2 g, 19 mmol)) in dry toluene (2 mL). The solution was stirred at room temperature overnight. The solvent was removed and the residue washed with hot petroleum ether to give **1** (4.8 g, 89%):

^{1}H NMR (300 MHz, DMSO) δ 10.23 (s, 1H), 8.28 (s, 1H), 8.24 – 8.10 (m, 2H), 7.89 – 7.81 (m, 2H), 4.64 (t, J = 5.2 Hz, 1H), 3.73 – 3.64 (m, 2H), 3.64 – 3.43 (m, 6H), 2.50 (dt, J = 3.7, 1.8 Hz, 2H).

^{13}C NMR (75 MHz, DMSO) δ 180.11, 146.38, 141.81, 124.55, 120.29, 72.18, 68.09, 60.22, 43.87.

A solution of **1** (4.8 g, 16.84 mmol) EDC (3.39 g, 17.68 mmol) and DMAP (catalytic amount) dissolved in dry dichloroethane (20 mL) was stirring at 0^{0} C for 15 min in a bath water/ice. A solution of thioctic acid (3.64, 17.68 mmol) in dichloroethane (30 mL) were added. After 24 h at room temperature chloroform was removed under reduced pressure and the mixture was extracted with diethyl ether. The organic layer was washed with brine, dried over $MgSO_4$ and concentrated. The product was purified by colum chromatography yield **L1** (4.5 g, 57%) as yellow oil.

^{1}H NMR (300 MHz, CDCl3) δ 10.22 (s, 1H), 8.22 (s, 1H), 8.16 (d, *J* = 9.2 Hz, 2H), 7.87 (d, *J* = 9.3 Hz, 2H), 4.17 (s, 2H), 3.73 – 3.62 (m, 6H), 3.58 – 3.47 (m, 1H), 3.20 – 3.01 (m, 2H), 2.42 – 2.25 (m, 4H), 1.89 – 1.75 (m, *J* = 33.1 Hz, 1H), 1.67 – 1.45 (m, *J* = 24.5 Hz, 5H), 1.41 – 1.25 (m, 2H).

^{13}C NMR (75 MHz, CDCl3) δ= 180.07, 172.70, 146.32, 141.74, 124.40, 120.13, 68.15, 63.04, 56.02, 54.83, 43.60, 39.87, 39.52, 38.09, 34.04, 33.28, 28.11, 24.21 ppm.

HRMS (ESI): m/z calcd. for $C_{19}H_{27}N_3O_5S_3$ ([M+H]+), 474.1186 (100%), found 474.1193.

Synthesis of L2

A solution of Triethylene glycol (5.82 g, 38.83 mmol) EDC (2.06 g, 10 mmol) and DMAP (catalytic amount) dissolved in dry chloroform was stirring at 0^0 C for 15 min in a bath water/ice. A solution of thioctic acid (2g, 9.71 mmol) in chloroform (50 mL) were added. After 24 h at room temperature chloroform was removed under reduced pressure and the mixture was extracted with diethyl ether. The organic layer was washed with brine, dried over $MgSO_4$ and concentrated. The product was purified by colum chromatography (ethyl acetate: hexane, 3:7) yield **L2** (1.273 g, 40%) as yellow oil.

^{1}H NMR (300 MHz, CDCl3) δ 4.30 – 4.18 (m, 1H), 3.79 – 3.66 (m, 4H), 3.63 – 3.50 (m, 1H), 3.24 – 3.05 (m, 1H), 2.81 – 2.74 (m, 1H), 2.46 (dtd, J = 12.0, 6.5, 5.5 Hz, 1H), 2.36 (t, J = 7.4 Hz, 1H), 1.90 (dq, J = 12.8, 7.0 Hz, 1H), 1.75 – 1.61 (m, 2H), 1.48 (ddd, J = 11.5, 8.4, 6.3 Hz, 1H).

^{13}C NMR (75 MHz, CDCl3) δ= 173.62, 72.61, 70.60, 69.32, 63.45, 61.93, 56.48, 40.36, 38.62, 34.72, 34.05, 28.86, 24.73 ppm.

HRMS (ESI): m/z calcd. for $C_{14}H_{27}O_5S_2$ ([M+H]+), 339.1294 (100%), found 339.1296.

Preparation of the Functionalized AuNPs:

All glassware was thoroughly cleaned with freshly prepared aqua regia (HCl/HNO_3, 3:1), rinsed thoroughly with deionized water and dried in air. GNPs with a diameter of around 13 nm were synthesized as reported previously.[1] Briefly, an aqueous 38.8 mm trisodium citrate solution (10 mL) was added to a boiling solution of 1 mm $HAuCl_4$ (100 mL) and the resulting solution boiled for 30 min until a red solution was obtained. This solution was cooled to room temperature and then stored in a refrigerator at 4 °C for use. The GNPs were modified by ligand-exchange reaction at room temperature as follows: A 0.01 M aqueous NaOH solution (20 µL) was added to the as-prepared citrate-capped GNPs (10 mL). Then **L2** (100 µL, 10^{-3} M in ethanol) and the appropriate amount of ligand **L1** (500 µL, 10^{-3} M in DMSO) were added simultaneously and the solution was stirred overnight. To purify the GNPs, the mixture was centrifuged for 20 min at 14000 rpm and the supernatants were decanted. Then the resulting GNPs were resuspended in Milli-Q water (**GNP1** $4 \cdot 10^{-10}$M). The size and shape of the modified GNPs were characterized by TEM. The UV/Vis spectra absorbance spectra of the modified AuNPs were recorded.

Calculation of LOD

The limit of detection for the succinate dianion was obtained from the plot of the ratio of the absorbance intensities at 530 and 615 nm (A_{615}/A_{530}) versus succinate concentration (in µM). LOD was calculated by using the equation (1), where K=3; S_b is the standard deviation of the blank and m is the slope of the calibration curve.

$$\mathrm{LOD} = \mathrm{K} \cdot \frac{S_b}{m} \quad (1)$$

Titration studies

In this case to 1000 µL of GNP1 (150 µL, $6. 10^{-11}$M in water) (obtained by dilution of 150 µL of the original solution of GNP1 $4 \cdot 10^{-10}$M) were added 100 µL of each dicarboxylate TBA salt (1·mM, corresponding to a final concentration of 90.9 µM). The solution was allowed to stand for 5 min in the air and the corresponding UV-vis spectra was recorded

Competitive studies

The same experimental procedure previously described for the dicarboxylate titration was followed for the competitive studies. In this case to 900 µL of **GNP1** ($6.7 \cdot 10^{-11}$M in water) (obtained by dilution of 150µL of the original solution of **GNP1** $4 \cdot 10^{-10}$M) were added 100 µL of each dicarboxylate TBA salt (1·mM, corresponding to a final concentration of 100 µM). The solution was allowed to stand for 5 min in the air and the corresponding UV-vis spectra was recorded. In absence of C4, no color changes were observed and the UV-vis spectra were almost identical to the original NPs. However in the presence of all the dicarboxylates (C2, C3, C5, C6, C7 plus C4, with a final concentration of 100 µM for each dicarboxylate) a clear change in the color of the solution were observed with the corresponding red shift in the UV-spectrum indicative of the aggregation process.

For the mixture of the dicarboxylate, we prepared each dicarboxylate solution as a TBA salt (6mM), 100 µL of each on were taken obtaining 600 µL of a solution 1mM as a final concentration in each dicarboxylate. of this solution 100 µL was taken and added to de **GNP1**

Figure S1. ^{1}H NMR and ^{13}C NMR spectrum of 1-(2-(2-hydroxyethoxy)ethyl)-3-(4-nitrophenyl)thiourea **1** in DMSO at 300 and 75 MHz

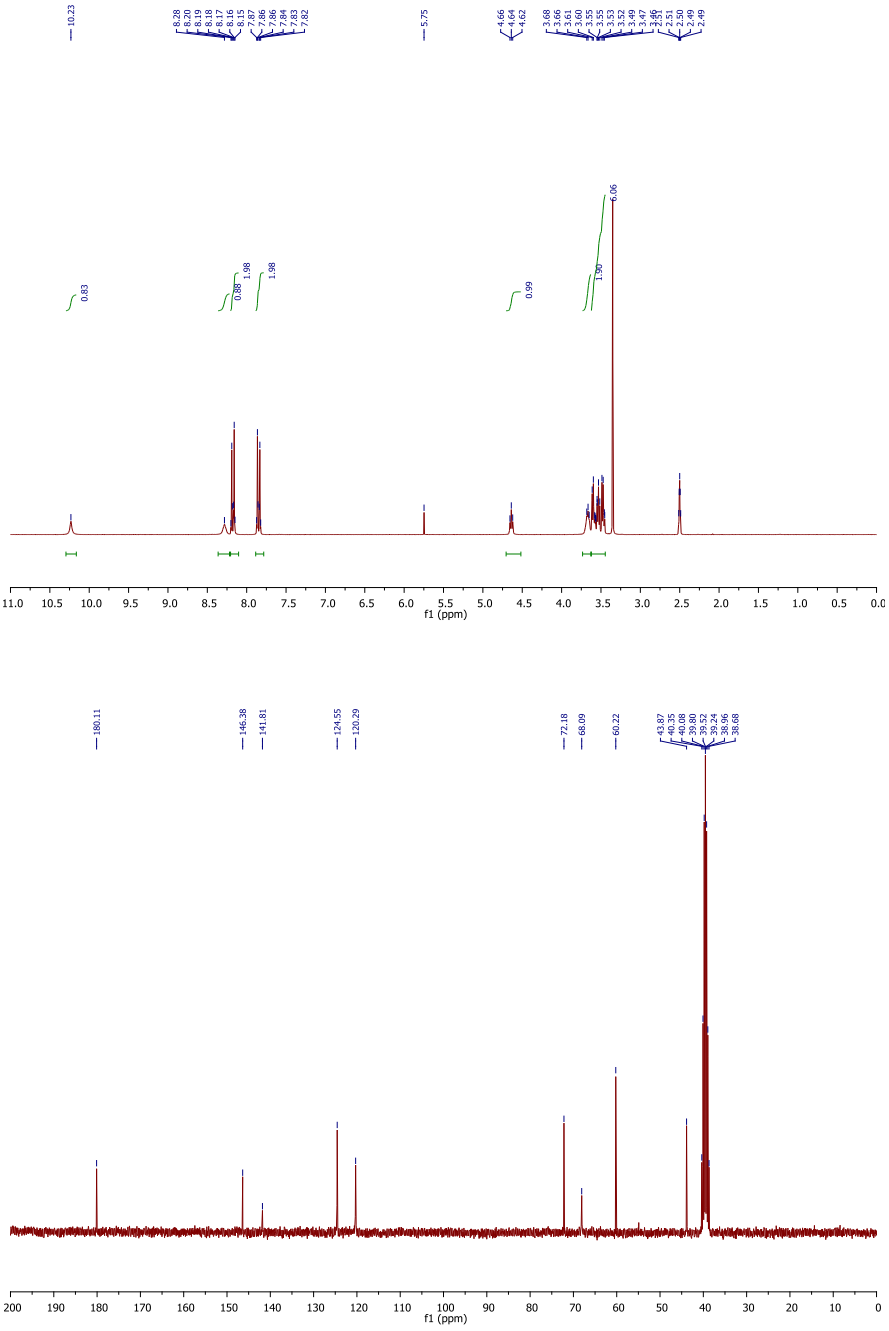

Figure S2. ^{1}H NMR and ^{13}C NMR spectrum of compound **L1** in DMSO at 300 and 75 MHz

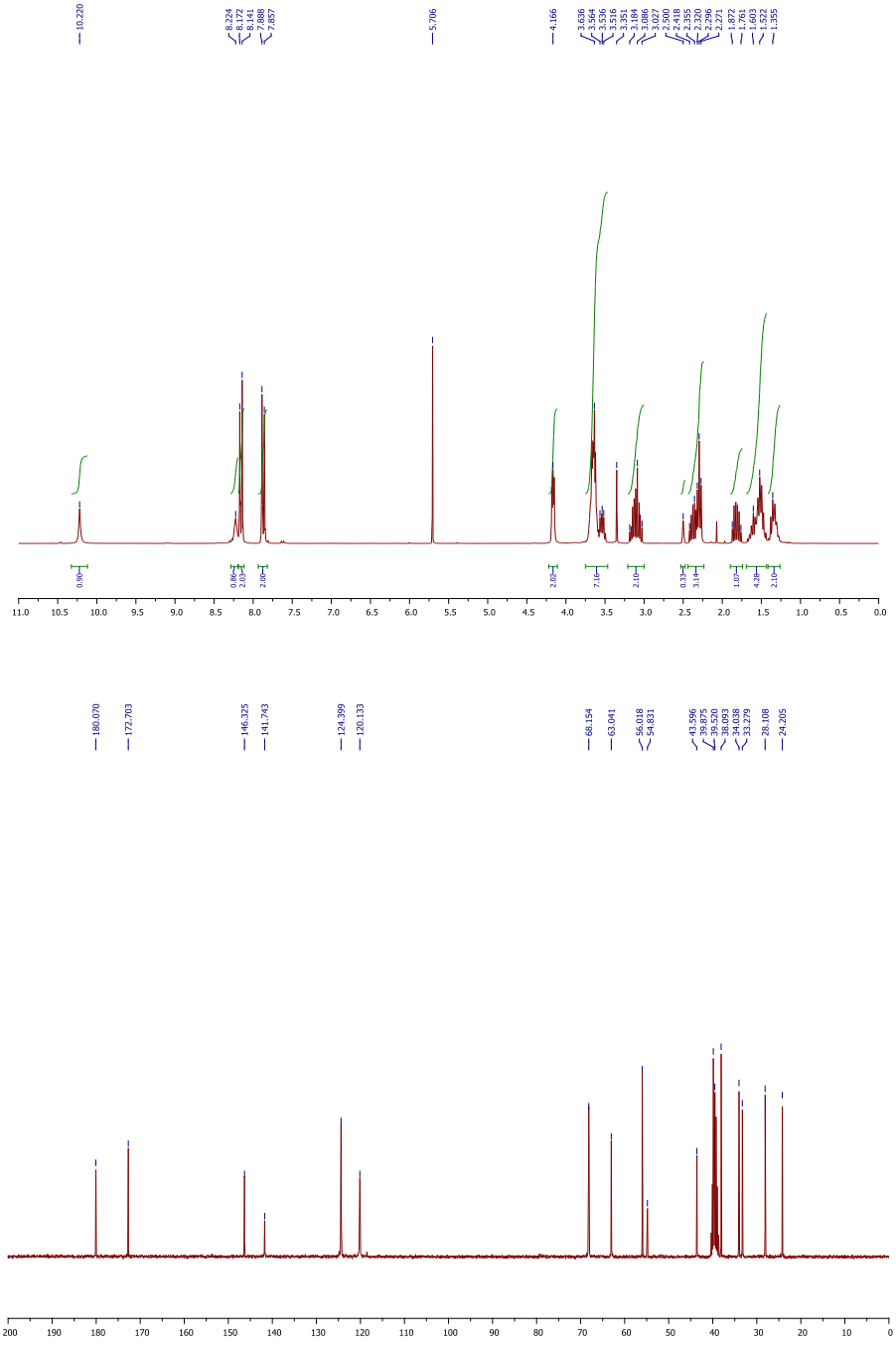

Figure S3. ^{1}H NMR and ^{13}C NMR spectrum of compound **L2** in $CDCl_3$ at 300 and 75 MHz

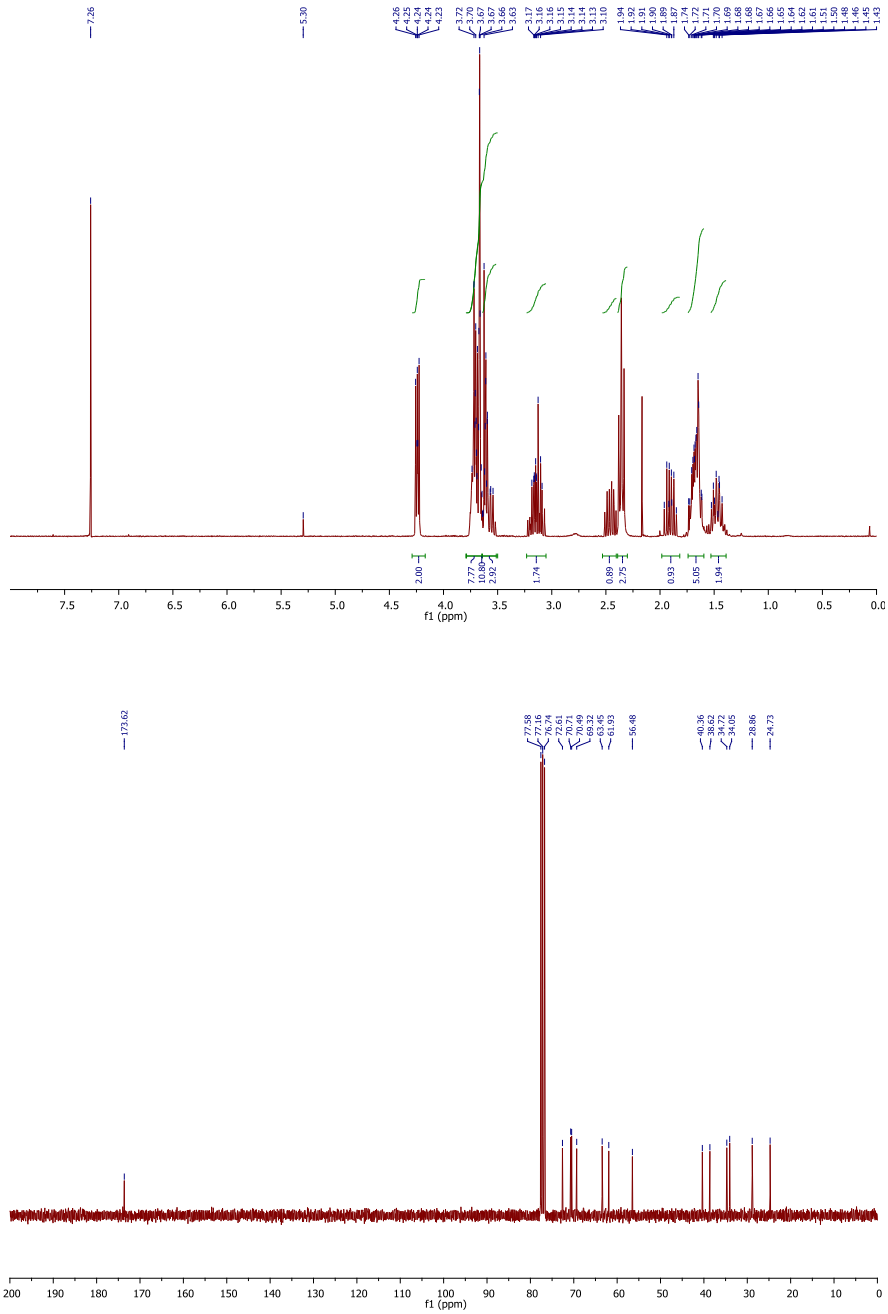

Figure S4. UV-spectra of a solution of **L1**,**L2**-AuNPs ($4 \cdot 10^{-10}$ M) and after addition of an excess (*100 µL of a solution of 1 mM* of different dicarboxilate salts (1mM in water)

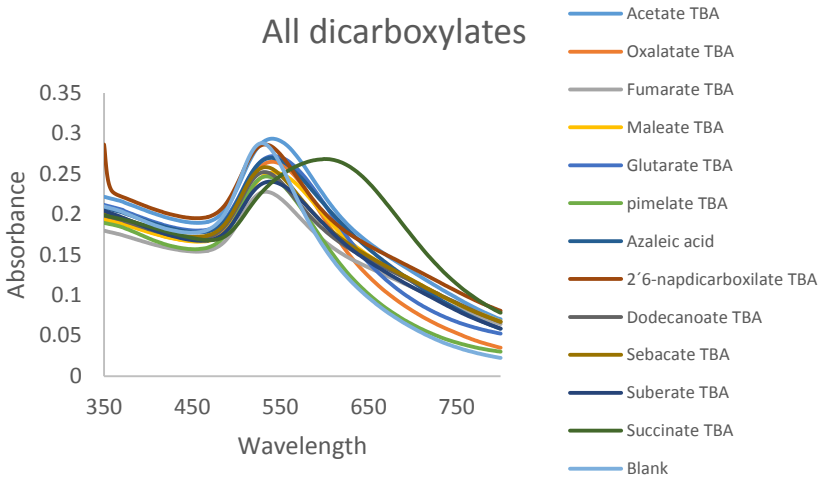

Figure S5. UV-vis spectra of the titration of **GNP1** ($6.67 \cdot 10^{-11}$ M) in water upon addition of increasing amounts of tetrabutylammonium acetate (2µM each)

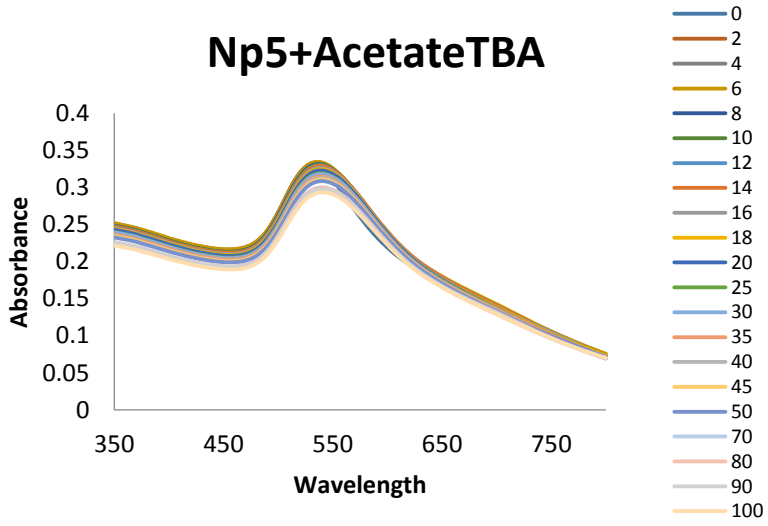

Figure S6. Comparative titrations: Plots A615/A530 versus dicarboxylate concentration obtained with **GNP1**

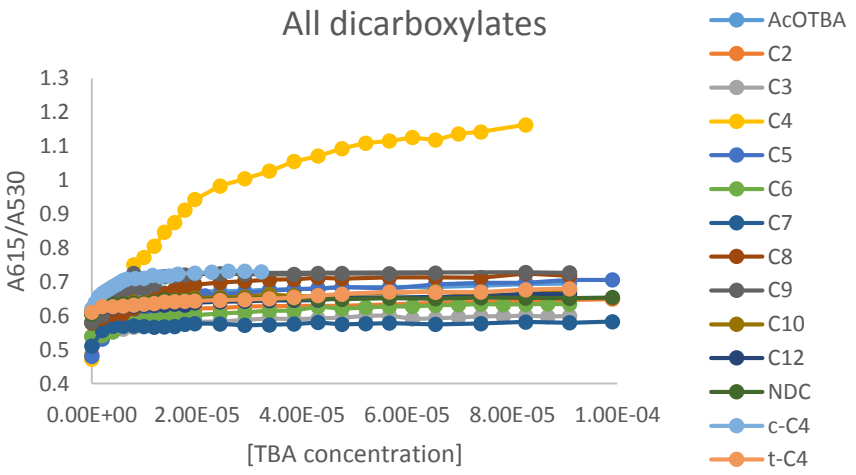

Figure S7. Competitive studies**.**

All the measures were referred to the succinate (C4)

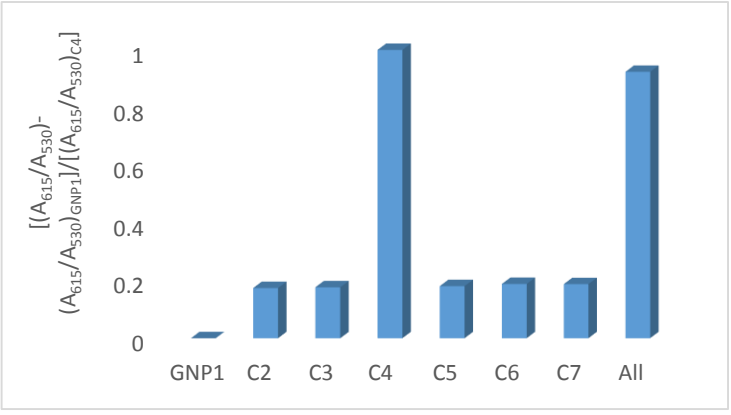

CHAPTER 5:
Discrimination of ω-amino acids.

5.1. Amino acids and their biological role.

α-Amino acids in their zwitterionic form are very important targets for molecular recognition due to their importance in biological processes.[98]Because of increasing attention paid to human health, and diagnosis and treatment of diseases, many efforts have been directed to the development of new methods toward α-amino acid analysis. However, less attention has been devoted to study linear aliphatic ω-amino acids even though they also play important biological roles.[99]. Structurally, amino acid neurotransmitters, such as β-alanine or GABA, are extremely simple molecules possessing an anionic carboxylate ($–COO^-$) on one end and a cationic ammonium ($–NH_3^+$) on the other end of the chain.

Glycine is a non-essential α-amino acid synthesized by animals, microorganisms, and plants. It is the simplest amino aid and the only one that is not optically active. Glycine is an essential precursor of important biological molecules such as proteins, and a key substance in many metabolic reactions; it is the major inhibitory neurotransmitter in the spinal cord and brain stem, and an anti-inflammatory, cytoprotective, and immune modulating substance.[100]

β-Alanine is the simplest β-amino acid. Structurally intermediate between α-amino acid and γ-amino acid neurotransmitters; β-alanine, contribute to the most fundamental processes of brain and to the pathogenesis of the disorders that affect these processes. In general, β-alanine satisfies a number of the prerequisite classical criteria for being a neurotransmitter: β-alanine occurs naturally in the central nervous system (CNS), it is released by electrical stimulation through a Ca^{2+} dependent process, it has binding sites, and inhibits neuronal excitability. Thus, a variety of data suggest that β-alanine should be considered as a small molecule neurotransmitter.[101]

γ-Aminobutyric acid (GABA) is the chief inhibitory neurotransmitter in the mammalian central nervous system. It plays the principal role in reducing neuronal excitability throughout the nervous system. In humans, GABA is also directly responsible for the regulation of muscle tone.[102]

---

[98] A. M. Costero, G. M. Rodríguez-Muñiz, S. Gil, S. Peransi, P. Gaviña, *Tetrahedron*, **2008**, 64, 110-116.

[99] H. Wang, A. Yu, b. Wiman, S. Pap, *Eur. J. Biochem*., **2003**, 270, 2023-2029.

[100] R. Y. Gundersen, P. Vaagenes, T. Breivik, F. Fonnum and P. K. Opstad, *Acta Anaesthesiol Scand*., **2005**; 49, 1108—1116

[101] K. E. Tiedje, K. Stevens, S. Barnes, D. F. Weaver; *Neurochem Int*., **2010** , 57, 177-188

[102] M. Watanabe, K. Maemura, K. Kanbara, T. Tamayama, H. HayasakiIn, *Int. Rev. Cytol,* **2002**, 213, 1–47.

5-aminopentanoic acid is a lysine degradation product. It is a metabolite of cadaverine. High levels of 5-aminovalerate in biofluids may indicate bacterial overgrowth or endogenous tissue necrosis. 5-aminovalerate is a normal metabolite present in human saliva, with a tendency to elevated concentration in patients with chronic periodontitis. It is also known as an antifibrinolytic amino acid analog and so it functions as a weak inhibitor of the blood clotting pathway.[103]

6-Aminohexanoic acid is an effective inhibitor for enzymes that bind that particular residue. Such enzymes include proteolytic enzymes like plasmin, the enzyme responsible for fibrinolysis. For this reason it is effective in treatment of certain bleeding disorders.[104]

Basic amino acids, aliphatic biogenic di- and polyamides and ω-amino acids are all interrelated bioactive species that share biosynthetic metabolic pathways. For this reason it is very important to develop new sensors to detect these species.

5.2. Heteroditopic receptors and sensors for amino acids.

Heteroditopic receptors for ion pairs and zwitterionic species are a class of supramolecular compounds able to bind simultaneously cationic and anionic guests. These type of ligands have shown applications in several fields such as selective extractions of nuclear waste products or solubilization of metal salts and their transport through lipophilic membranes.

An optical chemosensor consists of a molecule incorporating a binding site, a chromophore or fluorophore, and a mechanism for communication between the two. Analyte binding thus produces a change in the chemosensor optical properties (absorption or fluorescence).

Metal complexes are versatile as receptors because they can target a variety of Lewis basic guests through open coordination sites. Typically, metal-coordination events occur with large enthalpies relative to other monovalent

[103] K. R. Cole, F. J. Castellino, *Arch. Biochem. Biophys.*, **1984**,229, 568-575.
[104] T. J. Vander Salm, J. E. Ansell, ON Okike, T. H. Marsicano, R. Lew, W. P. Stephenson, K. Rooney, *J Thorac Cardiovasc Surg*, **1988**, 95, 538-540.

contacts, such as hydrogen bonding or electrostatic interactions. This enables the facile study of coordination-driven events in competitive solvents.[105]

There are many examples in the literature, but here there are some selected references about fluorescence sensors with fluorescein derivatives for detection of amino acids. For instance, Fabbrizzi *et al*. reported an *off-on* chemosensing ensemble for selective recognition of the ambidentate imidazole residue of histidine over the carboxylate group of natural amino acids via the indicator-displacement assays (IDAS).[106] The strategy of Lawrence d. Margerum and coworkers.[107] was accomplished though the introduction of an indicator in the host-guest system capable of competing with the guest for the recognition site on the host receptor. PAMAM dendrimer monolayers, immobilized on glass and modified with Ni(II)–NTA moieties at the termini, show generational dependent responses as histidine (His) selective sensors via indicator displacement assays.

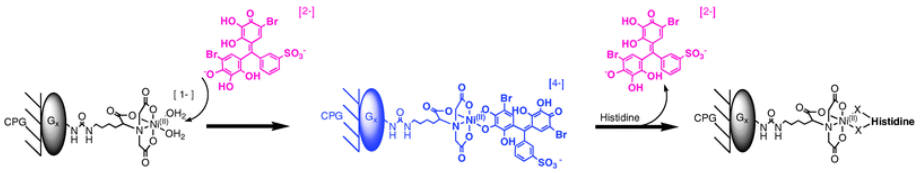

Figure 1: Strategy developed by Lawrence D. Margerum and coworkers.

The recognition and sensing of amino acids and their derivates has been investigated in both metal-containing and purely organic systems. As guest for metalloreceptors, α- amino acids are notable for their ambidentate character[108] and their ability to form strong complexes with a variety of metal ions.[109]

Aslyn also used the indicator displacement assays (IDAS) strategy to detect α-amino acids that bind coordinatively with a metal complexes.[110] The receptor was

[105] J. A. McCleverty, T. J. Meyer, *Compr. Coord. Chem. II*, **2004**, 43, 5073-5075.
[106] a) M. A. Hortala´, L. Fabbrizzi, N. Marcotte, F. Stomeo, and A. Taglietti, *J. Am. Chem. Soc*., **2003**, 125, 20-21. b) L. Fabbrizzi, F. Foti, S. Patroni, P. Pallavicini, A. Taglietti, *Angew. Chem.Int. Ed*., **2004**, 43, 5073-5075.
[107] M. J. Greaney, M. A. Nguyen, C.-C. Chang, A. Good and L. D. Margerum, *Chem. Commun*., **2010**, 46, 5337-5339.
[108] K. Severin, R. Beck, *Angew. Chem. Int. Ed*., **1998**, 37, 1634-1654.
[109] H.Aït-Haddou, S. L. Wiskur, V. M. Lynch, E. V. Anslyn, *J. Am. Chem. Soc*., **2001**, 123, 11296-11297
[110] J. F. Folmer-Andersen, V. M. Lynch, and E.V. Aslyn, *Chem. Eur. J*., **2005**, 11, 5319-5326.

found to discriminate His from other zwitterionic α-amino acids using a fluorescein derivate as an indicator, see Figure 2.

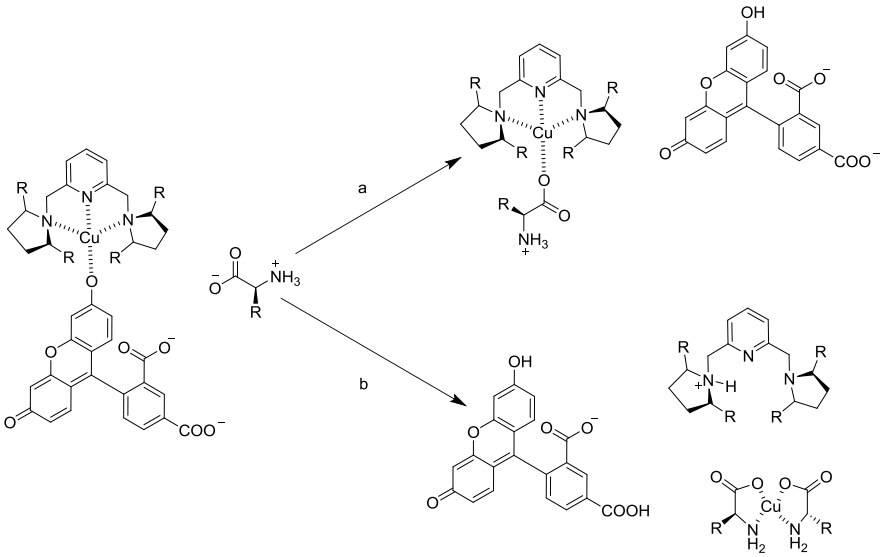

Figure 2: Two pathways for the displacement of the fluorophore by an amino acid: a) standard indicator displacement b) the complex breaks for Cu (II) to give Cu (II)-amino acid complex.

Tae *et al.* reported a Au(I)complex with a rhodamine hydroxylamine derivatized with a 2-deoxyribose to detect cysteine (Cys) and homocysteine (Hcy) in water (see Figure 3). In presence of Au^{+}, only Cys and Hcy produce dramatic enhancements in the fluorescence intensities of **1-Au+.** The recognition of Cys could be attributed to the binding of the thiol of cys to gold ion. The colorless probe changes to a red color, and this change is associated with the binding of the metal complex to the cysteine. Other amino acids exhibitrd no color changes with the metal complex under the same conditions.[111]

[111] Y.-K. Yang, S. Shim and J. Tae, *Chem. Commun*., **2010**, 46, 7766.

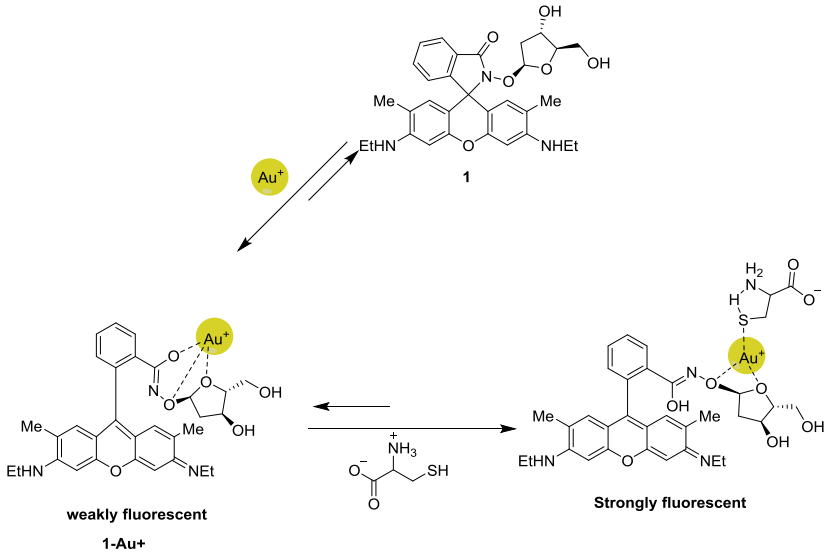

Figure 3: Mechanism of the colorimetric and fluorogenic detection of Cys by sensor 1-Au+.

Costero's group reported a heteroditopic ligand able to perform solid-liquid extraction of ω-amino acids. The prepared ligands for dissolving linear aliphatic amino acids into organic solvents. The prepared host contain in its structure a crown ether moiety for cation recognition, a thiourea group susceptible to be used as anion binding site and a naphthalene as a fluorophore unit.[112]

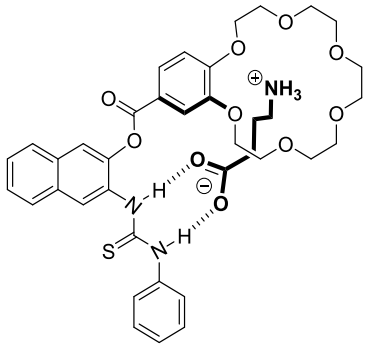

Figure 3: Heteroditopic receptor for detection of GABA by Costero's group.

[112] A. M. Costero, G. M. Rodríguez-Muñiz, S. Gil, S. Peransi, P. Gaviña, *Tetrahedron*, **2008**, 64, 110-116.

5.2. Fluorescein as a signaling unit.

The election of this fluorophore as signaling unit was based on its bright fluorescence, high emission quantum yields, good biocompatibility and the special spectral characteristics of the dye.[113] Fluorescein is one of the most commonly used fluorophores due to its high molar absorptivity, large fluorescence quantum yield and high photostability, in addition, the fluorescein unit absorbs and emits light in the visible region.

In aqueous solutions, fluorescein can exist in up to four different prototropic forms (cation, neutral, monoanion, and dianion) depending on pH, although, in the physiological pH range, only the dianion and monoanion forms are important. Fluorescein and its derivates have been widely employed as fluorescent labels because of their favorable spectral characteristics in water and aqueous media. In the visible range, the absorption maximum of the dianion in water is at 490 nm and its extinction coefficient is 8.36×10^4 M^{-1} cm^{-1}. The monoanion has two absoption maxima in the visible range, one at 454 nm and the other at 474 nm, the extinction coefficients being 3.03×10^4 and 3.14×10^4 M^{-1} $cm^{-1,}$ respectively. The emission spectra of both anion and dianion forms have their maxima around 515 nm. The dianion has a fluorescence quantum yield of 0.93, while for the monoanion it is 0.37.[114]

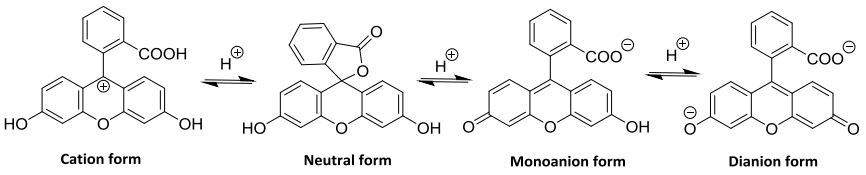

Figure 4: Fluorescein prototropic forms

Both the phenol and carboxylic acid functional groups of fluorescein are almost ionized in aqueous solutions above pH 9. Only the monoanion and dianion forms of fluorescein are fluorescent. In DMSO the predomint form is the monoanion.

---

[113] X. F. Zhang, *Photochem. Photobiol. Sci.*, **2010**, 9, 1261-1268.

[114] L. Crovetto, R. Rios, J. M. Alvarez-Pez, J. M. Paredes, P. Lozano-Velez, C. Valle and E. M. Talavera, *J. Phys. Chem. B*, **2008**, 112, 10082–10085.

5.3. Objectives

The aim of this work was to obtain a selective response towards ω-amino acids over other ionic species. The "binding site-signaling subunit" approach was selected for the chemosensor design. The detection system was designed in such way that, upon coordination of the zwitterionic form of ω-amino acid in the binding site, a modulation of the absorption and emission band of the sensor was induced.

We focused on the design of a fluorescein based chemosensor for the naked-eye detection of ω-amino acids. The election of this fluorophore as signaling unit was based on its bright fluorescence, high emission quantum yields, good biocompatibility and the special spectral characteristics of the dye.[115] Moreover, fluorescein isothiocyanate is commercially available, and reacts easily with amino groups to give the corresponding thiourea derivates

With this in mind, we have appended a thiourea group as H-bonding donor at the side of the phenyl ring as a carboxylate binding site. On the other hand, the carboxylate moiety of the anion or dianion open forms of fluorescein would act as cation binding site for the ammonium group.

In principle the simultaneous complexation of ω-amino acids with the anionic and cationic receptors of the fluorescein derivative shouldinduce some appreciable changes in its absorbance and emission spectra, which would indicate the presence of amino acids. At the same time, only ω-amino acids with an optimal chain length to complez simultaniusly to the thiourea group and the fluorescein carboxylate unit would lead to strong optical responses.

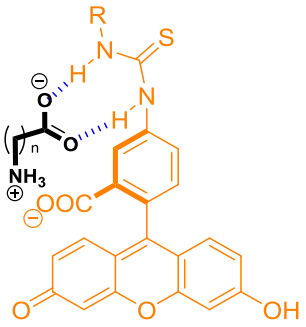

Figure 5: Design of our sensor strategy.

[115] X. F. Zhang, *Photochem. Photobiol. Sci.*, **2010**, 9, 1261-1268.

5.4. A simple system for ω-amino acid discrimination based on a thiourea modified fluorescein

A simple system for ω-amino acid discrimination based on a thiourea modified fluorescein

Almudena Martí,[a][b] Ana M. Costero,*[a][b] Pablo Gaviña,*[a][b] Margarita Parra,[a][b]

[a] Centro de Reconocimiento Molecular y Desarrollo Tecnológico (IDM), Unidad Mixta Universidad de Valencia-Universidad Politécnica de Valencia, Spain Fax: +34 963543151 E-mail: ana.costero@uv.es, pablo.gavina@uv.es

[b] Departamento de Química Orgánica, Universidad de Valencia, Dr. Moliner 50, 46100-Burjassot (Valencia), Spain.

Eur. J. Org. Chem. DOI: 10.1002/ejoc.201500991

Abstract

A novel thiourea modified fluorescein derivative was synthesized by reaction of fluorescein isothiocyanate and 2-(2-aminoethoxy)ethan-1-ol. UV-vis absorption and fluorescence emission studies demonstrate that this heteroditopic receptor is able to discriminate among linear aliphatic ω-amino acids with different chain lengths.

Introduction

Over the last decades, a large number of receptors and sensors for either cations or anions have been prepared and evaluated, and both cation and anion recognition are now well-established branches of supramolecular chemistry. More recently, the combination of cation and anion recognition centres in the same molecule has led to the development of more elaborate heteroditopic receptors, able to bind ion pairs or zwitterionic species.[1] On the other hand, the study of molecular recognition of biological molecules such as amino acids by synthetic receptors is a classical field that merges the principles and applications of supramolecular chemistry.[2] Within this area the most studied receptors and sensors are those involved in the recognition of α-amino acids due to their special importance in living organism.[3] However, many of the reported ligands only bind the carboxylate moiety,[4] or the functional group present in the side chain of the amino acid, such as the thiol moiety in cysteine.[5]

Whereas there is a large number of colorimetric or fluorimetric sensors for detecting a-amino acids, less attention has been devoted to the recognition of linear aliphatic ω-amino acids,[3b,6] even though they also play important biological roles. Thus, γ-aminobutyric acid (GABA) is an important neurotransmitter, 5-aminopentanoic acid is a metabolic product of cadaverine, and 6-aminohexanoic acid presents fibrinolytic properties.[7]

Here we report a new simple fluorescein derivative **L1** for detecting ω-amino acids. Fluorescein is a dye extensively used in fluorescent probes due to its excellent photophysical properties, such as long-wavelength absorption and emission, high fluorescence quantum yields and high photostability.[8] The neutral closed form of fluorescein with a spirolactam structure is not fluorescent but its anion and dianion forms are strongly fluorescent. These properties have made fluorescein useful in the design of chemosensors for anions,[9] cations[10] and neutral molecules.[11]

The described compound **L1** would be able to act as a useful receptor for the selective discrimination between different classes of ω-amino acids in their zwitterionic form. The recognition process is based on the complexation of both the anionic and the cationic moieties of the zwitterion with the corresponding thiourea and carboxylate receptor sites of the fluorescein derivative. The ligand was designed with an additional 2-ethoxyethanol chain, which could be used to anchor the compound to different solid supports. In addition, the hydroxyl group could also be involved in the complexation of the zwitterionic guest through additional hydrogen bond formation

Results and Discussion

The synthesis of ligand **L1** was carried out as described in Scheme 1. Fluorescein isothiocyanate and 2-(2-aminoethoxy)ethan-1-ol were refluxed in methanol during 24 h to obtain the corresponding thiourea with a 97 % yield.

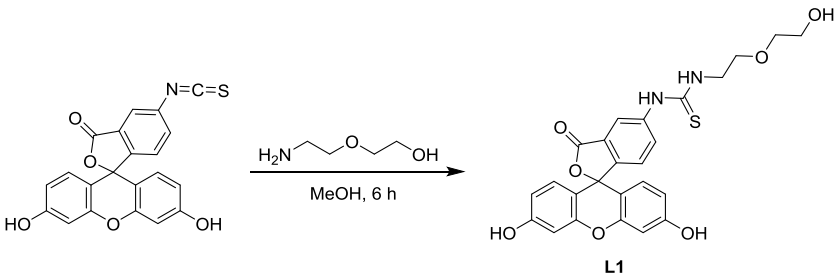

Scheme 1. Synthesis of Ligand L1

The spectroscopic properties of **L1** were evaluated in DMSO solution. As shown in Figure 1, **L1** (10^{-5} M in DMSO) exhibits maximal absorption bands at 461, 490 and 531 nm that could be related to an equilibrium between the neutral form, the anion and the dianion as showed by the corresponding deconvolution of the spectrum (Figure 1). In fact, it has been reported that for the parent compound fluorescein in DMSO-H_2O solution (91.3 wt% in DMSO), the neutral species shows an absorption band at 450 nm, the anion shows two bands at 460 and 490 nm and the dianion shows an absorption band at 520 nm with a shoulder at shorter wavelength that overlaps with one band of the anion.[12]

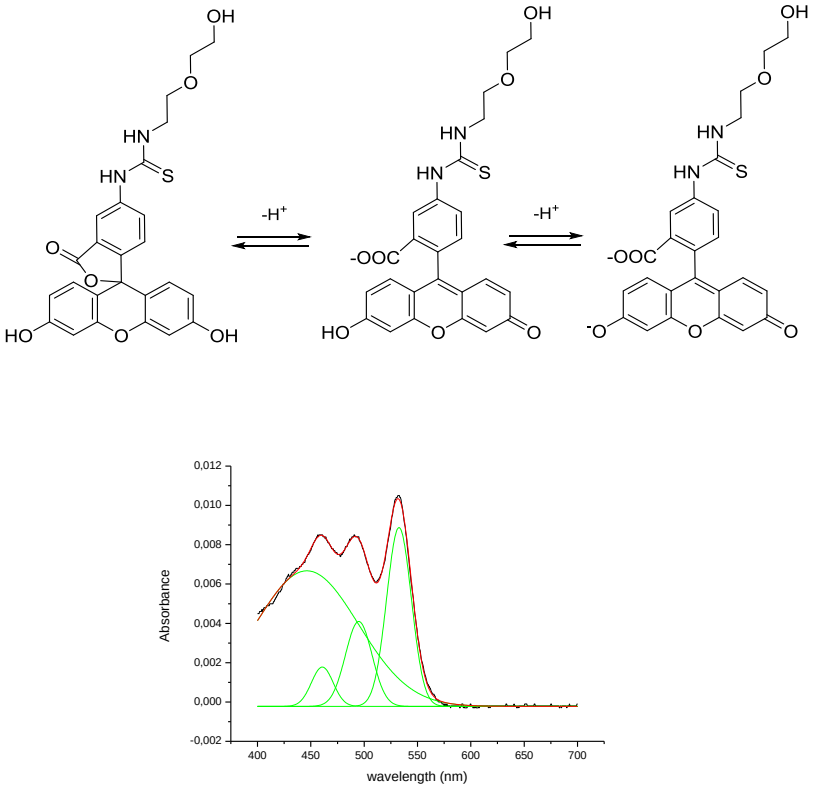

Figure 1. (Up) Protolytic equilibria of L1 in DMSO. (Bottom) UV spectrum of L1 10^{-5} M in DMSO (black), deconvolution bands (green), theoretical spectrum (red).

The presence of the thiourea moiety in the ligand makes it useful for interacting with carboxylate compounds. In addition, the presence of a free carboxylate group in the anion and dianion forms of **L1** allows it to interact with the ammonium group of the amino acids in their zwitterionic form. Thus, the thiourea should act as a carboxylate binding site whereas the carboxylate would act as a cation recognition centre. The geometry of the ligand should give rise to different interactions with the target molecules, depending on the length of the studied zwitterions, and in consequence, different photophysical responses should be achieved.[6a,13] For this reason, our first studies were focused on the evaluation of the behaviour of DMSO solutions of **L1** in the presence of various zwitterionic ω-amino acids of different chain lengths (glycine (**1**), β-alanine (**2**), GABA (**3**), 5-aminopentanoic acid (**4**), 6-aminohexanoic acid (**5**) and 8-aminooctanoic acid (**6**)). In all cases, addition of increasing amounts of each ω-amino acid to 10^{-5} M DMSO

solutions of **L1** induced a hypsochromic shift of the main absorption band together with a hyperchromic effect (Figure 2, up)

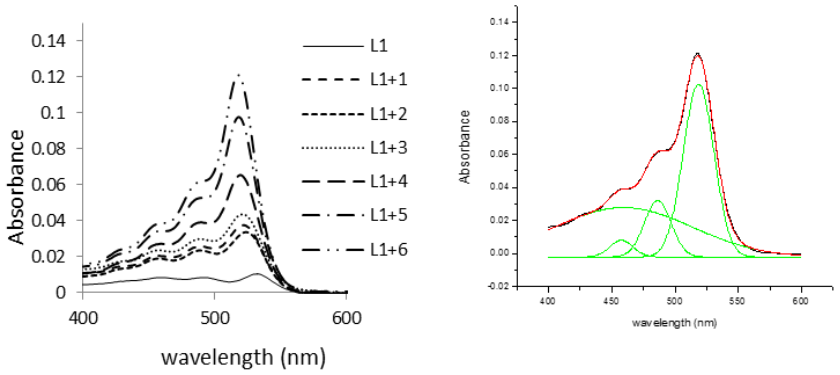

Figure 2. (Left) UV-vis spectra of L1 (10-5 M DMSO) free and in the presence of 5 equiv of the studied ω-amino acids 1-6. (Right) UV-vis spectrum (including deconvolution) of L1 (10-5 M DMSO) in the presence of 5 equiv of 8-aminooctanoic acid (6).

The observed hypsochromic shift can be related to the interaction between the carboxylate group of the amino acid and the thiourea moiety directly attached to the phenyl ring of the ligand. This interaction enhances the electron-donor ability of the thiourea moiety, giving rise to a blue shift of the main absorption band.[14] The hyperchromic effect observed in the presence of the studied amino acids can be due to a displacement of the protolytic equilibrium towards the dianionic complex as shown in the deconvolution of the corresponding UV-vis spectrum (see Figure 2 (bottom) for 8-amino octanoic acid (**6**); for the other amino acids see Figure S-2). It is worth noting that the hypsochromic effect is no longer observed after the addition of more than 1 equiv of the amino acid whereas the hyperchromic effect is still appearing (Figure 3). This behaviour suggests that until the addition of ca. 1 equiv of amino acid, complexation of the thiourea moiety of the different fluorescein species is taking place, together with the displacement of the protolytic equilibrium towards the dianion form. When all the thiourea carboxylate complexes are formed, the excess amino acid only gives rise to an increment of the concentration of the dianionic complex.

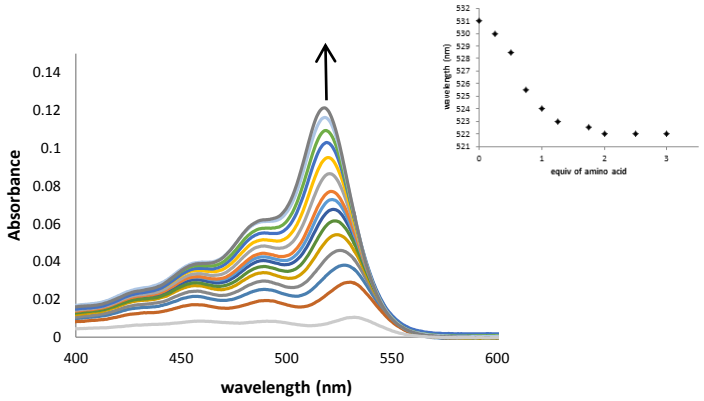

Figure 3. (Left) UV-vis titration of L1 (10-5 M DMSO) in the presence of increasing amounts (0-5 equiv) of 8-aminooctanoic acid (6). (Right) Hypsochromic shift of the main absorption band, corresponding to the dianion form, at increasing amounts of 6

As it was expected, the addition of 5 equiv of TBAOH to **L1** gave rise to similar, although more pronounced, hyperchromic and hypsochromic effects in the UV-vis spectrum (see Figure S-3), as a consequence of the acid-base reaction, giving rise to the complete deprotonation of the system including the thiourea moiety.[15]

When comparing amino acids of different chain lengths, the hypsochromic shift (ca. 11-15 nm for 5 equiv of amino acid) as well as the hyperchromic effect increase as the chain length does (see Figure 4 and Table S1), being the absorbance increment at the l_{max} higher than 10-fold in the presence of 5 equiv of 8-aminooctanoic acid (6).

As previously discussed, the free carboxylate group of **L1** in its anion and dianion forms is very likely involved in the complexation of the ammonium moiety of the target molecule. Thus, the differences observed among the different amino acids could be a structural effect related to the influence of the distance between both coordinating groups in the interaction with the ligand. To corroborate this suggestion, studies with 12-aminododecanoic acid (**7**) were undertaken (Figure S-4). The hyperchromic effect of this longer chain amino acid on **L1** was smaller than that observed with 6-aminohexanoic and 8-aminooctanoic acid but stronger than that with 5-aminopentanoic acid (Figure 4).

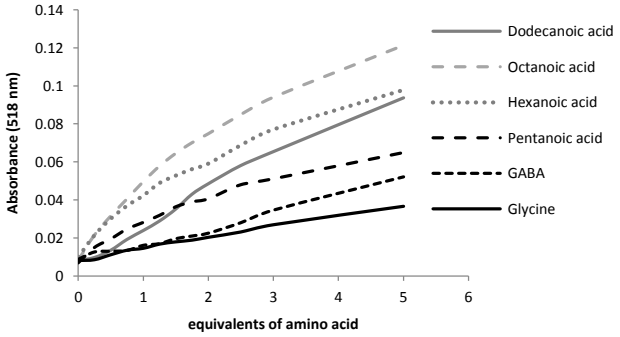

Figure 4. Absorbance at ?max at increasing concentrations of the studied amino acids.

Moreover, to verify if the complexation by **L1** involves the simultaneous binding of the carboxylate and the ammonium moieties of the amino acids, experiments with an equimolecular mixture of butanoic acid and propylamine were carried out. The mixture of these two compounds generates "in situ" an alkyl carboxylate and an alkyl ammonium with similar acid-base properties than those of the ammonium and carboxylate moieties in zwitterionic 8-aminooctanoic acid. As can be seen in Figure 5, although a similar hypsochromic shift of the main absorption band was observed in both cases, the hyperchromic effect induced by the amino acid was stronger than that observed with the equimolecular mixture of alkyl carboxylate and alkyl ammonium. Finally ^{1}H NMR experiments were carried out with **L1** and **6**. Due to solubility reasons, these experiment were developed in CD_3OD, a very competitive solvent. Under these conditions, changes were observed in both the amino acid and **L1**. Thus, the ^{1}H NMR signal corresponding to the methylene next to the carboxylate in the amino acid is slightly upfield shifted; on the other hand, the signal of the aromatic proton *ortho* to the thiourea and the carboxylate group of the fluorescein is upfield shifted whereas the peaks corresponding to H_1 and H_2 in the xanthene moiety are downfield shifted (see Figure S-5). These results confirm the simultaneous complexation of both the carboxylate and the ammonium group of the amino acid to **L1** and the importance of an optimum chain length for a cooperative coordination.

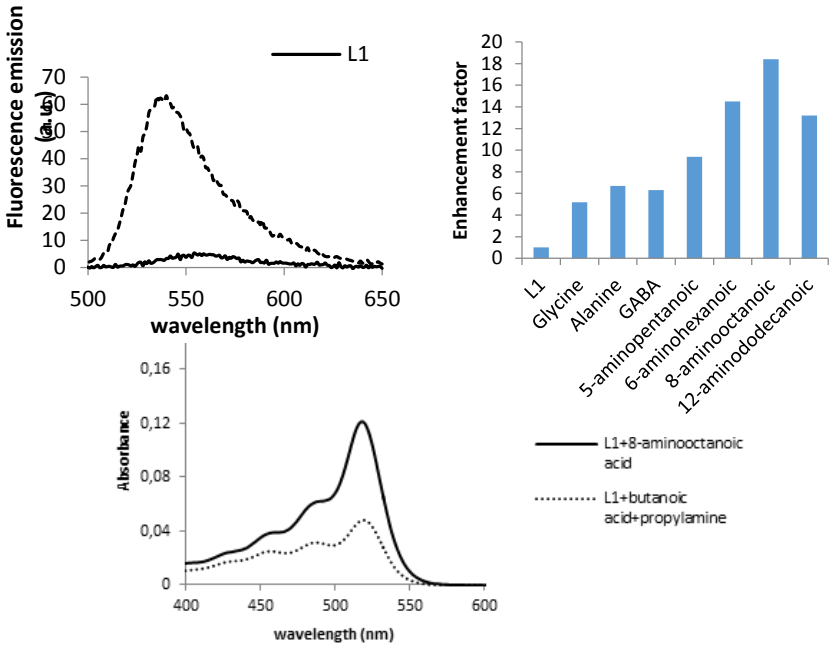

Figure 5. UV-vis spectra of L1 (10-5 M DMSO) in the presence of 5 equiv of 8-aminooctanoic acid (6) and 5 equiv of an equimolecular mixture of butanoic acid and propylamine.

Regarding the fluorescence emission behaviour, **L1** in DMSO solution is weakly fluorescent showing an emission band at 556 nm (λ_{exc} = 490 nm). Upon addition of increasing amounts of the studied amino acids a strong enhancement of the fluorescence emission was observed (Figures 6 up and S-6), together with a moderate hypsochromic shift (ca. 16 nm). The fluorescence behaviour of **L1** with the different amino acids followed a similar trend to that observed in the UV-vis studies, i.e. an increase in the fluorescence emission enhancement of **L1** as the chain length of the linear w-amino acid increases, reaching a maximum for 8-aminooctanoic acid (**6**), and decreasing again for the longer 12-aminododecanoic acid (**7**) (Figure 6 bottom). As the most fluorescent species in fluorescein derivatives is the dianion, the observed enhancement of the fluorescence supports the idea of a complex containing the xanthene moiety in its dianionic form.

Figure 6. (left) Fluorescence of L1 (10^{-5} M DMSO) free and in the presence of 5 equiv of 8-aminooctanoic acid (λ_{exc} = 490 nm). (right) Fluorescence enhancement

factor observed for L1 (10^{-5} M DMSO) in the presence of 5 equiv of amino acids 1-7.

A tentative structure for the complex between the dianion form of **L1** and 8-aminooctanoic acid (**6**), obtained using low-level calculations, is depicted in Figure 7. The structure shows that simultaneous coordination with both, the thiourea and the carboxylate moieties of **L1**, can occur, but more interestingly, also the phenolate seems to be involved in the complexation of the ammonium group, providing an additional stabilization of the complex. This interaction would also explain the displacement of the protolytic equilibria towards the dianion form of **L1** upon complexation, giving rise to the observed hyperchromic effect of the UV-vis band and the enhancement in the fluorescence emission. In amino acids with shorter chains, the interaction with the phenolate moiety is weaker and for this reason, the response both in UV and in fluorescence is weaker. In addition, the hydroxyl group of the 2-ethoxyethanol chain also seems to participate in the complexation, giving rise to an additional anchoring point.

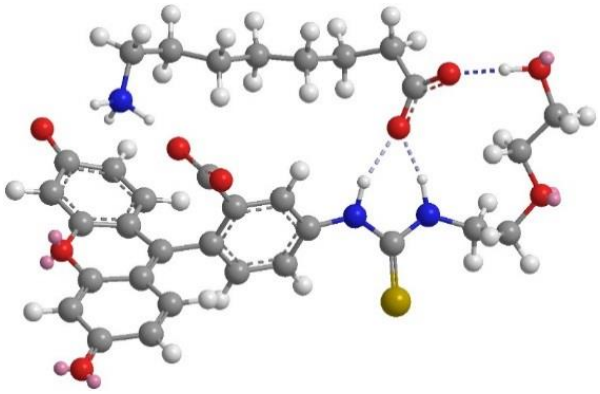

Figure 7. Proposed structure for the complex between the dianion of L1 and 8-aminooctanoic acid (6).

Conclusions

In summary, we have developed a new simple fluorescein derivative as amino acids receptor able to discriminate between amino acids with different chain lengths. The prepared heteroditopic ligand presents a carboxylate group able to complex the ammonium group and a thiourea moiety able to complex the amino acid carboxylate. An additional hydroxyl group has been included in the structure

that is able to cooperate in the recognition process. The chain length of the amino acid is of crucial importance for the cooperative coordination of the different binding sites present in the ligand.

Experimental Section

General: All reagents were commercially available, and were used without purification. Silica gel 60 F254 (Merck) plates were used for TLC. 1H-NMR and 13C-NMR spectra were recorded on a Bruker 300 MHz spectrometer. Chemical shifts are reported in ppm with tetramethylsilane as an internal standard. High resolution mass spectra (HRMS) were recorded in the positive ion mode on a VG-AutoSpec mass spectrometer. UV-vis absorption spectra were recorded using a 1 cm path length quartz cuvette on a Shimadzu UV-2101PC spectrophotometer. All measurements were carried out at 293 K (thermostated).

Synthesis of L1: 2-(2-Aminoethoxy) ethanol (71 µL, 0.7 mmol) and fluorescein isothiocyanate (300 mg, 0.7 mmol) were dissolved in methanol (10 mL). The reaction mixture was stirred under argon atmosphere and refluxed in methanol for 24 h. The solvent was removed, the residue was dissolved in dichloromethane (10 mL), and then 30 mL of diethyl ether were added to precipitate the product. After washing the precipitate with small amounts of diethyl ether an orange solid (332 mg, 97%) was obtained. ^{1}H NMR (300 MHz, DMSO-D6): δ = 8.38 (br. s, 1H), 8.29 (s, 1H), 7.74 (d, J = 8.4 Hz, 1H), 7.15 (d, J = 8.4 Hz, 1H), 6.67–6.47 (m, 6H), 4.05 (br. s, 1H), 3.70–3.40 (m, 8H), 2.86 (t, J = 5.3 Hz, 1H) ppm. ^{13}C NMR (75 MHz, DMSO-D6): δ = 188.4, 180.5, 168.7, 161.2, 152.6, 152.4, 141.4, 129.2, 124.2, 114.1, 113.6, 110.1, 102.3, 79.2, 72.2, 68.3, 68.1, 60.2, 43.8 ppm. HRMS (ESI): m/z calcd for $C_{25}H_{23}N_2O_7S$ ($[M+H]^+$) 495.1225; found 495.1206.

Acknowledgements

We thank the Spanish Government and European FEDER funds (MAT2012-38429-C04-02) for support. A. M. is grateful to the Spanish Government for a fellowship. SCSIE (Universidad de Valencia) is gratefully acknowledged for all the equipment employed.

Keywords: fluorescein derivative • amino acids • discrimination• sensing• thioureas

References

[1]. S. K. Kim, J. L. Sessler, Chem. Soc. Rev. 2010, 39, 3784–3809.

[2]. A. R. Urbach, V. Ramalingam, Isr. J. Chem. 2011, 51, 664-678.

[3]. a) Y. Zhou, J. Yoon, *Chem. Soc. Rev*. **2012**, *41*, 52-67; b) J. H. Lee, J. S. Kim, J. Vicens *Chem. Soc. Rev*. **2011**, *40*, 2777–2796; c) A. Galán, D. Andreu, A. M. Echavarren, P. Prados; J. de Mendoza, *J. Am. Chem. Soc*. **1992**, *114*, 1511-1512. Buryak, K. Severin, *J. Am. Chem. Soc*. **2005**, *127*, 3700-3701; b) X. Lou, L. Zhang, J. Qin, Z. Li, *Langmuir* **2010**, *26*, 1566–1569; c) Y-X. Zhang, P.-Y. Zhao, L.-P. Yu, *Sens. Actuators, B* **2013**, *181*, 850–857; d) S. Qian, H. Lin, *RSC Adv.* **2014**, *4*, 29581–29585; e) J. Wang, H.-B. Liu, Z. Tong, C.-S. Ha, *Coord. Chem. Rev*. **2015**, *303*, 139-184.

[4]. a) A. dalla Cort, P. de Bernardin, L. Schiaffino, Chirality 2009, 21, 104-109; b) J. F. Folmer-Andersen, V. M. Lynch, E. V. Anslyn, Chem. Eur. J. 2005, 11, 5319-5326.

[5]. a) Y.-K. Yang, S. Shim, J. Tae, Chem. Commun. 2010, 46, 7766-7768; b) F. Huo, J. Kang, C. Yin, Y. Zhang, J. Chao, Sensor Actuat-B-Chem 2015, 207, 139-143.

[6]. a) A. Buryak, K. Severin, J. Am. Chem. Soc. 2005, 127, 3700-3701; b) X. Lou, L. Zhang, J. Qin, Z. Li, Langmuir 2010, 26, 1566–1569; c) Y-X. Zhang, P.-Y. Zhao, L-P. Yu, Sensor Actuat B-Chem, 2013, 181, 850–857; d) S. Qian, H. Lin, RSC Adv. 2014, 4, 29581–29585.

[7]. a) A. P. de Silva, H. Q. N. Gunaratne, C. McVeigh, G. E. M. Maguire, P. R. S. Maxwell, E. O'Hanlon, Chem. Commun. 1996, 2191-2192; b) A. M. Costero, G. M. Rodríguez-Muñiz, S. Gil, S. Peransi, P. Gaviña, Tetrahedron, 2008, 64, 110-116.

[8]. J. R. Lakowicz Principles of Fluorescence Spectroscopy, 3rd (ed. Springer) New York, 2006, pp. 67-69.

[9]. a) S. K. Asthana, A. Kumar, N. K. K. Upadhyay, Tetrahedron Lett. 2014, 55, 5988-5992; b) F. Zheng, F. Zeng, C. Yu, X. Hou, S. Wu, Chem. Eur. J. 2013, 19, 936-942; c) X.-F. Yang, L. Wang, H. Xu, M. Zhao, Anal. Chim. Acta 2009, 631, 91-95; d) J.-S. Wu, H. J. Kim, M. H. Lee, J. H. Yoon, J. H. Lee, J. S. Kim, Tetrahedron Lett. 2007, 48, 3159-3162; e) X. Zhang, Y. Shiraishi, T. Hirai, Tetrahedron Lett. 2007, 48, 8803-8806; f) K. M. K. Swamy, Y. J. Lee, H. N. Lee, J. Chun, Y. Kim, S.-J. Kim, J. Yoon, J. Org. Chem. 2006, 71, 8626-8628.

[10]. a) T. Li; Z. Yang, Y. Li, Z. Liu, G. Qi, B. Wang, Dyes and Pigments 2011, 88, 103-108; b) X.-F. Yang, Y. Li, Q. Bai, Anal. Chim. Acta 2007, 584, 95-100.

[11]. N. Zhang, Y. Liu, L. Tong, K. Xu, L. Zhuo, B. Tang, Analyst 2008, 133, 1176-1181.

[12]. a) N. O. Mchedlov-Petrossyan, R. Salinas Mayorga, J. Chem. Soc. Faraday Trans 1992, 88, 3025-3032; b) R. Sjöback, J. Nygren, M. Kubista, Spectrochim. Acta A 1995, 51, L7-L21.

[13]. A. M. Costero, M. Colera, P. Gaviña, S. Gil Chem. Commun. 2006, 761-763.

[14]. X-F. Zhang, Photochem. Photobiol. 2010, 9, 1261-1268.

[15]. a) D. E. Gómez, L. Fabbrizzi, M. Licchelli, E. Monzani, Org. Biomol. Chem. 2005, 3, 1495-1500; b) C. Pérez-Casas, A. K. Yatsimirsky, J.

Org. Chem. 2008, 73, 2275-2284

SUPPORTING INFORMATION

A simple system for ω-amino acid discrimination based on a thiourea modified fluorescein

Almudena Martí, Ana M. Costero,* Pablo Gaviña,* Margarita Parra

[a] Centro de Reconocimiento Molecular y Desarrollo Tecnológico (IDM), Unidad Mixta Universidad de Valencia-Universidad Politécnica de Valencia, Spain

Fax: +34 963543151

E-mail: ana.costero@uv.es, pablo.gavina@uv.es

[b] Departamento de Química Orgánica, Universidad de Valencia, Dr. Moliner 50, 46100-Burjassot (Valencia), Spain.

Figure S.1: ^{1}H RMN (CD_3OD) and ^{13} C NMR (DMSO-d_6) spectra of compound L1 at 300 MHz and 75 MHz.

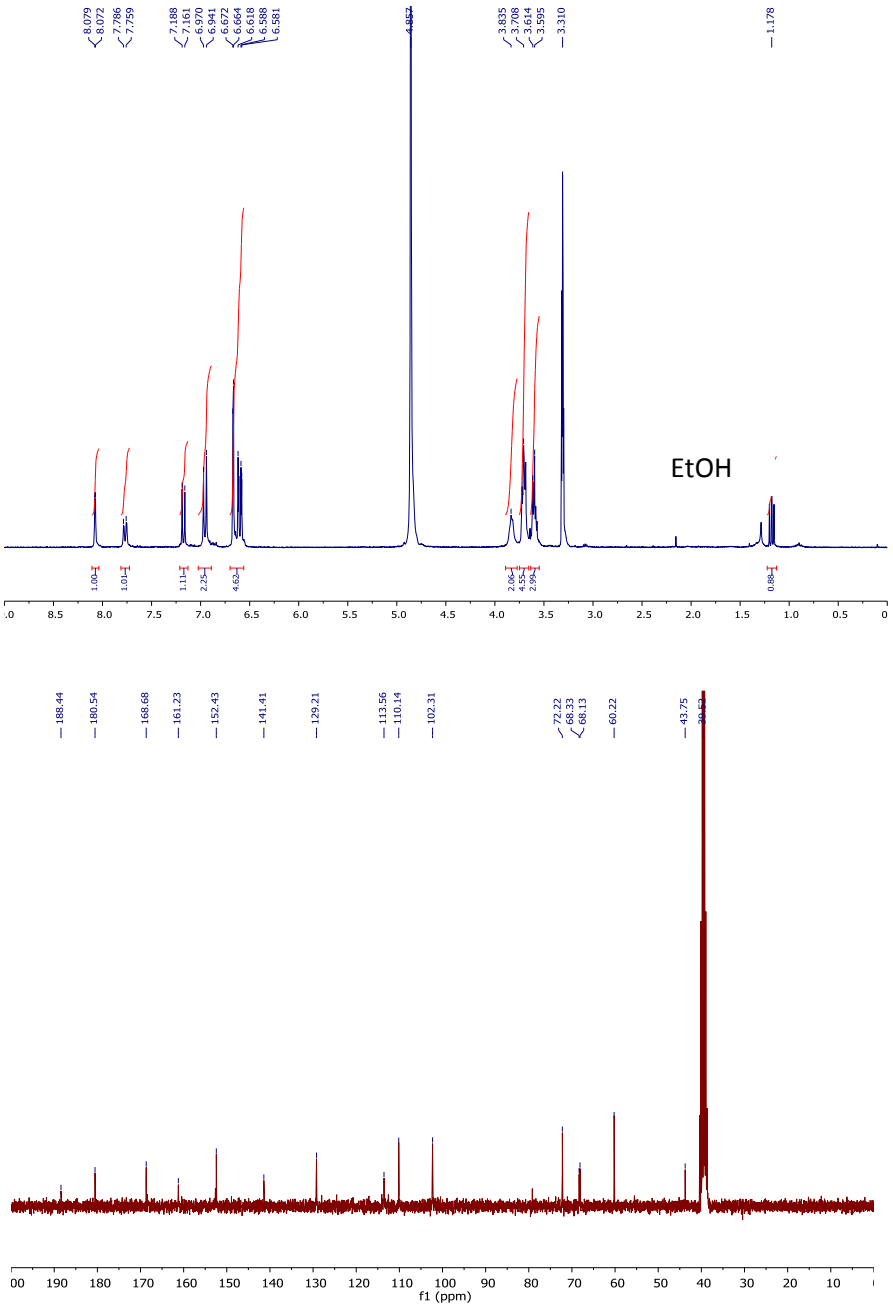

Figure S-2 : UV-vis spectrum (including deconvolution) of L1 (10^{-5} M DMSO) free and in the presence of 5 equiv of 1-6.

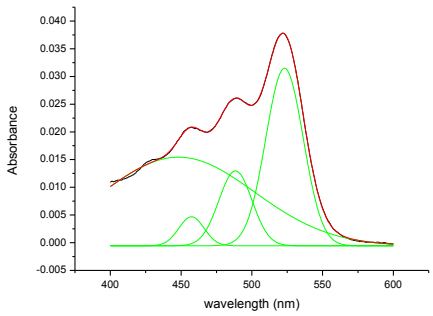

Glycine

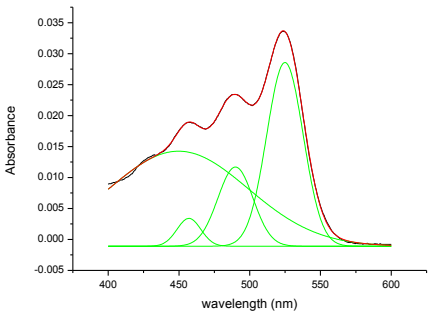

Alanine

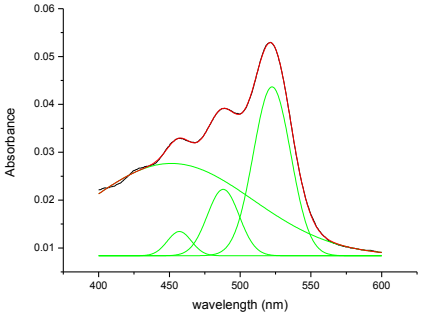

GABA

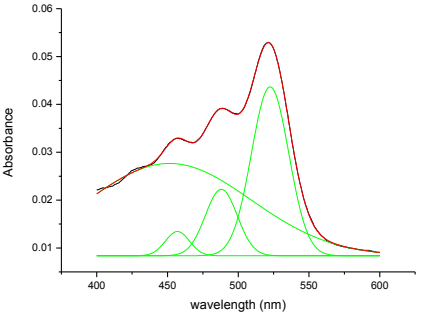

5-aminopentanoic acid

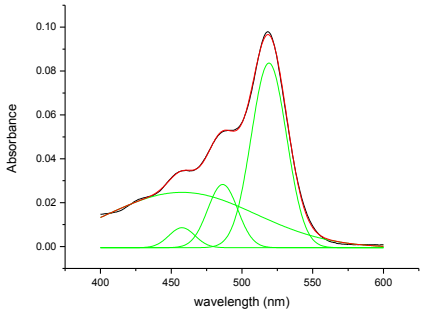

6-aminohexanoic acid

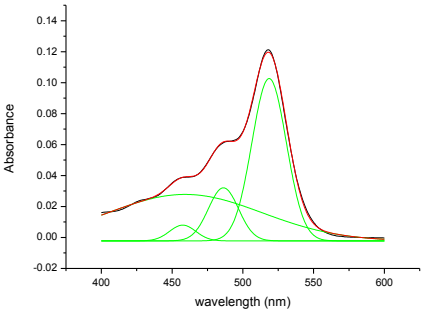

8-aminooctanoic acid

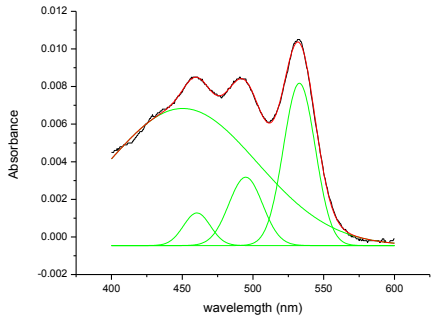

L1

Table S1. Changes observed in the UV-vis spectra of L1 (10^{-5} M DMSO) in the presence of 5 equiv amino acids **1-6**.

Amino acid	Hypsochromic shift λ_{max}(L1)-λ_{max} (nm)	Abs(λ_{max})/Abs(L1)
1	**10**	**3.6**
2	**11**	**4.2**
3	**11.5**	**5.0**
4	**12**	**6.2**
5	**14**	**9.3**
6	**15**	**11.7**

Figure S-3: UV-vis absorption spectra of L1 (10^{-5} M DMSO), and L1 upon addition of 5 equivalents of TBAOH, to confirm the formation of the dianion form of fluorescein.

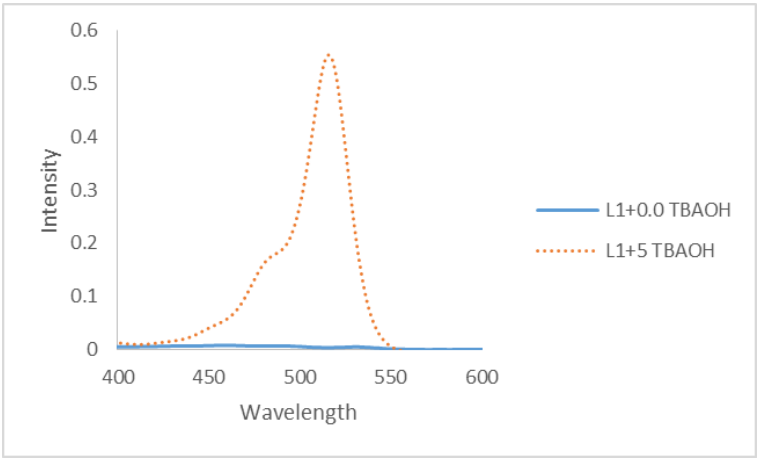

Figure S-4. UV-vis spectra of L1 (10^{-5} M DMSO) free and in the presence of 5 equiv of the studied ω-amino acids 5-7.

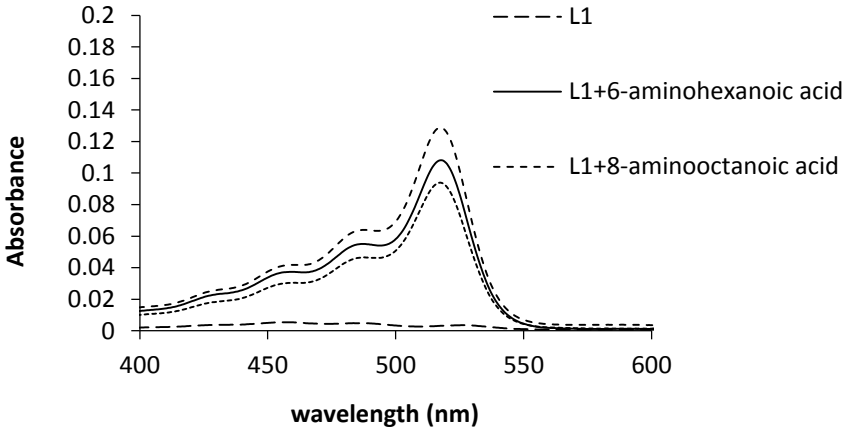

Figure S-5: ^{1}H-NMR spectra (CD_3OD, 300 MHz) of L1 in the presence of increasing amounts of 8 aminooctanoic acid (6) (0–2 equivalents). a) Aliphatic part (6); b) aromatic region (L1)

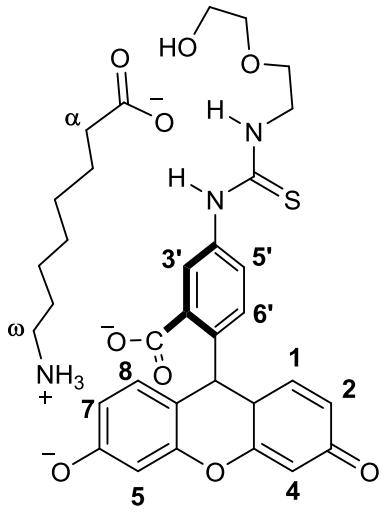

a)

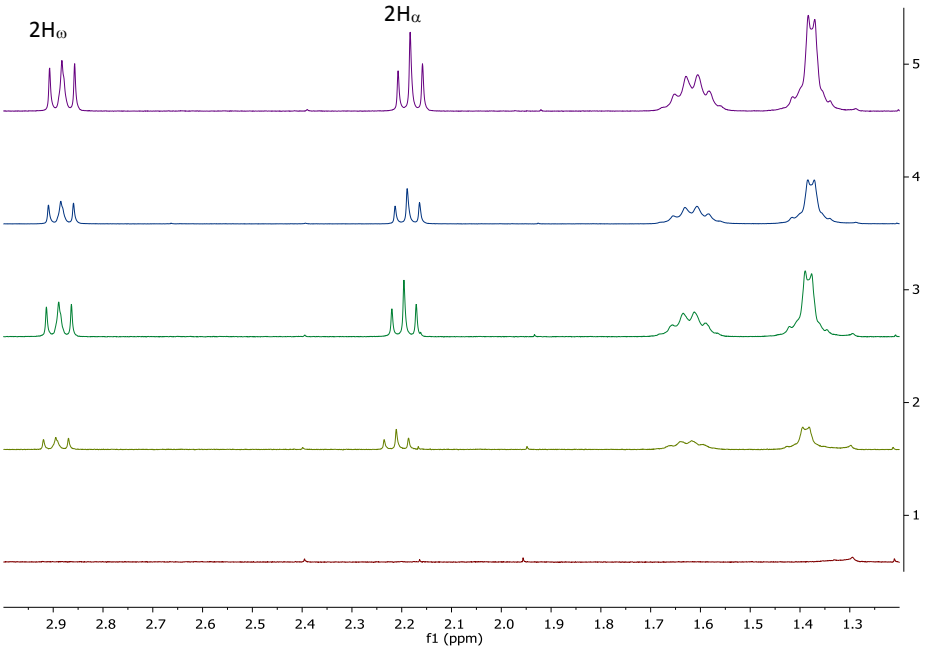

b)

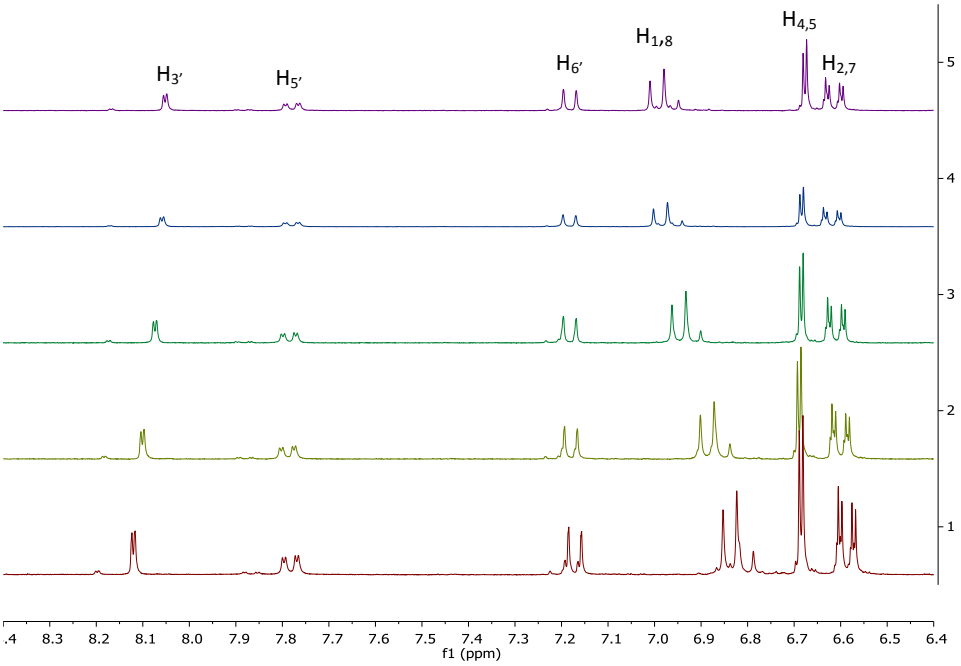

Figure S-6: Fluorescence spectra of L1 (10^{-5} M DMSO) free and in the presence of 5 equivalents of the studied ω-amino acids 1-

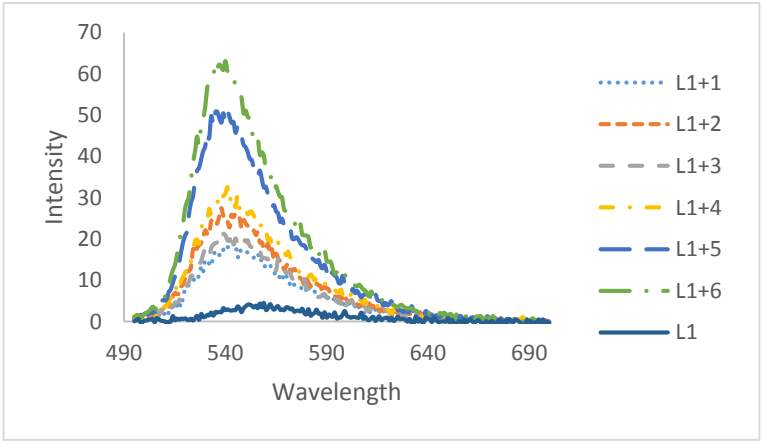

CHAPTER 6:
Conclusions

Today's world requires new methods and technologies for the detection and sensing of biological or environmentally important species, more quickly and selectively. Chemosensors and probes stand out for their selectivity and specificity over others as they can be designed specifically for a particular analyte.

Among chemosensors, those with optical properties are most interesting, as they do not require advanced instrumentation for measurements.

In the present thesis we have designed, synthesized and evaluated several chemosensors and probes for the selective detection of contaminating or biologically species, including the chemical warfare simulants.

The design, synthesis and evaluation of these sensors have been divided into discrete sections. These sections describe chemosensors for nerve agent simulants, chemosensors for nitric oxide gas, chemosensors for carboxylic acid dianions, and the development of a new sensor to detect amino acids in their zwitterionic form.

In the Introduction, the main aspects of molecular recognition and optical sensing were described. In particular the chemistry and optical properties of gold nanoparticles (AuNPs) were emphasized, in order to understand the basis of the colorimetric sensing strategy of the new prepared sensors based on functionalized AuNPS.

In Chapter 2, different colorimetric probes for nerve agents, based on azo pyridine- or triaryl carbinol-functionalized gold nanoparticles were reported. In the first case, azo pyridine-modified AuNPs were tested in aqueous solution and in the second case the detection experiments using AuNPs functionalized with triaryl carbinol derivatives were carried out in dimethylformamide. We demonstrated their capabilities of detecting these nerve agents at low concentrations and in the presence of other interferents.

In the third Chapter, a new sensor for the selective detection of nitric oxide in the gas phase was described. The design, synthesis and characterization of azide- and alkyne-functionalized AuNPs was reported. Subsequently the chromogenic response to the different gaseous species was evaluated and we were able to state that our sensor displayed a great selectivity towardsNO (g), with remarkably low limits of detection, in the ppm range, and with the additional advantage that the color changes could be observed by naked eye.

In Chapter 4, the use of thiourea derivatives for detection of ω-dicarboxylates is described. In a first approach we designed a fluorescein-based sensor capable of detecting the presence of dicarboxylates of different lengths by modulating its fluorescence intensity. In a second approach, gold nanoparticles functionalized with a thiourea derivative were synthesized and characterized to be used in colorimetric dicarboxylate sensing. a high selectivity towards succinic acid dianion was observed. As far as we know, this chemosensor may be the first example in the literature for specific colorimetric detection of succinate dianion versus other dicarboxylates of different change length.

Finally, in Chapter 5, the design, synthesis, and evaluation of a heteroditopic optical sensor for ω-amino acids in their zwitterionic form is reported. The new probe, based on thiourea-functionalized fluorescein, is capable of discriminating among ω-amino acids of different chain lengths, on the basis of their absorbance or fluorescence emission intensities.

Gracias al Ministerio de Economía y Competitividad (Secretaría de estado de investigación, Desarrollo y Innovación) por concederme una beca de Formacioón de Personal Investigador (FPI).